peripheral nerves

by

Mohammed Kismet Hossain-Ibrahim

Department of Anatomy and Developmental Biology

University College London

May, 2007

A thesis submitted to the University of London

in partial fulfilment of the requirements for the degree of

Doctor of Philosophy

ProQuest LLC
789 East Eisenhower Parkway
P.O. Box 1346
Ann Arbor, MI 48106-1346

Declaration

I, Kismet Hossain-Ibrahim, confirm that the work in this thesis is my own. Where information has been derived from other sources, I confirm that this has been indicated in the thesis. None of this work has been submitted for any other qualification at this or any other university.

M.K.Hossain-Ibrahim

May, 2007

Abstract

This thesis examines the roles of inflammation and the chondroitin sulphate proteoglycan NG2 in regeneration of injured axons in the adult mammalian nervous system, against a background suggesting that inflammation around the cell bodies of axotomised neurons enhances axonal regeneration and that NG2 is a major inhibitor of CNS axonal regeneration.

1) Lipopolysaccharide was placed on / injected in motor cortex of rats, with or without concomitant injury of the cervical corticospinal tract (CST). The inflammatory response and expression of the growth-associated genes c-jun, ATF3, SCG10 and GAP-43 was investigated by immunohistochemistry or in situ hybridisation. Retrograde labelling identified CST neuron cell bodies, and anterograde tracing of CST axons identified axonal sprouting / regeneration. Lipopolysaccharide-induced inflammation promoted upregulation of GAP-43 (briefly), c-jun and SCG10 (for two weeks) in CST neurons, but did not enhance regeneration of injured CST axons.

2) Axonal regeneration was examined in the CNS and PNS of NG2 knockout mice. CNS regeneration was assessed following dorsal column injury in ascending axons with cholera toxin-conjugated horseradish peroxidase (CT-HRP) and in descending CST axons with anterograde labelling with biotinylated dextran amine (BDA), as well as transganglionic labelling of transected dorsal roots with CT-HRP. PNS regeneration after sciatic nerve crush was assessed anatomically by: retrograde labelling (from the

hindpaw) of L4/5 dorsal root ganglion cells; immunohistochemistry to detect sensory axons in hindpaw skin; silver-cholinesterase staining of soleus motor axons / end plates; EM counts of tibial and digital nerves. Functional recovery was assessed by the (motor) toe spreading reflex and (sensory) responses to von Frey hairs. There was neither anatomical nor functional evidence for significant effects on CNS or PNS axonal regeneration in the knockout mice. These findings suggest that NG2 is not a major inhibitory factor in the failure of CNS regeneration and is not important for successful axonal regeneration in the PNS.

Acknowledgements

I would like to take this opportunity to offer my gratitude to my supervisors, Professors Patrick Anderson and Bob Lieberman, to allow me to pursue my life-long desire to study CNS regeneration in their laboratory. Their expert guidance, patience and constant reminder of the human side of lab-based research, especially for a clinician like myself, kept me inspired and allowed me to complete these studies.

My heartfelt thanks, however, go to my wife Zareen, whose love and support goes beyond words in helping me through my research that, at times, felt too much to bear. Both she and my daughter, Parisa, have been an inspiration to me.

The other members of Pat and Bob's laboratory have been a pleasure to work with, and I thank Julia MacNally (Winterbottom), Greg Campbell, Kia Rezajooi, Matt Mason and Dave Hunt for their assistance, advice and friendship. Though many people helped from other labs, I would like to mention my gratitude towards Mark Turmaine for his expert technical assistance with electron microscopy, Prof. Maria Fitzgerald for her assistance with the functional studies, Dr. Linda Greensmith and Jim Dick for their assistance with silver cholinesterase experiments and Dr. Bill Stallcup for supplying the NG2 knockout mice and anti-NG2 antibody.

I thank members of the West Midlands Deanery and academic department of neurosurgery in the Queen Elizabeth University Hospital, Birmingham for letting me

take 3 years out of the neurosurgery training programme to complete these studies and then granting me the sabbatical that allowed me to write up this thesis. In particular, I would like to thank Prof. Garth Cruickshank and Mrs. Ros Mitchell for their faith in my abilities, advice and encouragement.

This research was funded by the Wellcome Trust, with a Lang Research Fellowship from the Royal College of Surgeons of England assisting in the final few months of experimental studies.

Finally, I would like to thank my parents for always allowing me to pursue my interests and encouraging me to work hard throughout life, and I praise the memory of my grandfather, Prof. Md. Ibrahim, who inspired me to become a doctor.

Publications

The following publications relate to work reported in this thesis; paper 1 relates to chapter 5, paper 2 to chapter 3 and paper 3 to chapter 6.

1. Hunt, D, **Hossain-Ibrahim, MK**, Mason, MR, Coffin, RS, Lieberman, AR, Winterbottom, J, and Anderson, PN (2004). ATF3 upregulation in glia during Wallerian degeneration: differential expression in peripheral nerves and CNS white matter. BMC Neurosci. 5: 9

2. **Hossain-Ibrahim, MK**, Rezajooi K, MacNally JK, Mason, MRJ, Lieberman, AR, and Anderson, PN (2006) Effects of lipopolysaccharide-induced inflammation on expression of growth-associated genes by corticospinal neurons. BMC Neurosci. 7: 8

3. **Hossain-Ibrahim, MK**, Rezajooi, K, Stallcup, WB, Lieberman, AR, Anderson PN (2007). Analysis of axonal regeneration in the central and peripheral nervous systems of the NG2-deficient mouse. BMC Neurosci. 8: 80

Table of Contents

Declaration 2

Abstract 3

Acknowledgements 5

Publications 7

Table of Contents 8

Index of Figures 18

Index of Tables 21

List of abbreviations used 22

1 Introduction 24

1.1 Peripheral nerve regeneration 25

1.1.1 Response in the distal stump 26

1.1.2 Peripheral nerve cell body response and conditioning lesions 29

1.2 Causes of failure of CNS regeneration 34

Intrinsic Factors: 35

1.2.1 Realising the regenerative potential of many CNS neurons with peripheral nerve grafts 35

1.2.2 Variation in the cell body response of CNS neurons to injury 36

1.2.3 Importance of growth-associated genes 38

1.2.4 Inflammation and the cell body response of CNS neurons 42

1.2.5 Role of microglia in axonal regeneration 43

1.2.6 LPS-induced cerebral inflammation 46

Extrinsic factors: 47

1.2.7 Response of non-neuronal cells to injury 48

1.2.8 The glial scar 48
1.2.9 Chondroitin sulphate proteoglycans and NG2 50
1.2.10 Semaphorins 57
1.2.11 Tenascins 60
1.2.12 Ephrins 62
1.2.13 Myelin and other inhibitory factors 64
1.2.13.1 Nogo 65
1.2.13.2 Oligodendrocyte myelin glycoprotein (OMgp) 66
1.2.13.3 Myelin-associated glycoprotein (MAG) 67
1.2.13.4 Nogo receptors and co-receptors 68
1.2.13.5 Role of Nogo-A in axonal regeneration 73
1.2.13.6 Summary 79
1.2.14 Lack of trophic support and a growth promoting substrate 80
1.2.14.1 Nerve growth factor 80
1.2.14.2 Brain Derived Neurotrophic Factor (BDNF) 82
1.2.14.3 Neurotrophin-3 85
1.2.14.4 Neurotrophin 4/5 (NT-4/5) 86
1.3 Summary of techniques used to assess spinal cord regeneration 88
1.4 Attempts to stimulate CNS regeneration 91
1.5 Experimental aims of the studies described in this thesis 101
1.5.1 Inflammation, growth associated protein expression and CST regeneration.. 101
1.5.2 ATF3 upregulation in glia during Wallerian degeneration in peripheral nerves and CNS white matter 105
1.5.3 Axonal regeneration in the NG2 deficient mouse 107
2 Chapter 2 – Methods 108

2.1 Effects of topical lipopolysaccharide-induced inflammation on expression of growth-associated proteins / genes by corticospinal neurons 110

2.1.1 Animals 110

2.1.2 Application of lipopolysaccharide 110

2.1.3 Retrograde tracing with Cholera Toxin B (CTB) or Fluorogold (FG) 111

2.1.4 Control Studies: Facial nerve injury 115

2.1.5 Perfusion and histological processing 115

2.1.6 Quantification of OX42-labelled microglia 120

2.2 Corticospinal tract injury and anterograde tracing with Biotinylated Dextran Amine (BDA) 120

2.2.1 Perfusion and histological processing 121

2.2.2 Quantification of anterogradely labelled corticospinal tract axons 122

2.3 Effects of LPS-induced inflammation on regeneration following lumbar dorsal root transection 126

2.3.1 Animals and surgery 126

2.3.2 Dorsal root injury 127

Controls for spared axons 129

2.3.3 Histological processing 129

2.4 Effects of LPS injections into motor cortex on expression of growth-associated proteins 132

2.4.1 Animals 132

2.4.2 Injection of LPS 132

2.4.3 Perfusion and histological processing 133

2.5 Effects of zymosan-induced inflammation on glial cells, Nogo-A and expression of growth-associated proteins by corticospinal neurons 134

2.5.1 Animals 134

2.5.2 Application of zymosan 134
2.5.3 Retrograde tracing with Fluorogold (FG) 135
2.5.4 Positive control: facial nerve injury 135
2.5.5 Perfusion and histological processing 135
2.6 Effects of zymosan on the regenerative response of the CST axons to a cervical lesion 139
2.6.1 Animals 139
2.6.2 Corticospinal tract injury and anterograde tracing with BDA with or without concomitant application of zymosan 139
2.6.3 Perfusion and histological processing 140
2.6.4 Quantification of anterogradely labelled corticospinal tract axons 141
2.6.5 Quantification of anterogradely-labelled CST axons giving branches across the midline 142
2.7 ATF3 expression in glia during Wallerian degeneration, in peripheral nerves and CNS white matter 143
2.7.1 Animal utilisation and surgical procedures 143
2.7.2 Sciatic nerve resection 143
2.7.3 Sciatic nerve cut and reanastamosis 144
2.7.4 Sciatic nerve transection or crush 144
2.7.5 Dorsal root transection 144
2.7.6 Antibodies and immunohistochemical techniques 145
2.7.7 Statistical analysis 146
2.8 Axonal regeneration in the NG2-deficient mouse 147
2.8.1 Animals 147
2.8.2 Phenotyping 147
2.8.3 CNS injury models 148

2.8.3.1 Dorsal column and sciatic nerve conditioning lesions 148
2.8.3.2 Dorsal root injury 150
2.8.3.3 Controls for spared axons 150
2.8.3.4 Corticospinal tract injury and labelling 150
2.8.4 PNS injury models; functional analysis 153
2.8.4.1 Sciatic nerve injury 153
2.8.4.2 Assessment of functional recovery after sciatic (and saphenous) nerve injury 153
2.8.4.3 Facial nerve injury and assessment of functional recovery 154
2.8.5 PNS injury models; anatomical studies 154
2.8.5.1 Retrograde labelling of DRG cells 154
2.8.5.2 Silver-cholinesterase histochemistry 156
2.8.5.3 PGP 9.5 immunohistochemistry 157
2.8.5.4 Electron Microscopy 157
2.8.5.5 Retrograde labelling of facial motor neurons 159
2.8.5.6 Statistical analysis 162
2.9 NG2 expression in injured sciatic nerve 162
2.10 NG2 expression in glabrous hindpaw skin 162
Chapter 3 - Results 166
3 LPS-induced inflammation, growth-associated protein / gene expression and axonal regeneration 167
Background 167
Results 167
3.1 LPS-induced inflammation and growth-associated protein / gene expression 167
3.1.1 Positive and negative control studies 167
3.1.2 Assessing LPS- induced inflammation in cortex 171

3.1.2.1 Microglial / Macrophage response 171
3.1.2.2 Astrocytic response 178
3.1.3 Expression of growth-associated proteins / genes by CST neurons 181
3.1.3.1 Unoperated and Sham operated control cortex 181
3.1.3.2 LPS-treated cortex 182
3.1.3.3 Effect of CST injury in cervical spinal cord on growth–associated protein / gene expression 188
3.2 LPS-induced inflammation and CST regeneration 196
Background 196
Results 196
3.2.1 CST sprouting 196
3.2.2 BDA placement 197
3.3 Effects of LPS-induced inflammation on regeneration following lumbar dorsal root transection 201
Background 201
Results 201
3.3.1 LPS-induced inflammation and dorsal root regeneration 201
3.4 Effects of LPS injections into motor cortex on expression of growth-associated genes 208
Background 208
Results 208
3.4.1 Effect of LPS injections into cortex on microglia 208
3.4.2 Effect of LPS injections into cortex on expression of growth-associated proteins 212
4 Chapter 4 - Results 219

4.1 Effects of zymosan-induced inflammation on glial cells, Nogo-A and expression of growth-associated genes by corticospinal neurons 220

Background 220

Results 220

4.1.1 Assessing zymosan-induced inflammation in motor cortex 220

4.1.1.1 Zymosan application 220

4.1.1.2 Control experiments 221

4.1.1.3 Localisation of CST neurons 221

4.1.2 Effects of zymosan-induced inflammation in motor cortex on glial cells and Nogo-A 222

4.1.2.1 OX42 immunohistochemistry 222

4.1.2.2 GFAP immunohistochemistry 226

4.1.2.3 NG2 immunohistochemistry 229

4.1.2.4 Nogo-A immunohistochemistry 233

4.1.3 Effects of zymosan-induced inflammation on expression of growth-associated proteins by corticospinal tract neurons 236

4.1.3.1 c-Jun 236

4.1.3.2 ATF3 236

4.1.3.3 SCG10 237

4.2 Effects of zymosan on CST regeneration 244

Background 244

Results 244

4.2.1 Effect of cortical zymosan on sprouting of CST axons at a cervical lesion site 244

4.2.2 Effect of cortical zymosan on branching of CST axons across the midline proximal to a cervical lesion 248

Chapter 5 – Results 252

5 ATF3 expression in glia during Wallerian degeneration in peripheral nerves and CNS white matter 253

Background 253

Results 254

5.1 ATF3 expression in peripheral glia 254

5.1.1 Sciatic nerve resection 254

5.1.2 Sciatic nerve transection and reanastomosis 258

5.1.3 Sciatic nerve injury in mice 261

5.1.4 Identity of ATF3+ cells 261

5.1.5 Controls 262

5.2 ATF3 expression in CNS glia 265

5.2.1 Dorsal root transection 265

Chapter 6 – Results 268

6.1 Axonal regeneration in the NG2 deficient mouse 269

Background 269

Results 269

6.1.1 Analysis of phenotype 269

6.1.2 NG2 in injured sciatic nerve 270

6.1.3 NG2 in skin of plantar hindpaw 270

6.2 CNS injury models 273

6.2.1 Dorsal column injury 273

6.2.2 Dorsal root injury 276

6.2.3 Corticospinal tract injury 276

6.3 Functional recovery after peripheral nerve injury 282

6.3.1 Sciatic nerve crush and transection 282

6.3.2 Facial nerve crush 283

6.4 Anatomical studies after peripheral nerve injury 288

6.4.1 Retrograde labelling of DRG cells 288

6.4.2 Reinnervation of denervated endplates in the soleus muscle 292

6.4.3 Sensory reinnervation of hindpaw glabrous skin 295

6.4.4 Axon counts in digital nerves after sciatic nerve crush 298

6.4.5 Axon counts in the tibial nerve after sciatic nerve crush 298

6.4.6 Facial motor nucleus neuron counts after facial nerve injury 302

7 Chapter 7 - Discussion 304

7.1 LPS-induced inflammation around corticospinal neuron cell bodies results in their expression of growth-associated proteins, but does not stimulate axonal regeneration 305

7.2 Local and systemic LPS-induced inflammation does not stimulate dorsal root regeneration 311

7.3 Effects of zymosan-induced inflammation on motor cortex 315

7.4 Effects of cortical zymosan application on regeneration of injured CST axons.... 321

7.5 ATF3 upregulation in glia during Wallerian degeneration: differential expression in peripheral nerves and CNS white matter 324

7.6 Axonal regeneration in the NG2 deficient mouse 329

7.6.1 NG2 as a facilitator of regeneration in peripheral nerves 331

7.6.2 Potential confounding factors 332

7.6.3 Other roles of NG2 334

7.7 Concluding remarks 336

7.7.1 Inflammation-induced expression of growth-associated proteins in motor cortex, and the effect on injured CST regeneration 336

7.7.2 Axonal Regeneration in the NG2 deficient mouse 338

Appendix 339

Bibliography 344

Index of Figures

Figure 1-1 Intracellular signalling mechanisms of glial inhibitors and GAP-43 77

Figure 2-1 Summary of design and procedures for LPS experiments. 113

Figure 2-2 Diagrammatic representation of dorsal root injury model. 128

Figure 2-3 Diagrammatic representation of dorsal column injury model..... 149

Figure 2-4 Diagrammatic representation of experiments retrogradely labelling DRG neurons with DiAsp after sciatic nerve crush..... 155

Figure 2-5 Diagrammatic representation of facial nerve injury experiments 161

Figure 3-1 Immunostaining of facial nucleus positive control tissue. 169

Figure 3-2 Microglial responses to LPS application..... 173

Figure 3-3 Microglial response around identified CST neuron after LPS application. 175

Figure 3-4 Astrocytic response to LPS application. 179

Figure 3-5 Expression of c-Jun after LPS application. 183

Figure 3-6 Expression of ATF3 after LPS application. 186

Figure 3-7 Expresssion of SCG10 after LPS application..... 189

Figure 3-8 Co-localisation of retrograde label and c-Jun or SCG10. 191

Figure 3-9 GAP-43 mRNA expression after LPS application. 193

Figure 3-10 Anterograde labelling of CST axons after spinal cord injury and LPS application. 198

Figure 3-11 Transganglionic labelling of axons after DR injury and LPS application on to DREZ. 204

Figure 3-12 Microglial / macrophage responses to DR injury and I-P LPS injection. 206

Figure 3-13 Expression of OX42 after intracortical LPS injection. 210

Figure 3-14 Expression of c-Jun after intracortical LPS injection. 213

Figure 3-15 Expression of ATF3 after intracortical LPS injection. 215

Figure 3-16 Expression of SCG10 after intracortical LPS injection 217

Figure 4-1 Microglial / macrophage response to zymosan application. 224

Figure 4-2 Astrocytic response to zymosan application. 227

Figure 4-3 NG2-cell response to zymosan application. 231

Figure 4-4 Response of Nogo-A to zymosan application. 234

Figure 4-5 Expression of c-Jun after zymosan application. 238

Figure 4-6 Expression of ATF3 after zymosan application. 240

Figure 4-7 Expression of SCG10 after zymosan application. 242

Figure 4-8 Anterograde labelling of CST axons after spinal cord injury and zymosan application. 246

Figure 4-9 Histograms comparing sprouting of BDA-labelled CST axons 21 days after cervical injury. 250

Figure 5-1 Sciatic nerve resection 256

Figure 5-2 Counts of ATF3+ nuclei in proximal and distal nerve stumps 259

Figure 5-3 ATF3 in distal nerve stumps 263

Figure 5-4 Localisation of ATF3 in distal stumps and CNS. 266

Figure 6-1 Phenotyping of tailsnips and NG2 expression in injured sciatic nerve and hindpaw 271

Figure 6-2 Transganglionic labelling with CT-HRP of dorsal column axons after spinal cord injury. 274

Figure 6-3 Transganglionic labelling with CT-HRP of dorsal roots after transection and conditioning lesion. 278

Figure 6-4 Anterograde labelling with BDA of the CST after spinal cord injury. 280

Figure 6-5 Functional recovery after sciatic nerve injury. 284

Figure 6-6 Anatomical and functional correlates of regeneration after facial nerve injury 286

Figure 6-7 Retrograde labelling of DRGs after sciatic nerve injury 290

Figure 6-8 Silver-cholinesterase stained motor end plates after sciatic nerve injury. . 293

Figure 6-9 PGP 9.5 immunohistochemistry for axons in plantar hindpaw skin after sciatic nerve injury 296

Figure 6-10 Electron microscopy of regenerating axons in the digital & tibial nerves300

Figure A-1 Course of descending corticospinal axons 340

Figure A-2 Expression of c-Jun and variable tissue damage after zymosan application to cortex 342

Index of Tables

Table 2-1 Animal utilisation for experiments on the effect of cortical LPS on expression of growth-associated proteins / genes. 125

Table 2-2 Experimental procedures for studies of LPS and regeneration after dorsal root transection 131

Table 2-3 Animal utilisation for studies of the effects of zymosan on motor cortex .. 138

Table 2-4 Utilisation of NG2 knockout mice 164

Table 3-1 Number and morphology of cortical layer V microglia after sham-operation or LPS application 177

Table 3-2 Expression of cortical growth-associated proteins / genes in unoperated,.. 195

Table 3-3 Quantification of CST axons - LPS experiments 200

Table 4-1 Quantification of CST axons - zymosan experiments 249

List of abbreviations used

ABC	Avidin Biotin Complex
AP	Area postrema
ATF	Activating transcription factor
BDA	Biotinylated Dextran Amine
BDMA	Benzyldimethylamine
BDNF	Brain derived neurotrophic factor
BSA	Bovine serum albumin
C4	4th cervical vertebral level
C6	6th cervical vertebral level
cAMP	Cyclic adenosine mono phosphate
ChABC	Chondroitinase ABC
CNS	Central nervous system
CNTF	Ciliary neurotrophic factor
CR3	Complement receptor type 3
CREB	cAMP response element-binding
CSF	Cerebrospinal fluid
CSPG	chondroitin sulphate proteoglycan
CST	Corticospinal tract
CTB	Cholera toxin-subunit B
CT-HRP	Cholera toxin-subunit B horseradish peroxidase conjugate
DAB	3-3' diaminobenzidine tetrahydrochloride
DABCO	1,4-diazabicyclo[2,2,2] octane
Db-cAMP	Dibutyrl cAMP
DCN	Dorsal column nuclei
DDSA	Dodecenyl succinic anhydrite
DLCST	Dorsolateral corticospinal tract
DNA	Deoxyribonucleic acid
dpo	Days post operation
DREZ	Dorsal root entry zone
DRG	Dorsal root ganglion
E	Embryonic day
ECM	Extracellular matrix
EDTA	Epidermal growth factor receptor
EM	Electron microscopy
Eph	Ephrin
FG	Fluorogold
FITC	Fluoroscein isothiocyanate

GAGs	Glycosaminoglycans
GFAP	Glial fibrillary acidic protein
GPI	Glycosyl-phosphatidylinositol
HCl	Hydrochloric acid
HRP	Horseradish peroxidase
HSP27	Heat shock protein 27
ICH	Immunohistochemistry
IL	Interleukin
ISH	In situ hybridisation
JNK	Jun N-terminal kinase
KO	Knockout
LPS	Lipopolysaccharide
MAG	Myelin associated glycoprotein
Na Cl	Sodium chloride
N-CAM	Neural cell adhesion molecule
NGF	Nerve growth factor
NgR	Nogo-66 receptor
NGS	Normal goat serum
NP	Neuropilin
n.s.	Not-significant
NT	Neurotrophin
OEC	Olfactory ensheathing cells
OMgp	Oligodendrocyte myelin glycoprotein
OPC	Oligodendrocyte precursor/progenitor cell
P	Postnatal day
PB	Phosphate buffer
PBS	Phosphate buffered saline
PFA	Paraformaldehyde
PGP	Protein gene product
PNS	Peripheral nervous system
RGC	Retinal ganglion cell
SCIP	suppressed cAMP-inducible POU protein
SD	Standard deviation
SNpc	Substantia nigra pars compacta
SSC	Standard saline citrate
STAT3	Signal tansducer and activator of transcription-3
TLR	Toll-like receptor
TBS	Tris-buffered saline
TBST	TBS+Triton X-100 (0.5%)
TNT	TBS + Tween 20 (0.05%)
WT	Wild-type

1 Introduction

Axons regenerate in the peripheral nervous system (PNS) and central nervous system (CNS) of lower vertebrates (Singer et al., 1979), but the CNS is incapable of regenerating with any degree of functional significance in adult higher vertebrates. As early as 2640 B.C., medical literature has documented a patient with spinal cord injuries as "One having a dislocation in a vertebra of his neck, while he is unconscious of his two legs and his two arms, and his urine dribbles. An ailment not to be treated." (Edwin Smith Papyrus, ca. 1700 B.C.; translated into English by James H. Breasted, 1930). Even today, the consequences of this in every day life are clear to see, with spinal cord injury having devastating effects on the lives of the (typically young) victims and their family (McDonald and Sadowsky, 2002). Whereas lesions in the CNS result, at the most, in abortive sprouting of axons proximal to the injury site (Ramón y Cajal, 1928, reprinted 1991), injured axons in peripheral nerves are attracted to the nerve stump distal to the lesion (Anderson and Turmaine, 1986; Abernethy et al., 1992), through which they regenerate, often resulting in functional recovery. However, even in the PNS, aberrant target reinnervation is a common problem, causing neuropathic pain and incomplete motor recovery (see Ruijs et al., 2005).

The first experiments to suggest that the innate difference between the regenerative ability of the PNS and CNS could be altered were performed by Tello (1911). He implanted a peripheral nerve graft in to the CNS and demonstrated invasion of the graft by axons, presumably from the CNS. However, the origin of the regenerating axons could not be proved until the discovery of anterograde and retrograde tracers.

After Richardson et al. (1980) used horseradish peroxidase to conclusively show that CNS axons had regenerated into peripheral nerve grafts implanted into spinal cord - and later in brain (David and Aguayo, 1981; Benfey and Aguayo, 1982), it was clear that, given the right environment, CNS axons could regenerate. In the 25 years since those landmark experiments, two main theories aim to explain the lack of CNS regeneration in adult mammals:

1. Lack of an intrinsic CNS cell body response adequate enough to support axonal regeneration;
2. The inhibitory environment of CNS tissue that does not support axonal regeneration.

In order to understand the axonal response to CNS injury, it is prudent to study the events that result in successful regeneration of injured PNS axons, with the aim of translating as many of these mechanisms as possible to the CNS and thereby stimulate axonal regeneration (reviewed by Chen et al. (2007)).

1.1 Peripheral nerve regeneration

Axons injured in the PNS successfully regenerate due to two main factors:

1. the massive response at the lesion site and distal stump of an injured peripheral nerve that results in a milieu conducive to axon growth and target reinnervation;
2. neurons with axons in peripheral nerves show a very strong response to axotomy, upregulating genes and proteins necessary for regeneration.

1.1.1 Response in the distal stump

After peripheral nerve injury, whether chemical or mechanical, the axon distal to the lesion undergoes Wallerian degeneration (Waller, 1850), a histological description of the progressive destruction of the axonal cytoskeleton and myelin sheaths. Subsequent experiments have shown that Schwann cells in the distal stump endocytose axonal debris and the myelin sheath and then transfer the remaining debris to macrophages (Beuche and Friede, 1985; Fernandez Valle et al., 1995), which clear the route for axons by removing the vast majority of myelin debris (Stoll et al., 1989;Perry et al., 1995). The Schwann cells de-differentiate, proliferate and extend processes within the basal lamina tubes that used to surround the former distal nerve fibres to form bands of Büngner (Salzer et al/, 1980). These not only act as an anatomical guiding structure, but also a chemical guide through their expression of neurotrophic molecules, both surface bound and diffusible (Nathan, 1987; Hikawa and Takenaka., 1996; see Stoll et al., (2002) and Makwana and Raivich, (2005) for review. The proliferating Schwann cells also fill the gap produced by axotomy, by migrating from proximal and distal stumps, to form a continuous substrate for regeneration to occur (Ramón y Cajal 1928). They rapidly produce interleukin-1 (IL1), which stimulates NGF release from Schwann cells (Lindholm et al., 1987), IL6 and TNFα (also produced by macrophages) and other cytokines. Although the exact role of the cytokine cascade is not known, it is likely to stimulate not only inflammatory-cell mediated myelin clearance, but also the injured cell body response. Cell body responses and survival or regenerative responses of dorsal root ganglia (DRG) neurons to axotomy are suppressed in mice with null mutation of the gene for either leukaemia inhibitory factor (LIF) (Corness et al., 1996; Sun and Zigmond, 1996; Cafferty et al., 2001) or IL-6 (Murphy et al., 1999; Cafferty et al., 2004), but see (Cao et al., 2006). However, macrophages are not essential, as complete

removal of myelin from some Schwann cells can occur without their recruitment (achieved by prior whole animal irradiation), but macrophages accelerate the removal of myelin in the later stages of Wallerian degeneration (Perry et al., 1995b). It has also been suggested that macrophages mediate the transformation of the distal nerve environment into one that supports stable neurites (Luk et al., 2003).

Successful target reinnervation is guided by appropriate guidance molecule / receptor binding. For example, the L2/HNK-1 epitope, which mediates binding of neural cells to laminin (Hall et al., 1993) is more strongly expressed on Schwann cells previously associated with motor axons, and regenerating motor axons are more attracted to it and cause it to be much more upregulated after injury to a peripheral nerve than sensory neurons (Martini, 1994). Pathway specificity is also gained by pruning off those collaterals which have grown into the inappropriate nerve branch (Brushart, 1993). 'Motor' Schwann cells also express different trophic factors than sensory ones (Brushart et al., 1995; Hoke, 2006) and this may account for preferential motor (and sensory) regeneration.

Schwann cells upregulate pleiotrophin during Wallerian degeneration (Blondet et al., 2005), nerve growth factor (NGF; Heumann et al., 1987), brain derived neurotrophic factor (BDNF; Meyer et al., 1992), glial-cell line derived nerve factor (GDNF; Hammarberg et al., 1996; Hoke et al., 2003) and neurotrophin-4 (NT-4), but not NT-3 (Funakoshi et al., 1993), vascular endothelial growth factor (VEGF; Samii et al., 1999) and insulin-like growth factor-1 (IGF-1; Pu et al., 1995), which interestingly is predominantly expressed by macrophages 7 days after injury (Cheng et al., 1996b). Although NGF is essential for embryonic neuron development (Greene and Shooter,

1980) and is thought to enhance neuronal regeneration (Lindsay, 1988), experiments with antibodies blocking the action of NGF suggest that it is not vital for regeneration (Diamond et al., 1992). However, one study suggests that BDNF is important for regeneration (Boyd and Gordon; 2003). Even the loss of one copy of the trkB gene (that encodes for the BDNF receptor) impairs motor axon regeneration and mice deficient in its other receptor, p75, have decreased motorneuron survival after injury (Boyd and Gordon, 2001). Interestingly, ciliary neurotrophic factor (CNTF) mRNA and protein is downregulated in neurons following sciatic nerve crush (Rabinovsky et al., 1992), which is unexpected, as CNTF has been shown to protect newborn motorneurons from cell death after injury (Sendtner et al., 1990). A separate study also demonstrated a decrease in neuronal CNTF mRNA after sciatic nerve injury, but the downregulation in Schwann cells after loss of axonal contact was followed by re-expression with ensuing regeneration, and extracellular CNTF protein levels rose to above normal levels (Sendtner et al., 1992). The initial downregulation of CNTF by Schwann cells after peripheral nerve injury, means that it is unlikely to have a neurotrophic function, but it may play a role in signalling. The nuclear transcription factor signal transducer and activator of transcription-3 (STAT3), is the downstream target of activated CNTF receptor. STAT3 activates the transcription of many genes (Akira., 1999). If STAT3 is conditionally knocked out of neurons, post-traumatic cell death is increased, suggesting that STAT3 has a neurotrophic role (Schweizer et al., 2002). Knocking out CNTF delays phosphorylated STAT3 expression in neuronal cell bodies suggesting that, ultimately, CNTF has a neurotrophic role via STAT3 signalling (Makwana and Raivich, 2005).

Schwann cells synthesise surface-bound cell adhesion molecules, such as N-CAM, L1, CHL1 (a close homologue of L1) and N-cadherin, which are found at points of contact

with axons and are preferred substrates for axonal growth (Nieke and Schachner, 1985; Rutishauser et al., 1985; Rathjen, 1988; Shibuya et al., 1995). Schwann cell N-CAM and L1 bind homophilically to similar molecules on the surface of growth cones (Martini and Schachner, 1988). However, *in vitro* studies have shown that the form of L1 on Schwann cells is not able to directly interact with L1 on growth cones (de Angelis et al., 2001; Jacob et al., 2002), suggesting that there are other heterophilic ligands on Schwann cells to which neuronal L1 binds, which then regulates correct sorting and ensheathment of axons (Itoh et al., 2005). Schwann cells also upregulate laminin and tenascin-C on their basal laminae, which are both thought to guide successful regeneration (Salonen et al., 1987; Martini et al., 1990, Luckenbill-Edds, 1997; Chen et al., 2005). Absence of the laminin gamma 1 gene, which codes for laminin-2 protein in peripheral Schwann cells, causes a significant decrease in the number of axons crossing into the distal portion of crushed sciatic nerve for up to 30 days (Chen and Strickland, 2003). One of the receptors for laminin is the alpha7 beta1 integrin, which is upregulated by neurons after PNS injury (which successfully regenerate), but not in injured CNS neurons (which do not regenerate). In the same study, genetic deletion of the alpha7 subunit integrin gene resulted in approximately 40% reduction in the speed of motor axon regeneration following facial axotomy and a significant delay in target reinnervation (Werner et al., 2000).

1.1.2 Peripheral nerve cell body response and conditioning lesions

Axotomy of peripheral nerves elicits morphological and cytological changes in the appearance of their cell bodies (Lieberman, 1971). Subsequently, it was shown that

these changes reflect the changes in proteins being produced after peripheral nerve injury (McQuarrie, 1978; Skene and Willard, 1981). It is now thought that the strong cell body response of neurons with axons in peripheral nerves promotes neuronal survival and vigorous axonal regeneration. Gene array analysis has shown that over 200 genes are upregulated or downregulated in sensory and sympathetic ganglia after axotomy, but only just over 20 genes have altered expression in neurons (Costigan et al., 2002). Changes include increased production of the transcription factors c-Jun (Jenkins and Hunt, 1991) and ATF3 (Tsujino et al., 2000), with downregulation of ATF2 after axotomy (Herdegen et al., 1997; Martin-Villalba et al., 1998), but the downstream genes that they control are still unknown. Growth cone molecules such as GAP-43 and CAP-23 (which control actin dynamics; (Frey et al., 2000; Laux et al., 2000) and SCG10 (which controls tubulin dynamics; (Riederer et al., 1997)) are upregulated (van der Zee et al., 1989; Woolf et al., 1990; Chong et al., 1992; Mason et al., 2002). The importance of the growth-associated genes c-Jun, ATF3, GAP-43 and SC10 to axonal regeneration are discussed in Section 1.2.3.

Cytoskeletal changes after peripheral nerve injury include upregulation of tubulins (Hoffman et al., 1988; Miller et al., 1989) and downregulation of neurofilaments (Hoffamn et al., 1987; Tetzlaff et al., 1988); note that neurofilaments maintain axon diameter, rather than longitudinalgrowth. Cell adhesion molecules including L1, CHL1 are upregulated in many types of neurons (Zhang et al., 2000; Kiryushko et al., 2004). However, it is still uncertain which, if any, of these molecules is necessary for regeneration: mice deficient in NCAM and L1 still regenerate axons (Franz et al., 2005; Jakeman et al., 2006) and GAP-43 and CAP-23 knockout mice do not live long enough for regeneration experiments (personal communication, P.Anderson). The studies that have been performed on GAP-43 knockout mice (Strittmatter et al., 1995) and studies

with mice that overexpress GAP-43 (Aigner et al., 1995) both suggest roles in axonal pathfinding.

Growth-promoting factors continue to be discovered, such as oxidised galectin-1, which is upregulated by neurons after facial nerve injury; galectin-1 knockout mice have a reduced rate of functional recovery after facial crush injury (McGraw et al., 2004). Oxidised galectin-1 is upregulated by axons and Schwann cells after sciatic nerve injury (Horie et al., 1999) and, though its exact mechanism of action is still unclear, it has been shown to stimulate neuronal regeneration by promoting macrophages to release growth-promoting factors (Horie et al., 2004).

Around the cell bodies of axotomised sensory and autonomic neurons, macrophages accumulate, with accumulation of microglia around perikarya of motor neurons in CNS tissue (Lu and Richardson, 1993; Hu and McLachlan, 2002). They are thought to produce molecules that aid injured motorneuron survival (Raivich, 2002), but are not essential for regeneration. For example, following a crush injury to the sciatic nerve, C57/BL/Ola mice (which undergo extremely slow Wallerian degeneration) motorneuron axons regenerate into soleus muscle at a similar rate to normal mice, despite the presence of many intact axons and a paucity of macrophages (Lunn et al., 1989). However, sensory regeneration in these mice is delayed (Brown et al., 1991). There is evidence that motorneurons are intrinsically able to regenerate more vigorously than sensory neurons after injury (Fawcett and Keynes, 1990) but it is not possible to tell whether it was the lack of Wallerian degeneration or the lack of macrophages that led to poor sensory regeneration in the C57/BL/Ola mice. Gene deletion of IL-6 reduces inflammatory changes around axotomised facial motorneurons, which results in a

moderate decrease in the rate of axonal regeneration (Klein et al., 1997). However, mice lacking macrophage colony stimulating factor, which markedly reduces microglial proliferation as well as early lymphocyte recruitment, does not affect the speed of axonal regeneration (Raivich and Kreutzberg, 1994; Kalla et al., 2001). Similarly, continuous infusion of cytosine-arabinoside, which selectively inhibits microglial cell proliferation following peripheral nerve injury, made no difference to hypoglossal nerve axonal regeneration and target reinnervation after injury (Svensson and Aldskogius, 1993).

Regeneration of axons in the PNS is also dependent on:

1. age of the animal;
2. distance of the axotomy site from the cell body;
3. whether a conditioning lesion has been performed.

Rat motorneurons are most sensitive to injury in the first two weeks after birth (Schmalbruch, 1987). After sciatic nerve transection and surgical repair, 6 day old rats have significantly lower numbers than adult rats of motorneurons surviving up to 14 months later (Watanabe et al., 1998). There then appears to be a period of stability followed by a decline in axonal regenerative potential. Studies have shown that aged rats have a slower rate and degree of recovery after peripheral nerve injury (Verdú et al., 1995), with slower regeneration (Black and Lasek, 1979; Navarro et al., 1988) that involved fewer axons (Tanaka and Webster, 1991; Vaughan, 1992) than young animals. Peripheral nerves axotomised close to the neuronal cell body elicit a greater regenerative response than those injured distally (Lieberman, 1971), presumably because the lesioning stimulus is greater and there is a shorter distance required for

regeneration-associated molecules to travel from the cell body. These findings suggest that the cell body response is important to regeneration. However, the greater lesioning stimulus of proximal axotomy also results in more cell death. Fewer DRG neurons survive a proximal axotomy of sciatic nerve compared to a distal one (Ygge, 1989), but there is no such difference in injured hypoglossal nerve (Törnqvist and Aldskogious, 1994).

The best evidence for the importance of the neuronal cell body response to axotomy comes from experiments with DRG neurons, as they have a stem process that branches both into the PNS (sciatic nerve) and into the CNS (dorsal roots become the dorsal column). Injuring dorsal roots results in regenerating fibres stopping at the border with the CNS, known as the dorsal root entry zone (DREZ) (Carlstedt et al., 1988). Dorsal root injury also results in a smaller cell body response than injuring sciatic nerves: c-Jun is more transiently upregulated, with almost no increase in GAP-43 (Schreyer and Skene, 1993; Jenkins et al., 1993a; Chong et al., 1994; Broude et al., 1997); neurofilament is also less downregulated (Oblinger and Lasek, 1988; Greenberg and Lasek, 1988). As a consequence, central axotomy results in poor regeneration. However, this poor regenerative effort can be overcome with a concomitant injury of the peripheral branch (a 'conditioning lesion') of the same nerve. This was first shown by Richardson and Verge (1987) who demonstrated a four-fold increase in the rate of dorsal root regeneration following dorsal root crush. When injuring the same nerve in the CNS – i.e. transecting the dorsal columns – there is minimal sprouting and no regeneration across the lesion. However, a small proportion of these transected primary sensory axons will regenerate into a peripheral nerve graft inserted into the spinal cord. If the peripheral processes of these neurons is subjected to a conditioning lesion, the numbers of axons invading the graft increased by up to a factor of one hundred,

maximal when performed a week prior to cord lesioning (Richardson and Issa, 1984; Oudega et al., 1994). Later it was shown that axons transected in the dorsal column without a growth-promoting peripheral nerve graft can be stimulated to sprout much more into the lesion, through grey matter around the lesion and even regenerate across the lesion, if a conditioning lesion is performed as well (Neumann and Woolf, 1999; Bavetta et al., 1999). Thus, the growth-inhibitory environment of the CNS can be overcome by a vigorous enough cell body response. However, the response of intrinsic CNS neurons to axotomy varies considerably. This and the other factors contributing to the lack of regeneration in the CNS will be discussed in the next section.

1.2 Causes of failure of CNS regeneration

The causes of the failure of CNS neurons to regenerate their axons after injury can be divided into two groups. Intrinsic factors are those that are related to the response of the axotomised CNS neuron and mechanisms that may alter this regenerative response, notably expression of growth-associated genes/proteins; extrinsic factors are those that are related to inhibitory molecules, physical barriers, lack of neurotrophic support and response to injury of non-neuronal cells in the CNS environment that injured axons are attempting to regenerate through. Certainly both sets of factors need to be overcome for successful CNS regeneration to occur, and there are probably interactions between the two. These intrinsic and extrinsic factors are described in more detail below.

Intrinsic Factors:

1.2.1 Realising the regenerative potential of many CNS neurons with peripheral nerve grafts

It has been shown that many CNS neurons can regenerate axons if provided with an environment conducive to growth. For example some CNS axons regenerate readily into peripheral nerve grafts inserted into the brain or spinal cord or attached to severed optic nerves (Richardson et al., 1980; Berry et al., 1986) – the latter experiment unequivocally showed that regenerated axons originated from axotomised CNS neurons, and not from collateral sprouting of uninjured neurons. Regeneration relies on living cells in these grafts, presumed to be Schwann cells, as regrowth of axons fails if grafts are cleared of living cells by repeated freeze-thawing prior to implantation (Berry et al., 1988). Placing a graft in the vitreous humour stimulates retinal ganglion cell (RGC) regeneration across an optic nerve transection (Berry et al., 1996), suggesting that growth-promoting factors are released from peripheral nerve grafts. However, not all classes of CNS neuron regenerate into peripheral nerve grafts. This has been shown by experiments in which grafts have been placed into the thalamus, striatum and cerebellum, resulting in significant regeneration of neurons from the thalamic reticular nucleus, substantia nigra pars compacta (SNpc), globus pallidus and deep cerebellar nuclei, but not of thalamic projection, striatal projection or Purkinje neurons (Dooley and Aguayo, 1982; Benfey et al., 1985; Morrow et al., 1993; Woolhead et al., 1998; Chaisuksunt et al., 2000).

Variation in regenerative abilities of neurons is also seen in the spinal cord. For example, rubrospinal axons show a high propensity to regenerate into peripheral nerve grafts placed in the low cervical cord (Richardson et al., 1982b; Ye and Houle, 1997; Blits et al., 2000), though one study demonstrated CST regeneration through intercostals nerve grafts (Cheng et al., 1996a). The variation in CNS neurons' innate ability to regenerate is in part due to the strength of their cell body response (see section 1.2.2), their differing sensitivity to neurotrophic factors (see section 1.2.14) and expression of receptors for inhibitory molecules (Hunt et al., 2002b).

1.2.2 Variation in the cell body response of CNS neurons to injury

A 'conditioning lesion' of the peripheral process of DRG axons alters the expression of many genes in the DRG cell bodies that are associated with regeneration (Schreyer and Skene, 1993; Lu and Richardson, 1995; Chong et al., 1996; Broude et al., 1997) and can improve the regenerative ability of their axons within the CNS (Richardson and Riopelle, 1984; Neumann and Woolf, 1999; Bavetta et al., 1999). It appears that the regenerative ability of different classes of CNS neurons is correlated with their ability to express these growth-associated genes and proteins – e.g. c-Jun (Jenkins and Hunt, 1991; Vaudano et al., 1993; Jenkins et al., 1993a), SCG10 and CAP-23 (Mason et al., 2002), ATF3 (Takeda et al., 2000; Tsujino et al., 2000; Campbell G. et al., 2004) and GAP-43 (Reh et al., 1987; Skene, 1989; Campbell et al., 1991; Vaudano et al., 1995). GAP-43, cJun, L1 and CHL1 are upregulated after peripheral nerve graft implantation into the cerebellum by deep cerebellar nuclei (which successfully regenerate into the graft), in contrast to a modest upregulation of c-Jun only in (non-regenerating) Purkinje

cells– but only after axotomy close to Purkinje cell bodies (see Anderson et al., 1998; Anderson and Lieberman, 1999).

This leads us to the finding that in the CNS, as seen in the PNS, proximal axotomy elicits a greater regenerative response than distal axotomy (Lieberman, 1971), but at the expense of a greater proportion of neurons undergoing cell death. This is seen with intraorbital vs. intracranial RGC axotomy (Misantone et al., 1984; Aguayo, 1985; Sievers et al., 1987; Sievers et al., 1989), in L1 vs. C5 dorsal column lesions (Loewy and Schader, 1977) and septal cholinergic neuron lesions (Sofroniew and Isacson, 1988). The reasons are unclear, but it is of interest that the both c-Jun and ATF-3, which are upregulated after, and associated with neuronal regeneration are both associated also with cell death (Ham et al., 1995; Herdegen et al., 1997b; Hai et al., 1999; Mashima et al., 2001; Hartman et al., 2004).

The decreasing regenerative response with greater distance of the lesion from the cell body is seen with peripheral nerve graft insertion into the spinal cord at different levels, which results in more regeneration into grafts by local neurons (Richardson et al., 1984). Grafts apposed to a severed optic nerve result in greater RGC regeneration if placed 2mm from the retina than when placed 7mm away (Richardson et al., 1982a; Berry et al., 1986). Correlating with this is a greater expression of growth-associated genes and downregulation of neurofilament mRNAs with a cervical injury to rubrospinal axons compared to a thoracic injury (Tetzlaff et al., 1991; Jenkins et al., 1993b; Fernandes et al., 1999), and with proximal axotomy of RGCs compared to distal axotomy (Doster et al., 1991; Hull and Bahr, 1994). Even CST neurons, which fail to

upregulate growth-associated genes after spinal injury, are made capable of doing so following intracortical injury (Tetzlaff et al., 1994; Mason et al., 2003).

1.2.3 Importance of growth-associated genes

c-Jun

The transcription factor c-Jun is expressed by many different cell-types, and can dimerise either with itself to form homodimers or with other proteins such as JunB, JunD, c-Fos or CREB/ATF family members, amongst others, to form heterodimers. Its activity is regulated through the phosphorylation of two serine residues within the amino terminal of the protein by the c-Jun N-terminal kinase (JNK). Its widespread expression in brain decreases posnatally to the basal levels seen in adult CNS and PNS (Herdegen et al., 1991; De Leon et al., 1995). It has been implicated in both neuronal cell death and survival after injury (Jenkins and Hunt, 1991; Estus et al., 1994; Behrens et al., 1999) and is consistently upregulated after axotomy in regenerating neurons (Herdegen et al., 1997b; Vaudano et al., 1998; Raivich et al., 2004), with levels falling in neurons following successful regeneration, and elevated levels falling in Schwann cells when they remyelinate axons. There is a correlation between the ability of CNS neurons to upregulate c-Jun and regeneration up peripheral nerve grafts, with the exception of SNpc neurons, which show modest c-Jun upregulation despite growing axons up grafts (Chaisuksunt et al., 2003). The functional importance of c-Jun has been shown in mice lacking neuronal c-Jun. These mice have decreased expression of growth-associated molecules, with reduced axonal regeneration and less cell death after axotomy (Raivich et al., 2004); see (Raivich and Behrens, 2006) for review.

ATF3

ATF3 is also a transcription factor that is induced in many cell types by a range of stresses, its induction being correlated with cellular injury. It is thought to be a key regulator of cell stress responses (Hai and Hartman, 2001). ATF3 has been shown to prevent cell death and be a neurite growth-promoting factor in cultured neurons, apparently acting through HSP27 (Nakagomi et al., 2003) and is expressed after axotomy (Takeda et al., 2000; Tsujino et al., 2000). Contrary to Tsujino's (2000) claims that it is neuron specific, it now appears that ATF3 is expressed in the glial cells through which neurons regenerate following sciatic nerve injury (Hunt et al., 2004; see chapter 5). It is also co-expressed with c-Jun in the CNS neurons capable of regenerating through peripheral nerve grafts (Campbell et al., 2005). Co-localisation studies indicate that ATF3 and c-jun mRNA are co-expressed in several types of neuron after injury. Transfecting ATF3 alone into two neuron-like cell lines did not cause neurite outgrowth; c-Jun expression alone caused some outgrowth, but co-expression of both ATF3 and c-Jun greatly increased neurite outgrowth (Pearson et al., 2003), highlighting their synergistic growth-promoting roles.

Gap-43

GAP-43 is a 43kDa growth-associated protein noted to be important in neurite outgrowth (Skene and Willard, 1981). It is found at the growth cone during neurite extension, where it is membrane-bound and contacts axon guidance molecules, resulting in signal transduction, which culminate in cytoskeletal rearrangements. Strongly expressed by neurons during development and regeneration, levels diminish upon target (re-)innervation (see review by Benowitz, and Routtenberg, (1997)). It is also detected in presynaptic nerve terminals, remaining present at low levels throughout adulthood in

classes of neuron thought to be particularly plastic, implying multifunctional roles. Interestingly, the promoter sequence for the gap-43 gene contains an AP-1 binding site (Weber and Skene, 1998), suggesting that c-Jun plays a role in the high-level of gap-43 mRNA detected in many injured neurons, perhaps in conjunction with ATF3. GAP-43 is upregulated in the successfully regenerating axons of the peripheral nervous system, and in DRG neurons given a conditioning lesion that stimulates regeneration in CNS tissue (see section 1.1.2). Like c-Jun and ATF3, GAP-43 expression is positively correlated with intrinsic CNS neuronal ability to regenerate through peripheral nerve grafts (see Anderson et al., 1998).

SCG10

SCG10 is a member of the stathmin family of ubiquitous cytosolic proteins. It is believed to be neuron specific and expressed during development of the PNS and CNS Anderson and Axel, 1985; it has a high level of co-expression with GAP-43 in the embryonic rat brain (Sugiura and Mori, 1995). Although tightly bound to the Golgi apparatus (Lutjens et al., 2000; Charbaut et al., 2005), it is present in axons and some dendrites and accumulates in growth cones (Stein et al., 1988). Here, its membrane attachment uses the same covalent attachment mechanism as GAP-43 (Skene and Virag, 1989), the prevention of which abolished growth-cone targeting (Lutjens et al., 2000). SCG10 promotes disassembly of microtubules and counteracts microtubule assembly (Riederer et al., 1997), producing instability in the growth cone that is necessary for both forward motion and turning (Letourneau and Ressler, 1984; Bamburg et al., 1986; Williamson et al., 1996; Challacombe et al., 1997). Overexpression of SCG10 in PC12 cell lines increased frequency and speed of neurite outgrowth (but only in the presence of NGF (Riederer et al., 1997)), suggesting a role in neurotrophically-guided neurite outgrowth. Its high expression in adult hippocampus and cerebellar cortex suggests a

predeliction for long axons or ones with extensive dendritic arbours, prompting Himi et al., (1994) to believe it may play a role in synaptic plasticity, as suggested for GAP-43.

It has been hypothesised that GAP-43 and SCG10 are important for axonal elongation, through their role in cytoskeletal dynamics (Benowitz and Routtenberg, 1997; Riederer et al., 1997; Caroni, 1997). Motor and DRG neurons upregulate these molecules soon after axotomy. Expression decreases markedly following target reinnervation, but remains high if reinnervation is prevented by cut and ligation experiments, suggesting that contact with target tissues regulates expression of these molecules (Mason et al., 2002). Together with its location and role in microtubule reorganisation, these findings make SCG10 a suitable candidate for a regeneration-associated protein.

The *in vivo* effects of ATF3, GAP-43 and SCG10 expression individually on axonal regeneration are difficult to assess. It is not clear whether ATF3 knockout mice (Hartman et al., 2004) completely lack the protein in neurons but in any case, no axonal regeneration experiments on such animals have been reported, although it is noted that they appear grossly normal and are viable. GAP-43 deficient mice show neuroanatomical abnormalities but their CNS has been described as grossly normal with no interference in nerve growth rates (Strittmatter et al., 1995); hence GAP-43 is unlikely to be essential for axonal growth but probably is required for successful axonal pathfinding. No SCG10 knockout animals have been described.

Certainly, no single growth-associated molecule is able to drive regeneration on its own. Transgenic overexpression of individual growth-associated molecules has induced some sprouting (Buffo et al., 1997), but has not turned non-regenerating neurons into regeneration-competent cells, even when presented with favourable environments such

as implanted sections of peripheral nerve or Schwann cells (Mason et al., 2000; Rossi et al., 2001). However, overexpression of GAP-43 and CAP23 together, greatly enhanced the ability of ascending dorsal column axons to regenerate into peripheral nerve grafts placed in the spinal cord without a conditioning peripheral lesion (Bomze et al., 2001). Even growth-refractory Purkinje cells can be made to increase axonal outgrowth into predegenerated (but not fresh) peripheral nerve grafts by overexpressing GAP-43 and L1 in transgenic mice (Zhang et al., 2005). This regeneration can be improved further by transducing graft Schwann cells to produce polysialic acid (a growth permissive molecule) (Zhang et al., 2007). It would appear that a combination of ameliorating intrinsic and extrinsic factors is necessary for successful CNS regeneration to occur.

1.2.4 Inflammation and the cell body response of CNS neurons

The most encouraging results in the field of CNS regeneration have been seen with studies of injured dorsal columns, possibly reflecting their greater ability to regenerate, but also reflecting our ability to manipulate their cell body environment, located in dorsal root ganglia. It has been postulated that inflammation near the cell bodies of axotomised neurons enhances axonal regeneration. Injection of corynebacterium into the DRG prior to crushing the dorsal spinal root results in a four-fold increase in regenerating fibres (Lu and Richardson, 1991). Subsequently, it was found that 2-4 days after sciatic nerve transection macrophage numbers increase in injured DRGs (Lu and Richardson, 1993). Injection of corynebacterium into uninjured DRGs raises neuronal c-Jun and GAP-43 mRNA to similar levels to those found during regeneration after nerve injury. The upregulation of c-Jun precedes macrophage influx, suggesting that

inflammation alone isn't the pre-requisite factor for growth-associated gene upregulation and successful regeneration (Lu and Richardson, 1995).

Similarly, the greatest regeneration of RGC axons across an optic nerve injury has been achieved after stab injury to the lens (Leon et al., 2000; Fischer et al., 2000). Even with an intact optic nerve, the lens injury promotes GAP-43 expression by RGCs, unlike optic nerve injury alone or needle injury of the eye with no lens injury (Leon et al., 2000; Lorber et al., 2002). The growth-promoting effect may depend on inflammation in the retina, as macrophages enter the eyeball after lens injury and it is possible to produce regeneration of RGC axons by injecting the pro-inflammogen zymosan into the eyeball without lens injury (Leon et al., 2000). *In vitro*, media conditioned by activated macrophages stimulated adult RGCs to regenerate their axons (Yin et al., 2003). The principal molecule mediating this was recently found to be a calcium-binding protein, termed oncomodulin (Yin et al., 2006), which is secreted by macrophages, binds to RGCs and requires the elevation of cAMP to exert its neurotrophic effects. However, the intact lens has been shown to provide additional trophic factor(s) in rat (Lorber et al., 2002) and mouse models (Lorber et al., 2005), suggesting that lens and macrophage-derived factors act synergistically to stimulate optic nerve regeneration. Myelination of axons in the optic nerve may also be stimulated by the effects of zymosan, as shown with injection of OPCs and zymosan into the eyeball (Setzu et al., 2006).

1.2.5 Role of microglia in axonal regeneration

Wallerian degeneration in the CNS is much slower than in the PNS, as is the clearance of myelin debris. Unlike degenerating peripheral nerve, where there is recruitment of a large number of macrophages (see Section 1.1.1), there is a much slower increase in their numbers in CNS tracts undergoing Wallerian degeneration (Perry et al., 1987).

There is also a difference in morphology, with CNS macrophages taking on the form of microglia, which appear to be less active phagocytes than PNS macrophages (Perry and Brown, 1992).

Microglia are the resident macrophages of the CNS parenchyma, are morphologically highly differentiated macrophages and have a ramified quiescent (downregulated) phenotype at rest (Perry and Gordon, 1991), although *in vivo* imaging shows that they are actively monitoring the CNS environment with motile processes (Nimmerjahn et al., 2005; Davalos et al., 2005). They are upregulated within milliseconds after a variety of insults, such as excitotoxic lesions and even if there is no evidence of neuronal degeneration, such as spreading depression and epileptic activity (Perry et al., 1995a). They thicken and retract their processes and may eventually adapt a morphology indistinguishable from monocytes giving rise to macrophages. The plethora of mechanisms by which microglia may be activated also tends to also cause them to proliferate and alters their gene expression. This results in altered actin binding (potentially with micotubules or the plasma membrane to affect motility), cell adhesion and signalling, and antigen presentation (Moran et al., 2004). The most significant of these changes may be the increase of complement type 3 receptor within hours of neuronal injury (Graeber et al., 1988) and MHCII upregulation (Kreutzberg, 1996; reviewed by Aloisi (2001)).

Microglial activation occurs in the CNS around facial, hypoglossal and spinal motor neurons after axotomy (Aldskogius, 2001; Raivich, 2002). These injuries occur in the periphery, suggesting that microglia are sensitive to signals communicated from axotomised neurons, in particular macrophage-colony stimulating factor (Kalla et al., 2001). In contrast to those around regenerating facial nucleus neurons, microglia in the red nucleus do not divide, show only minimal hypertrophy and do not become closely

applied to the neurons after section of the rubrospinal tract (Barron et al., 1990; Tseng et al., 1996; Streit et al., 2000). Axotomised rubrospinal neurons atrophy and it has been suggested that this may be related to a lack of perineuronal microglial activation (Streit, 2002). However the importance of microglia around axotomised neurons for axonal regeneration in peripheral nerves or the CNS has not been demonstrated (Perry and Brown, 1992; Perry et al., 1995a). Indeed Kalla et al. (2001) have shown that animals lacking macrophage-colony stimulating factor, which show an absence of a microglial response to injury, exhibit little difference from non-transgenic animals in the regeneration of their motor axons in peripheral nerves. Similarly, Svennson and Aldskogius virtually eradicated the local microglial cell population in the hypoglossal motor nucleus following hypoglossal nerve injury with an intraventricular infusion of a mitotic inhibitor, cytosine arabinoside. They demonstrated that the neuronal response, the rate of axon outgrowth, axon maturation and target reinnervation were all unaffected by such treatment (Svensson and Aldskogius, 1993a; Svensson and Aldskogius, 1993c).

It has been suggested that the main role of microglia around axotomised neurons is in immune surveillance (Raivich et al., 1999; Ling et al., 2001). Microglial activation may serve a protective function in the CNS, but the cytokine profile of microglia may be altered if they are subjected to excessive or sustained activation (Hanisch, 2002). *In vitro* studies have shown microglia to be capable of producing cytotoxic molecules such as nitric oxide, free oxygen radicals, proteases, arachidonic acid intermediates and excitatory amino acids (Banati et al., 1993; Lee et al., 2002). They produce cytokines including TNF-α (Lee et al., 2002) and IL-1β (Quan et al., 1994), which could lead to tissue damage or enhance cell repair, and release a range of factors in vitro that may be neuroprotective and pro-regenerative (see (Raivich et al., 1999) for review).

During development, as well as removing cellular debris and temporary or inappropriately connected axons (Ashwell, 1990; Ashwell, 1991), microglia also play a role in neuronal differentiation through the release of trophic factors (Nagata et al., 1993; Jonakait et al., 1996; Mazzoni and Kenigsberg, 1997). The expression of nerve growth factor and brain-derived neurotrophic factor by cultured microglia are increased following stimulation with lipopolysaccharide (LPS) (Miwa et al., 1997; Nakajima et al., 2001). Neurotrophin 3 (NT-3) is present in some brain microglia, and *in vitro*, addition of LPS increased NT-3 expression by microglia (Elkabes et al., 1996; Elkabes et al., 1998). *In vivo*, striatal microglia activated by kainic acid injection, produced thrombospondin which stimulated neurite outgrowth (Chamak et al., 1994). Implantation of cultured microglia into lesions of dorsal spinal cord enhanced sprouting of neurites into the lesion site (Rabchevsky and Streit, 1997; Prewitt et al., 1997). In theory, the expression of factors produced by microglia may be altered in a manner that would actively support neuronal regeneration, for example with LPS.

1.2.6 LPS-induced cerebral inflammation

LPS, an endotoxin derived from the cell wall of E.coli, is a potent inflammatory agent (Burrell, 1990), that has been used extensively in previous experimental studies in CNS and other tissues to study the effects of inflammation (Andersson et al., 1992). LPS is not directly chemotactic and pro-inflammatory signals have to be transduced initially by resident cells (see Andersson et al., 1992); in the CNS it is believed that microglia play this role (Ling et al., 2001) and their limited reactions may partially account for some of the muted character of the inflammatory response in the brain (Perry et al., 1998).

Although the effects of LPS application onto the surface of the cerebral cortex have not been studied, its injection into cerebral cortex is followed by an increased number of recruited macrophages, activation of local microglia and, later, by activation of astrocytes (Perry et al., 1995a; Montero-Menei et al., 1996). Neutrophils are not recruited, in contrast to what occurs after LPS injection into peripheral tissues (Andersson et al., 1992), which may explain the absence of overt damage to the brain. Effects of LPS injections into brain include activation of complement (Boos et al., 2005) and production of the cytokines TNF-α and IL-1 (Quan et al., 1994; Cai et al., 2003), both of which can be either neurotrophic or lead to neuronal damage depending on their level of expression (Cajal, 1991; Miller et al., 1994; Hiebert et al., 2002). In slices of parietal cortex exposed to LPS, there is rapid glutamate and noradrenaline release, which causes inappropriate neuronal excitation (Wang and White, 1999). Neurons have been shown to express membrane histone H1 receptors that bind LPS and may provide a pathway for direct action of LPS on neurons (Bolton and Perry, 1997). However, *in vitro* studies suggest that LPS exerts its effects on CNS neurons via glial cells (Weis and Humpel, 2002). The Toll-like receptor 4 (TLR-4) acts as an LPS receptor on microglia (Laflamme and Rivest, 2001; Rivest, 2003), but is absent from cortical neurons (Lehnardt et al., 2003).

Extrinsic factors:

Research on extrinsic factors has concentrated on the inhibitory effects of the glial scar, namely NG2, and one inhibitory component of myelin, namely Nogo (and subsequently the Nogo receptor complex). Although the following section therefore concentrates on these molecules, the other extrinsic causes of CNS axons failing to regenerate should

not be downplayed. The intracellular pathways by which they are thought to act are summarised in Fig. 1.1 (page 77).

1.2.7 Response of non-neuronal cells to injury

We have seen that the PNS responds to injury by rapidly filling the gap formed by nerve transection. In contrast, there is an absence of CNS tissue within spinal cord lesions, which are either cystic or filled with a fibrous scar. This finding is species dependent, with mice usually having fibrotic, tissue-filled scars (Ma et al., 2001) and rats typically having cysts after injury, as found in humans (Bunge and Pearse, 2003). Cyst formation is thought to involve secondary insults, such as excitotoxicity, causing apoptosis and necrosis (Beattie et al., 2000). In rodents, lesion sites fill with blood and macrophages, are then invaded by meningeal cells, endothelial cells and Schwann cell, together with axons, which are usually of peripheral origin (Zhang et al., 1997). There are few astrocytes within the lesion, rather they form part of a hypertrophic gliotic scar around the lesion (Farooque et al., 1995), which contains many molecules thought to be inhibitory for axonal regeneration.

1.2.8 The glial scar

Surrounding a CNS injury site is an area of astrogliosis (Berry et al., 1996; Zhang et al., 1997) where chondroitin sulphate proteoglycans (CSPGs) and tenascins are upregulated (McKeon et al., 1991; Laywell et al., 1992; Zhang et al., 1997; Davies et al., 1999; Tang et al., 2003), and meningeal fibroblasts accumulate (Krikorian et al., 1981), which

express semaphorins (Pasterkamp et al., 1999; Pasterkamp et al., 2001; Niclou et al., 2003). Both astrocytes and meningeal cells upregulate ephrins after spinal cord injury (Miranda et al., 1999; Bundesen et al., 2003). The inhibitory properties of these molecules are discussed below. One should note that each individual molecule in this region may seem to play a potential or even weak role in blocking axonal regeneration, but the evidence that the scar as a whole is a profoundly inhibitory region, is strong.

Following injury, astrocytes proliferate and form a dense meshwork of hypertrophic processes that interact with meningeal fibroblasts to form a glia limitans, which has its own basal lamina (Bunge et al., 1994; Zhang et al., 1997; Shearer and Fawcett, 2001) containing extracellular matrix (ECM) molecules such as laminin and collagen (Timpl, 1996). This process is thought to prevent further spread of damage to the rest of the CNS. The ECM molecules and other 'stop signals', rather than the physical density of the astrocytic mesh of the glial scar, are some of the factors stopping axonal regeneration. For example, most regenerating dorsal root axons appear to form synaptic terminals with the purely astrocytic barrier of the DREZ rather than grow past it (Liuzzi and Lasek, 1987), but a few axons are able to penetrate the DREZ, often along blood vessels (Chong et al., 1999). Disrupting ECM formation with 2,2'–dipyridine allows regeneration in the injured fimbria-fornix (Stichel et al., 1999), but not the CST (Weidner et al., 1999)– presumably because in injured spinal cord external meningeal cells are present, which are a separate source of collagen IV (Hermanns and Werner, 2001). Injured CNS axons do not grow through the glial scar in a number of injuries, including those to the corpus callosum (Davies et al., 1997) and dorsal columns (Bavetta et al., 1999). Interestingly, the few axons that breach the glial scar after limited injury to the corticospinal tract become myelinated by the Schwann cells (that later enter the lesion centre) and are eventually able to enter the lesion site, but end there with

a massively extended terminal (Li and Raisman, 1995). Davies et al., (Davies et al., 1997; Davies et al., 1999) attributed axonal growth arrest to the presence of CSPGs in the glial scar, although not all groups ascribe to this view (Lips et al., 1995). Subsequently, much research has concentrated on the inhibitory capacity of this family of molecules (Bovolenta et al., 1997; Fawcett and Asher, 1999).

1.2.9 Chondroitin sulphate proteoglycans and NG2

There are many different types of CSPGs, which are made up of chondroitin sulphate linear polysaccharides (repeating disaccharide units of N-acetylgalactosamine and glucuronic acid), known as glycosaminoglycans (GAGs), attached to different core proteins. Members of the CSPG family in the mammalian CNS include aggrecan, versican, neurocan, brevican, neuroglycan D, NG2, the receptor-type protein tyrosine phosphatase PTPb and its splice variant phosphacan (Hartmann et al., 1991; Carulli et al., 2005).

Their ability to block neurite outgrowth has been attributed to the GAG sidechains (Yamada et al., 1997; Talts et al, 2000), the core proteins (Dou and Levine, 1994; Schmalfeldt et al., 2000), or both (Fidler et al., 1999; Ughrin et al., 2003), depending on which CSPG was studied. GAG sulphation pattern results in varying inhibitory activity (Gilbert et al., 2005). They have also been shown to block the growth-promoting ability of molecules, such as L1, N-CAM, Ng-CAM and laminin (Grumet et al., 1993; Friedlander et al., 1994; Smith-Thomas et al.. 1994) It has been suggested that CSPGs act as molecular barriers, preventing the growth of axons into inappropriate regions during development (Snow et al., 1990; Snow and Letourneau, 1992; Pindzola et al.,

1993; Landolt et al., 1995).They tend to be expressed on the cell surface of reactive astrocytes and meningeal cells (McKeon et al., 1991) and oligodendrocyte progenitor cells (Levine, 1994), both *in vitro* and in the glial scar that surrounds CNS lesions (Rudge and Silver, 1990; Snow et al., 1990; Snow et al., 1991). They are not evenly distributed at CNS lesion sites, with differing patterns of expression temporally and spatially (Tang et al., 2003). In brief, neurocan and NG2 are rapidly upregulated in and around spinal injury sites and phosphacan and brevican are more slowly upregulated; phosphacan, NG2 and tenascin C are strongly expressed in spinal cord lesions by invading meningeal cells compared to neurocan being strongly expressed by glia at the lesion margins. The receptor for CSPGs has not yet been discovered, but they are known to activate RhoA (Monnier et al., 2003) and they require PKC intracellular signalling to mediate their inhibitory effects on axonal regeneration (Sivasankaran et al., 2004). The mechanism appears to involve EGFR and intracellular calcium Koprivica et al., 2005. Among a variety of CSPGs expressed by a growth-inhibitory astrocyte cell line (Neu 7), NG2 was found to be the one with by far the strongest inhibitory effects on neurite growth (Fidler et al., 1999), resulting in NG2 becoming the focus of much research into the inhibitory properties of the glial scar.

NG2 expression

NG2 is a large transmembrane proteoglycan, with a large ectodomain and a short cytoplasmic tail (Nishiyama et al., 1991; Stallcup, 2002). It is expressed in many different tissues, especially during development, but in the adult mammalian brain and spinal cord, it is expressed predominantly by a subset of glial cells with astrocyte-like morphology and the antigenic characteristics of oligodendrocyte progenitor cells (Nishiyama et al., 1999). These cells are present throughout white and grey matter at a density similar to that of oligodendrocytes and microglial cells and have been shown to

respond to neuronal and astroglial signals by raising intracellular calcium (Wigley et al., 2007; Ziskin et al., 2007). It has been proposed that they constitute a novel class of glial cells (for which the term synantocytes or polydendrocytes has been proposed, but I shall use the term NG2+ cells) with as yet poorly understood roles in adult nervous system function (Nishiyama et al., 1999; Butt et al., 2002b; Peters, 2004). NG2+ cells accumulate around CNS lesions and become rounded, making it difficult to distinguish whether NG2 immunoreactivity seen inside the lesion is from glia or from cells of other origin. It is possible that some of the NG2+ cells in the lesion are non-myelinating Schwann cells, although the expression of NG2 by Schwann cells remains controversial (Schneider et al., 2001; Martin et al., 2001; Morgenstern et al., 2003). One current concept is that the NG2+ cells are a form of neural stem cell, as *in vivo* studies show that they are the major dividing population in the CNS (Horner et al., 2000; Dawson et al., 2003) and they can differentiate into oligodendrocytes (or astrocytes) (Polito and Reynolds, 2005). Recent evidence shows that NG2+ cells proliferate around CNS lesion sites and if these reactive cells are placed *in vitro*, they can differentiate into oligodendrocytes (Yoo and Wrathall, 2007), suggesting that they have the potential to fill CNS lesion cavities. However, current thinking links them to the glial scar that forms instead.

There is evidence from studies *in vitro* that NG2, like most other CSPGs, inhibits neurite outgrowth in culture (Dou and Levine, 1994), and possesses several domains that cause growth cone collapse (Ughrin et al., 2003). It has also been shown that antibodies against NG2 block its inhibitory effects on neurite growth (Fidler et al., 1999; Chen et al., 2002b), but it is still not clear whether the core protein or the GAG sidechains are the main site of inhibitory activity. *In vivo*, NG2 is present at sites at which regenerative growth of axons within or into the CNS is arrested, notably around

CNS injury sites and at the DREZ, where NG2+ cells proliferate and accumulate after injury (Levine, 1994; Zhang et al., 2001; Jones et al., 2002; Chen et al., 2002a; Rezajooi et al., 2004; McTigue et al., 2006); see reviews by Butt et al., (2002b) and Nishiyama, (2007).

Chondroitinase ABC

Findings such as those above have led to a widespread belief that NG2 is one of the major inhibitors of axonal regeneration within or into the mammalian CNS after injury (Levine et al., 2001). *In vitro*, neutralisation of NG2 on meningeal cells with an antibody promotes neurite extension (Shearer et al., 2003). Moreover, *in vivo* studies with an antibody called chondroitinase ABC (ChABC), which removes sidechains from CSPGs leaving only a disaccharide stub, has been claimed to promote axonal regeneration through CSPG-rich CNS lesions. Experiments with hyaluronidase, which has chondroitinase activity, showed some enhancement of retinal ganglion cell axon regeneration in crushed optic nerves ((Tona and Bignami, 1993)) and some enhancement of sprouting by injured nigrostriatal axons ((Moon et al., 2003)). ChABC has been reported to stimulate axons of the nigrostriatal tract to regenerate to their targets (Moon et al., 2001), although this tract has been found to have a greater innate propensity to regenerate axons than most others (Woolhead et al., 1998; Anderson and Lieberman, 1999). It is in the injured spinal cord that the most encouraging results have been found. A single application of ChABC was reported to greatly enhance the regeneration of dorsal spinocerebellar axons into a peripheral nerve graft placed in the thoracic spinal cord (Yick et al., 2000). The experiment was repeated by the same group *without* a peripheral nerve graft and using ChABC placed in Gelfoam at the lesion site. They showed that up to 12% of spinocerebellar neurons in the L1 segment had taken up the retrograde label – i.e. they had regenerated through the scar to (at least) the site of

Fluorogold label injection in cervical cord – some 30mm. Impressive results have been achieved with intrathecal infusion of ChABC after crush injury to the cervical cord of adult rats, with regeneration of injured dorsal column axons up to 4mm rostral to the lesion and CST axons up to 5mm caudal to borders of the lesion. Chondroitin sulphate GAGs were degraded at the lesion site and post-synaptic activity below the lesion after electrical stimulation of corticospinal neurons was restored, with functional recovery of locomotor and proprioceptive behaviours promoted, compared to controls (Bradbury et al., 2002). Partial crush lesions are more likely to spare axons than transection injuries (some axons distal to the lesion were seen in controls), and the location of the regenerating axons was not entirely clear. One of the findings was of increased branching of CST fibres into grey mater, although there was no anatomical evidence of these fibres then bypassing the lesion. Other research groups have since shown ChABC treatment after CNS injury to stimulate motor and bladder function recovery (Caggiano et al., 2005), rubrospinal regeneration (Yick et al., 2004) and dorsal root regeneration into the spinal cord (Steinmetz et al., 2005). It has also been used to successfully enhance axonal regeneration into and beyond grafts of olfactory ensheathing glia and/or Schwann cells in the spinal cord (Fouad et al., 2005).

These findings would suggest that the GAG sidechains are the site of axonal inhibition, but the paucity of lengthy axonal regeneration through a lesion seen in the published anatomical figures, combined with statistically significant improvements in behavioural scores after spinal cord injury suggest that ChABC exerts its effects via axonal sprouting and synaptic plasticity with remodelling of spinal circuits rostral and caudal to injury sites rather than by lengthy regeneration of transected axons (see section 1.2.13.5 regarding IN-1 antibody to Nogo). ChABC is a protein extracted from bacteria and may therefore contain impurities and/or elicit an immune response. It is interesting to note

that the experiments of Bradbury et al (2002) produced upregulation of GAP-43 in cervical DRG neurons. Do GAGs in the spinal cord suppress the expression of GAP-43 or was this a direct effect of a multifunctional antibody? Similarly, the enhanced regeneration seen by Fouad et al., (2005) using tissue grafts may have been due to ChABC's action on the graft cells (see Kim et al., (2006) regarding the effect of ChABC on transplanted embryonic cells in spinal cord injury). Cafferty et al., (2007) used the *gfap* promoter to express ChABC in astrocytes and reported that transected corticospinal axons extended within the lesion site, but not caudal to it in the transgenic mice, with no significant improvement in motor function recovery. It therefore appears that functional recovery (and the sprouting that presumably is the cause of this recovery) is due to ChABC *antibody*. There is good evidence that chondroitinase can enhance axonal sprouting in CNS grey matter and the resulting functional plasticity (Tropea et al., 2003; Corvetti and Rossi, 2005; Massey et al., 2006), reviewed by (Bradbury and McMahon, 2006). ChABC has been shown to stimulate sprouting above and below a cord lesion, even in uninjured axons (Barritt et al., 2006). After dorsal column crush, injured CST and intact serotonergic descending axons as well as uninjured primary afferents showed robust sprouting. ChABC in uninjured controls did not induce sprouting in any system, indicating that some form of denervation is required for this effect to occur. Similar sprouting has recently been reported in a study that claims to improve functional recovery following peripheral nerve repair, by injecting ChABC antibody into the ventral horn of spinal cord; they demonstrated increased axonal sprouting in the spinal cord grey matter with MAP-1B-P immunohistochemistry (Galtrey et al., 2007). Separate investigators have used a monoclonal antibody that specifically *neutralises* NG2 to promote regeneration of sensory axons into the lesion site when applied to dorsal column lesion sites, and when combined with a conditioning lesion of the sciatic nerve, resulted in regenerative growth of axons rostral to the lesion

site (Tan et al., 2006). It would be interesting to see if treatment with this mononclonal antibody would also result in functional recovery after spinal cord injury.

The role of NG2 in inhibition of axons is not clear

In addition to abundant evidence for the presence in the CNS of other molecules which are thought to inhibit regenerative axonal growth (including Nogo, myelin associated glycoprotein and oligodendrocyte myelin glycoproteins), there are numerous findings that cast doubt on the general validity of the view that NG2 is a major axon growth inhibitor and suggest the need for further investigation. For example, AN2, the mouse homologue of NG2, does not inhibit outgrowth of mouse DRG cell neurites growing on a laminin substrate (Schneider et al., 2001) and mouse cerebellar granule cells adhere to and extend neurites on substrates containing AN2 (Niehaus et al., 1999). Also, whereas NG2 inhibits neurite outgrowth from rat cerebellar granule cells plated on a substrate of L1 (an axon-growth-promoting cell adhesion molecule), it has no effect on the outgrowth of neurites from DRG cells on the same substrate (Dou and Levine, 1994) suggesting that the inhibitory effects of NG2 are exerted selectively on only some types of neuron. There is also evidence that regenerating CNS axons may grow through regions rich in NG2+ cells (Jones et al., 2003; McTigue et al., 2006). Moreover, in very recent work, it has been shown that NG2+ cells promote neurite outgrowth from hippocampal and neocortical neurons *in vitro,* and that both *in vitro* and *in vivo* NG2+ cells are preferentially and extensively contacted by axonal growth cones (Yang et al., 2006). This is in keeping with earlier evidence that NG2+ cells may receive synaptic input from glutamatergic axons (Bergles et al., 2000; Lin and Bergles, 2004).

The presence of NG2 in the normal and regenerating PNS raises further questions about its roles. NG2 is expressed by fibroblast-like cells and microvascular pericytes in peripheral nerves (Zhang et al., 2001; Morgenstern et al., 2003; Rezajooi et al., 2004), is present at nodes of Ranvier (Martin et al., 2001; Rezajooi et al., 2004) and may also be expressed by a subset of non-myelinating Schwann cells (Schneider et al., 2001). Moreover, the peripheral axons of DRG neurons in the sciatic nerve regenerate through the prominent cap of NG2+ cells that forms over the proximal stump following resection of the nerve, and continue to grow along the distal stump in close proximity to NG2+ cells (Rezajooi et al., 2004). Such observations suggest that NG2 has no generalised inhibitory effect on regenerating PNS axons or that it is involved in subtle focal inhibitory functions directed at preventing profuse branching of the axons and/or perhaps serving to confine regenerating axons to the bands of von Büngner.

I have attempted to answer some of these inconsistencies regarding the role of NG2 in the nervous system with the studies performed and described in this thesis. The aims and basis of these studies are summarised at the end of this chapter.

1.2.10 Semaphorins

Semaphorins, tenascins and some proteoglycans, are involved in the guidance of developing axons to their targets during development, by binding to receptors on growth cones that activate intracellular cascades which result in changes to the cytoskeleton and pathfinding via contact inhibition (Goodman, 1996; Guan and Rao, 2003; Huber et al., 2003). The same molecules seen in development are often expressed in the adult nervous system and/or upregulated after CNS injury, which leads one to believe that

they play a role in inhibiting, or at least regulating, axonal regeneration (De et al., 2002; Koeberle and Bahr, 2004); see (Pasterkamp and Verhaagen, 2006) for review.

Semaphorins form a family of secreted and membrane-bound proteiens that can either repel or attract axons. Membrane-associated Semaphorin-4D, -5A and -6A are expressed by oligodendrocytes (Moreau-Fauvarque et al., 2003; Cohen et al., 2003; Goldberg et al., 2004; Kerjan et al., 2005). Semaphorin-4D is strongly inhibitory for postnatal sensory and cerebellar granule cell axons (in stripe assays) and is transiently upregulated in oligodendrocytes after CNS lesions (Moreau-Fauvarque et al., 2003). It is therefore thought to be an inhibitory factor for axonal regeneration, expressed in myelin. Semaphorin-3 proteins are the most studied, and bind to neuropilins on neuron receptor complexes that also have plexin subunits to transduce signals (Raper, 2000). Other cell surface molecules may be part of the receptor complex, including L1, which is thought to transduce a repulsive signal from Semaphrin-3A to CST neurons. Fibroblast expression of Semaphorin-3A in CNS lesions has already been mentioned, but they also secrete Semaphorin-3b, -3C, -3E and 3F in the lesion (Pasterkamp et al., 1998a; De Winter et al., 2002). Semaphorin-3A and a component of its receptor, neuropilin-1 (NP-1) are also upregulated after optic nerve injury (Nitzan et al., 2006). However, after spinal cord injury, though Semaphorin-3A (Hashimoto et al., 2004) and Semaphorin-4F mRNA are upregulated, neuropilin-2 (NP-2) rather than neuropilin-1 was upregulated in axotomised motorneurons (Lindholm et al., 2004); NP-2 is a co-receptor for Semaphorin-3F (Scarlato et al., 2003). Another puzzling observation is that although Semaphorin-3A is upregulated within the lesions of transected spinal cord, it is not upregulated after contusion injury of the spinal cord (De Winter et al., 2002). Instead of being upregulated within the lesion site, Semaphorin-3A expression is limited to a fibrotic rim of meningeal cells surrounding the injury site. Though contusion

lesions are just as inhibitory to axonal regeneration as transections, this discrepancy may simply be because meningeal cells tend not to invade the lesion site itself after spinal cord contusion injuries.

The presence of Semaphorin receptor components on injured CNS neurons suggests that they may be sensitive to the repulsive effects of Semaphorins-3 molecules. This is seen with DRG neurons transected in the dorsal column with a conditioning lesion, which would usually stimulate sprouting into the lesion. DRG collaterals expressing both NP-1 and plexin-A1 failed to grow into scar tissue expressing Semaphorin-3A, although they did manage to grow over areas of strong tenascin-C and CSPG expression (Pasterkamp et al., 2001). Interestingly, Semaphorin-5A can be made to be an attractive axon guidance cue or an inhibitory one by interaction with HSPGs and CSPGs respectively (Kantor et al., 2004)– this may be particularly relevant to the failure of optic nerve regeneration, where Semaphorin-5A is constitutively expressed (Goldberg et al., 2004), but CSPG levels rise after injury at the lesion site (Butt et al., 2002b). It is not known whether CSPGs are able to convert other semaphorins to an inhibitory role in vivo, but ChABC releases cell surface bound Semaphorin- 3A *in vitro* (de Wit et al., 2005), implying that such release of inhibitory Semaphorin-3A may be one of the mechanisms by which ChABC ameliorates axonal regeneration. One CSPG, NG2, is expressed on polydendrocytes (oligodendrocyte precursor cells (OPC)) found in and around CNS lesions. Semaphorins (including -3A) may regulate OPC reaction to injury, as they can induce them to retract processes and orientate their migration (Cohen et al., 2003).

Selective inhibition of Semaphorin-3A after spinal cord transection (with fungal-derived SM-216289 administered into the lesion site for 4 weeks) appears to substantially enhance regeneration and/or preservation of injured axons, increase myelination and axonal regeneration in the lesion site, decrease cell death and markedly enhance

angiogenesis (Kaneko et al., 2006). The increased angiogenesis may be due to the finding that NP-1 is expressed in blood vessels in CNS lesion scars (Pasterkamp et al., 1999). Semaphorin-3A downregulation is seen after peripheral lesion of motorneuron axons (but with no change in levels of semaphorin receptor proteins and signalling molecules) (Pasterkamp et al., 1998b; Gavazzi et al., 2000), which regenerate vigourously. Intraspinal injury of motorneurons, in the ventral funiculus, results in increased levels of Semphorin-3A, and poor regeneration (Lindholm et al., 2004) – again correlating Semaphorin-3A with failed axonal growth. Scarlato et al., (2003) found that Semaphorin-3A, -3F, NP-1 and NP-2 are all upregulated after sciatic nerve crush in the distal stump and suggested that semaphorins may play a role in guiding regenerating axons in the adult PNS.

1.2.11 Tenascins

The expression of Tenascin-C around CNS lesions (e.g. (Fitch and Silver, 1997; Tang et al., 2003) has been attributed to meningeal cells (Zhang et al., 1997; Deller et al., 1997). Co-cultures of astrocytes and meningeal cells, upon which RGCs were plated, resulted in extension of neurites over the astrocytic component, but avoidance or contact termination with meningeal cells (Hirsch and Bahr, 1999). Tenascin-C has distinct adhesive, anti-adhesive and neurite outgrowth promoting sites and differentially regulates neurite growth depending on whether it is surface-bound, or soluble (Meiners et al.; Gotz et al., 1996). Initially Tenascin-C was thought to be present in the DREZ, where injured dorsal root axons stop regenerating (Pindzola et al., 1993). Later immunohistochemical and *in situ* studies revealed that Tenascin-R (and NG2) are present at the DREZ, with Tenascin-C upregulated in injured dorsal *roots* (Zhang et al.,

2001). Clearly, the role of Tenascin-C following dorsal root injury does not provide strong evidence for its role in preventing regeneration. Its presence in the distal stumps of injured peripheral nerve (Martini, 1994), and the ability of pre-conditioned DRG neurons to grow over it in dorsal column injury scars (see paragraph above), suggests that it may play a role that is more permissive for regeneration.

Tenascin-R glycoproteins are expressed as 160 and 180 kD isoforms by oligodendrocytes and OPCs, secreted into the ECM, and upregulated at CNS lesion sites after injury (Pesheva et al., 1989; Fuss et al., 1993; Wintergerst et al., 1993; Angelov et al., 1998; Probstmeier et al., 2000). Expression is regulated by cytokines and growth factors including TNFα and platelet-derived growth factor (Jung et al., 1993; Probstmeier et al., 1999). Tenascin-R can promote and inhibit axon growth, depending on what it is bound to. Neurites are inhibited if its EGF-like domain (in rats), or the 2^{nd}-3^{rd} fibronectin-III like domains (in chickens) binds to neuronal GPI-linked Rc protein F3/F11 (Brummendorf et al., 1993; Pesheva et al., 1993; Norenberg et al., 1995; Xiao et al., 1999). Removal of GAG side chains from Tenascin-R 160 with ChABC promotes cell adhesion (Probstmeier et al., 2000). Tenascin-R blocks neurite adhesion and outgrowth on fibronectin by inhibition of integrin/RGD-dependent adhesion to it (Pesheva and Probstmeier, 2000). Tenascin-R isoforms interact heterophilically with fibronectin and collagen 1, but not with either collagen IV or laminin (Faissner and Kruse, 1990; Pesheva et al., 1994).

Although Tenascin-R is inhibitory to the outgrowth of RGCs *in vitro* (Becker et al., 2000), it is present in the regenerating optic nerves of zebrafish (Becker et al., 2004), suggesting a role in axonal guidance via contact inhibition in this anatomical location and species, compared to an inhibitory role in the mammalian DREZ.

1.2.12 Ephrins

Ephrins are membrane-bound ligands for the Eph family of tyrosine kinases. They play a role in neuronal pathfinding during development via contact inhibition (Pasquale, 2005). There are two groups of Ephrins - A and B - which are GPI linked or integral membrane proteins respectively. The Ephs are divided into A and B subclasses depending on their ligand affinity and sequence similarity, though some functional interactions between classes do occur. Cell-cell contact is required for them to mediate repulsion via the Rho family of small GTPases, particularly RhoA (Stein et al., 1998; Kullander and Klein, 2002). There can be co-expression of ligands and receptors on neurons, which can modulate receptor sensitivity (Iwamasa et al., 1999; Eberhart et al., 2000).

Expression in the adult nervous system

Most tissues stop expressing ephrins postnatally, but, along with ephs, they remain present in human, primate and rodent brain and spinal cord (Liebl et al., 2003; Hafner et al., 2004; Sobel, 2005; Xiao et al., 2006). Ephrin B3 is found in adult myelin and is as potent as Nogo, MAG and OMGp *combined* in causing retraction of and repulsing neocortical neurites (Benson et al., 2005). Its role in development is that of a midline guidance marker for EphA4-positive corticospinal tract axons (Dottori et al., 1998; Kullander et al., 2001); reviewed by Harel and Strittmatter, (2006).

Ephrin expression by astrocytes (Miranda et al., 1999) has been implicated in gliosis and scar formation. Following partial transection of the spinal cord, reactive astrocytes upregulate ephrin B2 and meningeal cells upregulate EphA4 (Bundesen et al., 2003).

EphA4 is expressed in cortical neurons after spinal cord contusion (Miranda et al., 1999), as well as some astrocytes and oligodendrocytes (Willson et al., 2002). It accumulates in lesioned CST neurons, conferring them with susceptibility to inhibitory ephrins, such as those found in the glial scar. Cell surface signalling between ephrins and Ephs can occur 'in reverse' – i.e. with Eph receptors acting as ligands to transduce signals into cells. Thus, the astrocyte upregulation of ephrinB2 and meningeal cell upregulation of EphA4 may allow bidirectional signalling between these cell types that limits meningeal infiltration into cord and initiates the development of a glia limitans at the injured surface of the cord (Bundesen et al., 2003).

Role in regeneration

EphA4 null mice with hemisection of the spinal cord display reduced astrogliosis and CSPG expression at the lesion site, with enhanced motor recovery (Goldshmit et al., 2004). The use of tracers in these experiments is more anatomically credible than use of 5-HT or MAP-1B immunohistochemistry by other groups. The tracers demonstrated anterogradely labelled fibres crossing the lesion site, with retrograde labelling of corticospinal and rubrospinal cell bodies, as well as other brainstem nuclei. The neurite inhibitory findings of Benson et al., (above) also suggest a role for EphB3 in axonal regeneration.

1.2.13 Myelin and other inhibitory factors

Not only is the glial scar an inhibitory barrier to regeneration, but there is strong evidence that CNS myelin contains molecules which repel growing axons. These include Nogo (Chen et al., 2000), myelin-associated glycoprotein (McKerracher et al., 1994) and myelin oligodendrocyte glycoprotein (Kottis et al., 2002). Semaphorin-4A and Ephrin B3 are also found in myelin, and were discussed in the previous section, together with the glial scar derived semaphorins and ephrins.

The inhibitory nature of myelin was first postulated by Berry, (1982), who noted that chemical ablation of growth-permissive monoaminergic neurons allowed their regeneration, but mechanical injury did not. The key difference in these injury models was that mechanical injury damaged myelin and Berry concluded that myelin breakdown products are inhibitory. *In vitro* studies later showed that CNS myelin inhibited neurite outgrowth (Schwab and Caroni, 1988; Caroni and Schwab, 1988b), predominantly due to two molecules of ~250kDa and 35kDa (termed NI-250 and NI-35) (Caroni and Schwab, 1988b). A monoclonal function blocking protein raised against NI-250 (IN-1) reacted against both proteins (Caroni and Schwab, 1988a) and was subsequently administered to rats with spinal cord lesion with claims of axons regenerating 11mm past a thoracic corticospinal lesion compared to 2.6mm in controls (Schnell and Schwab, 1990) – note that this would not injure the dorsolateral corticospinal tract (DLCST). In retrospect, this appears to be a remarkable amount of regeneration, especially in control rats. Subsequent studies by the same group have moved away from claims of regeneration to interpretations based on sprouting of CST axons. Analysis of the 1990 paper reveals that the regenerating axons were in the region

of distal corticosopinal tract. This contrasts with their later studies, where regenerating axons were seen in the dorsal columns, lateral tracts and grey matter for up to 2mm, after pyramidotomy (i.e. lesioning rostral to the split of the CST into dorsal and ventral branches, which transects the entire CST – see Appendix Fig. A1) (Raineteau et al., 1999). It is therefore pertinent to question whether the 1990 experiments spared the most ventral part of the lesion or sprouting from the DLCST was not accounted for, which may have been the main - and still highly significant - effect of IN-1 treatment. At the time, however, these experiments prompted much excitement, and its encoding gene *nogo* was cloned (GrandPre et al., 2000; Chen et al., 2000; Prinjha et al., 2000). The Nogo protein, MAG and OMgp are the most-studied inhibitory molecules derived from myelin, and will be discussed with their receptors below. Other inhibitory molecules resident in myelin, such as Semaphorin-4A (see section 1.2.10 above) and ephrinB3, will be mentioned thereafter.

1.2.13.1 Nogo

Nogo is a member of the Reticulon family, and is also known as Reticulon 4 (others are Reticulon 1-3), named because they reside largely in the endoplasmic reticulum. There are three isoforms of Nogo: A, B and C (from largest to smallest) expressed in the adult nervous system, all generated by the *nogo* gene. An extracellular domain sequence (Nogo-66) is common to all isoforms and inhibits axonal extension with growth cone collapse (Fournier et al., 2001; GrandPre et al., 2002). Nogo-A also has inhibitory domains in its N-terminal sequence (Prinjha et al., 2002; Oertle et al., 2003). Nogo-A is found in CNS myelin where it is highly expressed by oligodendrocyte membranes, which suggests that it can be present on the cell surface and therefore able to interact with other proteins. However, data suggest that only 1-2% of total Nogo-66/A in

oligodendrocytes is actually expressed at the cell surface, which may be enough to exert axonal inhibition, but suggests that the other 98-99% plays another role in subcellular compartments.

The receptor to Nogo (NgR) is a glycosylphosphatidylinositol (GPI) -linked cell surface protein of 473 amino acids, which binds the Nogo-66 loop of the Nogo family of proteins with high affinity (Fournier, et al., 2001; Zander et al. 2007). The Nogo-66 receptor, NgR1, is also a functional receptor for MAG and OMgp, and it is therefore worth discussing these two other main inhibitory molecules found in myelin, before continuing with the evidence linking Nogo to inhibition of regeneration.

1.2.13.2 Oligodendrocyte myelin glycoprotein (OMgp)

OMgp is a GPI-linked cell surface CNS myelin protein that induces growth cone collapse and inhibits neurite outgrowth (Kottis et al., 2002; Wang et al., 2002b), (previously known as arretin (McKerracher et al., 1994)). Depending on its tissue of origin, it may possess the HNK-1 moiety (Mikol et al., 1990), which is also found on MAG, and which was mentioned earlier as being associated with selective motor axon regeneration of regenerating peripheral nerves (Low et al., 1994; Martini et al., 1994). It is expressed strongly by neurons (Habib et al., 1998) and glial cells that contact nodes of Ranvier (probably NG2+ cells) (Huang et al., 2005) with a putative role in suppressing formation of collaterals.

1.2.13.3 Myelin-associated glycoprotein (MAG)

MAG (or siglec 4a) is a transmembrane protein of the immunoglobulin superfamily, found in both Schwann cell and oligodendrocyte myelin membranes (Sternberger et al., 1979; Martini, 1994), where it plays a role in the formation and maintenance of myelin sheaths (Fruttiger et al., 1995; Carenini et al., 1997; Fujita et al., 1998; Marcus et al., 2002). MAG-mediated signalling (at least in the PNS) affects the diameter of myelinated axons by increasing expression of phosphorylated neurofilaments, but it is not known why there is degeneration of PNS axons if this signalling is disrupted (Quarles, 2007).

It was initially thought to promote neurite outgrowth from neonatal DRG cells *in vitro* (Johnson et al., 1989), but was subsequently found to inhibit axonal growth from adult DRG cells and cerebellar granule cells (Mukhopadhyay et al., 1994; McKerracher et al., 1994), suggesting a role in the age-related changes of mammalian regenerative ability. MAG binds tightly to the gangliosides GD1 and GT1b, that are expressed on axons (Calderon et al., 1995), but it is not clear if this is the mechaninsm of neurite inhibition used by MAG. McKerracher (2002) contemplated an inhibitory role induced by clustering gangliosides into lipid rafts that could activate Rho A, but the strongest evidence of its effects comes from the evidence that NgR1 is part of one neuronal functional receptor complex for MAG (see below).

The functional significance of MAG in the adult CNS is not clear. Although MAG is generally recognised as a potent inhibitor of axonal growth *in vitro*, MAG knockout mice show little or no enhancement of axonal regeneration in the spinal cord (Bartsch et

al., 1995; Li et al., 1996). However, there is evidence that MAG can be inhibitory to axonal regeneration in the slow-degenerating mutant mouse if the *mag* gene is inactivated, resulting in enhanced regeneration in the sciatic nerves of these mice (Schafer et al., 1996). Furthermore, MAG makes up the great majority of the neurite-outgrowth inhibiting substance released from myelin damaged in the CNS (suggesting that the release of Nogo from the cell surface is negligible), and a soluble form of MAG released in such a way inhibits neurite outgrowth from P6 DRG neurons (Tang, et al., 2001).

1.2.13.4 Nogo receptors and co-receptors

NgR1 has two structural homologues called NgR2 (RTN4RL2; NgRL3; NgRH1) and NgR3 (RTN4RL1; NgRL2; NgRH2) (Barton et al., 2003; Pignot et al., 2003; Lauren et al., 2003). NgR2 is a functional receptor for MAG (Venkatesh et al., 2005) and although its co-receptors are not yet discovered, gangliosides seem to be involved in MAG-mediated neurite inhibition (Yang et al., 1996; Vinson et al., 2001).

NgR1 mediates growth cone collapse in response to the three myelin proteins discussed above, and NGR2 is a receptor for MAG, but many neurons lack these receptors or co-receptors *in vivo* (Hunt et al., 2002b), which complicates claims that myelin is inhibitory to regeneration of these same neurons, due to Nogo, MAG or OMgp. MAG competes with Nogo-66 for binding to NgR (Domeniconi et al., 2002), which is also the site where IN-1 binds (Zander et al., 2007).

NgR1, 2 and 3 are unlikely to be the only receptors for Nogo-A, MAG and OMgp. Gangliosides interacting with MAG and oligodendrocytes do not express NgR, yet they show trophic effects with MAG (Gard et al., 1996). Furthermore, the N-terminal of Nogo-A is also inhibitory to neurites and prevents cell spreading (GrandPre et al., 2000; Fournier et al., 2001; Niederost et al., 2002; Prinjha et al., 2002), but no receptor for it has yet been found.

NgR is present in much higher levels in adults than in embryos (Fournier et al., 2001; Mingorance A, 2004), as one would expect, although two different *NgR* knockout mice are viable and healthy, suggesting that NgR is not vital to development.

NgR knockout mice show varying amounts of regeneration following spinal cord injury; genetic NgR deletion improved the ability of serotonin-containing but not CST fibres to regenerate after spinal cord injury (Kim et al., 2004; Zheng et al., 2005). Pharmacological NgR inhibition has resulted in more robust and reproducible effects in models of stroke and spinal cord injury (Lee et al., 2004; Li et al., 2004), where enhanced CST regeneration is seen following spinal cord injury, but growth is limited and proceeds along ectopic pathways. The discrepancy between genetic and pharmacological inactivation of NgR1 is not clear, but may include compensatory upregulation of other receptors during development of the mutant mice (Teng and Tang, 2005). *NgR* deficient mice upregulate Nogo-A until day P6 (Kim et al., 2004), which may have other as yet unidentified receptors, through which it may act. However, the fact that the neurons with the greatest expression of NgR1 (CST) do not regenerate in *NgR* knockout mice suggests that other factors are involved.

Co-receptors and signal transduction

NgR is not capable of transmembrane signal transduction because it is a GPI-anchored cell surface protein. Three other proteins have been found to be signal transducing co-receptors: p75, LINGO-1 and TROY (Wong et al., 2002; Wang et al., 2002b; Mi et al., 2004; Shao et al., 2005; Park et al., 2005).

p75 is a transmembrane protein belonging to the tumour necrosis factor receptor (TNFR) superfamily (Roux and Barker, 2002) and is necessary for MAG-induced inhibition of neurite outgrowth from adult DRG and postnatal cerebellar granule neurons (Yamashita et al., 2002). Its signalling has been shown to occur with NgR1 binding of Nogo-66, MAG or OMgp (Wang et al., 2002a). It has other roles when bound to different proteins, such as when bound to Trk family members, including a role in cell death (see Bronfman and Fainzilber, (2004).'Vice-versa', one can't exclude the possibility that neurotrophins may act to promote axonal sprouting (see section 1.2.14 below) by competitive inhibition of NgR rather than via Trk receptors. It may be significant that p75 is upregulated by several types of intrinsic CNS neurons after injury, including corticospinal neurons (Giehl, 2001) and Purkinje cells (Vaudano et al., 1998), neither of which has the capacity to regenerate axons. p75 knockout mice demonstrate enhanced sprouting of serotonergic (raphespinal) axons within the spinal cord and CGRP-containing primary afferents after dorsal rhizotomy (Scott et al., 2005). However, there was no enhancement of CST regeneration after dorsal hemisection (Zheng et al., 2005). The difference in results may reflect the greater regenerative ability of sympathetic, serotonergic and primary afferent neurons compared to CST neurons (at least into peripheral nerve tissue), suggesting that p75 is just one part of the multifactorial intracellular cascades that result in regeneration.

LINGO-1 is a transmembrane protein, found only in nervous tissue, which co-immunoprecipitates with NgR1 and p75, whose expression peaks at P1. The expression of all three co-receptor proteins is necessary for the downstream activation of RhoA in response to Nogo-66, MAG or OMgp (in the COS cell line; there is no such evidence in neurons yet) (Mi et al., 2004). LINGO-1 is apparently an obligatory co-receptor for NgR1, with either p75 or TROY required to complete the functional receptor complex (Mi et al., 2004). One study did not detect any LINGO-1 in the adult spinal cord (Carim-Todd et al., 2003), but it is upregulated in descending axonal tracts after spinal cord injury. LINGO-1 is also more predominantly expressed in Purkinje cells (which are refractory to regeneration), rather than cerebellar granule cells in adults (Mi et al., 2004). Transfection of a dominant negative LINGO-1 into embryonic cerebellar granule cells reduced the inhibitory effects of myelin, Nogo-66 and OMgp (Mi et al., 2004), but no regeneration experiments have been carried out using this construct. Its functional significance has recently been shown *in vivo* using soluble LINGO-1, which has an Fc fragment that acts as an antagonist to block binding of LINGO-1 to NgR1. LINGO-1-Fc treatment to rats after dorsal or lateral hemisection of the spinal cord decreased RhoA activation, promoted sprouting into the lesion and improved functional recovery (Ji et al., 2006)

TROY is a receptor in the tumour necrosis factor family (like p75) and binds to NgR1. It can replace p75 in the p75/NgR1/LINGO-1 complex to activate RhoA in the presence of myelin-derived inhibitory molecules and is more widely expressed in the CNS (and in a higher percentage of DRG neurons) than p75 is (Shao et al., 2005; Park et al., 2005). Transfection of P28 DRG neurons with a dominant negative TROY blocked the inhibitory effects of Nogo-66 and OMgp on neurite outgrowth (Park et al., 2005).

TROY knockout mice are healthy and fertile, and they have a greatly enhanced ability to grow neurites on myelin-derived inhibitory substrates (Shao et al., 2005).

The pathway from NgR binding to rearrangement of the actin cytoskeleton and subsequent growth cone collapse has not been fully elucidated, and is complicated by binding of p75 with other membrane-associated proteins (Fujitani et al., 2005). One can summarise current findings by stating that Nogo-66, MAG or OMgp binds to the tripartite receptor compromised of NgR1/LINGO-1/p75 or TROY. This probably stimulates intramembrane proteolysis of p75 (Domeniconi et al., 2005), activates PKC (Sivasankaran et al., 2004) and the epidermal growth factor receptor (EGFR; (Koprivica et al., 2005)), which releases RhoA from its inhibitor Rho-GDI (Yamashita and Tohyama, 2003) to activate it. Downstream, Rho kinase and the antagonistic effects of LIM kinase and Slingshot (a phosphatase enzyme) on cofilin, in the presence of calcium, result in growth cone collapse (see Ahmed et al., (2005) and Logan et al., (2006)). It is noteworthy that this growth cone collapse cascade is prevented by Schwann cell-derived factors that promote axon regeneration (Ahmed et al., 2006), although the presence of p75 in RGCs is disputed (Hu et al., 1999; Hirsch et al., 2000).

NgR1 and its ligands clearly play a part in limiting regeneration of some types of axon. None the less, since some neurons do not express NgR1 and since its inactivation has failed to produce significant regeneration of one class of axon (the corticospinal tracts) that express the receptor strongly, it is difficult to conclude that NgR1 signalling is the major cause of the failure of regeneration in the spinal cord. Surprisingly, inactivating NgR1 has been shown to allow rubrospinal and raphespinal axons to regenerate across complete transections of the spinal cord- i.e. through regions lacking the myelin-derived

inhibitors. This may be explained by the possibility that overcoming the inhibitory effects of some myelin-derived factors may upregulate neuronal growth-associated genes, altering the growth state of the neurons, so that regenerating axons can vigorously overcome other inhibitory influences. Such considerations may also explain the strong evidence that some neurons can regenerate axons through CNS white matter.

1.2.13.5 Role of Nogo-A in axonal regeneration

Studies on mice lacking *nogo-a/b* resulted in three different results of CST injuries from three different research groups, from no corticospinal regeneration (Zheng et al., 2003), through slight CST sprouting (Simonen et al., 2003)(*nogo a/a* knockouts), to significant regeneration and functional recovery (Kim et al., 2003)(NB: the mice with the greatest and least regeneration were both *nogo-a/b* knockouts). The disparity in findings could be explained by the effects of genetic background (see Dimou et al., (2006)) and/or compensatory changes of other molecules during development; for instance, Nogo-B was upregulated ten-fold in the *nogo a/a* knockouts. However the *nogo a/b* knockouts showed completely opposite results in different laboratories (Zheng et al., 2003); see Woolf (2003). The experiments were repeated by Steward et al., (2007), using the knockout mice of Kim et al., and Zheng et al. (i.e. both *nogo a/b* knockouts). Steward's group demonstrated that inadvertent injection of anterograde tracer into the ventricles below motor cortex and labelling of axons at the time of lesioning, resulted in false-positive labelling of axons below the cervical lesion site. Moreover, these incorrectly labelled axons had similar profiles to those seen by Kim et al., who had claimed regeneration occurred in their Nogo knockout mice, and did not occur with delayed

BDA labelling (Steward et al., 2007). This was countered by Kim's research group, who stated that only 5% (3 of 58) of their mice were labelled artefactually in this manner, and that there was still a statistically significant increase in ectopic sprouting of CST fibres in Nogo knockout mice, but accepted that it was far from complete (Cafferty et al., 2007).

If genetic deletion of the Nogo receptor does not stimulate regeneration, the transgenic expression of a soluble receptor antagonist appears to give better results (Li et al., 2005; Zheng et al., 2005). It is not known why genetic targeting of putative growth inhibitory molecules often fails but pharmacological targeting succeeds, but one can assume that pharmacological treatments have a broader mechanism of action. For instance, infusion of IN-1 into CSF almost certainly affected the cell bodies of, as well as the growth cones of, injured CST neurons.

Antibodies to Nogo

It is difficult (and provocative) to discount the results of the IN-1 antibody experiments, especially as their results were most conclusive with injured CST neurons, whose cell bodies contain very high levels of NgR1, Nogo-66 and Nogo-A mRNAs and recent evidence suggests that IN-1 acts on Nogo-66 and the N-terminal of Nogo-A (Zander et al., 2007). *In vitro*, IN-1 treatment promoted sprouting of uninjured Purkinje cell axons (Buffo et al., 2000). The effects of IN-1 were further enhanced by implantation of foetal spinal cord at the lesion site (Schnell and Schwab, 1993) and additional treatment with NT-3 (Schnell et al., 1994) with subsequent functional recovery (Bregman et al., 1995). Use of different antibodies – e.g. to the active sites of the Nogo-A specific region have given broadly similar behavioural results (Liebscher et al., 2005), but the regeneration

appears to be mainly through tissue adjacent to the lesion sites and grey matter distal to the lesion. Often no regeneration was seen through a lesion if there was a cyst or large scar (Brosamle et al., 2000; Liebscher et al., 2005), which is not surprising. More recent work with IN-1 has emphasised that it mainly promotes axonal sprouting above and around the lesion (Thallmair et al., 1998; Raineteau et al., 1999; Kartje et al., 1999) rather than growth through it. Even animals without axotomy had sprouting of CST fibres into abnormal territories (Bareyre et al., 2002). Moreover, after unilateral pyramidotomy, the IN-1 treatment resulted in behavioural recovery, but this was not later reversed by *re-lesioning* the CST rostral to the original injury (Z'Graggen et al., 1998). This showed that plasticity, rather than regeneration was responsible for the behavioural improvement. These findings correspond with other studies in which the motor improvement in injured animals seen with IN-1 treatment has been attributed potentially to enhanced plasticity of corticofugal axons or of the descending serotonergic system (Bregman et al., 1995; Bareyre et al., 2002).

A key point that is often overlooked is that Nogo-A is widely expressed in neurons (Josephson et al., 2001; Hunt et al., 2002a; Hunt et al., 2003) where it is expressed on the cell surface (Dodd et al., 2005). Therefore antibodies, such as IN-1 will not bind solely to myelin. It is expressed in groups of CNS neurons with varying innate abilities to regenerate - e.g. adult Purkinje cells and CST neurons, which are refractory to regeneration, as well as RGCs, which show a propensity to regenerate given the right environment - in their cell bodies (not their axons). All the neurons that respond to IN-1 in adult animals *in vivo* express Nogo-A mRNA and protein. IN-1 may function *in vivo* via neuronal binding to Nogo-A and *stimulating* a cell body response that drives regeneration. If Nogo-A is driven down axons, the scenario would resemble successfully regenerating adult peripheral nerves, which strongly express Nogo-A (Hunt

et al., 2003). Against this theory are reports that IN-1 does not stimulate DRG neurite outgrowth onto non-myelin substrates (Anderson et al., 2007) and immunohistochemical evidence of IN-1 binding to white matter *in vivo* (Huber et al., 2002; Mingorance, 2004). It may be that IN-1 has many actions *in vivo*, binding to other myelin products of injury and other molecules expressed by corticospinal neurons when delivered systemically (see Fournier et al., 2002), just as ChABC was postulated to do (above). Certainly this seems just as plausible as the idea that blocking only one of the major inhibitors in CNS myelin has such profound effects on axonal sprouting and regeneration.

both the 66 amino acid loop (Nogo-66) and the amino-terminal domain (amino-Nog are known to be inhibitory to axon outgrowth. The neuronal receptors and downstrea signalling pathways known to be involved in transducing these inhibitory signals are shown. Among the signalling components that are common to both CSPG and myel inhibition are the activation of RhoA and the rise in intracellular calcium. A gradien MAG receptor activation induces Ca release from internal stores, leading to a gradie of low-level [Ca] elevation that is highest on the side of the growth cone facing the MAG source. This causes repulsive growth cone turning. Coincident elevation of cA through a parallel signalling pathway can also lead to Ca release from internal stores creating a high-level [Ca] elevation that triggers attractive growth cone turning. Thu cAMP elevations can impinge on MAG-induced Ca signals and perhaps downstrean effectors to switch the growth cone turning response from repulsion to attraction. Whereas the signals downstream of RhoA that lead to the actin cytoskeleton are wel characterised (solid grey arrows), the relationship between components upstream of RhoA and the role of calcium influx are still ambiguous (dashed grey arrows). For example, calcium transients might activate protein kinase C (PKC), which is require for p75 cleavage by α-secretase66, or trigger the transactivation of epidermal growtl factor receptor (EGFR).

GAP-43 is upregulated in all known examples of successful axonal regeneration. It i bound to the plasma membrane and its binding to actin filaments can alter growth co morphology. Binding of PKC or calmodulin to GAP-43 is mutually exclusive. Phosphorylated GAP-43 stabilises long actin filaments, whereas calmodulin-bound dephosphorylated GAP-43 inhibits actin polymerisation and short filament extensio (He et al., 1997). $Pi(4,5)P_2$ are phosphoinositol second messenger lipids that are concentrated in the inner leaflet of cholestrol-rich membrane raft domains. GAP-43 functionally related proteins can stabilise $Pi(4,5)P_2$ in rafts, thus promoting actin and possibly microtubule stability, and leading to membrane protrusion essential for axo growth.

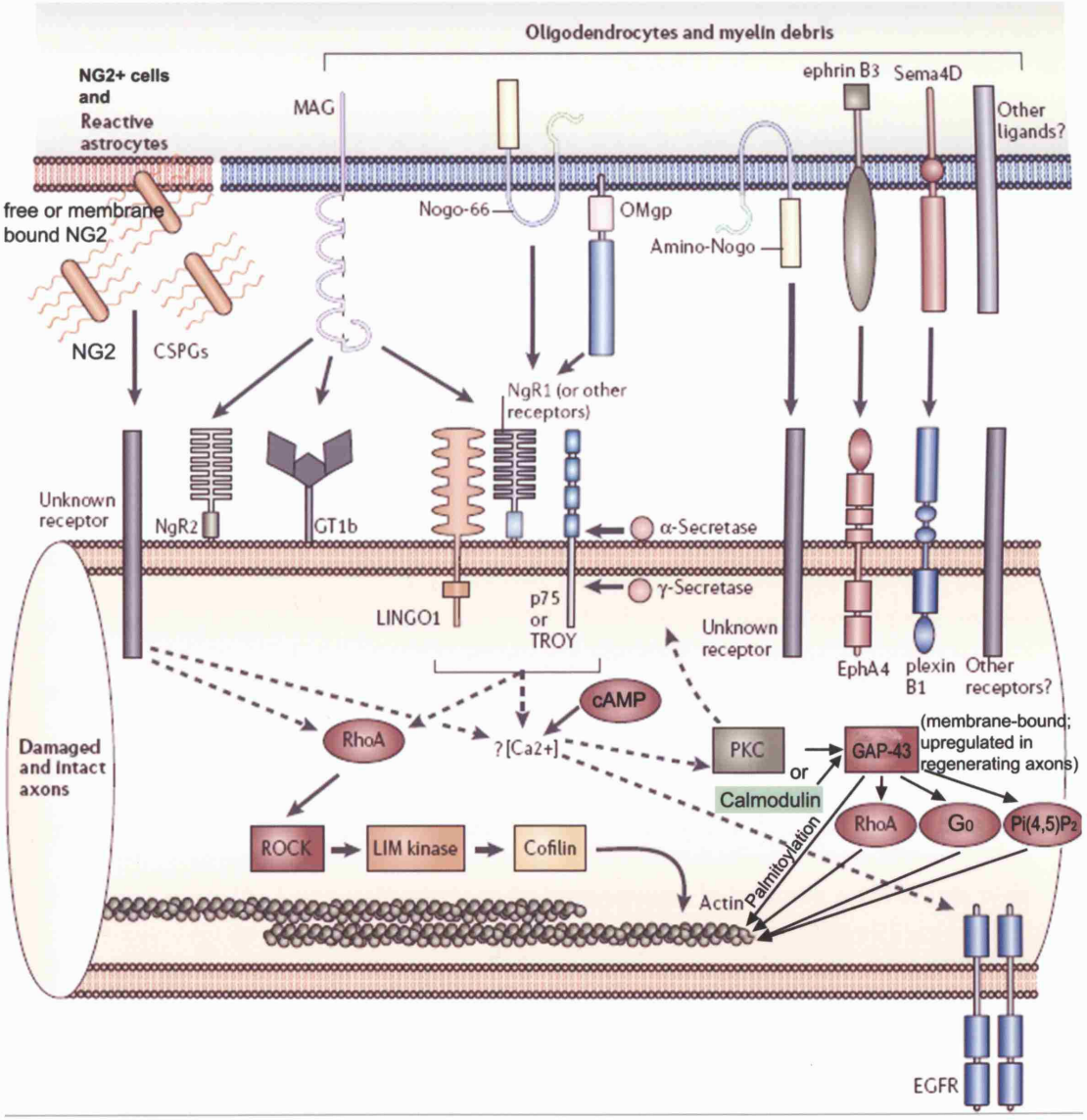
Oligodendrocytes and myelin debris
NG2+ cells and Reactive astrocytes
free or membrane bound NG2
NG2
CSPGs
MAG
Nogo-66
OMgp
Amino-Nogo
ephrin B3
Sema4D
Other ligands?
NgR1 (or other receptors)
Unknown receptor
NgR2
GT1b
α-Secretase
γ-Secretase
LINGO1
p75 or TROY
Unknown receptor
EphA4
plexin B1
Other receptors?
cAMP
RhoA
?[Ca2+]
PKC
or
Calmodulin
GAP-43
(membrane-bound; upregulated in regenerating axons)
RhoA
Go
Pi(4,5)P2
Palmitoylation
Damaged and intact axons
ROCK
LIM kinase
Cofilin
Actin
EGFR

1.2.13.6 Summary

It is unlikely that CNS myelin, containing MAG, OMgp and Nogo, is the key impediment to axon regeneration into and beyond lesion sites. Nogo is absent from CNS lesion sites (Hunt et al., 2002b; Hunt et al., 2003) and myelin is removed by 7 days after some injury models (Li et al., 1999), resulting in OPCs and meningeal cells being the major component of the subsequent scar (Levine, 1994; Stichel et al., 1995), both of which express NG2 (Jones et al., 2002; Shearer et al., 2003). Furthermore, transplanted adult DRG neurons have been shown to regenerate axons through undamaged CNS and even degenerating white matter (Davies et al., 1997; Davies et al., 1999) and given a strong enough stimulus, RGCs can regenerate through optic nerve white matter (Lorber et al., 2005). Blocking Nogo with the IN-1 antibody had no effect on the regeneration of ascending sensory axons (Oudega et al., 2000) although it was claimed to promote the regeneration of descending CST axons (Schnell and Schwab, 1990). This suggests that the effects of IN-1 (which is an IgM protein and thus less specific than IgG antibodies) may be in other parts of the CNS, rather than on the myelin distal to the lesion site. For example, when IN-1 was delivered via an intracerebral hybridoma graft to rats with pyramidotomy, cells in the spinal cord upregulated genes needed for axon growth, including actin, myosin and GAP-43 (Bareyre et al., 2002) and resulted in aberrant sprouting of CST neurons (although CST cell bodies were not examined).

1.2.14 Lack of trophic support and a growth promoting substrate

Neurotrophic factors are secreted soluble proteins whose actions on the nervous system include promoting cell survival, axon outgrowth and maintaining cellular morphology. There are a number of neurotrophic factors, but I shall concentrate on:

NGF, BDNF, NT-3 and NT-4.

In theory, BDNF, NT-3 and NT-4 all act like NGF (the first neurotrophin to be identified (Levi-Montalcini and Hamburger, 1951)), which is a target-derived molecule taken up after binding to its neuronal receptor as a complex and retrogradely transported to the cell body where it exerts its effects (Thoenen et al., 1988). However, BDNF and NT-3 act differently (DiStefano et al., 1992) and undergo anterograde transport in developing RGCs and primary sensory neurons, become stored in vesicles in axon terminals to be released when needed (von Bartheld et al., 1996).

1.2.14.1 Nerve growth factor

Studies with NGF resulted in the current theory regarding the role of neurotrophins in development. Excessive sympathetic and sensory neurons exist during development and the only neurons that survive to maturity are those that make functional connections with their target and retrogradely transport target-derived neurotrophic factors, such as NGF (Korsching and Thoenen, 1983). Adult primary sensory neurons remain sensitive

to NGF, although it is not vital for survival, but it retains the ability to stimulate neurite outgrowth.

Despite not being expressed in the adult spinal cord (Korsching and Thoenen, 1985), NGF is upregulated by meningeal cells and some Schwann cells of nerve roots around spinal cord compression or transection sites, peaking 1 day post-lesioning (Widenfalk et al., 2001). In the injured PNS, NGF is plentiful in axons and is upregulated by Schwann cells that also upregulate $p75^{NTR}$ (Taniuchi et al., 1986), possibly as a store to stimulate the regenerating axons as they grow through the $p75^{NTR}$-positive distal stump back to their original targets (Sandrock, Jr. and Matthew, 1987).

Neurotrophic factors are widely used to promote CNS regeneration *in vivo*. Continuous NGF infusion into the dorsal spinal cord is reported to promote the ingrowth of over a third of central processes of injured dorsal roots for several millimetres into spinal cord, compared to 3% ingrowth in untreated controls (Oudega and Hagg, 1996). The regenerating fibres were typically small diameter unmyelinated fibres, immunopositive for CGRP (these DRG neurons are known to express trkA, the NGF receptor). Implanting autologous grafts of fibroblasts genetically modified to express high levels of NGF promoted the growth of coerulospinal fibres and ventral motor axons, as well as CGRP immunoreactive primary sensory fibres, but not CST and raphespinal axons (Tuszynski et al., 1996). The axons did not exit the distal side of the lesion, and it is likely that this is because the neurotrophin concentration was highest within the lesion. More recent experiments using neurotrophins have therefore injected them directly into spinal cord distal to the lesion site, as well as within the lesion, with subsequent regeneration of axons across and out of a lesion to the injection site (Lu et al., 2004).

However, it appears that an absolutely continuous (gap-free) gradient of neurotrophins is necessary for successful regeneration, and axons do not grow past the site of injection (Taylor et al., 2006).

1.2.14.2 Brain Derived Neurotrophic Factor (BDNF)

BDNF has roles in the developing and mature CNS, including chemotaxis (Ming et al., 2002), neurotransmission (Yang et al., 2002), long-term potentiation (Kovalchuk et al., 2002), cortical inhibition (Huang et al., 1999) and neuroprotection (Jones and Reichardt, 1990).

Developing chick RGCs are dependent on BDNF between E6 and E11, which corresponds to the timecourse of their target innervation and apoptosis of superfluous RGCs (Rodriguez-Tebar et al., 1989). BDNF, like NGF, also has an antiapoptotic role on a subpopulation of developing primary sensory neurons. However, these neurons still depend on BDNF in adulthood, unlike NGF-dependent neurons, continuing to secrete BDNF themselves for autocrine regulation (Acheson et al., 1995). Studies with the BDNF knockout mouse have shown that trigeminal and facial sensory neurons and a subset of nodose-petrosal ganglion neurons (probably those involved in chemosensory regulation of respiration (Erickson et al., 1996) depend on BDNF for survival. Mice heterozygous for BDNF have some abnormalities in the morphology and physiology of serotonergic neurons (Lyons et al., 1999) and studies on conditional BDNF knockouts suggest that postnatal BDNF plays more of a role in maintaining post-synaptic 5-HT2A (and possibly other) receptors than pre-synaptic ones (Rios et al., 2006).

In adult brain, BDNF is present in hippocampus, amygdyla and neocortex (Ernfors et al., 1990; Phillips et al., 1990; Wetmore et al., 1990). In BDNF knockout mice, there is increased postnatal cell death of neurons in areas of the dentate gyrus and olfactory bulb that continuously regenerate neurons in adulthood (Linnarsson et al., 2000), confirming a role of BDNF in protection from apoptosis.

Peripheral nerve transection results in delayed BDNF upregulation in the distal stump, with peak expression several weeks after injury (Meyer et al., 1992) with knockout studies suggesting a role in regeneration (see section 1.1.1). Mice heterozygous for BDNF have delayed regeneration of periodontal Ruffini endings after transection of the inferior alveolar nerve (Harada et al., 2003).

In spinal cord, BDNF is found only in some neurons of lamina VII of the dorsal horn and some DRG neurons of varying size strongly express BDNF. There is no obvious regulation of BDNF expression after compression or transection of the cord (Widenfalk et al., 2001), although it is upregulated in spinal cord after treatment of injuries with IN-1 (Bareyre et al., 2002). Studies on regeneration of injured DRG primary afferents treated with exogenous BDNF give conflicting results. Directly infusing BDNF into spinal cord after dorsal root crush has been reported to promote their regeneration in ascending dorsal columns to a greater extent than NGF or NT-3 infusion, with no synergistic effect if all three neurotrophins are infused together (Oudega and Hagg, 1999). Intrathecal infusion of BDNF did not enhance axonal growth through the DREZ after dorsal root crush (Ramer et al., 2000).

Perhaps the most impressive results using BDNF to stimulate spinal cord regeneration have resulted from injecting it around the cell bodies of rubrospinal neurons to enhance the cell body response to cervical axotomy. This resulted in increases in cell body GAP-43 and Tα-1 tubulin mRNA and significant axonal growth into peripheral nerve grafts compared to vehicle-treated controls. Further to this, if the graft and BDNF injection was delayed for a year after cervical injury, the axons were still able to regenerate up the peripheral nerve graft, and it was discovered that the BDNF reversed some of the atrophy of the chronically injured rubrospinal neurons (Kwon et al., 2002; Plunet et al., 2002). CST axons again showed themselves to be more refractory to regeneration, with only an increase of sprouting at the proximal end of peripheral nerve grafts placed into cervical lesions, following BDNF application into sensorimotor cortex (Hiebert et al., 2002). There was no growth-associated protein upregulation and no regeneration into peripheral nerve grafts by injured rubrospinal axons when BDNF was injected into the spinal cord injury site (Kwon et al., 2004). This is not the case with injection of fibroblasts genetically modified to secrete BDNF into a hemi-cervical aspiration lesion, which resulted in regeneration of 7% of rubrospinal axons for 3-4 segments caudal to the injury, and improved functional motor recovery (Liu et al., 1999). In contrast, if this treatment was delayed by 6 weeks, there was limited regeneration and functional recovery (Tobias et al., 2003; Shumsky et al., 2003). It is therefore difficult to tell if peripheral nerve grafts or BDNF-expressing fibroblasts are more growth-conducive for injured rubrospinal axons, but it appears that combining the injury site altering qualities of a peripheral nerve graft with the cell-body stimulating effect of BDNF is necessary for rubrospinal regeneration to occur in chronically injured fibres. Recently, viral vector mediated transfection of BDNF into rubrospinal cell bodies has resulted in their upregulation of growth-associated genes GAP-43 and Tα1 tubulin with less damage to

the parenchyma around the red nucleus than neurotrophins injection directly (Kwon et al., 2007), although no concomitant spinal cord study was published.

1.2.14.3 Neurotrophin-3

NT-3 stimulates survival and outgrowth of neurites from embryonic placodes and the neural crest (Kalcheim et al., 1992). In developing peripheral nerves, it is thought to suppress myelination, which commences as levels of NT-3 decrease. It acts as an inhibitory modulator of the trkC receptor (Cosgaya et al., 2002). NT-3 knockout mice die perinatally from cardiac maldevelopment (Donovan et al., 1996), but also have severe neurological abnormalities including some missing primary sensory, proprioceptive and sympathetic neuronal subpopulations. In the adult brain, NT-3 mRNA is found only in CA1 and CA2 neurons in the hippocampus (Ernfors et al., 1990) and it is not detected in the spinal cord, even after injury (Widenfalk et al., 2001).

The developmental defects seen in knockout mice demonstrate the importance of NT-3. It is also the only neurotrophin to have been used experimentally that has stimulated regeneration of injured CST axons. After CST injury, NT-3 injections into cord significantly increased anterogradely labelled CST fibres, whereas BDNF made no difference and NGF injection led to a moderate increase only, compared to control injections. Addition of IN-1 antibody injections led to significant regeneration of CST fibres past the lesion, compared to NT-3 alone and controls (although there were no images of axons crossing the lesion) (Schnell et al., 1994). Grill et al., (1997) reported that injured CST axon regenerated past an aspiration lesion filled with fibroblasts expressing NT-3, compared to unmodified grafts or grafts engineered to express NGF

(which the group had shown to increase sprouting of other CNS tracts the year before) which led to no CST regeneration. The latter group later performed mid-thoracic spinal cord dorsal hemisection lesions, but with a three month delay before implantation of fibroblasts genetically modified to express human neurotrophin-3 (NT-3) into and distal to, the lesion cavity. Upon sacrifice 3 months later, NT-3-grafted animals exhibited significant growth of corticospinal axons up to 15 mm distal to the lesion site and showed a modest but significant improvement in locomotor scores compared to control-grafted animals (Tuszynski et al., 2003). Thus, even chronic CST lesions were found to respond to therapeutic intervention with NT-3.

Zhou et al., (2003) performed unilateral cervical CST transections in adult rats and overexpressed NT-3 in the motorneurons distal to the lesion by transfecting them with NT-3 expressing adenovirus, retrogradely uptaken by injecting it into the sciatic nerve. This resulted in increased neuronal plasticity, as demonstrated by increased numbers of fibres crossing the midline compared to controls. In a further study, they repeated the experiment and, in addition, stimulated the CST cell body response by administering BDNF or GDNF with an adenoviral vector via six injections into the sensorimotor cortex. This resulted in significantly more sprouting of axons at the injury site than NT-3 treatment alone (Zhou and Shine, 2003), highlighting the importance of the cell body response.

1.2.14.4 Neurotrophin 4/5 (NT-4/5)

NT-4/5 is widely expressed in the adult rodent CNS (Timmusk et al., 1993). It is strongly upregulated in the distal stump after peripheral nerve transection, but its role in

regeneration is not well studied. NT4 knockout mice have selective structural and chemical deficits in sympathetic ganglia and their preganglionic innervation (Roosen et al., 2001), but are viable. If the distal stump of a mouse common peroneal nerve is replaced with a peripheral nerve graft of a NT-4/5-deficient or heterozygote NT-4/5 mouse, then regeneration is impaired, compared to wild-type grafts (English et al., 2005). Interestingly grafts from BDNF heterozygote knockouts had similar lengths of regenerating fibres as wild-type grafts. The regeneration of Ruffini endings in the periodontal ligament in NT-4/5-deficient mice following transection of the inferior alveolar nerve was slower compared to wild-type mice, and was partially reversed by administration of NT-4/5 to the knockout mice (Jabbar et al., 2007).

It has become clear that in addition to their axon outgrowth promoting effects, neurotrophic factors may positively influence axon regeneration by changing the responsiveness of regenerating fibres to outgrowth inhibitory molecules. NT-3, NGF and BDNF modulate growth collapse responses to Semaphorin-3A (Tuttle and O'Leary, 1998; Dontchev and Letourneau, 2002). Both NGF and BDNF have been shown to protect embryonic chick DRG growth cones from Semaphorin-3A-induced growth cone collapse in a concentration-dependent manner (Dontchev & Letourneau 2002), whereas Semaphorin-3F antagonises NGF-induced TrkA signalling (Atwal et al., 2003). Exactly how and where neurotrophin and Semaphorin-3 signalling pathways intersect is still unknown.

1.3 Summary of techniques used to assess spinal cord regeneration

The optic nerve is considered a useful model for investigating the failure of regeneration after CNS injuries. It is composed of only one type of nerve fibre – the RGC axons – and is easy to access, being separate from the brain. All fibres can be seen to be transected, without much damage to surrounding tissue, which minimises extended inflammatory processes. The cell bodies of the axons being studied are also easily accessed, with pharmacological agents, viral vectors and tracers easily administered into the vitreous humour of the eyeball, where they can diffuse and reach all RGCs. Finally, functional recovery can be assessed by monitoring visual evoked potentials in the visual cortex or superior colliculus.

Spinal cord injuries in rats are difficult to study, as compression injuries (although more closely mimicking human injuries) result in very large cystic cavities (Bresnahan et al., 1991), which are impossible for axons to regenerate through. Transection injuries, although allowing detailed examination of the lesion site and axons within it, may result in sparing of fibres, especially at the bottom of the lesion (You et al., 2003). Transection injuries can result in return of function (Freeman, 1954); even removal of 2cm of a dog's spinal cord (and reapposition with plasma clot) eventually results in the animal regaining the ability to walk, if it can be kept alive for long enough (unpublished observations by Freeman, (*in* Heimburger, 2005)), and it is now clear that the injured spinal cord spontaneously forms new intraspinal circuits after injury (Bareyre et al., 2004). The functional recovery seen by investigators with some of the treatments mentioned in the preceding sections seems to be ameliorating this intraspinal circuitry formation. Compression injuries have different histopathological features to transection

injuries, and physically mimic human injury more closely and therefore seem to be the better model to use for looking at functional recovery.

However, some degree of regeneration across injury sites will always be required for complete spinal cord lesions and anatomical tracing techniques are the gold standard method for assessing regeneration following injury. The main risk with this technique is spread of the tracer to adjacent tissues. For example, if injected distal, but too close to the lesion site, the label may spread into the lesion and therefore label fibres that have merely reached the lesion site, rather than labelling those that have regenerated across the lesion to the injection site. This may have occurred in a study by (Yick et al., 2004) who performed lateral hemisections at C7, but injected Fluorogold at T1, when assessing the efficacy of ChABC treatment, with subsequently excellent regeneration. Inadvertent injection of tracer into the lateral ventricles (located just under the motor cortex used for CST labelling) has been discussed at the beginning of Section 1.2.13.5 (pages 73-4), when discussing the discrepancies of CST labelling in different types of Nogo knockout mice (Steward et al., 2007).

The anterograde tracer (for labelling descending axons) of choice tends to be biotinylated dextran amine (Li et al., 1997) or, less frequently, cholera toxin subunit B (CTB)(Hagg et al., 2005) injected near the cell bodies of the injured neurons. Retrograde tracers used to label ascending fibres include CTB or CTB conjugated to horseradish peroxidase (Chong et al., 1996; Chong et al., 1999).

Some axon tracts are easier to study than others. For example, the dorsal columns synapse at the gracile nucleus (dorsal column nucleus; DCN) in the medulla. These can easily be checked for spared axons, as it is unlikely that axons would regenerate across a

lesion and several centimetres up to the DCN in the timecourse that most studies are carried out in. The rubrospinal tracts are located entirely within the dorsolateral funinculus in rodents, and a lateral lesion will completely transect them. The corticospinal tract, so important for locomotion, is unfortunately the most difficult to lesion completely, unless performing a whole cord transection. Descending fibres decussate at the medulla where they also split to form the DLCST and the ventral CST (located immediately below the dorsal columns (see Appendix Fig. A1, which is taken, with permission, from Steward et al., (2004)). Tracing of DLCST axons in mice with selective lesions of the dorsal column revealed that DLCST axons arborise extensively throughout the dorsal and ventral horns and that the overall territory that the DLCST axons invade is similar to the territory innervated by the CST axons in the main tract (Steward et al., 2004). Thus, a dorsal column lesion deep enough to transect / crush the ventral CST may spare the DLCST, which will send branches into the grey matter caudal to a lesion. These branches would be indistinguishable from any ventral CST axons that managed to regenerate across or - more likely – around the lesion. Careful analysis should enable one to distinguish spared CST axons, which will be in the correct white matter tract distal to the lesion, straighter and broader than the more 'feeble' regenerating fibres, although this is often ignored (see Cafferty et al., (2007) in reply to Steward et al., (2007). Sprouting of lesioned CST axons distal to a lesion is in itself an interesting phenomenon (well illustrated in Bradbury and Macmahon's (2006) review), but may also be misinterpreted as regeneration. It therefore comes as no surprise that so many claims of CST regeneration have gone unrepeated or are not replicated in other laboratories.

1.4 Attempts to stimulate CNS regeneration

In discussing the causes of failure of CNS neurons to regenerate, experimental methods of providing a suitable environment for regeneration, stimulating the cell body, depleting the glial scar, reducing the effect of inhibitory factors and use of neurotrophins have been discussed. Complex interactions between these factors in the injured CNS have been highlighted by studies showing, for example, that neurotrophic stimulation (Cai et al., 1999; Logan et al., 2006) or a vigorous cell body response to axotomy may decrease axonal sensitivity to inhibitory molecules. It is clear that certain CNS neurons have the ability to regenerate, but finding a simple means to target such a broad range of factors that prevent CNS regeneration is difficult. Some experimental therapies have been shown to have a broader range of actions than expected and are briefly discussed below.

One of the most encouraging papers regarding approaches to breach the inhibitory glial scar of CNS lesions used EphA4 knockout mice (Goldshmit et al., 2004). Their results suggested that blocking EphA4 signalling could reduce astrogliosis around the lesion site as well as disinhibiting some axons attempting to regenerate. One should note that not all CSPGs are inhibitory to axonal regeneration. Decorin, a small leucine-rich proteoglycan which has a single chondroitin sulphate or dermatan sulphate side chain, reduces astrogliosis and extracellular matrix deposition following cortical stab wounds (Logan et al., 1999). When decorin was infused around partial spinal cord lesions in adult rats, there was a downregulation of the inhibitory CSPGs NG2, neurocan, phosphacan and brevican, and the reduced scarring allowed regenerating axon to grow across and out of the lesion site (Davies et al., 2004). Since decorin downregulates

EGFR on tumour cells and cell lines (Csordas et al., 2000, Zhu et al., 2005) and EGFR activation appears necessary for signalling from several axonal growth inhibitory molecules, decorin could also have a direct disinhibitory effect on regenerating axons.

RhoA has been explored as a potential target for encouraging CNS regeneration, as it involved in the downstream signalling of many inhibitory molecules, including Nogo-A, MAG, OMgp, (Niederost et al., 2002) Ephs (Wahl et al., 2000), semaphorins (but not Semaporin-3) (Driessens et al., 2001; Swiercz et al., 2002) and CSPGs (Jain et al., 2004; Schweigreiter et al., 2004). RhoGTPases and their downstream effector proteins are expressed in lesioned neurons, and blockage of RhoA, by treatment with C3 transferase or Rho kinase (ROCK) inhibitors (Y27632), has resulted in impressive anatomical and functional recovery in different models of spinal cord injury (Cai et al., 1999; Lehmann et al., 1999; Dergham et al., 2002; Fournier et al., 2003; Sivasankaran et al., 2004; Bertrand et al., 2005). Current therapeutic strategies aimed at inactivating Rho or its downstream effectors are, therefore, likely to neutralise the repulsive effects of not only Nogo and other myelin inhibitors, but also a subset of repulsive semaphorins.

Similar to RhoGTPases, cAMP has been targeted to try and stimulate regeneration in the injured CNS. cAMP signalling may have either a direct influence on neurons by stimulating the synthesis of neuropoietic cytokines or influence neighbouring non-neuronal cells (Cao et al., 2006). Neuronal cyclic nucleotide levels also have modulatory effects on signalling from inhibitory molecules *in vitro*. For example, they can change the response of Xenopus motor axons to MAG from repulsion to attraction (Song et al., 1998). Arginase-1 and polyamines (that arginase-1 catalyses the production

of) are downstream of cAMP in the pathway that reduces the effects of myelin-derived inhibitors (Cai et al., 2002). Arginase-1 has been proposed as a target for stimulating regeneration in the CNS and it is noteworthy that it is upregulated after axotomy in peripheral neurons which regenerate vigorously (Costigan et al., 2002; Boeshore et al., 2004).

The initial observation that increases in cAMP may render cultured neurons less sensitive to the actions of several growth inhibitory proteins (Cai et al., 1999; Qiu et al., 2002; Neumann et al., 2002) led to *in vivo* experiments that manipulated neuronal cAMP signalling in an attempt to achieve functional CNS regeneration. Conditioning nerve injuries, which allow DRG axons to regenerate their centrally projecting neurites, are thought to increase endogenous cAMP within DRG cell bodies (Wu et al., 2007). Microinjection of a cAMP analogue into lumbar DRGs mimicked this conditioning lesion, allowing elongation of subsequently plated DRG neurites over CNS myelin substrates and increased the regeneration of injured central sensory branches across spinal cord lesions (Neumann et al., 2002; Wu et al., 2007).

Levels of cAMP can be increased either by exogenous administration (such as dibutyrl-cAMP) or by inhibiting phosphodiesterases (PDEs), which are the only means of degrading this second messenger. Rolipram readily crosses the blood-brain barrier (Krause and Kuhne, 1988) and is a specific inhibitor of the PDE4 subfamily of PDEs, which account for 70-80% of all PDEs in neuronal tissue, (Jin et al., 1999) by preventing PDE hydrolysis. Its efficacy and safety has been documented when it was trialled for human use as an anti-depressant (it was not as effective as amitriptyline, and caused more nausea), so any translational research would be rapid.

Administration of cAMP analogues following injury stimulates regeneration of axonal projections in the lesioned rat spinal cord (Qiu et al., 2002; Neumann et al., 2002), although others saw no difference in regeneration with dibutyrl-cAMP injection into DRGs (Han et al., 2004). Spinal cord injury results in a drop in cAMP levels in sensorimotor cortex (i.e. where CST cell bodies are located); subcutaneous rolipram infusion was shown to prevent this (Pearse et al., 2004). In the same experiment, db-cAMP injections used in combination with Schwann cell grafts in thoracic cord lesions and subcutaneous rolipram infusion resulted in more sparing of axons and increased levels of their myelination within the lesion and promoted axonal growth and functional recovery after spinal cord injury.

Using the phosphodiesterase inhibitor rolipram increased the sprouting of serotonergic axons into foetal spinal cod grafts placed in cervical cord lesions of adult rats with improved motor response (Nikulina et al., 2004)– though, with the lack of axonal tracing in this study, the most likely explanation for the latter finding is plasticity of motor axonal circuitry. Transfecting DRG neurons with a constitutively active CREB (which mediates the effects of cAMP transcription) also increased sprouting into dorsal column lesions (Gao et al., 2004). Conversely, others found that cAMP did not have much effect on injured dorsal column axons, but the addition of NT-3 had more of an effect on sprouting than NT-3 alone (Lu et al., 2004). Regeneration of the rat optic nerve has also been stimulated by increasing cAMP around injured RGCs, although its effect was by potentiation of CNTF rather than a direct action by itself (Cui et al. 2003;Wu et al., 2007; Hu et al., 2007). It should be noted, however, that conditioning nerve injuries which allow DRG axons to regenerate their centrally projecting neurites, an effect thought to be dependent on increases in endogenous cAMP, do not promote

regenerative growth through Semaphorin-3-positive scar tissue (Pasterkamp et al., 2001).

Manipulation of the ECM is another potential target in regeneration studies. (Houle et al., 2006) used a peripheral nerve bridge applied to a complete aspiration hemisection at C3, and applied ChABC to the distal end of the graft placed in a dorsal quadrant aspiration cavity at C5. These rats had better functional outcomes than controls (that was greatly diminished if the PN graft was cut, indicating that the recovery was due to regeneration through the grafts) and crucially had evidence of axons emerging from the distal end of the graft into spinal cord, with histological evidence of synapse formation there. Chen et al., (2007), used adeno-associated virus to express L1 in neurons and glia of the spinal cord, with subsequent effects on both axons and the glial scar. They observed enhanced functional recovery after spinal cord injury, reduced NG2 and GFAP expression around the lesion, growth of 5-HT (descending) fibres distal to the lesion (although there were no images of axons in continuity regenerating through or round the lesion in their paper) and elevated levels of cAMP, CREB and MAPK1 (which reflected enhanced signal transduction mechanisms) in AAV-L1 treated spinal cords. However, co-expression of L1 and NGF in adenoviruses administered to injured spinal cord (but not co-expression of NGF and other CAMs) reduced neurite sprouting – compared to increased sprouting with NGF overexpression alone (Chaudhry et al., 2006). Co-expression of L1 and NGF *in vitro* does not reduce neurite outgrowth over astrocytes, and it is thought that the *in vivo* effect may be due to L1's role in Semaphorin 3a receptor signalling, with its overexpression potentiating the growth inhibitory effects of Semaphorin 3a signalling.

Several cellular transplantation strategies would seem to be vital for regeneration of axons, as CNS injury sites are either cystic or filled with an unorganised mesh of inhibitory and inflammatory cells, through which axons cannot grow. Genetically modified fibroblasts (Grill et al., 1997; Liu et al., 1999), olfactory ensheathing cells (OECs) (Li et al., 1997), Schwann cell bridges (Xu et al., 1994) and stem cells (Lu et al., 2003; Roskams and Tetzlaff, 2005) have been used to bridge either side of the lesion site. They have all resulted in limited success in terms of axonal regeneration (see Reier, (2004) for review and comments on translational research with cellular transplantation techniques). OECs have prompted much excitement and have been used in a single-blinded Phase I human trial (Féron et al., 2005) and represent one of the first examples of translational research in the field of spinal cord regeneration. Two neurosurgical groups, in China (Huang et al., 2003) and Portugal (Lima et al., 2006), have started treating patients with spinal cord injury, presumably under the guises of a trial. The following section therefore discusses what led to these intriguing trials.

OECs are unique glia in that they reside both inside and outside the CNS, in the olfactory bulb and olfactory nerve, where they assist newly generated axons from olfactory neurons to grow towards mitral cells within the olfactory bulb throughout adult life. It was found that when implanted near the DREZ, they allowed injured sensory afferents to grow past this barrier into the spinal cord (Ramon-Cueto and Nieto-Sampedro, 1994). Later, regeneration of adult rat axons in injured thoracic cord beyond a Schwann cell bridge (Ramon-Cueto et al., 2000) and across a dorsal column lesion was demonstrated (Lu et al., 2001), even when transplantation was delayed by one month (Lu et al., 2002). OEC transplantation into lesioned CST, after hemisection and complete transection of the spinal cord led to significant functional recovery, including phrenic nerve function (Li et al., 1997; Ramon-Cueto et al., 2000; Li et al., 2003). OECs

do not myelinate axons that make up the olfactory nerve, and whether they myelinate regrowing axons at the injury site after CST lesion is contentious, especially as some investigators have found Schwann cells within the transplanted olfactory tissue. One of the main theories regarding how OECs work is the 'pathway hypothesis of repair', whereby they produce growth factors to attract and guide axons, (Boruch et al., 2001; Woodhall et al., 2001; Lipson et al., 2003), penetrate host astrocytes (just as they penetrate at the edge of the brain to enter the olfactory bulb), and then form straight channels through the lesion site (which are seen in olfactory nerve by EM). The inhibitory surfaces of astrocytes are turned aside and regenerating axons within are shielded from inhibitory influences such as myelin or fibroblasts in surrounding tissue (Raisman and Li, 2007). It is not clear how the inhibitory constituents of the glial scar are reduced to allow exit out of these channels; there is poor evidence of axons exiting lesions for any significant distance and it is likely that OECs are stimulating functional plasticity distal to / with the few axons that do exit spinal cord lesions. In view of this, current strategies using OECs are starting to use genetic modification to further enhance the OEC grafts – e.g. transfection with NT-3 or BDNF (Ruitenberg et al., 2003) - with subsequent increases in tissue sparing and axonal sprouting. Transfection with NT-3 (*ex vivo*) in particular appears to promote long distance CST regeneration after injury, compared to OEC grafts alone (Ruitenberg et al., 2005).

However, not all studies have replicated the findings of axonal regeneration with OEC treatment, with minimal effect at the DREZ (Gomez et al., 2003; Riddell et al., 2004) or in primary afferents in spinal cord (Ramer et al., 2004b). Interestingly, the latter group found that OECs transplanted into spinal cord lesions facilitated Schwann cells in filling the lesion site and increased axonal sprouting into and across the lesion (although not of rubrospinal axons) (Ramer et al., 2004a). One explanation for these discrepancies,

especially those within the same laboratory, is because of varying responses of different tissues to OECs. Another reason is that researchers use different methods of accessing and purifying the OECs from the olfactory basal lamina. In their current clinical trial, the Australians aim to use absolutely pure OEC preparations, although this is difficult to prove (Féron et al., 2005); Raisman's group (due to start clinical trials with dorsal root injured patients) specifically use a formulation with olfactory nerve fibroblasts (Li et al., 2005) and there is speculation that the 'impure' Schwann cells may actually aid OEC-driven regeneration (see Oudega (2007). The accessibility of olfactory mucosa via autologous nasal biopsy (Feron et al., 1998) from which OECs can be grown (Bianco et al., 2004), has allowed rapid translation of this research from rodents to humans. Nevertheless, it is ironic that the human trials using OECs in spinal cord injury were initiated before specific analysis of OECs was performed in a clinically relevant spinal cord injury model.

Note that clinical trials are also taking place using transplantation of autologous activated microglia into spinal cord injury sites, which is claimed to stimulate axonal regeneration in experimental models in rodents (Rabchevsky and Streit, 1997; Schwartz et al., 1999) - see Schwartz and Yoles (2006) for review. The results of Phase I trials suggesting that it is a safe treatment (Knoller et al., 2005) and Phase II trials are now underway. However, with the exception of Prewitt et al., (1997) and Lazarov Spiegler et al., (1996), over ten years ago, similar findings of axonal regeneration have yet to be reproduced outside Schwartz's group - compared to over 50 publications regarding the benefits of OEC treatment - and will not be discussed further.

Some combination therapies aimed at targeting multiple factors that prevent CNS regeneration - e.g. both intrinsic and extrinsic influences - have been shown to act synergistically to enhance axon regeneration after spinal cord injury. They may yet lead to a 'magic shotgun' (as opposed to the 'magic bullet' panacea of cancer medicine) treatment to stimulate functional restoration of the injured spinal cord. The first published example of this combinatorial approach was by Lu et al., (2004) who performed cervical dorsal column transections in rats, with implantation of bone marrow stromal cells into the lesion, which prevented cyst formation. The intrinsic cell body response was stimulated by injection cAMP into the L4 DRG and the extrinsic environment made more conducive to regeneration by injecting NT-3 into and distal to the lesion. They found that the combination of the two treatments stimulated injured axons to regenerate into and beyond the lesion site, but regeneration beyond the lesion site did not occur with treatment using NT-3 or cAMP alone.

Fouad et al. (2005) attempted to address multiple impediments to regeneration by using a combinatory strategy after complete spinal cord transection in adult rats. They used ChABC to reduce inhibitory cues in the glial scar, Schwann to provide a growth-supportive substrate for axonal regeneration and injected OECs either side of the bridge to enable regenerated axons to exit the bridge to re-enter the spinal cord. The combination of Schwann cell bridge, olfactory ensheathing glia, and ChABC provided significant functional motor benefit compared with grafts only or untreated controls. However, there was no increase in the number of serotonergic axons in the caudal spinal cord. The effects of chondroitinase combined with a Schwann cell bridge only (no OEC injections) were not studied. That experiment could have shown whether enzyme treatment in combination with a spinal cord bridge can promote axonal growth beyond the bridge and affect motor function.

However, despite their advances, none of these studies show a vast improvement over all others and they do not always result in a synergistic effect. For example, although NgR antibody treatment increases axonal sprouting and functional recovery after spinal cord contusion, addition of rolipram as well did not make any difference (Wang et al., 2006). However an encouraging point to take from this study was that the NgR-Fc treatment was delayed by seven days and therefore much more closely mimicked the human setting of spinal cord injury, where any treatment in the UK is, at present, likely to be delayed until transfer of the patient to a spinal injuries unit. Although cellular transplantation studies are often delayed to avoid the early immune response, it is encouraging to see other experimental studies comparing acute and delayed timing of treatments to try and stimulate axonal regeneration - e.g. (Kwon et al., 2002; Nikulina et al., 2004). Administration of experimental therapies at the time of injury is clearly an impossible method to replicate in future human trials.

Combinatorial therapy appears to be the way forward in spinal cord regeneration treatment, but at present, research still needs to focus on which are the best therapies to combine. Although most research has concentrated on the inhibitory factors in myelin, this may be an oversimplification of what is occurring there, with many neurons not containing receptors for these proteins and, given the right stimulus, CNS axons can grow long distances within myelin-filled white matter tracts.

This thesis will study two of the areas showing great promise with respect to CNS regeneration:

1. Inflammation-induced stimulation of the cell body response and subsequent regeneration (Lu and Richardson, 1991; Leon et al., 2000);
2. The functional role of NG2, which is the most strongly upregulated CSPG at CNS injury sites (Jones et al., 2002; Tang et al., 2003).

1.5 Experimental aims of the studies described in this thesis

1.5.1 Inflammation, growth associated protein expression and CST regeneration

The greatest regeneration seen in dorsal column and optic nerve models of CNS injury were both a result of inflammation around the cell bodies of the CNS axons being stimulated them to regenerate (Lu and Richardson, 1991; Leon et al., 2000). Corticospinal neurons do not regenerate axons to any significant extent along peripheral nerve grafts inserted into the spinal cord or brainstem (Richardson et al., 1982b; Ye and Houle, 1997; Blits et al., 2000) and display upregulation of growth-associated genes only after intracortical lesion of their axons and not after spinal injury (Tetzlaff et al., 1994; Mason et al., 2003). Against this background, I have investigated the possibility that LPS-induced inflammation around the cell bodies of corticospinal tract neurons would enhance their expression of growth-associated genes (c-jun, ATF3, SCG10 and

GAP-43) and promote regeneration of their axons following spinal cord injury. It is of particular importance and interest to investigate these questions in relation to corticospinal neurons because their axons constitute the major descending motor pathway, and because they display very poor regenerative responses to injury.

Although zymosan has been used to produce inflammation in the retina and promote regeneration in crushed optic nerve, the eyeball is a highly 'immune-privileged' site, and more resistant to inflammation than cerebral cortex. It may be significant that LPS injection into the vitreous body was not a sufficient stimulus to induce regeneration of optic axons (Leon et al., 2000). However, zymosan particle injection into cortex caused substantial cavity formation and a glial scar (Fitch et al., 1999), whereas single injections of LPS into cortex caused minimal cavitation (Montero-Menei et al., 1994; Montero-Menei et al., 1996).

As my experiments aim to cause no damage to the corticospinal cell bodies located in layer V of the cerebral cortex, or their axons within the cortex, LPS is used as the inflammatory agent and is applied onto the surface of the cortex (Methods section 2.1 and Results section 3.1, 3.2). The degree of inflammation is gauged by examining the local microglial reaction and macrophage response with OX-42 antibody, which recognises the C3 complement receptor, which functions even in the absence of a phagocytic response (Kreutzberg and Barron, 1978). This is a useful antibody to use, as it recognises macrophages and all types of microglia (phagocytic, non-phagocytic and resting). Other markers do not recognise microglia unless they are phagocytic (when they resemble macrophages), such as OX-41, ED1 and ED2 (Graeber et al., 1988).

I also intended to not damage corticospinal neurons in the subsequent set of experiments where LPS solution was injected directly around CST neuronal cell bodies, to try to increase the local concentration of LPS and therefore exert a greater inflammatory stimulus around them (Methods section 2.4 and Results chapter 3.4). Lack of neuronal damage has been documented with *chronic* infusion of LPS into hippocampus. This forms a focal necrotic lesion at the infusion site with a surrounding region showing activation of astrocytes and macrophages, but significantly no loss of neurons (Szczepanik et al., 1996).

I then attempt to produce greater inflammation around CST cell bodies with topical application of zymosan with or without concomitant corticospinal tract injury and anterograde CST axonal labelling (Methods section 2.5 and Results chapter 4). Although it has not been studied extensively in brain, zymosan is known to be a cell wall preparation of the yeast *Saccharomyces cerevisiae*, that has been used for over 50 years both *in vivo* and *in vitro* as a phagocytic stimulus and one of the most inflammatory agents known (Pillemer et al., 1941; Di Carlo et al., 1958; Gantner et al., 2003). Zymosan is composed of β-glucans, mannans, chitins, and activates several macrophage receptors, including TLR2, dectin-1, the mannose receptor, and CD11b/CD18 (complement receptor 3). Recent reports theorise that simultaneous engagement of different macrophage receptors, such as TLR2 and dectin-1, by zymosan synergistically activates inflammatory pathways leading to increased TNF-α production and more of an oxidative burst than other inflammogens (Gantner et al., 2003; Brown et al., 2003). Dectin-1, a C type lectin that recognizes β-glucans, also signals independently of TLR2 by activating Syk kinase, leading to induction of IL-2 and IL-10 production (Rogers et al., 2005). An important role for zymosan and dectin-1 in

inducing chronic autoimmune arthritis via activation of innate immune mechanisms and cytokine production has been previously demonstrated (Yoshitomi et al., 2005).

In my zymosan experiments, I also investigate the astrocyte and NG2-glia response to a large inflammatory stimulus, using antibodies to GFAP and NG2, to compare with the findings in microglia. I also look at the expression of Nogo-A, because during development Nogo-A is expressed in all neuronal cell bodies and in growing axons. Nogo-A is downregulated later in development by most CNS neurons and excluded from the axons of others. Some intrinsic CNS neurons, notably retinal ganglion cells, Purkinje cells, some hippocampal neurons and corticospinal tract neurons, retain high levels of Nogo-A in their cell bodies (but not their axons) during adult life. In contrast to intrinsic CNS axons, mature and regenerating peripheral nerves express Nogo-A strongly in their axons (Hunt et al., 2003). Hence *axonal* Nogo-A expression appears to be correlated with the ability of the axons to grow, form fascicles and regenerate. Using immunohistochemistry to visualise Nogo-A in inflamed cortex would allow one to confirm this theory that Nogo-A may be a novel regeneration-associated molecule if injured CST neurons were stimulated to both regenerate and upregulate it.

As an adjunct, the effect of LPS-induced inflammation on regeneration of injured dorsal roots is also studied (Methods section 2.3 and Results section 3.3). Inflammation around the DRG cell bodies has been shown to mimic a conditioning lesion and promote dorsal root regeneration. However, the effect of inflammation around the inhibitory barrier of the DREZ is not known. In my experiments, dorsal roots are transected and LPS applied onto the DREZ. (CT-HRP labelled) regenerating axon fibres are then compared with uninflamed animals at the DREZ. Systemic LPS has been shown to have effects in the

brain (Bohatschek et al., 2001) and injured DREZ (Lazar et al., 1999), and increased rates of Wallerian degeneration in the spinal cord (Vallieres et al., 2006). I therefore prolong the inflammatory stimulus in a subgroup of mice with post-operative intraperitoneal injections of LPS; local and distant microglial/macrophage responses are analysed as well as regenerating dorsal root axons, to see whether sustained inflammation may promote regeneration across the DREZ.

1.5.2 ATF3 upregulation in glia during Wallerian degeneration in peripheral nerves and CNS white matter

Following injury to peripheral nerve trunks, the resident cells in the distal stump undergo proliferation and many changes in gene expression, and are joined by haematogenous monocytes. These events enable debris to be cleared, the extracellular matrix to be remodelled and the bands of Büngner to be made ready to receive the regenerating axons. Non-neuronal cells in the proximal stump are less affected than those in the distal stump. Transcription factors control the changes in gene expression that occur in the distal stump of an injured peripheral nerve, and it has been recognised for some years that an upregulation of c-Jun and c-fos in the non-neuronal cells occurs soon after injury and that Krox-20 and SCIP are upregulated (Zorick et al., 1996). Wallerian degeneration also occurs in the CNS distal to a site of axotomy. The best known features of responses of CNS glia to axotomy are the generation of reactive astrocytes and microglia. The transcriptional control of these cellular events is also poorly understood, but there is little upregulation of c-Jun in the degenerating optic nerve following crush injury (Vaudano et al., 1998). ATF-3 is one member of a large

family of bZip leucine zipper transcription factors that bind to promoters responsive to cAMP and phorbol ester at the related cAMP (CRE) and phorbol ester response elements and AP-1 sites (reviewed in Hai et al., 2001). ATF3 is particularly interesting in the context of axonal regeneration because it can form heterodimers with c-Jun (Hai and Hartman, 2001) and its regulation in axotomised neurons closely mimics that of c-Jun (Tsujino et al., 2000).

This thesis seeks to examine ATF3 expression in the non-neuronal cells of injured peripheral nerves or CNS glia during Wallerian degeneration. The DRG model of injury is used, as Wallerian degeneration distal to injury of the peripheral processes (sciatic nerve) occurs in the PNS, and Wallerian degeneration distal to injury of the central processes of the same group of neurons (dorsal root) occurs in the CNS.

1.5.3 Axonal regeneration in the NG2 deficient mouse

The full role of NG2 is yet to be elucidated and further experimental evidence is needed to prove the NG2 inhibitory hypothesis, discussed in Section 1.2.6.1 above. To determine whether the failure of CNS axons to regenerate after injury is due to the presence of NG2, mice in which NG2 is not expressed are studied in this thesis. My approach to elucidating the possible roles of NG2 in inhibiting axonal regeneration after injury is to compare regeneration and reinnervation in a variety of well-established CNS and PNS injury models, between age and sex-matched normal and NG2 knockout mice. Thus, axonal regeneration in the CNS after lesions of the corticospinal tract and dorsal column are studied, as well as at the dorsal root-spinal cord interface following dorsal root injury. As NG2 is expressed in the injured peripheral nervous system, regeneration and reinnervation in the peripheral nervous system following facial and sciatic nerve injuries is also examined.

Chapter 2 – Methods

Surgical procedures

All surgery was performed under aseptic conditions and was approved by the local ethical committee and by the Home Office under UK animal experimental legislation. Unless otherwise stated, all animals were initially anaesthetised with 4% halothane and anaesthesia was maintained with 1.5% halothane (plus oxygen and nitrous oxide 1:1).

Following surgery, all animals received intramuscular buprenorphine (20 mg/kg) opiate analgesic (Vetergesic; Alstoe Ltd., Yorks., UK) and recovered in a transparent incubator to allow checks for unexpected deficits.

Microscopy

All sections were analysed and digital images taken using a Zeiss Axiophot microscope equipped with Openlab image processing software (Improvision, Coventy, UK), except for BDA-labelled CST (chapters 2.1 and 2.5) and DiAsp-labelled DRGs (chapter 2.7.4.1), which were imaged with a Leica confocal microscope.

2.1 *Effects of topical lipopolysaccharide-induced inflammation on expression of growth-associated proteins / genes by corticospinal neurons*

2.1.1 Animals

Adult female Sprague-Dawley rats (220-250g; n = 66) were used.

2.1.2 Application of lipopolysaccharide

The scalp was incised in the midline and bilateral craniotomies performed to expose the surface of the motor cortex (localised according to the atlas of Paxinos and Watson (1998)). A 3mm x 4mm piece of parietal bone was removed from the cranium, centred 3mm caudal to the bregma and 2mm from the midline. The dura was opened and 500μg of LPS from Escherichia coli, serotype 055:B5 (Sigma, UK) was applied - as a powder - to the exposed pial surface of the right hemisphere (Fig. 2.1a). The powder dissolved to a paste on contact with the CSF and was kept in place by application of Gelfoam (Johnson & Johnson, Skipton, UK), which was anchored to the cranium with Histoacryl glue (B. Braun, Melsungen AG, Germany). In preliminary experiments it was found that if less than 500μg of LPS was applied to cortex, inflammation did not consistently extend as deep as layer V. As a control for the effects of surgery, the contralateral cortex was exposed but LPS was not applied. The scalp incision was closed with Michel clips and the animals allowed to recover. Survival times were 1 day (n = 3), 3 days (n = 8), 7 days (n = 6), 14 days (n = 4) and 1 month (n =4) after LPS application. A further 9

LPS-treated animals (survival 3 days to 1 month) also received a left corticospinal tract (CST) transection lesion at the time of LPS application in order to determine if concomitant axotomy is a requirement for growth associated protein expression. A C3/4 laminectomy was performed and microscissors used to cut the area between the left dorsal root entry zone and the right CST down to a depth of 2mm. The dura was closed and the wound closed in layers. In 6 other animals (survival 3 days (n = 3), 7 days (n = 1) and 14 days (n = 2)), the motor cortex was exposed unilaterally, Gelfoam applied on top of the burrhole and the scalp then closed (without the application of LPS). In 3 further animals (survival 3 days) the motor cortex was exposed but neither LPS nor Gelfoam were applied prior to closing the scalp, as a control for the possibility that the surgical procedure or the application of Gelfoam contributed to any of the effects observed (see Table 2.1).

2.1.3 Retrograde tracing with Cholera Toxin B (CTB) or Fluorogold (FG)

In order to identify the neuronal cell bodies giving rise to the CST in animals treated with LPS, the contralateral cervical spinal cord was injected with CTB (10mg / ml in sterile H_2O; List laboratories Inc, Campbell, CA, USA) in a further 5 rats. Three days before the animals were killed, a laminectomy was performed at C3/4, the dura opened, and 1.5µl of CTB was slowly injected into the CST, through a Hamilton syringe attached to a fine glass pipette (Fig. 2.1b). The dura and wound were closed in layers. The survival periods after LPS application for these animals were 3 days (n = 2), 14 days (n = 2) and one month (n = 1). Coronal sections of brain were processed for the visualisation of both growth associated proteins and CTB (described below). In a further 3 animals (survival 3 days) Gelfoam impregnated with 1.5µl of Fluorogold

(Molecular Probes, Oregon, USA) (diluted to 2% in sterile water) was inserted into a contralateral (left) C6 corticospinal tract lesion at the same time as LPS was applied to the cortex. Coronal sections of the brains of these three animals were immunostained with OX42 antibody in order to examine the relationships between microglia and CST cell bodies after LPS treatment (see below).

Figure 2-1 Summary of design and procedures for LPS experiments.

Fig. 2.1**a**. Unilateral application of lipopolysaccharide (LPS) to the pial surface of motor cortex through a cranial burrhole with sham operation on the contralateral side, to investigate the inflammatory response and expression of growth-associated proteins.

Fig. 2.1**b**. Unilateral LPS application to the pial surface and injection of Cholera toxin B or placement of Fluorogold (FG) (retrograde tracers) into the contralateral corticospinal tract (CST) at C4 or C6 respectively, to identify CST neurons displaying changes in growth-associated protein expression.

Fig. 2.1**c**. Application to the pial surface of LPS with injection of biotinylated dextran amine (BDA; anterograde tracer) into motor cortex and transection of contralateral CST. LPS application omitted in control animals.

a. LPS application to pial surface of cortex

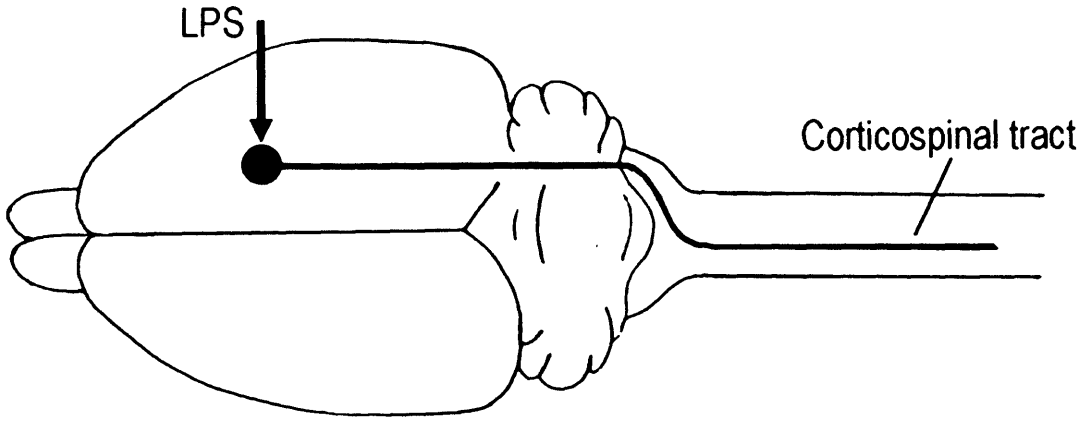

b. LPS application and retrograde tracer placement

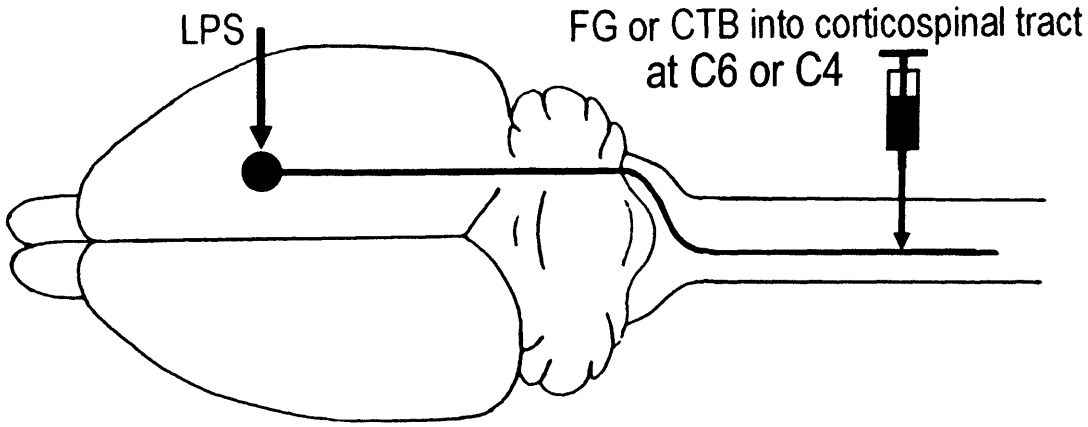

c. Corticospinal injury and anterograde tracer (BDA) +/- LPS application

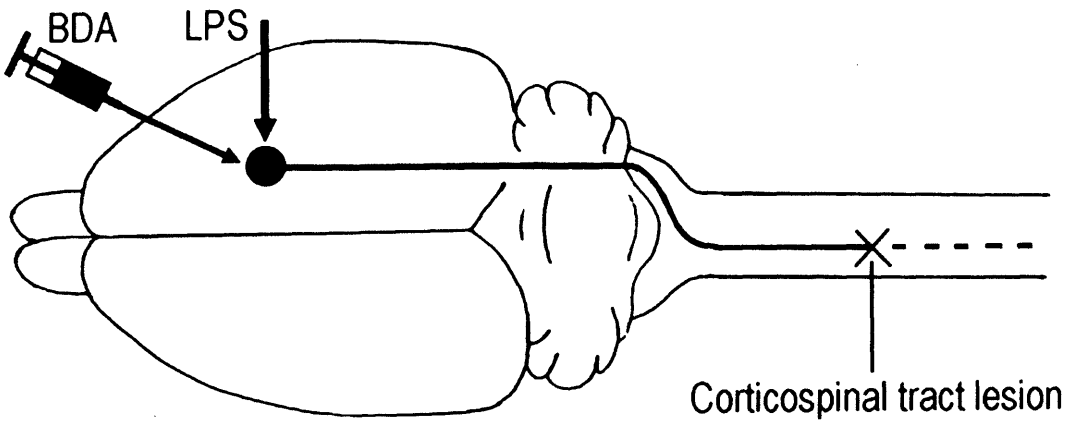

2.1.4 Control Studies: Facial nerve injury

As a positive control, expression of growth-associated proteins was induced in facial nucleus neurons by facial nerve injury – a well established experimental model to look at the cellular response of the injured brain (Kalla et al., 2001). In 6 adult rats, anaesthetised as described above, a 1cm skin incision was made posterior to the right ear, and the facial nerve exposed and crushed for 10 seconds with watchmakers' forceps proximal to its branch point. The skin incision was closed with Michel clips and all animals were killed after seven days.

2.1.5 Perfusion and histological processing

Animals were overdosed with halothane and intraperitoneal pentobarbitone, and perfused transcardially with 200ml of PBS followed by 350ml of 4% paraformaldehyde in 0.1M PBS (PFA). The brain, or pons (containing the facial nucleus) was removed and immersed in PFA fixative solution for 2 hours. Dissected tissue specimens were then cryoprotected for 40 hours in PBS containing 30% sucrose.

Antibodies

ATF3: polyclonal (raised in rabbit); dilution 1:800; source - Santa Cruz, CA, USA.

c-Jun: polyclonal (raised in rabbit); dilution 1:5000; source – Dr. A. Behrens (Cancer Research, UK), gift.

SCG10: polyclonal (raised in rabbit); dilution 1:3000; source – Dr. G. Grenningloh (University of Lausanne, Switzerland), gift.

OX42: monoclonal (raised in mouse); dilution 1:3000; source – Serotec, Oxford, UK.

GFAP: monoclonal (raised in mouse); dilution 1:800; source – Sigma, St. Louis, Missouri, USA

CTB: polyclonal (raised in goat); dilution 1:100,000 – List Biological Laboratories, CA, USA.

Single label immunohistochemistry

Coronal sections of brain through the motor cortex and pons (containing the facial nucleus) were cut at 40μm using a freezing microtome and collected in 0.1M PBS. Care was taken to ensure that every section to be reacted for growth-associated protein expression was immediately adjacent to a section reacted for CTB. All sections were then washed in 0.3% H_2O_2 for 15 minutes to remove endogenous peroxidase, followed by 3 x 5 minute PBS washes (or 0.1M tris-buffered saline (TBS) + 0.05% Tween 20 (TNT), for OX42 and CTB). Then followed a one hour wash in blocking solution, using 1% bovine serum albumin (BSA), 0.1% Triton-X and 10% normal goat serum (NGS) in PBS (for sections to be reacted with the antibodies against ATF3, c-Jun and SCG10) or 2% horse serum in TBS (for OX42, GFAP and CTB). Serial sections were incubated with primary antibody (made up in appropriate blocking solution) against ATF3, c-Jun SCG10, OX42, GFAP or CTB for 72 hours at 4°C. Sections of motor cortex and pons incubated with the appropriate blocking solution rather than with primary antibody, served as negative controls. After 3 washes in PBS / TNT, sections to be immunoreacted for ATF3, c-Jun and SCG10 were incubated for 2 hours in 1:200 goat anti-rabbit biotinylated secondary antibody (preincubated with 10% normal rat serum and microfiltered with a syringe-driver to adsorb non-specific anti-rat immune complexes). Sections to be immunoreacted for CTB were incubated in 1:200 horse anti-goat biotinylated secondary antibody and sections to be immunoreacted for OX42 or

GFAP were incubated in horse anti-mouse biotinylated secondary antibody (all diluted in appropriate blocking solution). After 3 further washes, ATF3, c-Jun, SCG10 and CTB sections were reacted with an avidin-biotin complex (ABC) kit (Vectastain, Burlingame, CA, USA) for 2 hours, again washed in PBS and finally reacted with 0.04% 3-3' diaminobenzidine tetrahydrochloride in 0.015% H_2O_2 in TBS until a brown reaction product appeared (usually about 12-15 minutes). OX42 sections were washed in TNT, incubated in streptavidin-conjugated horseradish peroxidase (streptavidin-HRP) (Vector Laboratories, Burlingame, CA, USA) for 1 hour at 1:200 in TBS, washed in TNT buffer, reacted with Tyramide Cy3 (NEN Life Science Products, Boston, USA) for 30 minutes at 1:400 in TBS and then washed in TBS. GFAP sections were washed in TNT, incubated in horse anti-mouse IgG FITC conjugate (Sigma, St. Louis, Missouri, USA) at 1:100 for 1 hour and then washed in TBS. Sections for fluorescence microscopy were mounted onto agar-coated slides and coverslipped immediately with glycerol containing 1,4-diazabicyclo[2,2,2]octane (DABCO). Sections reacted with ABC were dried overnight and dehydrated through ascending concentrations of alcohol, followed by Histoclear (National Diagnostics, Georgia, USA) before being mounted onto slides and coverslipped with DPX (Merck, Poole, UK).

Double label immunohistochemistry

The steps followed were the same as for OX42 immunofluorescence processing until the stage of incubation in primary antibody solution. At this point, primary antibody against ATF3, c-Jun or SCG10 was mixed with the antibody against CTB, made up in blocking solution containing 2% normal horse serum. Sections were then rinsed in TNT (3 x 5 minutes), incubated for 2 hours in 1:200 horse anti-goat biotinylated secondary antibody (made up in TNT), rinsed again in TNT and incubated for 1 hour in a mixture of 1:200 streptavidin-HRP and 1:100 donkey anti-rabbit FITC (made up in blocking

solution). After 3 further TNT washes, sections were reacted for 30 minutes in 1:400 Tyramide Cy 3, washed in TBS, mounted onto slides and coverslipped immediately with DABCO.

The steps followed for retrograde labelling with Fluorogold were the same as for single OX42 immunofluorescence processing up to the stage of incubation with the ABC kit. At this point, sections were instead incubated with 1:200 horse anti-mouse Alexa Fluor 568 (Molecular Probes, Invitrogen Corporation, Paisley, UK) for one hour, washed in TBS, mounted onto slides, coverslipped immediately with DABCO and photographed.

In situ hybridisation

An additional 16 animals were used for in situ hybridisation studies. Of these, 15 had unilateral LPS application to the pial surface of motor cortex as described above and 1 had a unilateral opening of dura only (as a control). They were sacrificed at 3 days (n = 4, plus 1 control), 7 days (n = 4), 14 days (n = 3) and 1 month (n = 4) after LPS application, by lethal overdose of halothane and intraperitoneal pentobarbitone. Their brains were removed and immediately frozen in Tissue-tek cooled with dry ice.

GAP-43 cRNA antisense probes were generated from pcDNA-GAP-43, which contains the 680 base pair open reading frame of rat GAP-43 cDNA and labelled with digoxigenin according to the manufacturer's recommendations using an RNA labelling kit (Boehringer Mannheim, Germany), as described by Mason et al. (2002). Sections derived from animals at all survival times were processed under identical conditions, at the same time.

Coronal cryostat sections of motor cortex directly under the area of LPS application were cut at a nominal thickness of 12μm, thaw-mounted onto slides coated with 3-aminopropyltriethoxy-silane, and fixed with 4% paraformaldehyde in PBS overnight at 4°C. After washing in PBS, sections were treated with 0.1M HCl, and washed in PBS, incubated in 0.1M triethanolamine containing 0.25% acetic anhydride, and then washed with PBS, dehydrated in an ascending ethanol series, and air dried. Prehybridisation was carried out at 37°C for 3 hours with a mixture of prehybridisation buffer / deionised formamide 1:1 (containing 50% formamide, 25mM ethylenediaminetetra-acetic acid (EDTA), 50mM, pH 7.6 Tris–HCl, 2.5x Denhardt's solution, 0.25mg/ml tRNA (Boehringer Mannheim), and 20mM NaCl). The digoxigenin-labelled GAP-43 probe was prepared at a concentration of 3μl/ml with hybridisation buffer containing 50% formamide, 20mM Tris–HCl (pH 7.50), 1mM EDTA, 1x Denhardt's solution, 0.5mg/ml tRNA, 0.1mg/ml poly (A) RNA (Sigma), 0.1M DTT, and 10% dextran sulfate. Hybridisation was performed overnight at 62°C. After hybridisation, sections were washed in 0.2x standard saline citrate (SSC), containing 30mM NaCl, and 3mM Na-citrate, pH 7.0 and then in 0.1x SSC / 50% formamide at the hybridisation temperature. Sections were equilibrated with buffer 1 (100mM Tris–HCl, 150mM NaCl, pH 7.5), incubated in modified buffer 2 (1% Boehringer blocking reagent, 0.5% BSA fraction from Sigma in buffer 1) and then incubated with alkaline phosphatase-coupled antibodies to digoxigenin (Boehringer Mannheim, Germany) at a dilution of 1:700 in modified buffer 2 overnight at 4°C. Sections were washed in buffer 1, equilibrated in buffer 3 (100mM Tris-base, 100mM NaCl, 50mM MgCl2, adjusted to pH 9.5), and developed in the dark with buffer 3 containing 0.34mg/ml 4-nitroblue tetrazolium chloride (Sigma), 0.175mg/ml 5-bromo-4-chloro-3-indolylphosphate (Sigma), and 0.25mg/ml levamisol (Sigma). Development was stopped by washing with buffer 4

(10mM Tris–HCl, 1mM EDTA, pH 8.0), following which the sections were dried and mounted in DPX beneath glass coverslips.

2.1.6 Quantification of OX42-labelled microglia

In three LPS-treated animals surviving 3 days, 14 days and 1 month after application of LPS, microglia were counted in layer V of cortex under the area of LPS application and under the area of the contralateral (control) burrhole. For each animal, activated and ramified microglia were counted within a counting frame of 400μm x 340μm superimposed on a digital image of layer V captured using a x20 objective lens. The number of activated and ramified microglia (means of 3 counts) was calculated as well as the relative proportions of activated and ramified microglia (expressed as percentages) for each survival time (see Table 2.1).

2.2 Corticospinal tract injury and anterograde tracing with Biotinylated Dextran Amine (BDA)

To study the effect of cell body inflammation on CST axon regeneration, the CST was lesioned at the same time as LPS was applied to the cerebral cortex (n = 4) or the dura opened without application of LPS (n = 4), and at the same time BDA was injected into the cortex to label CST axons (Figs. 2.1c and appendix Fig. A1). The spinal cord was exposed at C3/4 by laminectomy and the area between the left dorsal root entry zone and the midline was cut to a depth of 2mm with microscissors, and the cut extended to cross the midline, undercutting the midline spinal vein to minimise ischaemic damage. Overlying muscle and skin was sutured. Immediately thereafter, a midline incision was

made over the skull, a 4mm x 2mm burr hole made over the right parietal cortex, the dura opened and LPS powder (500μg) placed on the pial surface (LPS application omitted in control animals). Then BDA (Molecular Probes, Oregon, USA) dissolved in 0.1M phosphate-buffered saline (PBS) (10% solution) was injected into the cortex, about 1mm below the pial surface, through a Hamilton syringe attached to a glass micropipette. The micropipette was introduced into the cortex at a very shallow angle from the rostral edge of the burr hole and advanced 4mm in a caudal direction, and parallel to the cortical surface. The BDA solution (2.5μl) was injected as the pipette was slowly withdrawn to its entry point. The injection was then repeated, via the same entry point, but with the micropipette directed 1mm medial to the initial injection track, and repeated again, with the pipette directed 1mm lateral, thus delivering a total of 7.5μl BDA solution. The exposed area of cortex was covered with Gelfoam, the wound sutured and the animal checked upon recovery to ensure that no unexpected deficits were present. Survival time for all animals in this group was three weeks.

Any inflammatory response due to damage induced by the relatively large volumes of BDA injected (see Fig. 3.10d) would occur in both LPS-treated and control animals and would therefore not significantly impact on or obscure effects due to LPS

2.2.1 Perfusion and histological processing

Animals were sacrificed as described in Section 2.1.5 above. The cervical spinal cord and brainstem were removed and post-fixed in PFA for 2 hours. Tissue specimens were then cryoprotected in 30% sucrose and frozen in Tissue-Tek (Sakura, Zoeterwoude, Netherlands), cooled with dry ice.

BDA labelling immunohistochemistry

Serial horizontal cryostat sections through the spinal cord, encompassing the entire CST, and transverse sections of the medulla through the pyramids, were cut at 40μm and collected in 0.05M TBS. The free floating sections were rinsed in 0.05M TBS and 0.5% Triton X-100 (TBST), incubated in 0.3% H_2O_2 for 15 minutes, rinsed in TBST (2 x 10 minutes) and incubated at 1:200 dilution of ABC overnight at 4°C. They were then rinsed in TBST, incubated in Tyramide Cy3 at 1:400 for 30 minutes, rinsed in 0.05M TBS and mounted as above.

2.2.2 Quantification of anterogradely labelled corticospinal tract axons

In the four LPS-treated animals in which BDA was injected into motor cortex, and the four control animals (BDA injected; no LPS applied), consecutive serial horizontal sections through the entire cervical lesion site (9 sections per animal) and 12 transverse sections through the medulla were cut at a thickness of 40μm and scanned with a Leica confocal microscope. Projection images used an accumulation of 3 scans of each optical section and represent stacks of 20-25 optical sections merged together, with a resolution of 1024 x 1024 pixels. The source of these digital images was then blinded from the quantifier. Images were standardised to 500μm x 500μm. For the horizontal sections, a frame was made which hid each image from view except for a 60μm wide window, running transversely across the image, orientated perpendicular to the CST (corresponding to the white boxes in Fig. 3.10). The total number of BDA-labelled axons traversing this window, positioned 0.4mm rostral to the lesion site, were counted through the 9 serial images of the CST. The number of axons traversing the window and

branching within it were separately recorded from the serial horizontal sections and totalled for each animal. The total number of labelled CST axons in each animal was estimated by counting the number of labelled axons in a transverse section of the medullary pyramid, photographed at a magnification of 60x (mean of counts of 3 sections).

Anterograde labelling is variable, presumably because of variations in the uptake of BDA in the motor cortex, and can cause bias if *total* numbers of labelled axons or branch points are compared between animals. In order to normalise for differences in the tracing efficiency in individual animals, the total number of branch points was divided by the total number of labelled CST axons in the pyramid (Fig. 3.10c) to give a 'total sprouting ratio' for each animal. Another estimate of the proportion of the CST axons sprouting near the lesion was obtained by dividing the total number of branch points 0.4mm rostral to the lesion site by the total number of axons counted 0.4mm rostral to the lesion site to give a 'lesion site sprouting ratio' for each animal. After unblinding the results, the two sets of ratios for the 4 LPS-treated animals and the 4 control animals were analysed for significant differences by using the Mann-Whitney test. It should be noted that the number of labelled CST axons counted in the medulla gives a more accurate estimate of the total number of axons labelled with BDA than do counts close to the lesion site. Thus, the 'total sprouting ratio', which utilises the medullary count, is probably a better estimate of the injured CST regenerative response than the 'lesion site sprouting ratio'.

Correct BDA placement:

2 further animals had BDA injected into motor cortex, as described above, and after 21 days were analysed with the ABC immunohistochemistry method to visualise BDA crystals and damage done to cortex by the injection of 7.5µl BDA. 40µm freezing microtome-cut coronal sections were reacted in the same manner as the ATF3 experiments described above (see Fig. 3.10d).

Table 2-1 Animal utilisation for experiments on the effect of cortical LPS on expression of growth-associated proteins / genes.

Survival Time	Cortical LPS (with SCI) for IHC	Cortical LPS with retro-grade labelling	Cortical LPS for *in situ* hybridis-ation	Cortical LPS with SCI and antero-grade labelling	SCI with antero-grade labelling	Controls (Gelfoam not applied)
1 day	3					
3 days	5 (+3)	5	4 (+1 control)			3 (+3)
7 days	4 (+2)		4			1
14 days	2 (+2)	2	3			2
21 days				4	4	
1 month	2 (+2)	1	4			
Totals	16 (+9) = 25	8	15 (+1)	4	4	6 (+3)

Notes to Table 2-1: GAP = growth associated protein; IHC = immunohistochemistry; SCI = spinal cord injury (denotes animals with unilateral transection of corticospinal tract at C4).

Controls were animals in which the dura was opened unilaterally without application of LPS (in 6 of these animals Gelfoam was applied to the cortex; in 3 others no Gelfoam was applied). In addition, control exposure of the left cerebral cortex was carried out in all animals with unilateral LPS application.

This Table does not include 6 positive control animals in which the expression of growth associated proteins was examined in the facial nucleus following facial nerve injury and it also excludes 12 animals used in pilot studies to determine the optimal dose of LPS.

2.3 *Effects of LPS-induced inflammation on regeneration following lumbar dorsal root transection*

2.3.1 Animals and surgery

Adult female Sprague-Dawley rats (220-250g; n = 19) were divided into six experimental groups:

Controls: (dorsal root (DR) transection and conditioning sciatic nerve crush; n = 3);

LPS: (DR transection, conditioning lesion and LPS application on DREZ at the same time; n = 2);

Delayed LPS: (DR transection with conditioning lesion and LPS application onto DREZ after 1 week; n = 3)

Delayed + I-P LPS: (same as delayed LPS, plus intraperitoneal (I-P) injections of LPS solution every 3 days after LPS application; n = 5)

I-P LPS OX42: (DR cut with conditioning lesion, plus I-P LPS injections at 4 and 7 days. Analysis at 7 days with OX42 immunohistochemistry, to look for the microglial and macrophage response to injury; n = 3)

Control OX42: (DR cut with conditioning lesion; animals were analysed after 7 days with OX42 immunohistochemistry, to look for the microglial and macrophage response to injury; n = 3)

2.3.2 Dorsal root injury

The lumbar spine was exposed via a midline dorsal incision and a unilateral left L4 and L5 laminectomy performed to expose the lower lumbar dorsal roots. The L5 and L6 roots were identified, transected with microscissors and the cut ends reapposed and held together with fibrinogen (Sigma, Dorset, UK). The cranial portion of the transected L5 root was followed to the DREZ, visualised by removing the overlying vertebra's ipsilateral lamina. In 4 rats (LPS group), 500μg LPS powder was placed onto the DREZ, kept in place with Gelfoam, (3 control rats were not given LPS). Superficial muscles were sutured and the wound closed with clips. To maximise the regenerative response of injured ascending axons in the dorsal column, a conditioning peripheral nerve injury was performed at the same time as the dorsal column lesion on all animals. The ipsilateral sciatic nerve was exposed at mid-thigh level, crushed for ten seconds with watchmakers' forceps (No. 7) and the skin incision was closed with Histoacryl glue. Approximately 0.5ml sucrose octa-acetate and denatonium benzoate ('Stop 'n' grow'; Mentholatum, Glasgow, UK) was applied to the hindpaw on the injured side to prevent autophagy.

In the 2 groups with delayed LPS application, the animals were reanaesthetised after 1 week, the DREZ exposed and 500μg LPS powder was placed onto it at that time (rather than at the time of dorsal root injury. In the delayed + I-P LPS group, animals were then given additional intraperitoneal injections of 1mg LPS (suspension in 0.5mls PBS) every 3 days until sacrifice. After 25 days, the animals were reanaesthetised, the left sciatic nerve exposed and an incision made into the nerve proximal to the previous crush site. A fine glass micropipette attached to a Hamilton syringe was pushed into the nerve through the incision, and 1μl of cholera toxin conjugated to horseradish peroxidase (CT-HRP; solution of 0.042mg CT / 0.1mg HRP in 7μl sterile water; List Biological Laboratories, UK) was slowly injected into the endoneurium. The

micropipette was withdrawn and the sciatic nerve was ligated immediately above the incision in the nerve to prevent leakage of injectate. The skin incision was then sutured and the animals allowed to recover and survive for 3 further days. A further 6 animals were analysed 7 days after a DR cut (control OX42 group) or DR cut with I-P LPS injection at 4 and 7 days (I-P LPS OX42 group). See Table 2.2 for a summary of animal utilisation and diagram below for experimental procedure.

Figure 2-2 Diagrammatic representation of dorsal root injury model

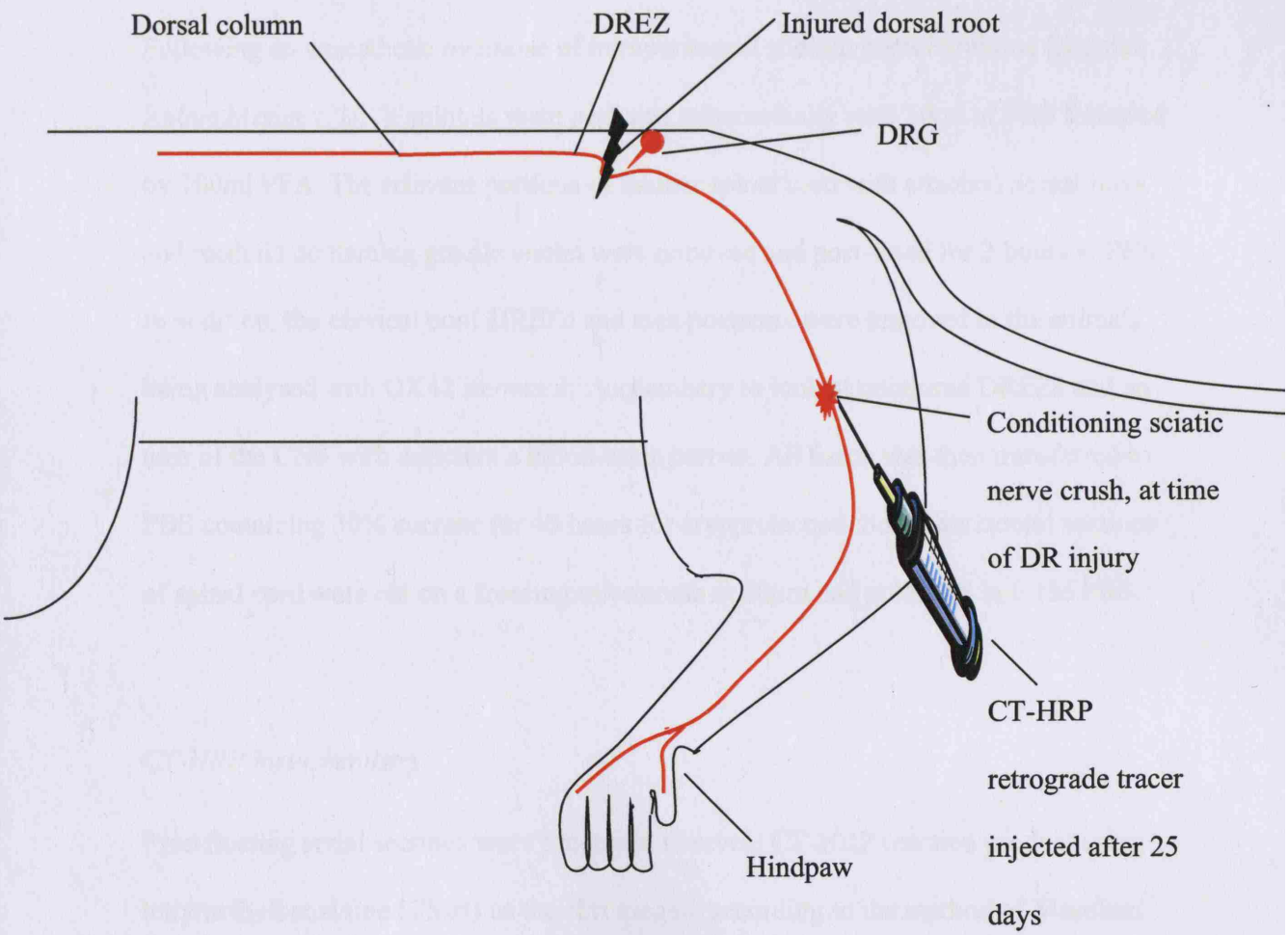

Controls for spared axons

Because incomplete dorsal column (or dorsal root) lesions might result in CT-HRP labelling of uninjured axons in the dorsal column, transverse sections were cut through the medulla at the level of the gracile nucleus in every animal in these two experimental groups. These sections were processed alongside the sections of the injury site. One animal showed evidence of axon sparing (labelled axons in or immediately caudal to the gracile nucleus) - see Results section 3.3 and Fig. 3.11a.

2.3.3 Histological processing

Following an anaesthetic overdose of intraperitoneal sodium pentobarbitone (Sagatal; Rhône Merieux, UK), animals were perfused transcardially with 50ml of PBS followed by 100ml PFA. The relevant portions of lumbar spinal cord with attached dorsal roots and medulla containing gracile nuclei were removed and post-fixed for 2 hours in PFA. In addition, the cervical cord DREZs and area postrema were removed in the animals being analysed with OX42 immunohistochemistry to look at uninjured DREZs and an area of the CNS with deficient a blood-brain barrier. All tissue was then transferred to PBS containing 30% sucrose for 48 hours for cryoprotection. Serial horizontal sections of spinal cord were cut on a freezing microtome at 40μm and collected in 0.1M PBS.

CT-HRP histochemistry

Free-floating serial sections were processed to reveal CT-HRP reaction product using tetramethylbenzidine (TMB) as the chromogen, according to the method of Mesulam and Brushart (1979). The sections were rinsed in dH_2O (6 x 5 minutes), then preincubated, on ice, for 30 minutes in a solution of 0.1% sodium nitroferricyanide, 5%

0.2M sodium acetate buffer (pH 3.3), 0.005% TMB (dissolved first in a volume of ethanol that amounted to 2.5% of the total solution) made up in dH_2O. A solution of 0.3% H_2O_2 was then added (2% of the total incubation mixture volume) and the sections incubated on ice until reaction product was visible (approximately 15 minutes) at which point the reaction was arrested by 6 x 5 minute washes in 0.02M sodium acetate buffer. Sections were collected on gelatinised slides, air dried overnight, rapidly dehydrated in ascending strength alcohol solutions and coverslipped with DPX (Merck, Poole, UK).

OX42 immunohistochemistry

Sections were washed in 0.1M PBS and reacted for OX42 as described in the Methods section for the cortical LPS experiments above (Chapter 2.1.5, pages 116-7).

Table 2-2 Experimental procedures for studies of LPS and regeneration after dorsal root transection

Group name	Experimental procedure	Number of animals	Survival
Control	Dorsal root cut	3	28d
LPS	Dorsal root cut + LPS on DREZ	2	28d
Delayed LPS	Dorsal root cut + LPS on DREZ after 1 week	3	28d
Delayed + I-P LPS	Dorsal root cut, LPS on DREZ after 1 week and I-P LPS injections every 3 days	5	28d
I-P LPS OX42	Dorsal root cut and I-P LPS injections at 4days and 7days	3	7d
Control OX42	Dorsal root cut for OX42 IHC	3	7d
	Total	19	

Notes to Table 2-2: All animals also had a conditioning sciatic nerve crush performed at the time of dorsal root transection. I-P = intraperitoneal; IHC = immunohistochemistry.

2.4 Effects of LPS injections into motor cortex on expression of growth-associated proteins

Following our experiments demonstrating upregulation of certain growth-associated proteins / genes in corticospinal cell bodies with topical application of LPS onto motor cortex, a preliminary study of the effects of intracortical injections of LPS solution into motor cortex was conducted.

2.4.1 Animals

Adult female Sprague-Dawley rats (220-250g; n = 5) were used.

2.4.2 Injection of LPS

In 4 animals a solution of 20mg/ml LPS dissolved in PBS was used for injections and a concentration of 10mg/ml in the fifth animal. LPS was added to PBS, which formed a suspension, which was warmed to 60°C and vigorously shaken for two minutes to form a solution. The animals had a right craniectomy performed centred over motor cortex (2mm caudal to the bregma and 2 mm lateral to the midline, according to the coordinates of Paxinos and Watson (1998), as described above). A microinjector (World Precision Instruments, Sarasota, FL, USA) fitted with a very fine bore Hamilton syringe was used to inject 0.25µl LPS solution to a depth of 1.4mm over 10 minutes. The cannula was left in situ for 2 minutes to prevent immediate leakage of injectate out of the puncture site in brain and then slowly withdrawn. 1 animal had 4 x 0.25µl LPS

injected, 2 animals had 4 x 1µl LPS injected; 1 animal had 1 x 1µl LPS injected and 1 animal had 1 x 1µl of 10mg/ml LPS injected. The craniectomy was covered with Gelfoam and the wound sutured. Three separate animals had a facial nerve crush performed as a positive control for expression of growth-associated proteins (as described above in Methods section 2.1). All animals survived for 3 days.

2.4.3 Perfusion and histological processing

Animals were overdosed with halothane and intraperitoneal pentobarbitone, and perfused transcardially with 200ml of PBS followed by 350ml of 4% paraformaldehyde in 0.1M PBS buffer. The brain was removed and immersed in PFA for 2 hours. Dissected tissue specimens were then cryoprotected for 40 hours in PBS containing 30% sucrose. Coronal sections of brain through the motor cortex and pons (containing the facial nucleus) were cut at 40µm using a freezing microtome and collected in 0.1M PBS.

Immunohistochemistry

After rinsing section in PBS (3x5 minutes), sections of motor cortex and pons (positive control tissue) were reacted at the same time for ATF3, c-Jun or SCG10 expression as described in the LPS experiment Methods section 2.1.5 above (see pages 114-117), using the ABC method. Other sections were reacted for OX42 immunofluorescence to investigate the microglial and macrophage reaction to LPS injection in cortex (see Methods section 2.1.5 above). Digital images were taken of sections for analysis.

2.5 *Effects of zymosan-induced inflammation on glial cells, Nogo-A and expression of growth-associated proteins by corticospinal neurons*

2.5.1 Animals

Adult female Sprague-Dawley rats (220-250g; n = 18) were used.

2.5.2 Application of zymosan

The surface of the right motor cortex was exposed as in the LPS experiments (see LPS Methods chapter 2.1.2, page 110). The dura was opened and 500μg of zymosan (Sigma, UK) was applied - as a powder - to the exposed pial surface of the right hemisphere. The powder was kept in place by application of Gelfoam, which was anchored to the cranium with Histoacryl glue. The contralateral cortex was exposed but zymosan was not applied as a control for the effects of surgery. The scalp incision was closed with Michel clips. Survival times were 1 day (n = 3), 3 days (n = 3), 7 days (n = 2), 17 days (n = 3) and 1 month (n =3) after zymosan application. In an attempt to reduce the risk of cortical damage, 2 animals (survival 3 days) had a solution of zymosan dissolved in PBS (6μl of 1% solution in 0.1M TBS) soaked on a 2mm x 2mm square of Gelfoam placed onto the exposed motor cortex and in 2 further animals (survival 2 days) the dura over the motor cortex was not opened, and zymosan powder was placed on top of the intact dura (see Table 2.3).

2.5.3 Retrograde tracing with Fluorogold (FG)

In order to identify the neuronal cell bodies giving rise to the CST in animals treated with zymosan, animals surviving 17 days and 1 month had Gelfoam impregnated with 1.5μl of FG placed into the contralateral cervical spinal cord 2 to 3 days before the animals were killed (see LPS Methods chapter 2.1.3, pages 111-2).

2.5.4 Positive control: facial nerve injury

As a positive control, expression of growth-associated proteins was induced in facial nucleus neurons by facial nerve injury. In 2 adult rats, anaesthetised as described above, a 1cm skin incision was made posterior to the right ear, and the facial nerve exposed and crushed for 10 seconds with watchmakers' forceps proximal to its branch point. The skin incision was closed with Michel clips and the animals were killed after seven days.

2.5.5 Perfusion and histological processing

Animals were overdosed with halothane and intraperitoneal pentobarbitone, and perfused transcardially with 200ml of PBS followed by 350ml of 4% paraformaldehyde in 0.1M PBS buffer. The brain was removed and immersed in fixative solution for 2 hours. Dissected tissue specimens were then cryoprotected for 40 hours in PBS containing 30% sucrose. Coronal sections of brain through the motor cortex or pons (containing the facial nucleus) were cut at 40μm using a freezing microtome and collected in serial order in 0.1M TBS.

OX42 immunohistochemistry

Sections were reacted as described in the LPS Methods section 2.1.5. Briefly, sections were washed in 0.3% H_2O_2 followed by 3 x 5 minute TNT washes, followed by a one hour wash in blocking solution. Sections were then incubated with primary antibody against OX42 (1:3000 diluted in blocking solution) for 72 hours at 4°C. Sections of motor cortex and pons incubated with blocking solution, rather than with primary antibody, served as negative controls. After 3 washes in TNT, sections were incubated in horse anti-mouse biotinylated secondary antibody, rinsed again and incubated in streptavidin-HRP, washed in TNT buffer, reacted with Tyramide Cy3 and then washed in TBS. Sections were then mounted onto agar-coated slides and coverslipped immediately with glycerol containing DABCO.

Nogo-A/NG2 and Nogo-A/GFAP double label immunohistochemistry

The steps followed were initially the same as for OX42 immunofluorescence processing except that the blocking solution contained an additional 10% normal goat serum. Sections were incubated with primary antibody against Nogo-A (1:5000 dilution; gift from Dr. R. Prinjha, GSK, UK) mixed with primary antibody against either GFAP (1:400) or NG2 (1:5000) in this blocking solution overnight at room temperature. After 3 washes in TNT, sections were incubated with goat anti-rabbit Alexa Fluor 488 (1:400 in TBS - to label the polyclonal anti-NG2 or anti-GFAP antibodies) mixed with horse anti-mouse biotinylated secondary antibody (1:200 to label the monoclonal anti-Nogo-A antibodies) for 2 hours, followed by 3 rinses in TBS and then 2 hours incubation with Streptavidin-Texas red (1:400) (Vector laboratories, Peterborough, UK). After 3 rinses in TBS, sections were rinsed with bisbenzimide (2.5μg / ml; Sigma, Dorset, UK) for 7

minutes as a non-specific label for cell nuclei, rinsed in TBS and then mounted onto agar-coated slides and coverslipped immediately with glycerol containing DABCO.

ATF-3, cJun and SCG10 immunohistochemistry

Sections for analysis by light microscopy were reacted as described in the LPS Methods section 2.1.5 (see pages 115-118). Briefly, sections were washed in 0.3% H_2O_2, followed by PBS washes, rinsed in blocking solution containing 10% normal goat serum and then incubated with primary antibody against ATF3, c- Jun or SCG10 for 72 hours at 4°C. Sections were then rinsed with PBS, incubated for 2 hours in 1:200 goat anti-rabbit biotinylated secondary antibody (preincubated with 10% rat serum and microfiltered), rinsed again and reacted for two hours with the ABC kit. After further washing, sections were reacted with DAB in 0.015% H_2O_2 in TBS until a brown reaction product appeared, washed, mounted onto slides and air dried, dehydrated, rinsed in Histoclear and coverslipped with DPX. Sections for immunoflourescence were washed in TNT rather than PBS, were rinsed in 10% normal goat serum made up in TBS rather than PBS and were incubated in this blocking solution for 72 hours at 4°C. They were then rinsed in TBS, and incubated with goat ant-rabbit Alexa Fluor 488 (1:400) for 2 hours, rinsed in TBS, mounted onto slides and coverslipped immediately with glycerol containing DABCO and photographed.

Table 2-3 Animal utilisation for studies of the effects of zymosan on motor cortex

Survival time	Cortical zymosan powder	Cortical zymosan solution	Zymosan on top of dura	Facial nerve controls
1 day	3			
2 days		2		
3 days	3		2	
7 days				2
17 days	3			
1 month	3			
TOTAL	12	2	2	2

2.6 Effects of zymosan on the regenerative response of the CST axons to a cervical lesion

2.6.1 Animals

Adult female Sprague-Dawley rats (220-250g; n = 10) were used.

2.6.2 Corticospinal tract injury and anterograde tracing with BDA with or without concomitant application of zymosan

To study the effect on CST axon regeneration of cortical inflammation more intense than that produced by LPS, the CST was lesioned at the same time as zymosan was applied to the cerebral cortex (n = 6) or the dura opened without application of zymosan (n = 4, controls). At the same time BDA was injected into the cortex to label CST axons (as described in the LPS experimental Methods section 2.2, page 121 and as depicted in Fig. 2.1c on page 114). In brief, a laminectomy was performed at C3/4 and a left dorsal hemisection was made to a depth of 2mm with microscissors, and the cut extended to cross the midline. Overlying muscle and skin was sutured. Immediately thereafter, a 4mm x 3mm burr hole was made over the right parietal cortex, the dura opened and zymosan powder (500μg) placed on the pial surface (zymosan omitted in control animals). Then 7.5μl BDA (10% solution in PBS) was injected into the cortex, about 1mm below the pial surface, through a Hamilton syringe attached to a glass

micropipette. The exposed area of cortex was covered with Gelfoam, the wound sutured and the animal allowed to recover. Survival time for all animals was 21 days.

Any inflammatory response due to damage induced by the relatively large volumes of BDA injected would occur in both zymosan-treated and control animals and would therefore not significantly impact on or obscure effects due to zymosan.

2.6.3 Perfusion and histological processing

Animals were overdosed with halothane and intraperitoneal pentobarbitone, and perfused transcardially with 200ml of PBS followed by 350ml of 4% paraformaldehyde in 0.1M PBS buffer. The spinal cord was removed and immersed in fixative solution for 2 hours. Dissected tissue specimens were then cryoprotected for 40 hours in PBS containing 30% sucrose. Serial horizontal sections through the spinal cord, encompassing the entire CST, and transverse sections of the medulla through the pyramids, were cut at 40μm with a freezing microtome and collected in 0.05M TBS. The free floating sections were rinsed in TBST, incubated in 0.3% H_2O_2 for 15 minutes, rinsed in TBST (2 x 10 minutes) and incubated at 1:200 dilution of ABC overnight at 4°C. They were then rinsed in TBST, incubated in Tyramide Cy3 at 1:400 for 30 minutes, rinsed in 0.05M TBS mounted onto slides and coverslipped with DABCO.

2.6.4 Quantification of anterogradely labelled corticospinal tract axons

For all animals, 9 consecutive serial horizontal sections through the entire cervical lesion site and 12 transverse sections through the medulla were scanned with a Leica confocal microscope. Image positioning was standardised by having the left (rostral) edge of each image placed over the mid-point (centre) of the CST lesion. Projection images used an accumulation of 3 scans of each optical section and represent stacks of 20-25 optical sections merged together, with a resolution of 1024 x 1024 pixels. The source of these digital images was then blinded from the quantifier. Using the same methodology as the LPS experiments, separate counts were made of the total number of BDA-labelled axons and their branches seen within a window, positioned 0.4mm rostral to the lesion site, through the 9 serial images of the CST and totalled for each animal. The total number of labelled CST axons in each animal was estimated by counting the number of labelled axons in a transverse section of the medullary pyramid, photographed at a magnification of 60x (mean of counts of 3 sections).

In order to normalise for differences in the tracing efficiency in individual animals, the total number of branch points was divided by the total number of labelled CST axons in the pyramid (Fig. 4.8d) to give a 'total sprouting ratio' for each animal. Another estimate of the proportion of the CST axons sprouting near the lesion was obtained by dividing the total number of branch points 0.4mm rostral to the lesion site by the total number of axons counted 0.4mm rostral to the lesion site to give a 'lesion site sprouting ratio' for each animal. As discussed in LPS Methods section 2.2.2, the medullary count is probably a better estimate of the injured CST regenerative response than the 'lesion site sprouting ratio' as it accounts for variations in the degree of BDA labelling. After

unblinding the results, the two sets of ratios for the zymosan-treated group were compared to the control animal group for statistical significance using the Mann-Whitney test.

2.6.5 Quantification of anterogradely-labelled CST axons giving branches across the midline

As a measure of potential plasticity from increased sprouting, I also counted the number of branches given off by the injured CST axons in the 10mm proximal to the lesion site that crossed the midline and entered the contralateral, uninjured CST. This was done in a blinded fashion in all 9 sections analysed per animal and sum total then divided by the medulla count (to take into account variable labelling of CST axons by BDA) to give a 'midline branching ratio'.

2.7 *ATF3 expression in glia during Wallerian degeneration, in peripheral nerves and CNS white matter*

2.7.1 Animal utilisation and surgical procedures

Adult female Sprague Dawley rats (n = 37) and adult C57BL/6 mice of both sexes (n = 13) were used.

2.7.2 Sciatic nerve resection

In 20 rats the left sciatic nerve was transected in mid thigh using microsurgical scissors, and 2–3 mm of the nerve excised to create a gap between the proximal and distal stumps. This allows slow regeneration of axons with few entering the distal stump before 16 days post operation (dpo) but variable and sometimes substantial numbers of axons present in the distal stump at 30 dpo. These animals were killed at 1 dpo (n = 4), 4 dpo (n = 3), 8 dpo (n = 3), 16 dpo (n = 3) and 30 dpo (n = 4). In a further 3 animals, the sciatic nerve was excised and the proximal stump was ligated and turned aside to prevent axonal regeneration into the distal stump; these rats were killed at 30 dpo.

Approximately 3 mm was resected from the left sciatic nerve of 7 mice, which were killed at 5 dpo (n = 2), 8 dpo (n = 2), 17 dpo (n = 2) and 30 dpo (n = 1).

2.7.3 Sciatic nerve cut and reanastamosis

In 9 rats the left sciatic nerve was transected (without resection) and reanastomosed with 10/0 sutures to allow rapid axonal regeneration into the distal stump. These rats were killed at 4 dpo (n = 3), 16 dpo (n = 3) and 30 dpo (n = 3).

2.7.4 Sciatic nerve transection or crush

In 4 mice the left sciatic nerve was transected. This allows rapid axonal regeneration because the ends soon become reapposed. These mice were killed at 4 dpo (n = 1), 8 dpo (n = 1) and 20 dpo (n = 2). In 2 further mice, the sciatic nerve was crushed. The injury site was marked with a 10/0 suture through the epineurium, as regeneration of axons would be rapid and so extensive that the lesion site would be difficult to visualise; the mice killed at 22 dpo.

2.7.5 Dorsal root transection

In 8 rats the left L3-6 dorsal roots were cut (surgery performed by Prof. P. N. Anderson). This produces Wallerian degeneration in the segment of dorsal root between the lesion and the spinal cord, in the dorsal root entry zone (DREZ) and in the ascending dorsal column (fasciculus gracilis) of the spinal cord rostral to the lesion. The animals were killed at 1 dpo (n = 3), 8 dpo (n = 3) and 30 dpo (n = 2).

All animals were killed by decapitation while deeply anaesthetised. Samples from operated and unoperated animals of the sciatic nerves and spinal cord were fresh-frozen in Tissue Tek cooled by dry ice.

2.7.6 Antibodies and immunohistochemical techniques

Fresh-frozen sections were cut at 20 μm, directly onto Superfrost Plus slides using a Bright cryostat and fixed in PFA. The sections were rinsed several times in PBS prior to incubation for 30 minutes at room temperature (RT) in blocking solution (0.1 M PBS, 5% NGS, 0.5% Triton-X 100). The samples were then incubated with primary antibodies, diluted appropriately in blocking solution, at RT overnight. After several rinses with PBS, rat sections were incubated with secondary antibodies, (Molecular Probes, UK) diluted in PBS, for two hours at RT. These were either monoclonal tetramethylrhodamine conjugated goat anti-mouse (to label neurofilament, GFAP, S100 or p75) or monoclonal Alexa Fluor-488-conjugated goat anti-rabbit (to label ATF3). For double-labelling experiments, the secondary antibodies were mixed together. Both secondary antibodies were adsorbed against rat serum prior to use. The sections were then rinsed several times in PBS before being stained with bisbenzimide (2.5μg / ml) for 7 minutes. After three more rinses in PBS, sections were coverslipped with DABCO and photographed. Mouse sections were treated as above, but after incubation in primary antibody were reacted using the ABC immunohistochemistry method described in Methods section 2.1.

Primary antibodies:

rabbit polyclonal anti-ATF3 (Santa Cruz);

rabbit polyclonal anti-neurofilament 200 kDa antibody (Sigma, UK);

mouse monoclonal antibovine glial fibrillary acidic protein (Sigma, UK);

mouse monoclonal anti-S100 (Sigma, UK);

mouse monoclonal anti-p75 (Sigma, UK).

Negative controls

Sample sections were incubated with blocking solution instead of primary antibodies, to ensure signal specificity.

2.7.7 Statistical analysis

All sections for statistical analysis were immunoreacted for ATF3, and stained with bisbenzimide (which labels all nuclei). The percentage of ATF3+ nuclei in rat tissue was calculated from comparable fields, photographed using a x20 objective, from each of three adjacent sections of injured sciatic nerve, per animal. These data were collated with those from at least two other animals, depending on the injury model and timepoint (see above). The group average and the standard error of the mean were subsequently calculated.

2.8 Axonal regeneration in the NG2-deficient mouse

2.8.1 Animals

Male and female adult mice, between 6 and 9 weeks old were used, with wild-type and transgenic mice matched for age and sex. For all experiments the animals were coded and randomised so that their phenotype was unknown at the time of surgery and in the course of data analysis. In animals with sciatic nerve or dorsal root injuries, approximately 0.5ml sucrose octa-acetate and denatonium benzoate (Mentholatum, UK) was applied to the hindpaw on the injured side to prevent autophagy. See Table 2.4 for a summary of utilisation of animals.

2.8.2 Phenotyping

NG2 knockout mice were bred with C57BL/6 wild-type mice (Harlan, UK) to produce a breeding stock of heterozygous mice, the offspring of which were phenotyped as follows. Tailsnips from all mice were sectioned at 12μm in a cryostat and mounted on gelatinised glass slides along with sections of tailsnips from known wild-type mice as a positive control. The sections were post-fixed for 5 minutes with PFA, rinsed (x3) in TNT, and incubated with 0.3% H_2O_2 for 15 minutes, rinsed again in TNT and placed for 1 hour in 10% normal goat serum, 1% BSA and 0.1% Triton X-100 made up in TBS. The polyclonal anti-NG2 antibody was then added (1:5000) and the sections incubated for 72 hours at 4°C. (A polyclonal antibody was used in preference to a monoclonal antibody because it would be expected to recognise many sites on the NG2 protein, and therefore be more likely to detect a (possibly functional) truncated form of NG2 in the KO mouse). The sections were then washed again in TNT (x3) and incubated in Alexa Fluor 488 - conjugated goat anti-rabbit biotinylated IgG secondary antibody (1:400;

Molecular Probes) for two hours, washed in TBS and coverslipped with DABCO anti-fade medium. Mice with no evidence of NG2 staining, following comparisons with positive control tissue (see Fig. 6.1), were designated as knockouts (KO) and used in experiments with age and sex matched C57BL/6 mice as wild-type (WT) controls. Homozygous mutants were viable, fertile, and morphologically indistinguishable from wild-type mice.

2.8.3 CNS injury models

2.8.3.1 Dorsal column and sciatic nerve conditioning lesions

A midline incision was made over the lower thoracic vertebrae, muscles overlying the spine were stripped and a bilateral laminectomy performed at T8 to expose the spinal cord. The dura was opened and two puncture holes were made with a fine insulin syringe needle, one immediately medial to the left dorsal roots and the second on the immediate opposite side of the midline. The points of a pair of straight-bladed microscissors were inserted vertically into the needle holes and the scissors closed to transect the left dorsal column. The insulin needle, marked at 2mm, was passed across the injury site to ensure a uniform depth of lesion. Superficial muscles were sutured and the wound closed. To maximise the regenerative response of injured ascending axons in the dorsal column, a conditioning peripheral nerve injury was performed at the same time as the dorsal column lesion. The ipsilateral sciatic nerve was exposed at mid-thigh level, crushed for ten seconds with watchmakers' forceps (No. 7) and the skin incision was closed with Histoacryl glue. After 25 days, the animals were reanaesthetised, the left sciatic nerve exposed and an incision made into the nerve proximal to the previous crush site. A fine glass micropipette attached to a Hamilton syringe was pushed into the

nerve through the incision, and 1μl of CT-HRP was slowly injected into the endoneurium. The micropipette was withdrawn and the sciatic nerve was ligated immediately above the incision in the nerve to prevent leakage of injectate. The skin incision was then sutured and the animals allowed to recover and survive for 3 further days (see Fig. 2-3 below)

Figure 2-3 Diagrammatic representation of dorsal column injury model

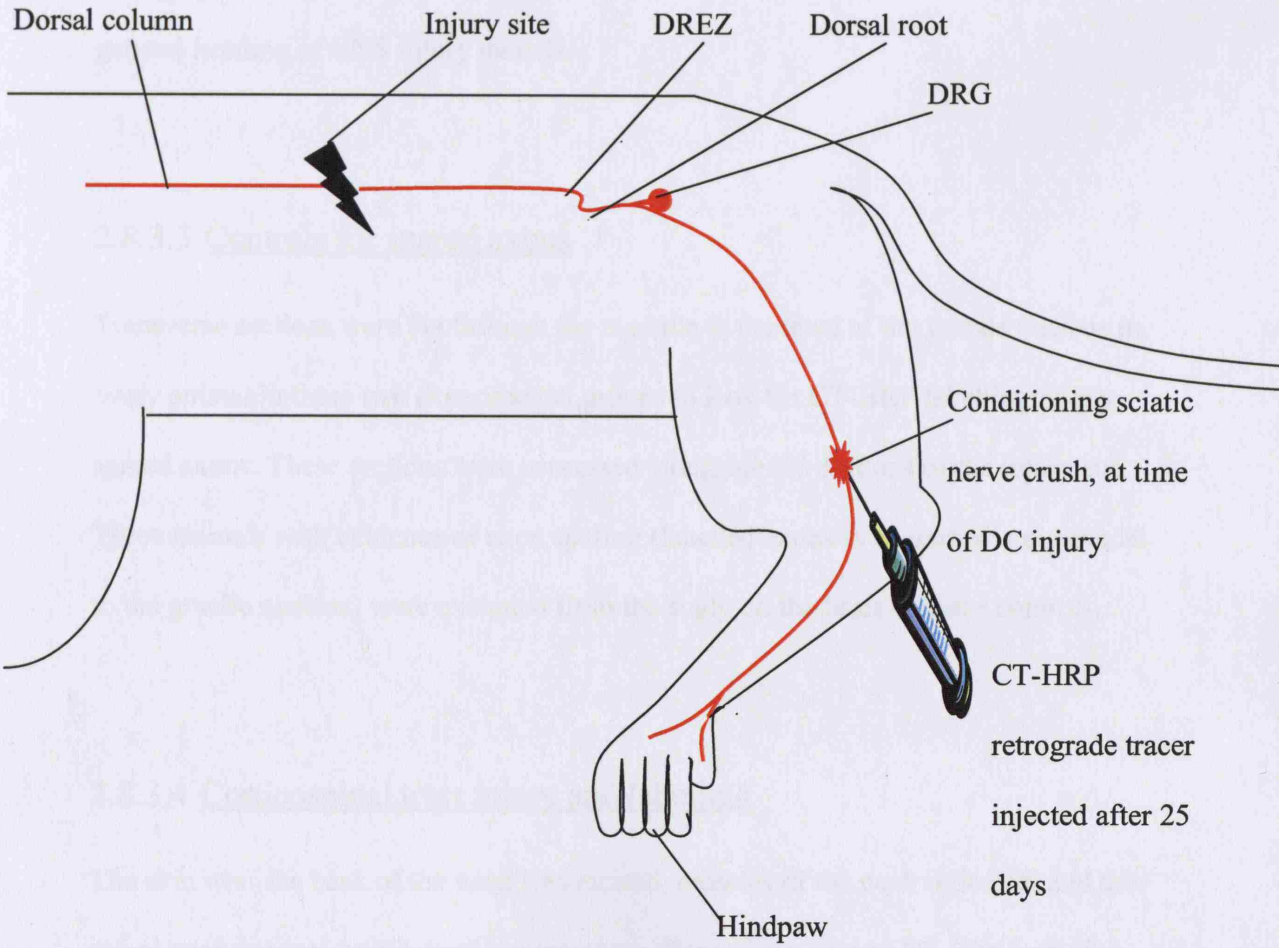

2.8.3.2 Dorsal root injury

The left L5 lumbar root was exposed via a hemilaminectomy, cut with a pair of microscissors and reapposed with fibrinogen and an ipsilateral concomitant sciatic nerve crush injury was performed (as described in the LPS experimental Methods section 2.3.2, page 127). After 25 days, the animals were reanaesthetised and 1μl of CT-HRP was injected into the sciatic nerve, as described above, in order to label axons in the dorsal root (see Fig. 2.2, page 128). As the purpose of these experiments was to test for the ability of regenerating axons to enter the CNS they are included under the general heading of CNS injury models.

2.8.3.3 Controls for spared axons

Transverse sections were cut through the medulla at the level of the gracile nucleus in every animal in these two experimental groups to look for CT-HRP labelling of any spared axons. These sections were processed alongside the sections of the injury site. Three animals with evidence of axon sparing (labelled axons in or immediately caudal to the gracile nucleus) were excluded from the study on the basis of these controls.

2.8.3.4 Corticospinal tract injury and labelling

The skin over the back of the neck was incised, muscles of the neck reflected, and the spinal cord exposed by bilateral laminectomy of vertebrae C6 and C7. The area of dorsal column between the DREZ and the midline on the left side was cut using a pair of microscissors, and the lesion was extended across the midline and checked to extend to a depth of 2mm below the dorsal surface of the cord with a marked needle. Care was

taken to undercut and avoid damage to the dorsal spinal vein. The dura was closed and overlying muscle and skin sutured. While the animals remained under anaesthesia, BDA (Molecular Probes, Oregon, USA; 10% solution in dissolved in 0.1M PBS) was injected into the contralateral sensorimotor cortex to anterogradely label corticospinal tract axons. A 2 x 1mm burr hole was made over the right parietal cortex, the dura opened, and a glass micropipette attached to a Hamilton syringe was pushed into the cortex from the rostral edge of the burr hole, at a very shallow angle and advanced for 2mm in a caudal direction. The pipette tip was kept almost parallel to the cortical surface and at a depth of no more than 1mm. BDA solution (1.7μl) was then injected while the pipette was slowly retracted to its entry point. The pipette was then advanced through the same entry point, for the same distance and at the same depth but directed slightly medially with respect to the first injection and a second aliquot of BDA (1.7μl) injected in the same manner as the first. Finally the process was repeated a third time, with the pipette tip directed slightly laterally with respect to the first injection. Thus a total of approximately 5μl BDA solution was injected, filling a large area of the right sensorimotor cortex. The burr hole was then covered with Gelfoam (Johnson & Johnson, Skipton, UK) and the scalp incision sutured. These operations were performed by D. K. Rezajooi.

Animals with dorsal column or dorsal root injuries survived for 28 days and those with CST injuries survived for 21 days. Following an anaesthetic overdose of intraperitoneal sodium pentobarbitone supplemented with halothane, they were perfused transcardially with 50ml of PBS followed by 100ml PFA. The relevant portions of cervical, thoracic or lumbar spinal cord and dorsal roots were removed and post-fixed for 2 hours in PFA. The tissue blocks, in some cases further dissected, were then transferred to PBS containing 30% sucrose for 48 hours. The cryoprotected tissue blocks were frozen in

Tissue-Tek cooled with dry ice. Serial horizontal sections of spinal cord were cut on a freezing microtome at 40μm and collected in 0.1M PBS.

BDA immunohistochemistry

Free floating sections, maintained in serial order, were reacted as described in the 'BDA labelling immunohistochemistry' section of the LPS experimental Methods (chapter 2.2.1, pages 121-2).

Sections were scanned with a Leica TCS NT confocal microscope. Projection images represented stacks of 10-20 optical sections merged together (2 scans at each optical section level), with a resolution of 1024 x 1024 pixels. Images from wild-type and knockout mice were acquired under identical exposure conditions.

CT-HRP histochemistry

Free-floating serial sections were processed to reveal CT-HRP reaction product using tetramethylbenzidine (TMB) as the chromogen, according to the method of Mesulam and Brushart (1979), as described in the LPS experimental Methods section 2.3.3, pages 129-30).

2.8.4 PNS injury models; functional analysis

2.8.4.1 Sciatic nerve injury

The left sciatic nerve was exposed via a 4mm longitudinal incision over the left mid-thigh above the level of origin of the sural nerve, and crushed for ten seconds with watchmakers' forceps (No. 7). In other mice, sciatic nerve crush was supplemented by excision of 3mm of the saphenous nerve at mid-thigh level, in order to control for the possibility that sensory recovery following sciatic nerve injury might result from sprouting of saphenous nerve axons (Devor et al., 1979; Kinnman and Aldskogius, 1986; Kinnman et al., 1992). In other mice, the left sciatic nerve was transected with microscissors at the same level as the crush lesions and the cut ends immediately reanastamosed with 2 x 10/0 sutures. The skin incisions were closed with Histoacryl glue.

2.8.4.2 Assessment of functional recovery after sciatic (and saphenous) nerve injury

Recovery of sensory function was assessed using Von Frey hairs. Animals were placed under a glass case on a taut nylon mesh and allowed to settle for 20-30 minutes, to allow the test to be performed without restraint and under conditions of minimal stress (Ren, 1999). The threshold thickness of Von Frey hair required to elicit a repeated withdrawal response was assessed in all animals, prior to nerve injury, by stimulating the lateral glabrous skin of the hindpaw. After injury, the time taken for mice to recover the ability to withdraw their paw in response to the same Von Frey hair as pre-

operatively was assessed twice daily and continued for two days after recovery of function. At each testing session, the contralateral, uninjured hindpaw was assessed for comparison. Motor function was tested immediately after the sensory assessment, by assessing (recovery of) the toe spreading reflex (involuntary spreading of the digits when the hindlimbs are raised off their supporting surface by lifting the mouse by the tail).

2.8.4.3 Facial nerve injury and assessment of functional recovery

The right facial nerve was exposed postero-inferior to the right ear and crushed immediately distal to the stylomastoid foramen for ten seconds with watchmakers' forceps. The skin incision was closed with Histoacryl glue. Functional recovery was monitored twice daily by visually checking for recovery of spontaneous whisker twitching and for the return of the blink reflex (elicited by irritating the cornea with a thin piece of cotton wool). The left side was examined at the same time as a positive control.

2.8.5 PNS injury models; anatomical studies

2.8.5.1 Retrograde labelling of DRG cells

After survival times of 3 - 88 days (Table 2.4), 1µl of DiAsp was injected into the lateral plantar skin of the hindpaws both ipsilateral and contralateral to the nerve injury, under general anaesthesia, using a glass micropipette attached to a Hamilton microsyringe (see Fig. 2.4). Two days later, the animals were overdosed with anaesthetic and the L4 and L5 DRGs on both sides removed and placed in PFA for 2

hours. The ganglia were then placed whole onto a cavity slide, coverslipped with glycerol containing DABCO, and examined and photographed immediately in a confocal microscope. An average of 25 images were collected through the entire thickness of the DRG. Retrogradely labelled cells (visible above a fixed luminescence threshold) were counted using Openlab image processing software. The exposure time for all images was kept constant to ensure valid comparisons between control and injured and between wild-type and knockout material.

Figure 2-4 Diagrammatic representation of experiments retrogradely labelling DRG neurons with DiAsp after sciatic nerve crush

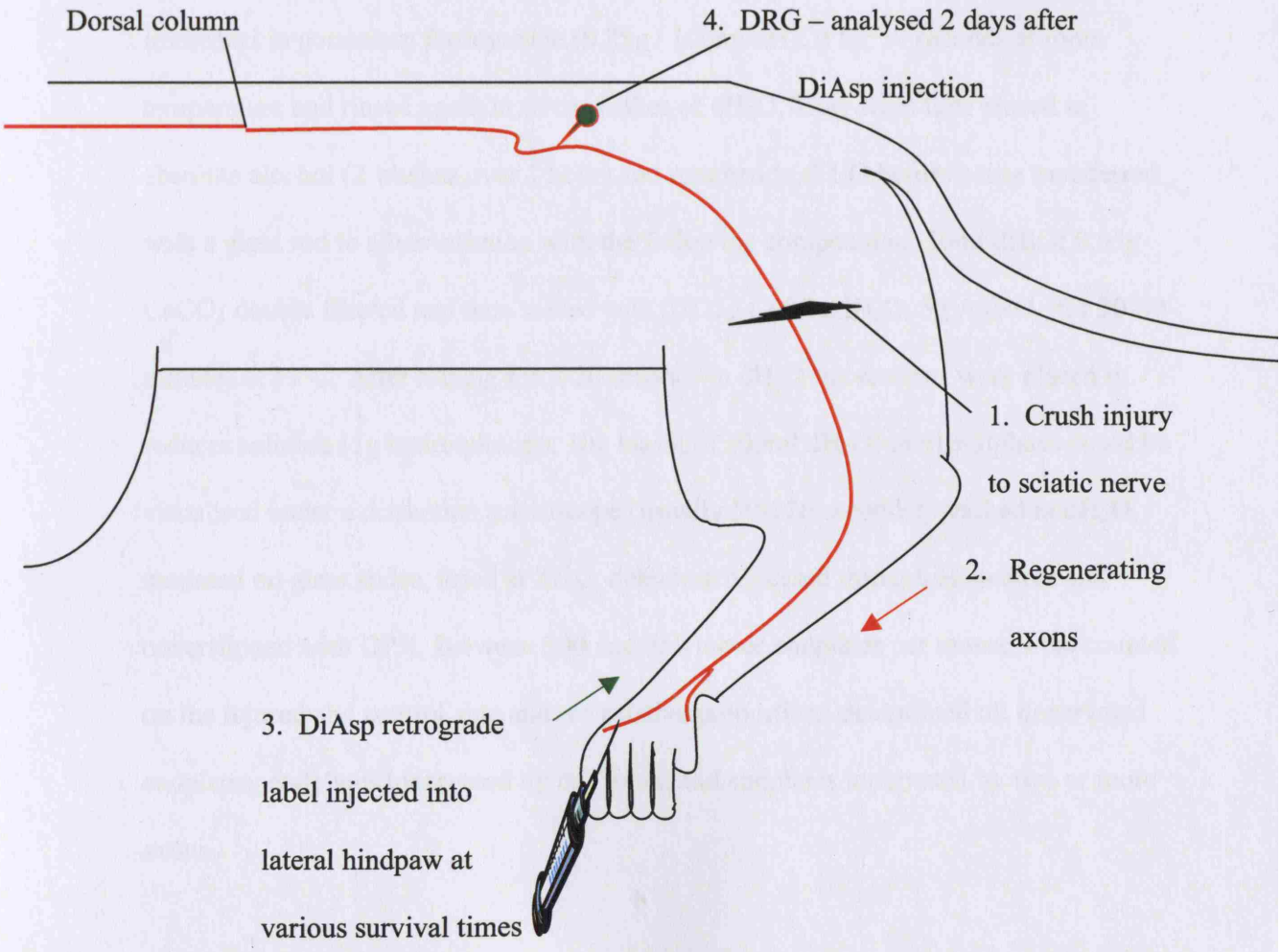

2.8.5.2 Silver-cholinesterase histochemistry

To examine reinnervation of muscle 7 and 10 days after sciatic nerve crush, animals were killed by overdose of anaesthetic and their right and left (control) soleus muscles removed and processed by the Method of Namba *et al.* (1967). The muscles were fixed, whilst slightly stretched, in buffered formol-calcium at 4°C for 6 hours, then placed in 10% sucrose at 4°C overnight. The muscles were cut at 40μm with a freezing microtome and the sections collected in chilled dH_2O. Sections were then incubated for 20 minutes on ice in the following medium: acetylthiocholine (10mg); 0.1M sodium hydrogen maleate (13ml); 100mM tri-sodium citrate (1ml); dH_2O (2ml); 5mM potassium ferricyanide (2ml); sucrose (3g). They were then rinsed in dH_2O and immersed in potassium ferricyanide (0.25g / 100ml dH_2O) for 30 seconds at room temperature and rinsed again in three washes of dH_2O. They were then placed in absolute alcohol (2 washes over 1 hour) and returned to dH_2O before being transferred with a glass rod to silver solution with the following composition: 50ml dH_2O; 0.05g $CaCO_3$ double filtered and then mixed with 0.025g $CuSO_4.5H_2O$; 5g $AgNO_3$, for 20-30 minutes at 37°C. After rinsing for 5-20 seconds in dH_2O the sections were placed in reducer solution (1g hydroquinone; 10g Na_2SO_4; 100ml dH_2O) until endplates could be visualised under a dissection microscope (usually 30-120 seconds), washed in dH_2O, mounted on glass slides, dried at 37°C, dehydrated, passed through Histoclear and coverslipped with DPX. Between 300 and 350 motor endplates per mouse were counted on the injured and control side and the relative proportions determined of: denervated endplates; endplates innervated by one axon; and endplates innervated by two or more axons.

2.8.5.3 PGP 9.5 immunohistochemistry

Reinnervation of skin was examined, after PGP 9.5 immunostaining of sensory axons, in mice surviving 17 days after sciatic nerve crush (as described above). The animals were killed by anaesthetic overdose and both hindpaws removed and placed into PFA for 3 hours, followed by immersion in 30% sucrose in TBS overnight. An area of lateral glabrous skin was dissected from each hindpaw and frozen in Tissue-Tek cooled with dry ice. Frozen sections were cut at a 12μm perpendicular to the skin surface, collected on glass slides, air dried for 30 minutes and washed with TBS before immersion for 30 minutes in a blocking solution of 10% normal goat serum in TBS containing 0.1% Triton X-100 and 1% BSA. Sections were then reacted overnight with PGP antibody (1:500 in blocking solution) in a sealed humidified chamber at room temperature. After 3 washes in TNT, the sections were incubated with goat anti-rabbit Alexa Fluor 488 (1:400 in TBS) for 2 hours, followed by one rinse in TNT and 2 rinses in TBS. Slides were coverslipped using DABCO and the lateral edge of glabrous hindpaw examined and photographed (using a x20 objective lens) from a random sample of 7 sections per foot. From these images, the total numbers of axons labelled with PGP 9.5 that had regenerated into the dermis were counted in the skin samples from the ipsilateral hindpaw of all mice (Table 2.4), and from the contralateral hindpaw of 3 wild-type and 3 knockout mice.

2.8.5.4 Electron Microscopy

The extent of axonal regeneration into distal nerve branches was analysed by EM in the same group of 12 mice used to examine skin reinnervation by PGP immunohistochemistry (17 day survival) and in an additional group of mice with identical unilateral sciatic nerve crush injury and 21 day survival. Following anaesthetic

overdose, the 4th toe of both hind feet was amputated and placed in fixative solution (2% paraformaldehyde and 2.5% glutaraldehyde in 0.1M PB) for 24 hours followed by immersion in 5% EDTA for 48 hrs at 4°C to soften bone. The toes were post-fixed in 1% OsO_4 in PB at 4°C for 1 hour, washed in PB followed by three washes in dH_2O, stained with 2% uranyl acetate (in dH_2O) for 40 minutes at 4°C, washed in dH_2O, dehydrated, passed through propylene oxide, placed in a 50:50 mixture of propylene oxide and Agar resin (12g Agar; 8g dodecenyl succinic anhydrite (DDSA); 5g methylnadicanhydride; 0.4ml benzyldimethylamine) for 45 minutes and then placed in fresh Agar resin overnight at room temperature on a rotator. Specimens were then placed in fresh resin for a further 24 hours before being placed in blocks in an oven at 60°C for 36 hours to polymerise the resin. Transverse semithin sections (ca. 1μm) of both ipsilateral and contralateral toes were cut on an ultramicrotome and stained with toluidine blue to localise dorsal digital nerves. Ultrathin transverse sections through the nerves were cut with a diamond knife, collected on Formvar-coated slot grids, stained with lead citrate for 10-15 minutes, and examined in a JEOL 1010 electron microscope operated at 60kV. Images were recorded on Kodak EM film 4489. In animals that had survived 17 days, numbers of unmyelinated axons in the dorsal digital nerves were counted. In the animals that survived 21 days, only remyelinating axons of all digital nerves of the 4th toe were counted.

Axonal regeneration in the tibial nerve, just below the lesion site was also examined by EM in an additional group of mice, 15 days after sciatic nerve crush. These animals were given an anaesthetic overdose and perfused transcardially with 50ml of PB followed by 100ml of 2% paraformaldehyde and 2.5% glutaraldehyde in PB. A segment of tibial nerve 5mm distal to the crush site was removed, post-fixed for 2 hours, osmicated (1 hour in 1% OsO_4 at 4°C), dehydrated and processed into Araldite resin

(10g DDSA; 10g Araldite (CY212); 0.8g dibutylphthalate) warmed for two minutes at 60°C and then mixed with 0.4ml BDMA. Following polymerisation, transverse thin sections of the tibial nerve 5mm distal to the crush site were stained with lead citrate, examined by EM and myelinated axons counted. Independent blinded counts were made by two observers to reduce the impact of bias in relation to identification criteria for axons.

2.8.5.5 Retrograde labelling of facial motor neurons

The extent of facial nerve regeneration after transection was assessed with the retrograde label Fluorogold (FG). The facial nerve was transected with microscissors immediately below the stylomastoid foramen and the cut ends apposed and held together by fibrinogen. They were anaesthetised 3 days before sacrifice and a 2 x 2mm piece of Gelfoam previously soaked with 4µl FG (2 granules dissolved in 100µl PBS) was placed below the skin of the right whisker pad (see Fig. 2.5, page 161). Note that anaesthesia was induced by a single intraperitoneal injection of 150 µl of 2.5% Avertin (tribromoethanol; Sigma, Deisenhofen, Germany) per 10g of body mass, as the nose cone used to deliver halothane would have covered the whisker pad. As a control FG was also applied to the contralateral whisker pad at the same time in most of the mice. After a further 3 days, the animals were overdosed with anaesthetic and perfused transcardially with PBS followed by PFA, as described above. A block of tissue including the pons and midbrain was dissected out and cryoprotected for 24 hours in PBS containing 30% sucrose. Frozen coronal sections through the pons (containing the facial nucleus) were cut at 40um, collected in PBS, mounted in serial order on slides, coverslipped with DABCO, examined and photographed immediately. Counts were made of labelled neurons in the injured and control side facial nucleus (above a fixed

luminescence threshold), using Openlab image processing software and the final number corrected for variability in the optical slicing of nuclei using Abercrombie's counting method (Abercrombie, 1946).

In other mice, DiAsp was used as the retrograde label as a control. The facial nerve was transected and 4µl DiAsp (2 granules dissolved in 100µl DMSO) soaked in a Gelfoam pad placed in the whisker pad 37 days after injury, after which the animals were allowed to survive for 3 days. The facial nucleus of these animals was analysed as described above.

In addition, 6 of the 8 mice used for functional assessment of facial nerve recovery after *crush* injury were also used for anatomical assessment by retrograde labelling with DiAsp. They were anaesthetised 12 days after the facial nerve crush and DiAsp placed in the whisker pad. After a further 2 days, the animals were given an anaesthetic overdose and their facial nuclei examined as described above.

Figure 2-5 Diagrammatic representation of facial nerve injury experiments

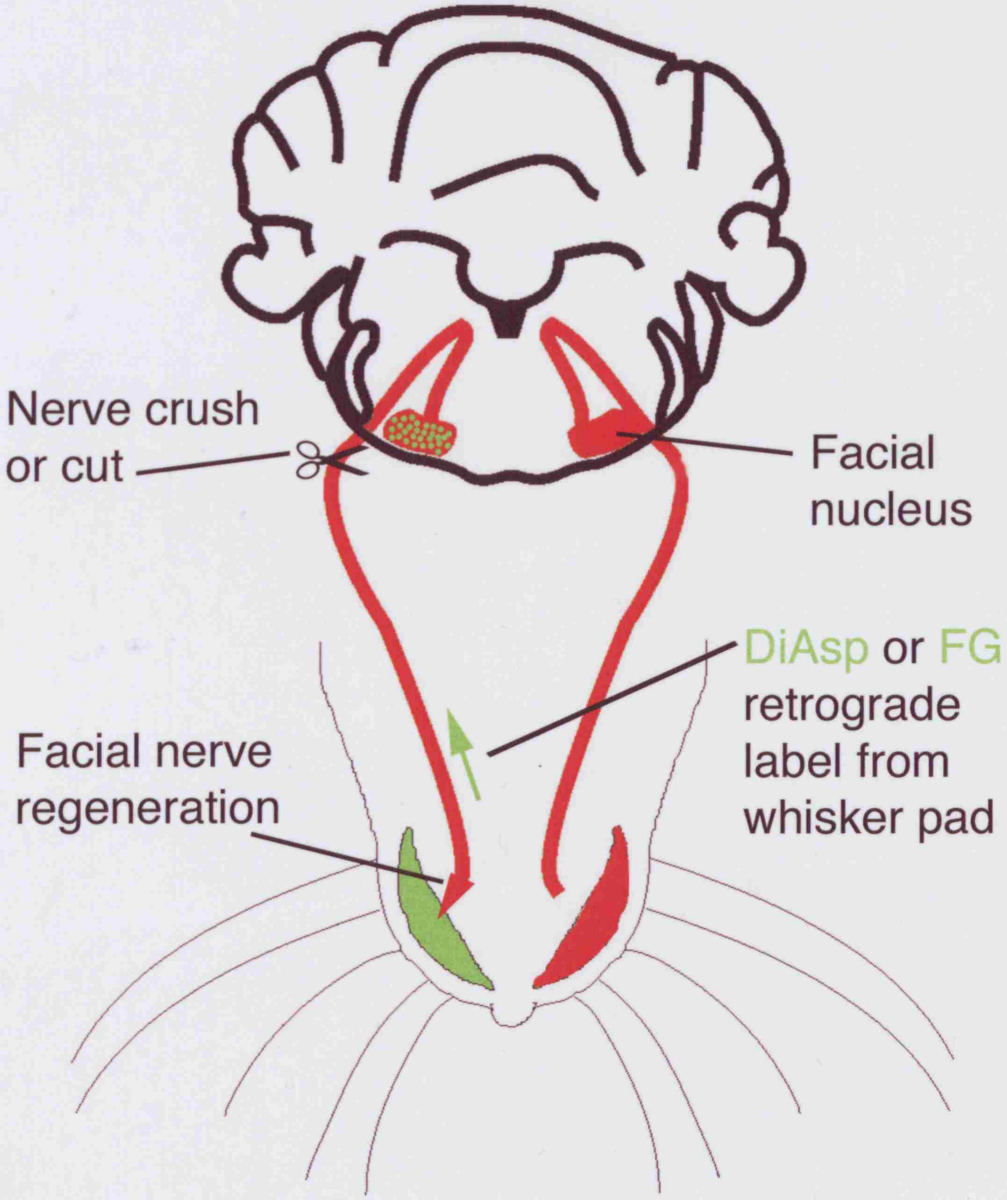

2.8.5.6 Statistical analysis

Differences between wild-type and knockout mice with respect to both functional and anatomical analyses of axonal regeneration were evaluated for significance by using Student's two-tailed unpaired t-test when there were 6 or more animals per experimental group, or a Mann-Whitney test if there were fewer animals or if the data from any group did not represent a normal distribution. In one experiment, the standard deviation of a group was zero, which precludes such statistical analysis and a two-tailed Fisher's exact test was used to calculate a p value. For all experiments, a p value of <0.05 was considered to be significant.

2.9 NG2 expression in injured sciatic nerve

In order to assess the localisation of NG2 in the injured sciatic nerve, a 3mm segment of sciatic nerve was excised in the mid thigh of two animals, and the animals allowed to survive for 7 days. Fresh frozen cryostat-cut sections of the proximal and distal stumps were double labelled with anti-NG2 and anti-neurofilament antibodies (as described in Methods chapters 2.8.2 (NG2 labelling) and 2.7.6 (neurofilament double labelling)).

2.10 NG2 expression in glabrous hindpaw skin

The localisation of NG2 in the lateral plantar hindpaw skin was assessed with immunohistochemistry. This was done in order to analyse the target territory of injured sciatic nerve that was the subject of some of the other experiments. For example, lateral plantar hindpaw skin was:

- injected with DiAsp to retrogradely label DRGs,
- tested with Von Frey hairs and
- immunoreacted with PGP 9.5.

Uninjured mice were fatally anaesthetised and fresh frozen cryostat sections of their hindpaws prepared for immunohistochemical analysis as described in the PGP 9.5 Methods section, chapter 2.8.5.3 (page 157). Sections were then immunoreacted with anti-NG2 antibody, as described in Methods chapter 2.8.2 (pages 147-8).

Table 2-4 Utilisation of NG2 knockout mice

Experimental procedure(s)	No. of mice		Survival period	Analysis performed
	KO	WT		
Sciatic nerve 3mm segment excision Uninjured lateral plantar foot	2 2	2 2	7d n/a	NG2 immunohistochemistry
Transection of DC at T8; conditioning lesion of ipsilateral sciatic nerve; subsequent injection of CT-HRP into sciatic nerve for TGL	8	6	21d	Regen growth by analysis of labelled sensory axons at/beyond DC lesion site
Transection of dorsal spinal cord at C6; simultaneous injection of BDA into contralateral sensorimotor cortex	6	6	21d	Regen growth by analysis of labelled CST axons at DC lesion site
Transection of L5 dorsal root; conditioning lesion of ipsilateral sciatic nerve; subsequent injection of CT-HRP into sciatic nerve for TGL	6	6	21d	Regen growth by analysis of labelled sensory axons in dorsal root and DREZ
Sciatic nerve crush Sciatic nerve crush; saphenous nerve resection Sciatic nerve transection	6 6 9	6 6 9	n/a n/a n/a	Recovery of foot withdrawal (sensory) and toe spreading (motor) reflexes

Sciatic nerve crush; subsequent injection of DiAsp into hindpaw skin	10	10	5d (2) 9d (2) 13d (8) 90d (8)	Extent of sensory axon regen by analysis of retrogradely labelled DRG cells
Sciatic nerve crush	9	12	7d (6) 10d (15)	Extent of motor regen by analysis of silver-cholinesterase preparations of soleus muscle
Sciatic nerve crush	6 6	6 6	17d 21d (EM only)	Sensory reinnervation of skin by PGP 9.5 IHC; regen of axons into digital nerves by EM
Sciatic nerve crush	6	8	15d	Regen of axons into distal nerve stump by EM
Facial nerve crush: subsequent application of DiAsp to whisker pad	4	4	14d	Recovery of whisker twitch and blink reflexes (n = 3+2), plus extent of axon regen by analysis of retrogradely labelled facial neurons (n = 4+4)
Facial nerve transection: subsequent application of FG or DiAsp to whisker pad	12	12	30d (FG, 8) 40d (DiAsp, 4)	Extent of axon regen by analysis of retrogradely labelled facial neurons

Key: KO = knockout; WT = wild-type; d = days post op; TGL = transganglionic labelling; CST = corticospinal tract; DC = dorsal column; DREZ = dorsal root entry zone; IHC = immunohistochemistry; EM = electron microscopy; FG = Fluorogold; Regen = regenerative / regeneration.

Chapter 3 - Results

3 LPS-induced inflammation, growth-associated protein / gene expression and axonal regeneration

Background

Inflammation around cell bodies of primary sensory neurons and retinal ganglion cells enhances expression of neuronal growth-associated genes and stimulates axonal regeneration. I have asked if inflammation would have similar effects on corticospinal neurons, which normally show little response to spinal cord injury.

Results

3.1 LPS-induced inflammation and growth-associated protein / gene expression

3.1.1 Positive and negative control studies

Positive controls: c-Jun and ATF3-positive nuclei were identified in the ipsilateral facial nucleus, one week after facial nerve crush. SCG10-positive cells were found in both facial nuclei, but immunoreactivity was greater in the facial nucleus ipsilateral to the crushed facial nerve (Fig. 3.1). These results were consistent for all animals.

Negative controls: When the primary antibody was omitted, no cells displayed immunoreactivity for c-Jun, ATF3 or SCG10 in brain or facial nucleus (Figs. 3.1a and b). No positive control tissue was used in the GAP-43 experiments; the contralateral and unoperated cortex was used as a negative control.

Figure 3-1 Immunostaining of facial nucleus positive control tissue.

Transverse section from the pons of adult rats (containing facial nucleus) 7 days after a unilateral facial nerve crush injury (inj; Figs. 3.1b, d, f and h) and no operation on the contralateral, control side (con; Figs. 3.1a, c, e and g), immunoreacted with either no primary antibody (Figs. 3.1a and b), c-Jun (Figs. 3.1c and d), ATF3 (Figs. 3.1e and f) or SCG10 (Figs. 3.1g and h).

When primary antibody was omitted, cells in the facial nucleus appeared the same on control (Fig. 3.1a) and injured sides (Fig. 3.1b), with a low level of background non-specific staining. c-Jun nuclei were faintly immunopositive in control facial nucleus (Fig. 4.1c), but were significantly more darkly stained in injured facial nucleus (Fig. 4.1d). ATF3-positive nuclei were identified in the injured facial nucleus only (Figs. 4.1e and f). The inset in Figs. 4.1e and f are magnified images of facial nucleus sections showing a similar result when reacted with an immunofluorescent secondary antibody, as a positive control for our immunoflourescent immunohistochemistry experiments. SCG10-positive cells were found in both facial nuclei, but immunoreactivity was greater in the facial nucleus ipsilateral to the crushed facial nerve (Figs. 3.1g and h). Scale bar in Fig. 3.1a = 200μm and applies to b – h; inset bar = 100μm and applies to both insets.

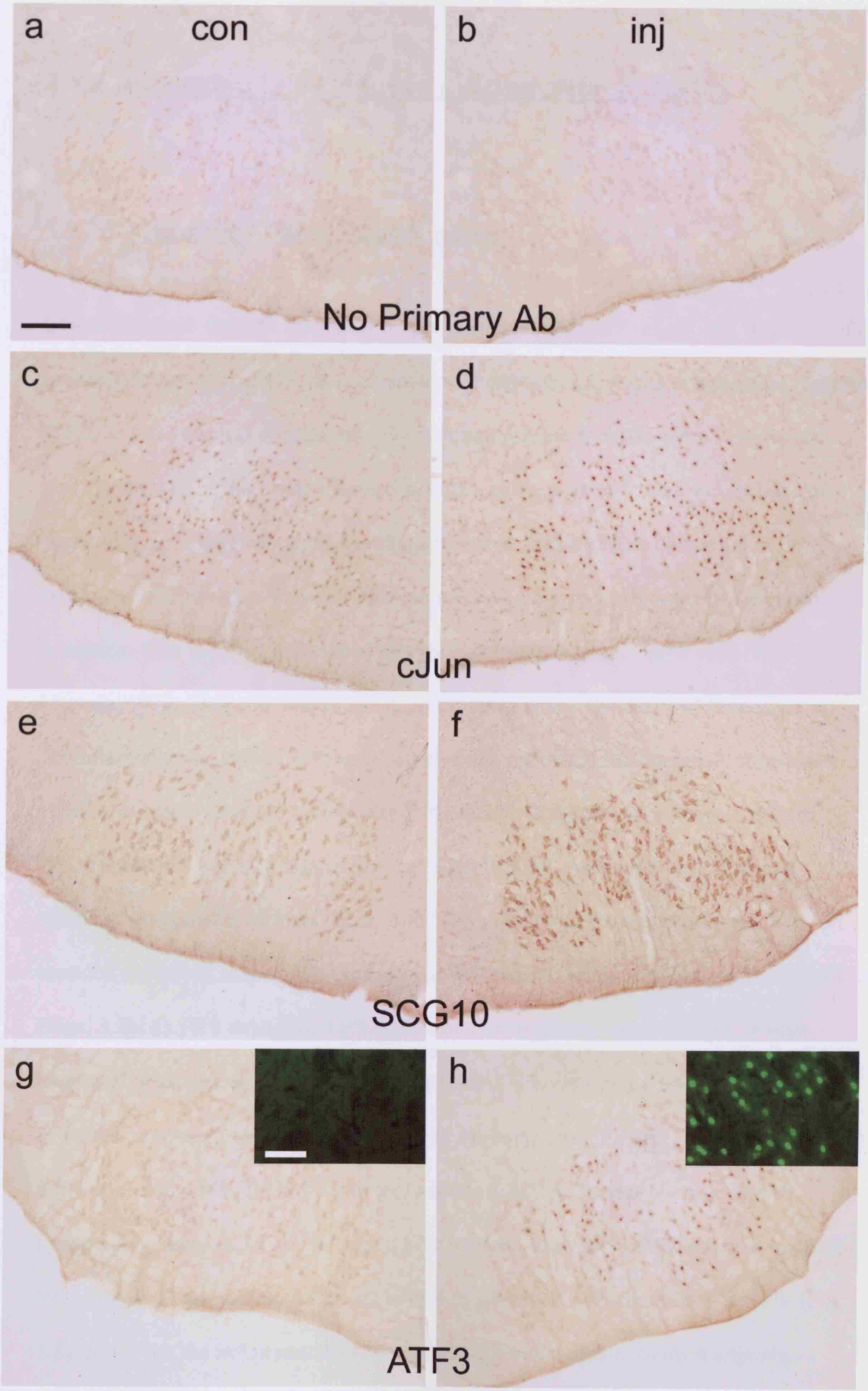
a
con
b
inj
No Primary Ab
c
d
cJun
e
f
SCG10
g
h
ATF3

3.1.2 Assessing LPS- induced inflammation in cortex

3.1.2.1 Microglial / Macrophage response

Coronal sections through the motor cortex to which LPS had been applied were immunostained with OX42, an antibody that recognizes the type 3 complement receptor (CR3) in mononuclear phagocytes, which is upregulated by activated microglia and macrophages (Aldskogius and Kozlova, 1998). In unoperated brains and on the side opposite to LPS application, and in sham-operated animals (dura opened; no LPS applied +/- Gelfoam), highly ramified microglia were present throughout the cortex, consistent with the well established morphology of resting microglial cells (Rio-Hortega, 1932; Ling and Wong, 1993). In brains in which the dura had been opened contralateral to the side of LPS application, there was some accumulation of rounded OX42-positive cells at the pial surface in the first 7 days after treatment but deeper layers contained ramified microglia (Fig. 3.2c). In LPS-treated cortex, microglial morphology was altered from the ramified form typical of the quiescent state, to a rounded amoeboid shape, with thicker proximal processes and loss of distal ramification (Figs. 3.2b, d). At 3 days after LPS application microglia numbers in layer V were increased, with a mean of 177 cells per unit area (136,000 μm^2), 91.4% of which were activated, compared to a mean of 69 cells in the contralateral cortex – of which only 0.5% were activated (Table 3.1). In the animals in which Fluorogold was used to retrogradely label corticospinal tract (CST) neurons, activated OX42-positive microglia were closely associated with the cell bodies of identified CST neurons in layer V (Fig. 3.3). However, the inflammatory response to LPS was variable. In most animals,

microglial activation was seen in all layers of the cortex beneath the site of LPS application, and extending up to 2mm on either side, for up to one week after application. In a few animals microglial activation was only evident in the outer two thirds of the cortex. Inflammation around layer V pyramidal neurons was always apparent beneath the site of LPS application. Two weeks after application, rounded, amoeboid microglia were rare and microglia with a ramified morphology predominated in both the ipsilateral and contralateral cortex (Figs. 3.2e, f). There were 75.3 microglia per unit area in control cortex, 0.4% of which were activated, compared to 79.3 microglia per unit area, of which 2.9% were activated, in LPS-treated cortex. At one month, the ipsilateral and contralateral cortex appeared identical in all animals, with only ramified microglial cells apparent. Thus, 500μg of LPS was sufficient to produce inflammation around layer V pyramidal neurons in all animals by 24 hours, which was maximal at 3 days and had subsided by two weeks after application.

Figure 3-2 Microglial responses to LPS application

Coronal sections of motor cortex, immunoreacted with OX42 antibody to visualise microglia / macrophages 3 days (Figs. 3.2a, b), 7 days (Figs. 3.2c, d) and 2 weeks (Figs. 3.2e, f) after unilateral application of LPS to the pial surface (Figs. 3.2b, d, f) or sham operations on the contralateral (contra), control side (Figs. 3.2a, c, e). **Here and in all other figures in Results chapters 3.1, 3.3. and 4.1, the pial surface is at the top and all sections are photographed below the craniotomy site, with the same exposure for all pairs of images taken at each survival time.**

Microglia from layer V are illustrated at higher magnification in the insets. Note that microglia are present throughout the full depth of cortex at all time points and are ramified in the control (contra) but are rounded and amoeboid and more numerous in the LPS-treated cortical tissue 3 days and 7 days after LPS application. The numerous immunoreactive cells at the pial surface on both sides of the brain (Figs. 3.2a, b) are likely to be macrophages of haematogenous origin induced by local damage due to craniotomy. Note the reduction in number of such cells at 7 days and that very few remain at two weeks. Scale bar in Fig. 3.2a = 200μm and also applies to Fig. 3.2b; scale bar in Fig. 3.2c = 200μm and also applies to Figs 3.2d - f (Figs 3.2a and b are of greater magnification than Figs. 3.2c - f); scale bar in the inset to Fig. 3.2a = 50μm and applies to all insets.

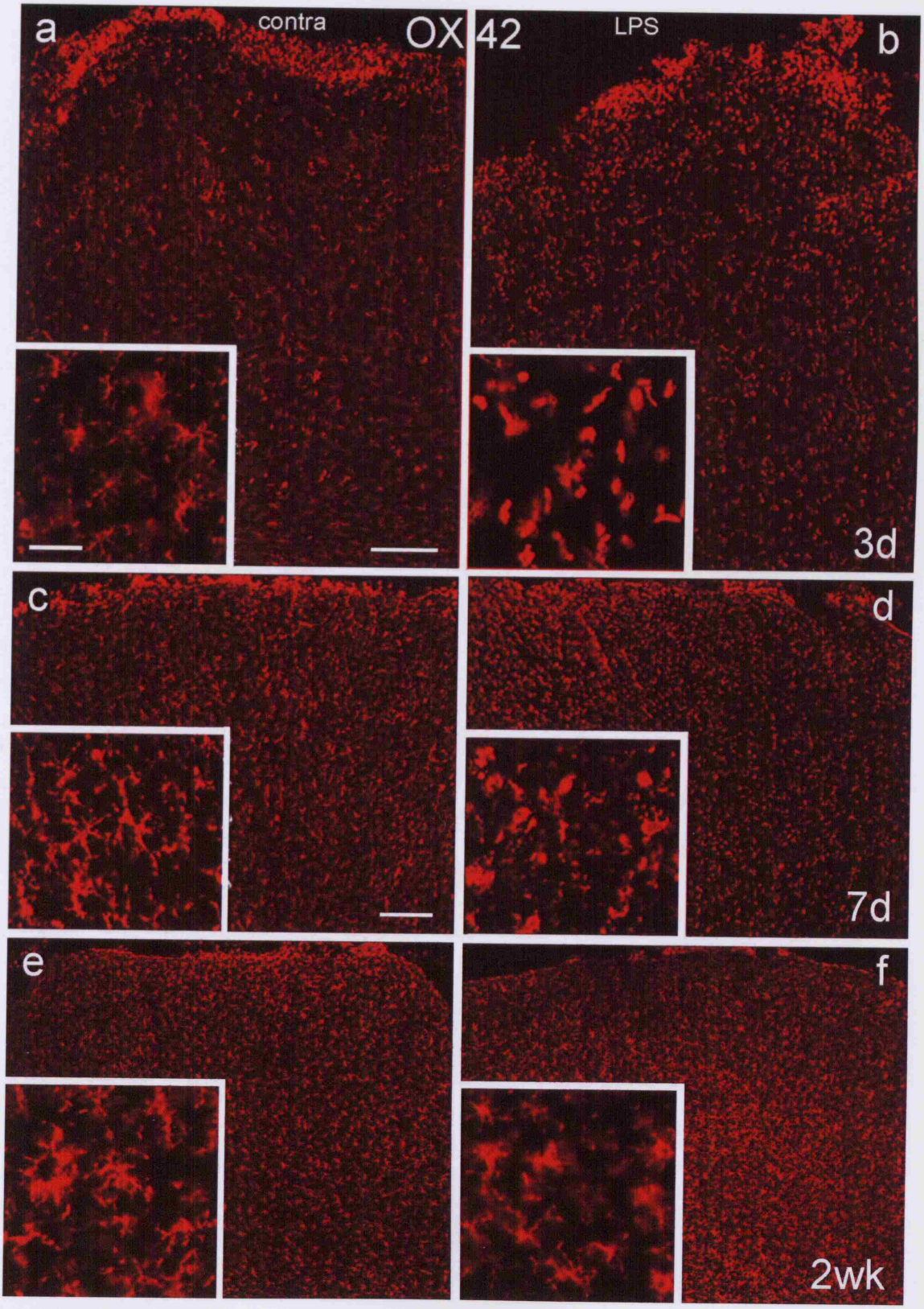
a
contra
OX 42
LPS
b
3d
c
d
7d
e
f
2wk

Figure 3-3 Microglial response around identified CST neuron after LPS application.

Coronal section of OX42-immunoreacted motor cortex (layer V) 3 days after LPS administration and simultaneous application of Fluorogold to a lesion of contralateral cord at C6. Note the very close association between microglial cell(s) (red) and the retrogradely-labelled (blue) CST neuronal cell body. Scale bar = 10μm.

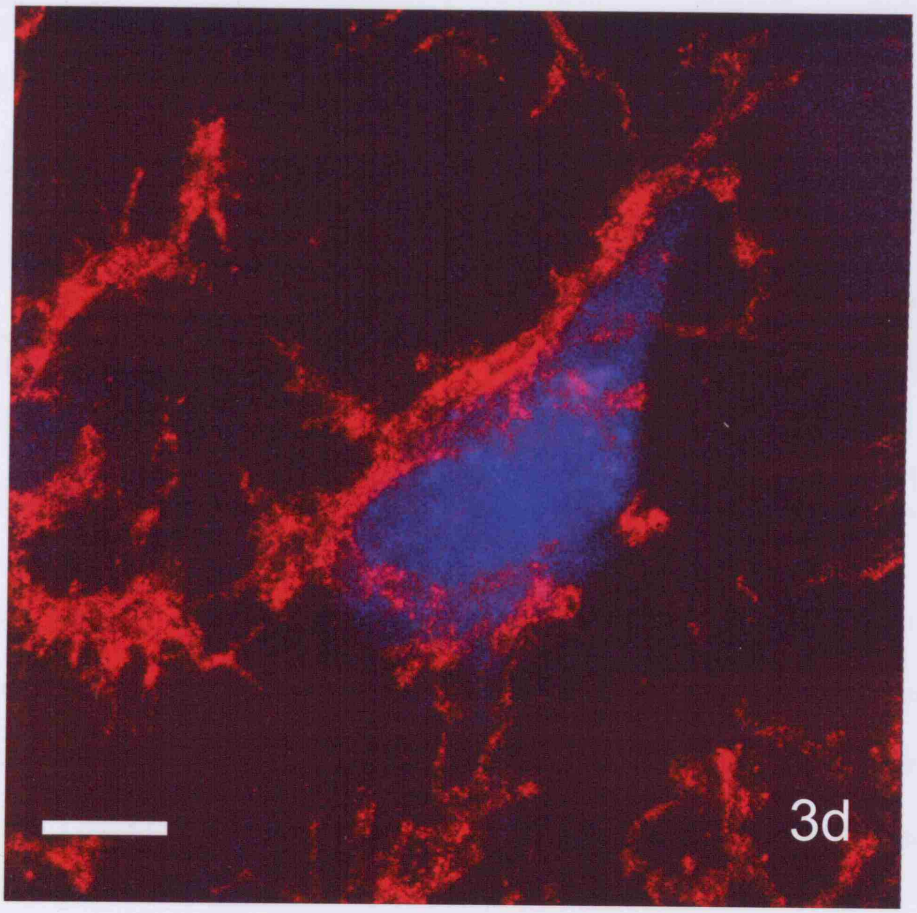
3d

Table 3-1 Number and morphology of cortical layer V microglia after sham-operation or LPS application

		Sham-operated		LPS-treated	
		Ramified microglia	Activated microglia	Ramified microglia	Activated microglia
3 days after LPS	Mean number	69	0.3	15.3	162
	% of total	99.5	0.5	8.6	91.4
14 days after LPS	Mean number	75.3	0.3	77	2.3
	% of total	99.6	0.4	97.1	2.9
1 month after LPS	Mean number	67	0	72	0
	% of total	100	0	100	0

Notes to table 3-1: All microglia within an area of 400μm x 340μm (136,000 μm^2) defined by a counting frame superimposed over a digitised image of layer V were counted and identified as either ramified (quiescent) or activated. Numbers represent means of 3 counts; % indicates relative proportions of ramified and activated microglia.

3.1.2.2 Astrocytic response

From 3 days to 2 weeks after the application of LPS, GFAP-positive astrocytes in the LPS-treated cortex showed hypertrophy of their processes and GFAP immunofluorescence near the inflamed pial surface was more intense (Fig. 3.4d) than in the contralateral cortex (Fig. 3.4c) or in unoperated controls. Astrogliosis was less marked in deeper layers of cortex. However, in some animals surviving for 3 days, there was a marked amount of swelling of LPS-treated cortex (and maximal microglial activation), consistent with the variable nature of LPS-induced inflammation, and GFAP immunoreactivity was reduced in parts of the swollen cortex directly under LPS application (Fig. 3.4b). The contralateral cortex (con) was swollen to a lesser degree under the site of the sham operation with a much smaller area of decreased GFAP immunoreactivity but similar level of GFAP signal intensity in layers I and II of cortex. Deeper in cortex, the LPS-treated cortex had brighter GFAP immunoreactivity than the control cortex, similar to animals with a less swollen motor cortex. The findings in animals with more swollen cortex are consistent with the findings in zymosan-treated animals (see chapter 4.1.2.2, page 226).

Figure 3-4 Astrocytic response to LPS application.

Coronal sections of GFAP-immunostained motor cortex below the area of LPS application (Figs. 3.4b and d) or sham operation (Figs. 3.4a and c) on the contralateral (contra), control side, 3 days after application of LPS. The animals shown in Figs. 3.4a and 3.4b have a markedly swollen cortex on the LPS-treated and (to a lesser extent) control cortex. In Fig. 3.4a, there is an area of decreased GFAP immunoreactivity (arrowhead) directly under the burrhole with a similar, but much larger area in Fig. 3.4b (arrows). In deeper layers of cortex and either side of the operation site, GFAP immunoreactivity is greater in the LPS-treated cortex. In contrast, the less swollen (and therefore less inflamed) cortex (Figs. 3.4c and d), has GFAP+ astrocytes present throughout the full depth of cortex and they are more brightly fluorescent in the LPS-treated cortex, with thicker processes than in the control cortex. Scale bars in Fig. 3.4a and 3.4c = 200μm and also apply to Figs. 3.4b and 3.4d respectively.

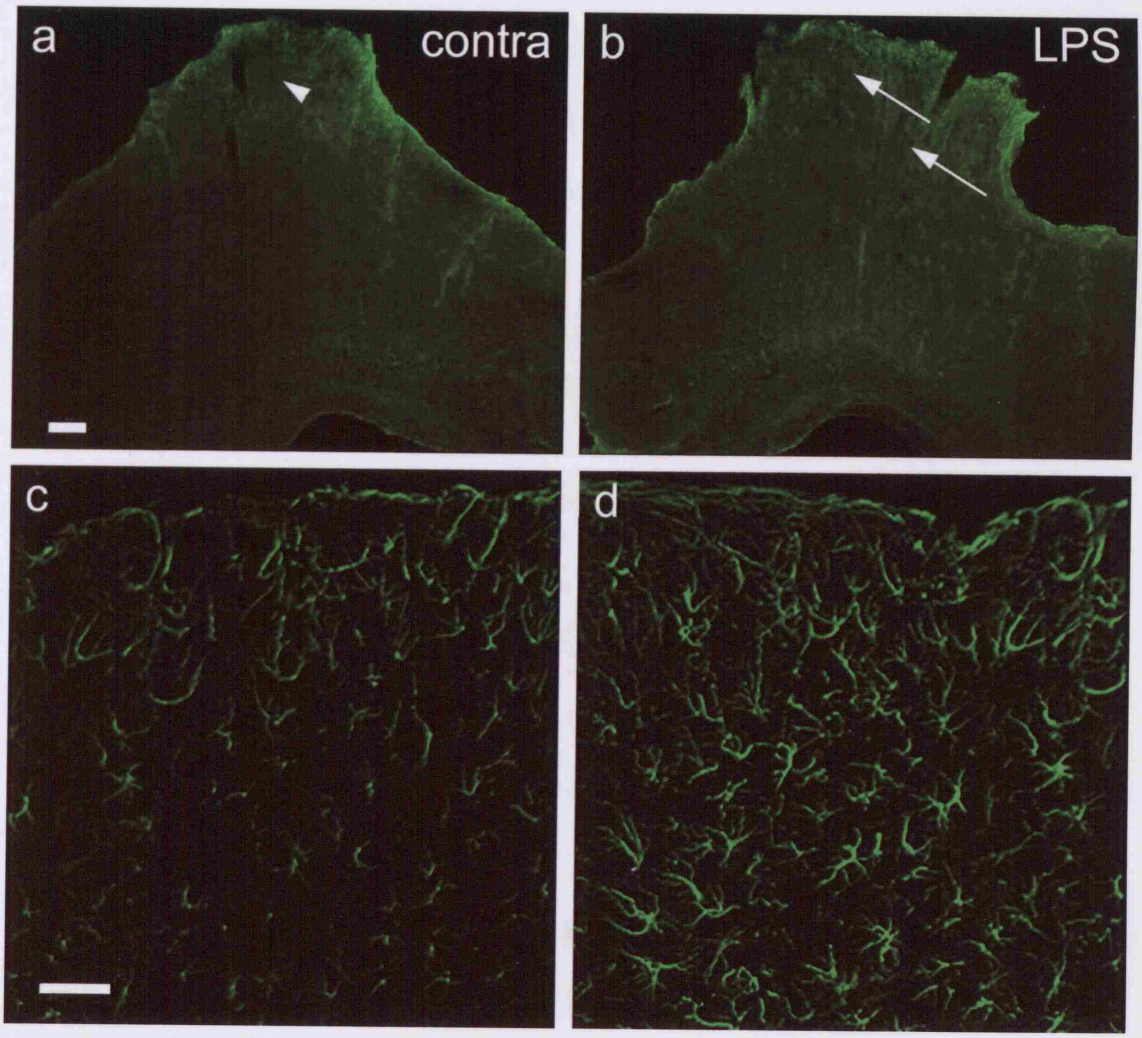
a
contra
b
LPS
c
d

3.1.3 Expression of growth-associated proteins / genes by CST neurons

Injection of CTB into the spinal cord at C4 invariably labelled layer V pyramidal cell bodies in the contralateral motor cortex. Sections immediately adjacent to those reacted for CTB were reacted for c-Jun, ATF3 or SCG10 (e.g. Figs. 3.5b, d). Other sections were reacted for both CTB and a growth-associated protein, allowing identification of the protein and CST neurons in the same section (Fig. 3.8).

3.1.3.1 Unoperated and Sham operated control cortex

Making a burr hole in the skull and opening the dura had some effect on c-Jun and ATF3 expression for up to 3 days. In unoperated cortex, c-Jun was weakly expressed in cells in layers II, III and V. There was a small increase in c-Jun expression by cells in layers I, II, III and V (mostly or entirely neurons) directly underneath the burr hole even without LPS application (Fig. 3.5a). In unoperated cortex there was no ATF3 expression whereas in sham-operated controls, ATF3 was expressed by very small numbers of layer I cells directly underneath the burr hole (< 5 per section). These ATF3-expressing cells had abnormal nuclei and were possibly apoptotic but could not be unequivocally identified. Expression of SCG10 protein and GAP-43 mRNA were not affected by opening of the dura. SCG10 was weakly expressed, in layer V neurons only, in the cortex contralateral to LPS application, and in sham-operated and unoperated animals. GAP-43 mRNA was present in neurons in all layers of the cortex, but most strongly in layers IV and V, contralateral to LPS application, in sham-operated and unoperated animals, confirming previous findings from this laboratory (Mason et al., 2003). The

presence or absence of Gelfoam made no difference to the expression of growth-associated genes in the cerebral cortex.

3.1.3.2 LPS-treated cortex

c-Jun

From 24 hours to two weeks after LPS application c-Jun was markedly upregulated in most neurons of layers II, III and V of the motor cortex (Figs. 3.5b, d). Retrograde labelling with CTB (Fig. 3.5 insets) and retrograde labelling combined with immunohistochemistry for c-Jun (Fig. 3.8) showed that CST neurons in layer V were among cells upregulating c-Jun in response to LPS application. By 1 month after application (Fig. 3.5f) there were no detectable differences between treated and control cortex.

Figure 3-5 Expression of c-Jun after LPS application.

Coronal sections of motor cortex 3 days (Figs. 3.5a, b), 2 weeks (Figs. 3.5c - e) and 1 month (Fig. 3.5f) after unilateral application of LPS, or sham operation (Figs. 3.5a, c), immunoreacted for c-Jun or CTB (insets to Figs. 3.5b, d and f). Note that, at 3 days c-Jun is detectable in layers II, III and V at low levels immediately below the craniotomy on the control side, but is almost undetectable more medially and laterally, and that c-Jun immunoreactivity is much stronger on the treated side, predominantly in layers II, III and V, immediately below the site of LPS application. Note also the marked increase in c-Jun immunoreactivity in layers II, III and V immediately below the burr hole and site of LPS application in Fig. 3.5d compared to the corresponding contralateral cortex in Fig. 3.5c. The framed area of layer V in Fig. 3.5d is enlarged in Fig. 3.5e to show details of immunostained nuclei. The insets to Fig. 3.5b and d are taken from the section immediately serial to the ones shown in Figs 3.5b and d and demonstrates that retrogradely labelled CST neurons occupy the same area (in layer V) as neurons displaying upregulation of c-Jun expression. Some of the retrogradely labelled cells in Fig. 3.5d are shown at greater magnification in the inset to Fig. 3.5f. Note also that at one month, c-Jun immunoreactivity in layers II and III of the experimental side still involves areas medial and lateral to the site of LPS application with almost no c-Jun detectable in layer V (c-Jun immunoreactivity in the contralateral cortex is weak and largely confined to layers II and III: not shown). Scale bar = 500μm and applies to Figs. 3.5a - d and f); bar in Fig. 3.5e = 20μm; bar in Fig. 3.5f inset = 50μm.

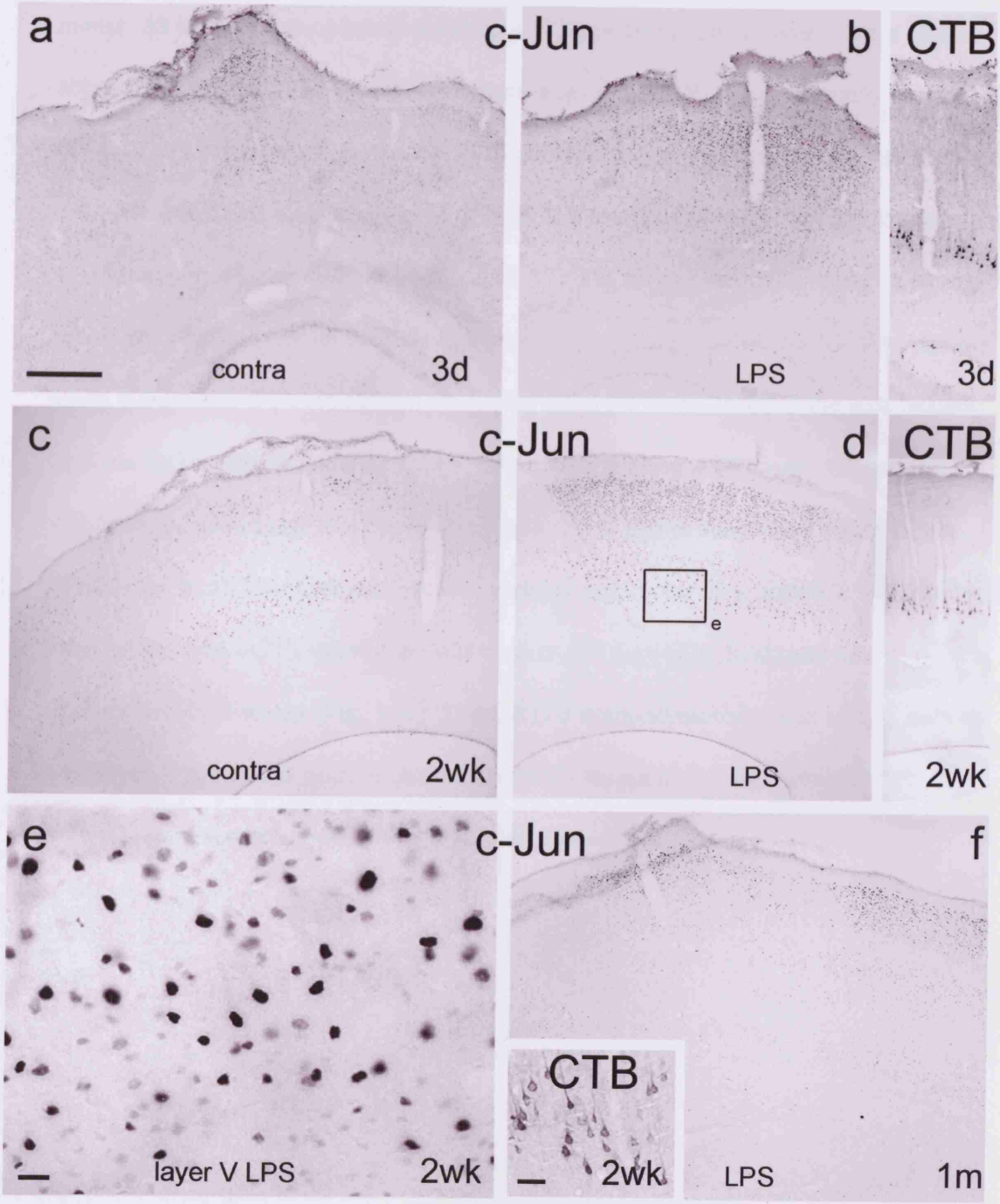
a
c-Jun
b
CTB
contra
3d
LPS
3d
c
c-Jun
d
CTB
e
contra
2wk
LPS
2wk
e
c-Jun
f
CTB
layer V LPS
2wk
2wk
LPS
1m

ATF3

By 24 hours after application of LPS, ATF3 was upregulated in very few neurons, confined to the region under the burr hole, and in numerous glia in the subcortical white matter. As in the sham-operated animals, ATF3-positive nuclei in layer I were often abnormally shaped. ATF3-positive neurons in layers II to VI were extremely sparse (<8 per section on the treated side; none on the contralateral side), but retained a normal morphology. ATF3 was upregulated in layer V pyramidal neurons but only in relatively small numbers of such cells. Expression of ATF3 in subcortical white matter glia was much more extensive than the neuronal expression; ATF3-positive nuclei were present up to 400μm into the contralateral hemisphere and for 2mm lateral to the area of LPS application (not illustrated). At 3 days, neurons expressing ATF3 were almost entirely confined to layers I and II under the burr hole and to glia in subcortical white matter (Figs. 3.6a, b, c). This upregulation was variable and appeared to correlate with the level of inflammation. ATF3 expression was weaker at 7 days (Fig. 3.6d) and had disappeared by 2 weeks (Fig. 3.6e). Thus, ATF3 immunoreactivity was seen in only a few layer V pyramidal neurons in animals with a maximal (i.e. full cortical thickness) inflammatory response and only at 24 hours after application.

Figure 3-6 Expression of ATF3 after LPS application.

Coronal sections of motor cortex immunoreacted for ATF3, 3 days (Figs. 3.6a - c), 7 days (Fig. 3.6d) and 2 weeks (Fig. 3.6e) after LPS application. Fig. 3.6a shows both the experimental and the medial part of the control cortex (midline at the vertical arrow) and demonstrates ATF3 immunoreactivity directly under the area of the burr hole and in the subcortical white matter on the experimental side. The superficial upregulation is localised, but immunoreactive cells in the white matter extend for 2 mm laterally and 400 μm across the midline. There is no ATF3 immunoreactivity in cortical neurons located in layers III to VI or in the contralateral (control) cortex. Fig. 3.6b is enlarged from the boxed area of cortex directly under the site of LPS application in Fig. 3.6a. Note the irregular shape of ATF3-positive nuclei, suggesting possible damage or apoptosis. Fig. 3.6c is enlarged from the boxed area of white matter in Fig. 3.6a. ATF3-positive nuclei are seen arranged in a linear fashion, suggesting that they are white matter glial cells. Fig. 3.6d, 7 days after LPS application shows reduced ATF3 immunoreactivity directly under the LPS application site (top arrowhead) and in the subcortical white matter (bottom arrowhead). Fig. 3.6e shows no ATF3 immunoreactivity 2 weeks after LPS application. The inset is from the immediately adjacent section, directly beneath the LPS application site and demonstrates CST neurons retrogradely labelled with CTB. No ATF3 immunoreactivity was seen in the area of cortex where the CTB-labelled CST neurons were located. Scale bar in Figs. 3.6a and e = 500μm; bar in Fig. 3.6b = 50 μm and also applies to Fig. 3.6c; bar in Fig. 3.6d = 200μm.

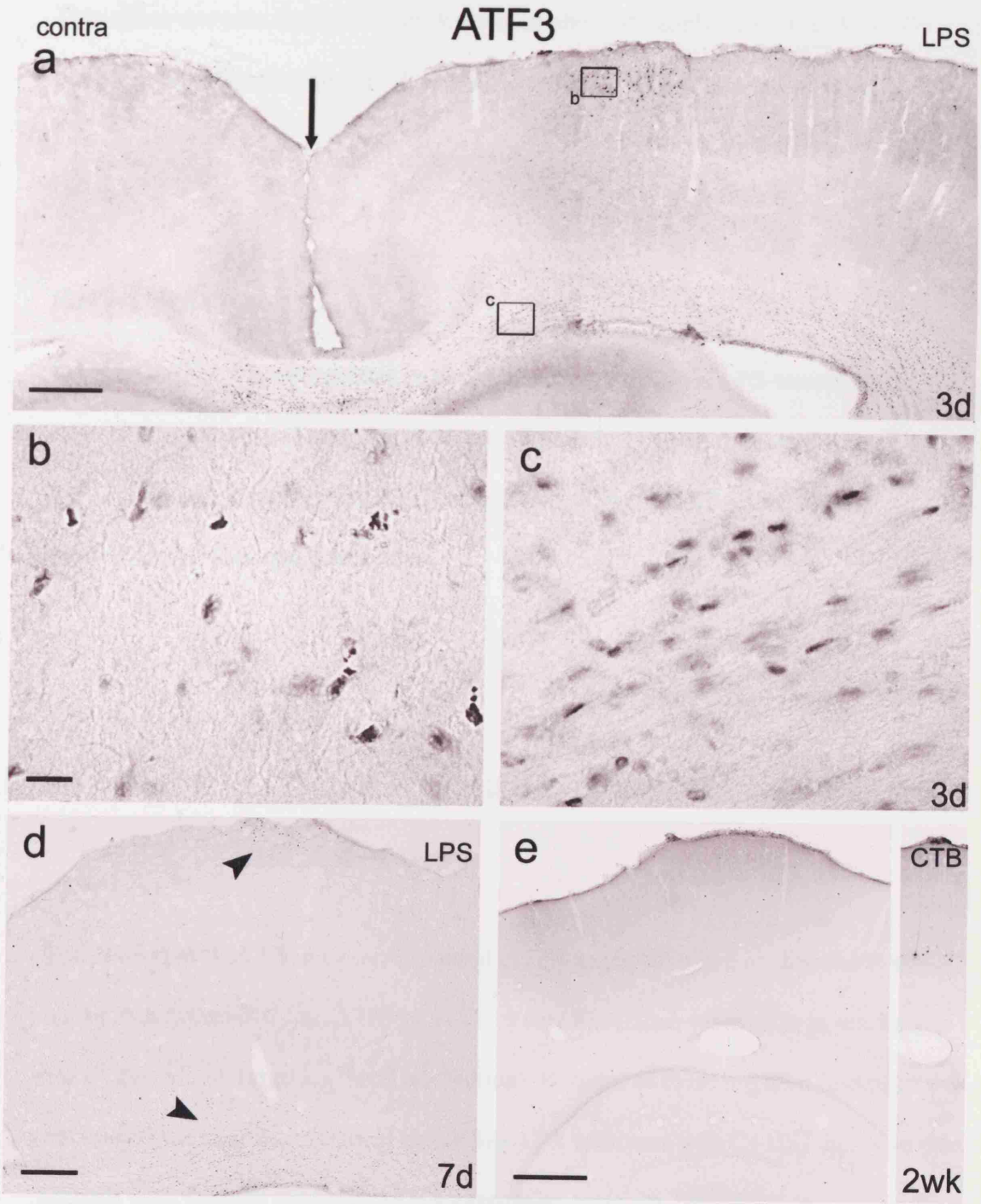
contra
ATF3
LPS
a
b
c
3d
b
c
3d
d
LPS
7d
e
CTB
2wk

SCG10

SCG10 was weakly upregulated by layer V pyramidal neurons and by no other cells. This effect was seen from 24 hours to 2 weeks after LPS application (Fig. 3.7). The cell bodies displaying upregulation of SCG10 were identified as CST neurons (Fig. 3.8b).

GAP-43 mRNA

GAP-43 mRNA was upregulated in neurons in layers II –VI of LPS-treated cortex, 3 days after application (Fig. 3.9b), most conspicuously in layer V. After 7 days (Figs. 3.9e, f), 2 weeks (not illustrated) or 1 month (Fig. 3.9g, h) GAP-43 expression resembled that in unoperated cortex.

3.1.3.3 Effect of CST injury in cervical spinal cord on growth–associated protein / gene expression

Transection of the CST at C4 contralateral to LPS application had no detectable effect on the expression of c-Jun, ATF3 or SCG-10 (not illustrated; referred to in brackets in the 2nd column of Table 2.1, Methods section). Because of these negative findings I did not investigate possible effects of combining LPS treatment with C4 CST injury in the animals used to study GAP-43 mRNA expression by *in situ* hybridisation.

Figure 3-7 Expresssion of SCG10 after LPS application.

Coronal sections of motor cortex immunoreacted for SCG10 (except for insets), 1 week (Figs. 3.7a - d) and 1 month (Figs. 3.7e, f) after LPS application. Control, contralateral cortex is shown in Figs. 3.7a, c and e, LPS-treated cortex in Figs. 3.7b, d and f. Note increased SCG10 immunoreactivity in layer V cells at one week in Fig. 3.7b compared to contralateral cortex (Fig. 3.7a), and absence of immunoreactivity in more superficial cortex. Fig. 3.7c is enlarged from layer V in Fig. 3.7a and Fig. 3.7d is enlarged from layer V in Fig. 3.7b. One month after LPS application there is only a background level of SCG10 immunoreactivity in layer V cells of both contralateral (Fig. 3.7e) and ipsilateral (Fig. 3.7f) cortex. The insets are from immediately serial sections to Figs. 3.7e and 3.7f and show retrogradely CTB-labelled CST neurons in layer V. Bar in Fig. 3.7a = 200μm and also applies to Figs. 3.7b, e, f and insets; bar in Fig. 3.7c = 50μm and also applies to Fig. 3.7d.

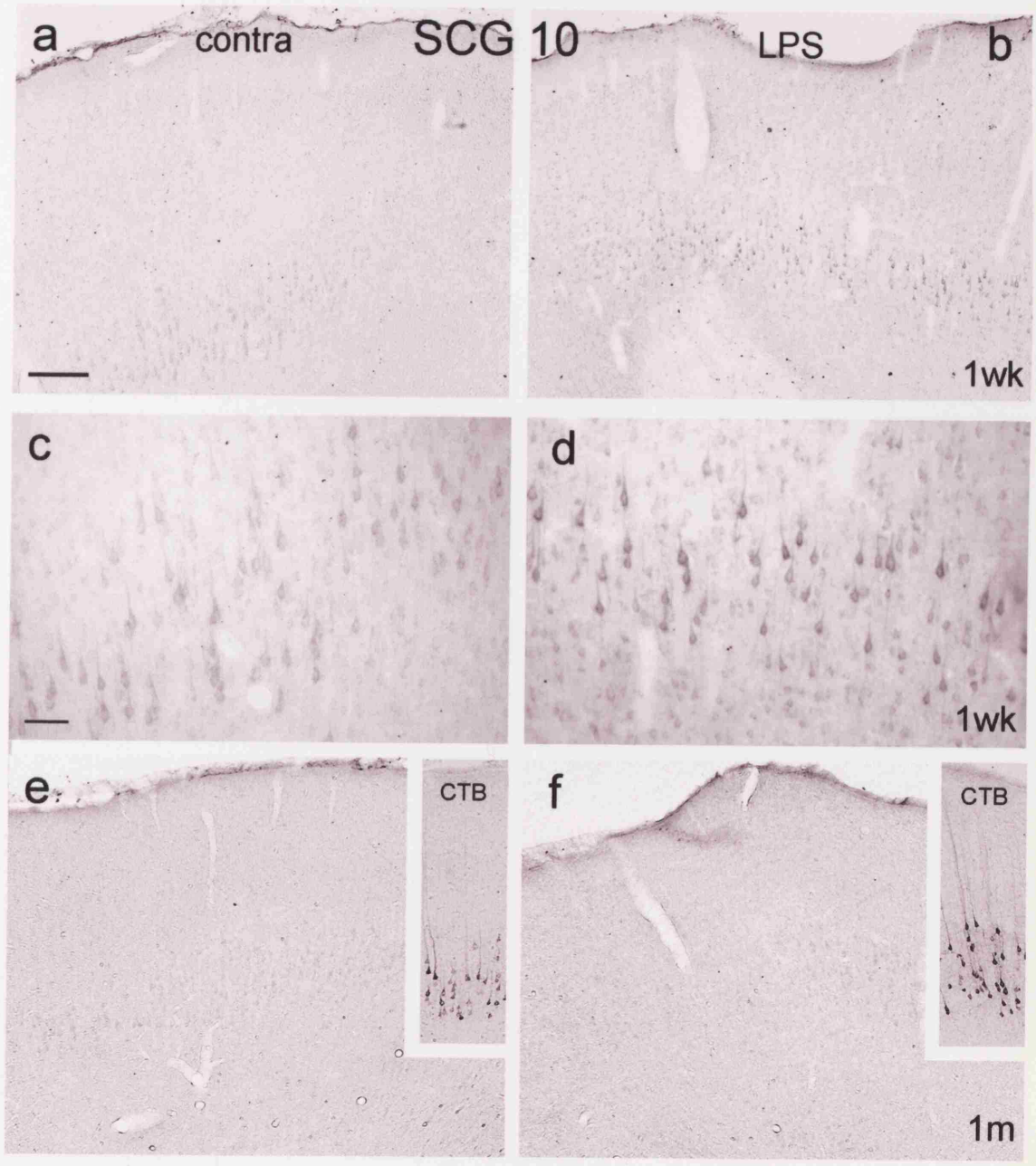
a
contra
SCG
10
LPS
b
1wk
c
d
1wk
e
CTB
f
CTB
1m

Figure 3-8 Co-localisation of retrograde label and c-Jun or SCG10.

CTB (red) in the cell bodies of CST neurons co-localised with c-Jun (Fig. 3.8a) or SCG10 (Fig. 3.8b) (green) in coronal sections of the motor cortex (layer V), 3 days after application of LPS and simultaneous injection of CTB into the CST at C4. Note that not all layer V neurons expressing c-Jun in their nuclei also show co-localisation with CTB (Fig. 3.8a). There is a higher degree of co-localisation between SCG10 and CTB (Fig. 3.8b). Confocal microscopy; scale bar = 20μm and applies to both images.

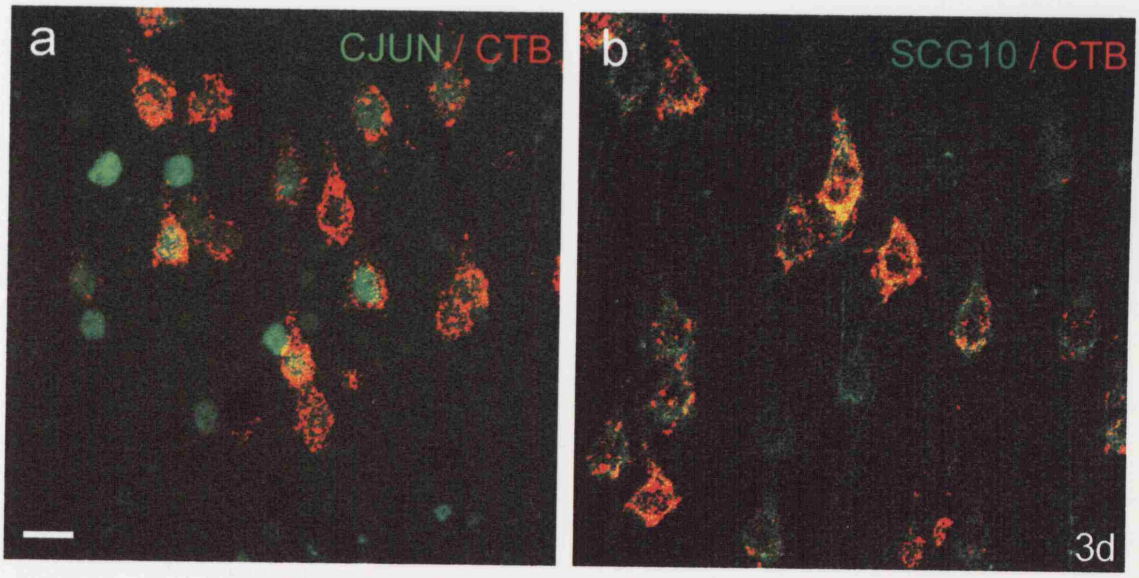
a
CJUN / CTB
b
SCG10 / CTB
3d

Figure 3-9 GAP-43 mRNA expression after LPS application.

Coronal sections of motor cortex hybridised with GAP-43 mRNA probe 3 days (Figs. 3.9a - d), 7 days (Figs. 3.9e, f) and 1 month (Figs. 3.9g, h) after unilateral application of LPS (Figs. 3.9b, d, f, h) or sham operations to the contralateral (control) side (Figs. 3.9a, c, e, g). Background levels of GAP-43 mRNA are seen in contralateral (control) cortex at 3 days but stronger expression is apparent in layers II-V of LPS-treated cortex. Areas of layer V in Figs. 3.9a and b are enlarged in Figs. 3.9c and d to better show differences in hybridisation signals. By 7 days (Figs. 3.9e and f), GAP-43 mRNA expression appears to be identical on both sides, and remains so one month after LPS application (Figs. 3.9g and h). Scale bar in Fig. 3.9a = 500μm and also applies to Fig. 3.9b; scale bar in Fig. 3.9c = 50μm and also applies to Fig. 3.9d; scale bar in Fig. 3.9e = 200μm and also applies to Figs. 3.9f - h.

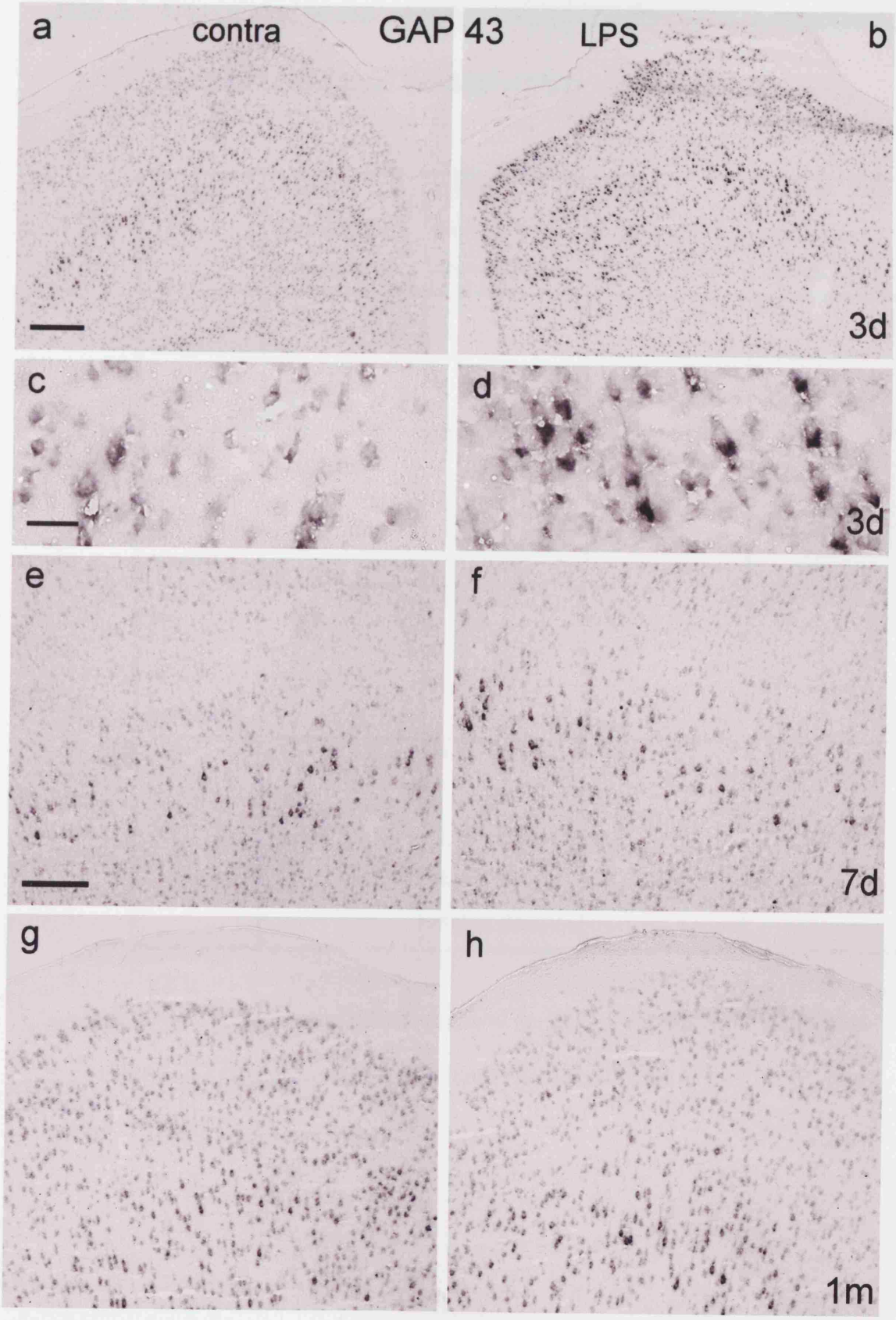
a
contra
GAP 43
LPS
b
3d
c
d
3d
e
f
7d
g
h
1m

Table 3-2 Expression of cortical growth-associated proteins / genes in unoperated, sham-operated and LPS-treated animals

Group	c-Jun expression cortical layers	ATF3 expression cortical layers	SCG10 expression cortical layers	GAP-43 expression cortical layers
Unoperated animals	-/+ II, III	-	-/+ V	+ II – VI
Control animals (dura opened)	+ II, III, V	+ I, II	-/+ V	+ II – VI
Cortex contralateral to LPS application	+ II, III, V	+ I, II	-/+ V	+ II – VI
LPS-treated cortex	+++ II, III, V[1]	++ I, II[2], V[4] & white matter glia[2]	+ V[1]	++ II – VI[3]

Notes to table 3-2: Superscript numbers refer to duration of expression of the growth-associated protein / gene after LPS application: [1] for up to 2 weeks; [2] for up to 7 days; [3] for up to 3 days; [4] for up to 24 hours

3.2 LPS-induced inflammation and CST regeneration

Background

Corticospinal neurons normally show little response to spinal injury. CST neurons also fail to upregulate growth-associated genes after spinal injury, but are capable of doing so following intracortical axonal injury (Tetzlaff et al., 1994; Mason et al., 2003). In the above study, topical LPS application onto the cortical surface induced inflammation around the cell bodies of CST neurons. My study examines whether the inflammation-induced expression of growth-associated genes c-jun, SCG10 and GAP-43 would stimulate the regeneration of their axons, following a lesion of the CST.

Results

3.2.1 CST sprouting

Application of LPS to motor cortex had no obvious effect on the numbers and morphology of microglia around the lesion site in the spinal cord, compared with controls (data not shown). Three weeks after spinal cord lesion, injured CST axons, anterogradely labelled with BDA, terminated proximal to the lesion site, many with swollen axonal tips, in both LPS-treated and control animals (Figs. 3.10a and b). No axons were seen to grow into or distal to the lesion cavity or to bypass the lesion site, or send branches around it. Thus, application of LPS to the cortex appeared to produce no enhancement of axon regeneration into or around the lesion site. There was no statistically significant difference between control and LPS-treated animals in either the

'total sprouting ratios' ($p = 0.2$; Mann-Whitney) or the 'lesion site sprouting ratios' ($p = 0.39$; Mann-Whitney). These data, summarised in Table 3.3, suggest that application of LPS to motor cortex has no effect on the sprouting response or regeneration of CST axons across a lesion. The application of LPS to cortex did not cause a significant reduction of labelled CST axons in the medulla ($p = 0.69$, Mann-Whitney test, n.s.; see Table 3.3 and Fig. 3.10c). This result demonstrates that the uptake and anterograde transport of BDA by CST neurons was unaffected by LPS-induced inflammation.

3.2.2 BDA placement

The correct placement of BDA in layer V of motor cortex (as described in Methods section 2.2, pages 120-121) was checked by reacting coronal sections of motor cortex injected with BDA 21 days previously with ATF3 antibody and the ABC method of immunohistochemistry. Cystic areas that were presumably sites of BDA injections were seen in the deeper layers of motor cortex, surrounded by very strongly immunopositive spots that were most likely to represent crystals of BDA, to which biotinylated secondary antibody would have bound (Fig. 3.10d).

Figure 3-10 Anterograde labelling of CST axons after spinal cord injury and LPS application.

Horizontal sections through spinal cord injury sites (Figs. 3.10a, b), and a transverse section through the medulla (Fig. 3.10c) 21 days after lesion of the CST at C4 with either simultaneous injection of BDA into contralateral motor cortex (Control) or injection of BDA into and application of LPS onto motor cortex (LPS). In both the LPS-treated (Fig. 3.10b) and control tissue (Fig. 3.10a), end bulbs are seen at the tips of large numbers of axons. There is little sign of axon branching into the contralateral CST, and the labelled axons extending into the lesion site are located in a strand of spared tissue that extends no more than 50μm. No axons appear to circumnavigate or regenerate beyond the lesion site. The white boxes correspond to the counting frame windows. Fig. 3.10c shows BDA-labelled CST axons in the pyramid of the medulla (midline at arrow). Fig. 3.10d is a coronal section of motor cortex, immunoreacted with ATF3 antibody 21 days after injection of BDA into motor cortex (3 x 1.4μl), demonstrating the cystic areas caused by injection of anterograde tracer are located within layer V of motor cortex, and a depression on the cortical surface caused by the trauma of needle injections. The strongly immunopositive black dots within the cortex and corpus callosum are probably macrophages that have taken up BDA. There is no ATF3 immunoreactivity within the injected cortex. Images 3.10a - c are confocal; * = lesion site; R = rostral; L = lateral; P = pyramid; scale bar in Fig. 3.10a = 100μm and also applies to Fig. 3.10b; bar in Fig. 3.10c = 200μm; bar in Fig. 3.10d = 500μm.

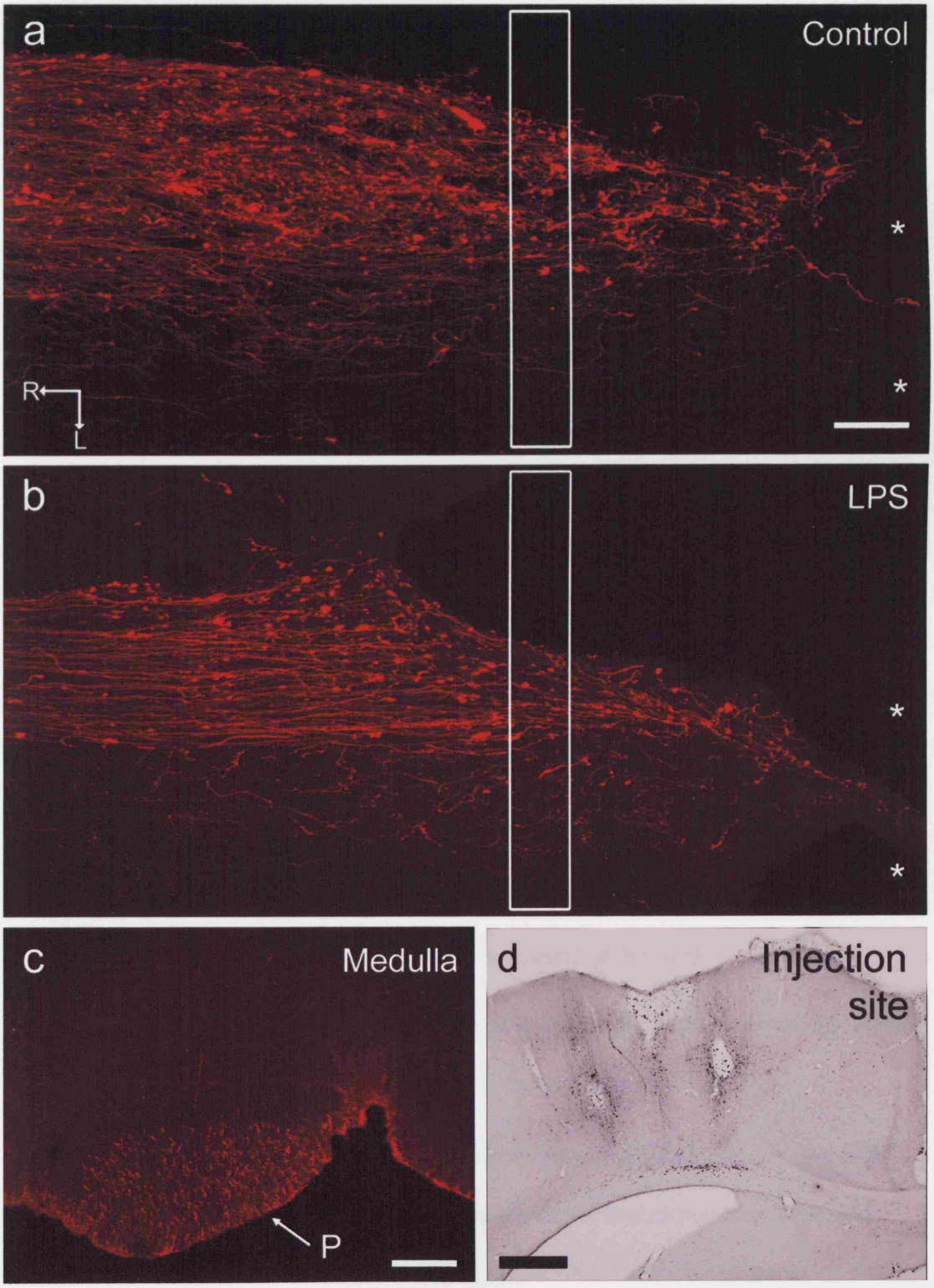
a
Control
R
L
*
*
b
LPS
*
*
c
Medulla
P
d
Injection
site

Table 3-3 Quantification of CST axons

	Lesion site axon total	Branching points	Medulla axon total	Total sprouting ratio	Lesion site sprouting ratio
LPS 1	133	52	466	0.11	0.39
LPS 2	123	100	788	0.13	0.81
LPS 3	146	54	685	0.08	0.36
LPS 4	301	128	519	0.25	0.42
LPS group mean ± SEM			614.5 ± 74.3	0.14 ± 0.04	0.5 ± 0.11
Con 1	150	162	998	0.16	1.08
Con 2	273	162	602	0.27	0.59
Con 3	200	78	323	0.24	0.39
Con 4	138	98	439	0.22	0.71
Control group mean ± SEM			590.5 ± 147.4	0.22 ± 0.02	0.69 ± 0.15
Mann-Whitney test p value for LPS-treated vs. control animals			0.69	0.2	0.39

Notes to table 3-3: BDA-labelled axons (and branch points) in 4 LPS-treated animals and 4 control animals (LPS not applied) were counted at two sites:

1) in 9 horizontal sections through the cervical spinal cord 0.4mm rostral to the lesion site, in a 60μm wide counting frame (labelled axons and branch points);

2) in transverse sections through the medulla (number of labelled axons in pyramid). Total sprouting ratio is the ratio between the number of branch points and the total number of labelled CST axons at the level of the medulla. Lesion site sprouting ratio is the ratio between branch points and labelled axons at the same level (0.4mm rostral to the lesion site); SEM = standard error of the mean

3.3 Effects of LPS-induced inflammation on regeneration following lumbar dorsal root transection

Background

It has been postulated that inflammation near neuronal cell bodies enhances axonal regeneration. Injured dorsal root axons do not regenerate into the spinal cord, but stop at the DREZ. However, injection of Corynebacterium into the DRG prior to crushing the dorsal spinal root results in a four-fold increase in regenerating fibres (Lu and Richardson, 1991). The injured CNS has a much delayed macrophage / microglial response to degenerating axons than the injured PNS (George and Griffin, 1994). I therefore investigated the possibility that LPS-induced inflammation around sites of dorsal root transection - and subsequent enhancement of the macrophage / microglial response - would enhance regeneration of their axons.

Results

3.3.1 LPS-induced inflammation and dorsal root regeneration

Each dorsal rootlet contains a cone of CNS tissue, the DREZ. Following dorsal root injury, astrocyte processes extend outward from the DREZ into the rootlets. Axons

regenerate along the rootlets towards the DREZ but only a few grow back into the spinal cord (Chong et al., 1999).

In my studies, a conditioning sciatic nerve crush was performed at the same time as dorsal root transection to improve the regenerative response (Richardson and Verge, 1987). In rats with a L5 dorsal root transection (controls) and rats with L5 transection plus LPS placement on the DREZ either at time of injury or a week later, labelled axons (transganglionic CT-HRP) were present in the dorsal root central to the injury site 28 days after injury. However, the great majority appeared to be have stopped at the DREZ (Fig. 3.11). The addition of intraperitoneal (I-P) LPS injections did not affect regeneration of injured dorsal root axons at the DREZ.

In summary, the finding of almost all axons stopping at the DREZ was consistent in all groups analysed: controls, LPS, delayed LPS and delayed + I-P LPS. One animal in the LPS-treated group had CT-HRP labelled cells in the Gracile nucleus (Fig. 3.11a) and was excluded.

Intraperitoneal LPS injections are known to cause a systemic inflammatory response that affects CNS tissue (Perry et al., 1995a). I therefore analysed 3 animals with a dorsal root cut that were given two I-P injections of LPS 4 and 7 days after the DR cut and compared them to 3 control animals (DR cut alone), with OX42 immunohistochemistry 7 days after injury to look for any differences in inflammation. Sections of dorsal root, DREZ and spinal cord were examined in the lumbar region and cervical region (to see what the effects of injury and I-P LPS were on distant DREZs). Sections through the area postrema (AP) were also analysed, as it is an area of CNS known to have a deficient blood-brain barrier (see Gross, 1992) to look for the effect of systemic LPS on microglia in this region also.

The lumbar roots and spinal cord in control animals demonstrated significant numbers of OX42+ rounded macrophages in the injured dorsal root central to the injury site (peripheral (sciatic) nerve not examined; Fig.3.12b) compared to the uninjured dorsal root (Fig. 3.12e). The adjacent lumbar spinal cord contained ramified microglia on both injured and control sides (Fig. 3.12a), with only a few extra activated microglia / macrophages (round OX42+ amoeboid cells) at the DREZ. In animals given 2 intraperitoneal injections of LPS after DR transection, there was a massive increase in the numbers of round OX42+ cells in the injured dorsal root and DREZ (presumed macrophages) compared to control animals - see Fig. 3.12d. The uninjured, contralateral dorsal root had very few macrophages (Fig. 3.12f) – a very modest increase from the control DR injury animals. Injury to lumbar dorsal roots did not have an effect on cervical dorsal roots in control animals or the I-P LPS injected animals, with ramified microglia present in the spinal cord and DREZ and no macrophages or microglia in the dorsal roots joining the DREZ (Figs. 3.12 g – j). The AP had a uniform distribution of ramified microglia in the control group (Fig. 3.12k); in animals given I-P LPS, a few (< 8 per section) macrophages were present on the surface of the AP and the majority of microglia in the AP had a degree of distal process retraction, with some microglia also demonstrating enlarged somata also (Fig. 3.12l), signifying their (partial) activation. In summary, DR transection causes influx of macrophages to the central portion of the dorsal root, with minimal effect on macrophages and microglia in the lumbar spinal cord adjoining the DREZ and no effect on cervical DREZs and spinal cord. Addition of 2 I-P injections causes dense accumulation of macrophages in the dorsal root, DREZ and adjacent lumbar spinal cord, with presumed microglial activation locally, but no effect on the cervical DREZs and spinal cord.

Figure 3-11 Transganglionic labelling of axons after DR injury and LPS application on to DREZ.

Horizontal sections of spinal cord, proximal dorsal roots and transverse section of medulla containing gracile nucleus (Fig. 3.11a), in control (Fig. 3.11b), LPS-treated (Figs. 3.11a, c – e) and delayed LPS-treated rats (Fig. 3.11f) injected with CT-HRP, visualised with (orange / gold) TMB histochemistry 28 days after DR injury.

In Fig. 3.11a, some cells in the gracile nucleus are retrogradely labelled with CT-HRP (e.g. arrow) indicating that the DR injury was incomplete in this animal. Fig. 3.11b shows most labelled axons in the dorsal root (DR) turning away from the DREZ, but two axons are seen entering the spinal cord (SC) grey matter for a little over 100mm (arrowheads). No axons in any group entered the dorsal columns (not illustrated). Fig. 3.11b plus shows the majority of retrogradely-labelled axons stopping at the DREZ. One axon penetrates grey matter and then gives off many branches (see box). Fig. 3.11d is an enlargement of the boxed area in Fig. 3.11c, showing that none of the branches of the DR axon that entered the spinal cord (arrow) exceed 50μm in length and they sprout in different directions. Fig.3.11e show a labelled DR axon stopping at the DREZ, with a swollen tip indicative of abortive regeneration. Fig. 3.11f shows many CT-HRP-labelled axons in an injured L5 DR that all end at the DREZ. This image highlights the variable uptake of CT-HRP, though the result is the same as the other experimental groups (I-P LPS group data not illustrated). Scale bar in Figs. 3.11a and b = 100μm; bar in Fig. 3.11c = 200μm; bar in Fig. 3.11d = 50μm; bars in Figs. 3.11e and 3.11f = 20μm; DC = dorsal column.

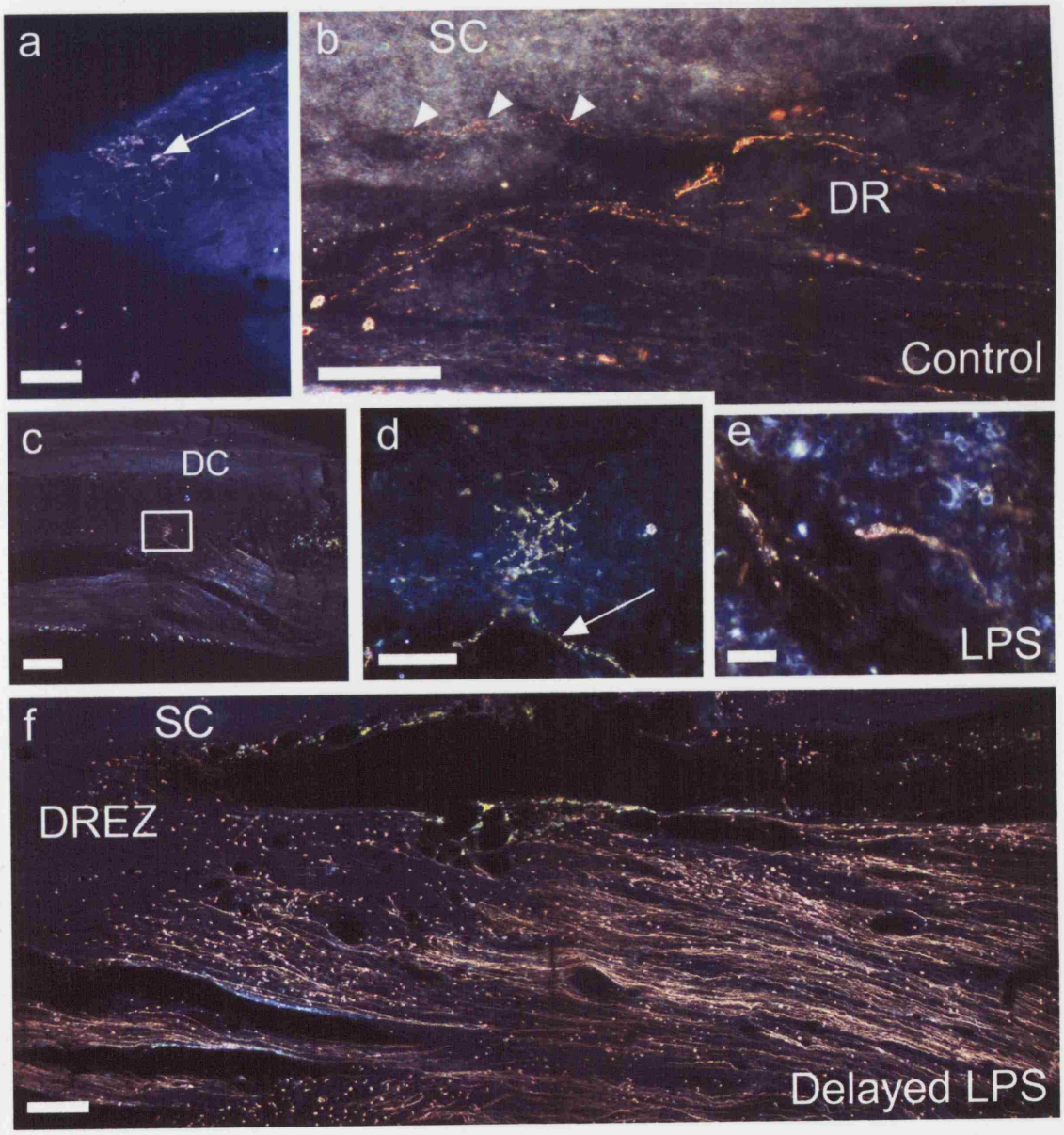
a
b
SC
DR
Control
c
DC
d
e
LPS
f
SC
DREZ
Delayed LPS

Figure 3-12 Microglial and macrophage responses to DR injury and I-P LPS injection.

Horizontal sections of spinal cord (Figs. 3.12 a – j) and transverse sections of medulla, containing the area postrema (AP) (Figs. 3.12 k and l) in animals 7 days after a L5+L6 DR transection (control; Figs. in left half of plate) or DR transection plus two I-P injections of LPS (LPS; Figs. in right half of plate), immunoreacted with OX42.

Fig. 3.12**a**, shows a control animal (DR cut only) with the lumbar spinal cord containing ramified (resting) microglia. DRs entering from the left contain many macrophages on the injured side (top), with no OX42+ macrophages on the uninjured side (bottom; enlarged in Fig. 3.12**e**). Fig. 3.12**b** is a magnified image of an injured L5 DR showing the macrophages within it, and very few macrophages / activated microglia in the adjacent spinal cord. Figs. 3.12**c** and 3.12**d**, from a rat given I-P LPS, contains massive numbers of rounded OX42+ macrophages in the DR and adjacent spinal cord on the injured side, with very few macrophages in the uninjured DR (Fig. 3.12**f**). Microglia are ramified on the control side, but appear amoeboid and activated in the injured side. Figs. 3.12**g – j** show that DRs and DREZ in cervical spinal cord appear the same on the injured (Figs. 3.12**g** and **h**) and uninjured (Figs. 3.12**i** and **j**) sides, with ramified microglia in CNS tissue and no macrophages in the DRs, whether I-P LPS was administered (Figs. 3.12h and j) or not. Fig. 3.12**k** demonstrates ramified microglia in the AP of the control animals. In Fig. 3.12**l**, there are a few macrophages on the surface of the AP and most microglia in the AP have some retraction of their processes, with some having enlarged cell bodies. Scale bar in Figs. 3.12a and c = 500μm; bar in Fig. 3.12b = 100μm and also applies to Fig. 3.12e; bar in Fig. 3.12d = 50m; bar in Fig. 3.12f = 200mm and also applies to Figs. 3.12g – j; bar in Fig. 3.12k = 100μm and also applies to Fig. 3.12l. DR = dorsal root; SC = spinal cord; AP = area postrema; inj = injured side of cord; uninj = uninjured side of cord.

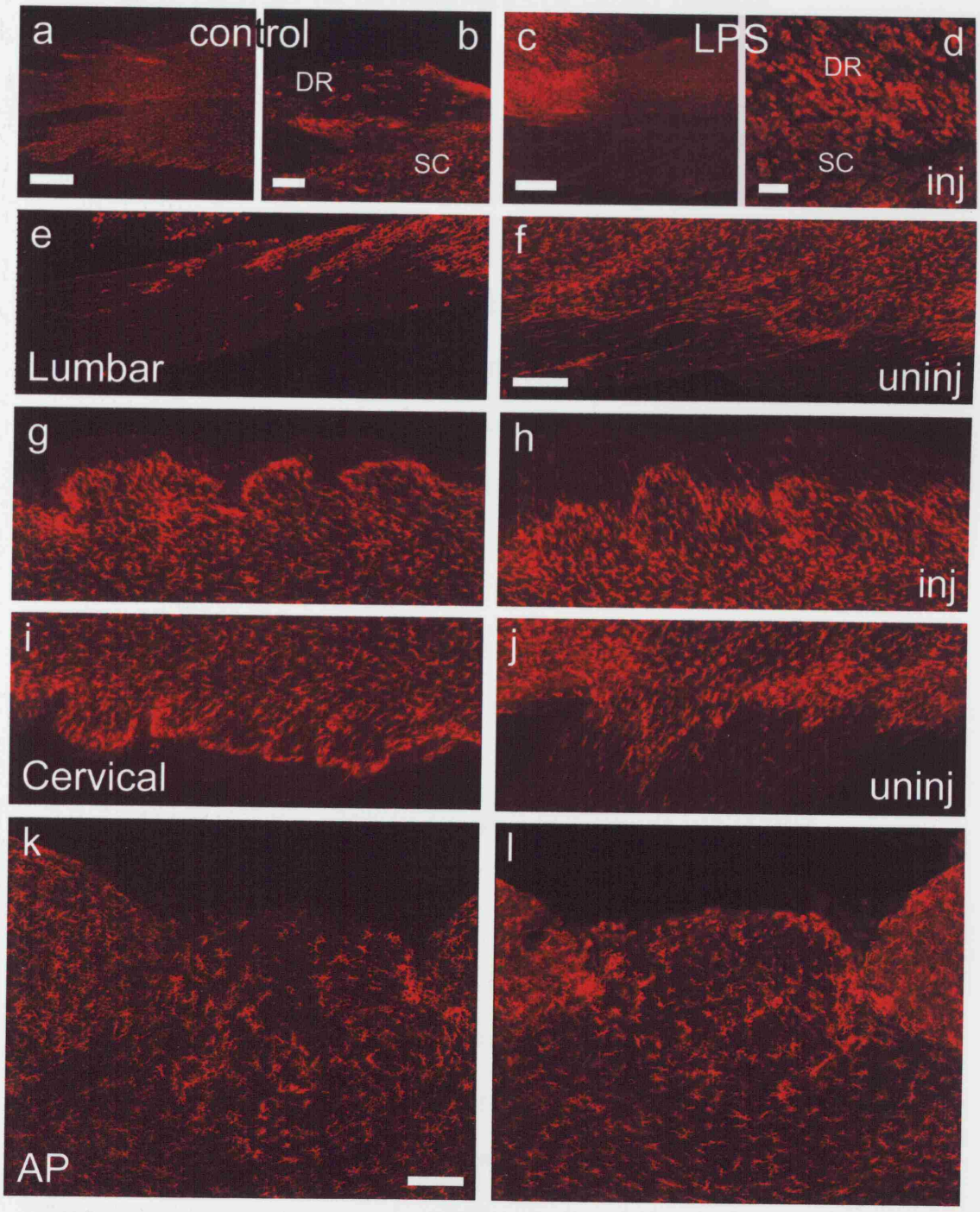
a
control
b
DR
SC
c
LPS
d
DR
SC
inj
e
Lumbar
f
uninj
g
h
inj
i
Cervical
j
uninj
k
AP
l

3.4 Effects of LPS injections into motor cortex on expression of growth-associated genes

Background

Following my experiments demonstrating upregulation of certain growth-associated genes in corticospinal cell bodies with topical application of LPS onto motor cortex, a preliminary study of the effects of intracortical injections of LPS solution into motor cortex was conducted. The aim was to produce a stronger inflammatory stimulus in layer V of cortex, around corticospinal cell bodies in an attempt to stimulate a greater upregulation of growth-associated proteins than that seen with topical LPS application.

Results

3.4.1 Effect of LPS injections into cortex on microglia

OX42

All animals were analysed 3 days after intracortical injection of LPS solution into layer V of motor cortex. OX42 immunohistochemistry allowed localisation of the injury tract (Fig. 3.13), as well as the reaction of microglia and macrophages. There was localised damage to cortex around the needle puncture site (Fig. 3.13c). In the control cortex, microglia were ramified. In the LPS-injected cortex, activated microglia were present throughout the depth of cortex for approximately 500μm on either side of the needle

tracts, with characteristic rounded cell bodies and retraction of dendritic processes. OX42 immunoreactivity was maximal around the site of LPS injection in layer V of cortex, with activated cells present for up to 2mm on either side of the distal injection site in lower layers of cortex and laterally along the subcortical white matter tracts. There appeared to be an increase in the number of microglia in the areas of activation compared to the control side, with no destruction of tissue in layer V. One animal had 3 small cysts are present at the site of injection (Fig. 3.13d), which may represent pathology secondary to inflammation or represent direct trauma from the injections that this animal received. Anatomical findings were otherwise similar in all 5 animals analysed, though the volume of tissue affected was less in the animal given a single injection of LPS, rather than 4 separate injections. There appeared to be no difference if 10mg/ml or 20mg/ml LPS solution was used as the injectate.

Figure 3-13 Expression of OX42 after intracortical LPS injection.

Coronal sections from motor cortex of adult rats 3 days after unilateral injection of LPS into the motor cortex (Figs. 3.13b - d) with no operation on the contralateral (con), control side (Fig. 3.13a), immunoreacted with OX42 antibody to visualise microglia / macrophages.

In the control (con) cortex, microglia are ramified. In the injured (inj) cortex, activated microglia are present throughout the depth of cortex on either side of the needle tracts; they are rounded and amoeboid and possibly more numerous. Fig. 3.13c shows the damage done to cortex by needle insertion (arrow), with OX42 immunoreactivity maximal around the site of LPS injection in layer V of cortex and spreading laterally along the subcortical white matter tracts. Fig. 3.13d demonstrates activated, rounded microglia from layer V in a separate animal at higher magnification, where 3 small cysts are present at the site of injection (*). Scale bar in Fig. 3.13a = 200μm and also applies to Fig. 3.13b; scale bar in Fig. 3.13c = 200μm; scale bar in Fig. 3.13d = 50μm.

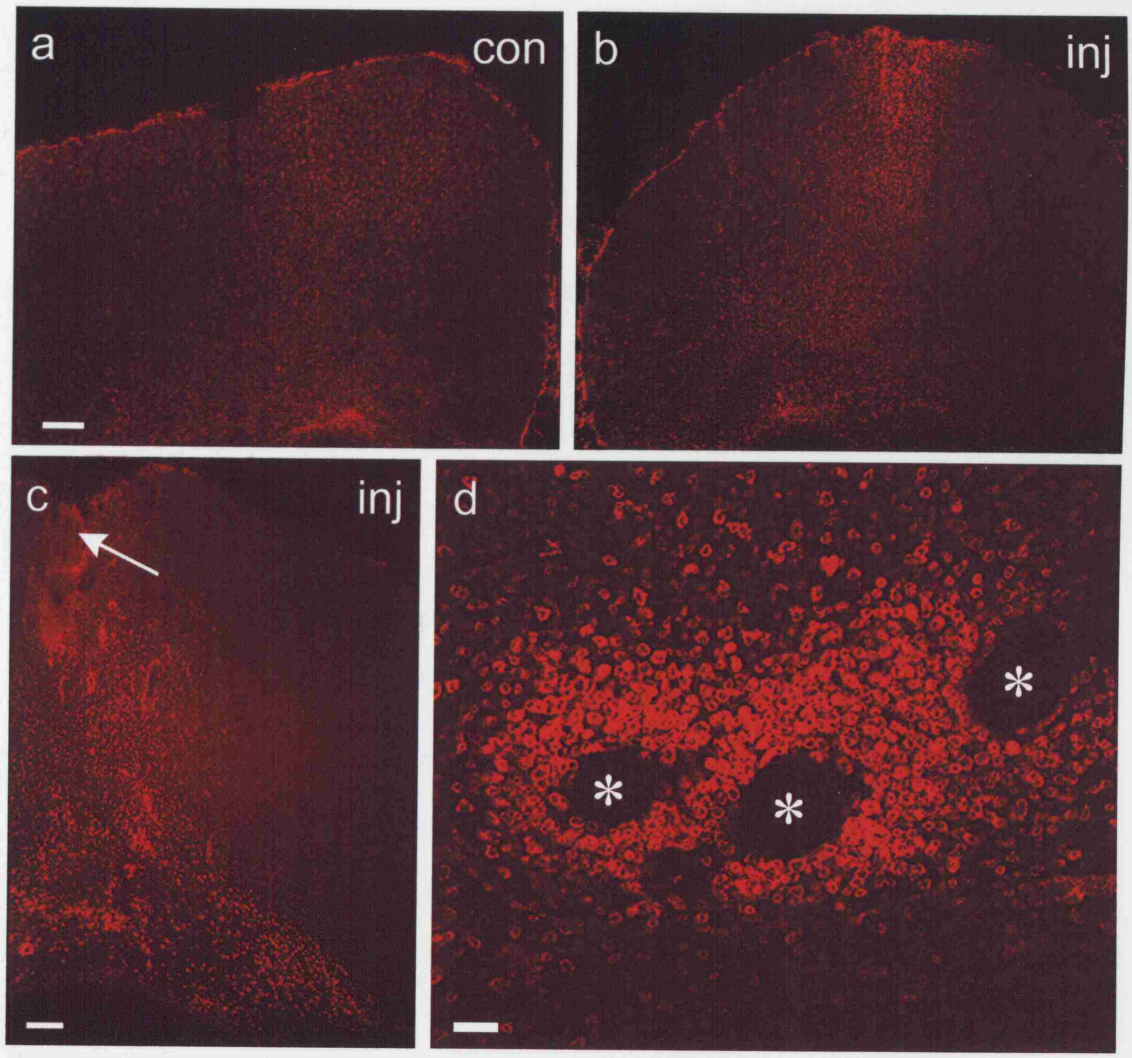
a
con
b
inj
c
inj
d

3.4.2 Effect of LPS injections into cortex on expression of growth-associated proteins

c-Jun

The uninjected, contralateral cortex showed background levels of c-Jun immunoreactivity (Fig. 3.14a). LPS-injected cortex had a gradient of increased c-Jun immunoreactivity, mainly in the top layers of cortex and reducing down to layer V, around the site of LPS injection (Figs. 3.14 b and d).

ATF3

There were no ATF3 immunopositive nuclei in the cortex contralateral to LPS injection. There was very localised ATF3 immunoreactivity around the site of the injection tract, at the site of LPS injection in layer V of cortex and below the injection site in the corpus callosum. Fig. 3.15b shows cortex damaged by the injection needle and, in this animal, ATF3 upregulation is mainly in the areas of cortex immediately adjacent to damaged cortex.

SCG10

In the control cortex, there was a background level of SCG10 immunoreactivity, maximal in layer V neurons (Figs. 3.16 a and c). There was increased neuronal SCG10 immunoreactivity in the top layers of cortex around the site of damage to the cortical surface by needle penetration, and also spreading laterally from the site of LPS injection, in layer V of cortex.

Figure 3-14 Expression of c-Jun after intracortical LPS injection.

Coronal sections from motor cortex of adult rats 3 days after unilateral injection (inj) of LPS into the motor cortex with no operation on the contralateral, control side (con), immunoreacted with c-Jun antibody.

Fig. 3.14a shows background levels of cortical c-Jun immunoreactivity. Fig. 3.14b demonstrates the gradient of c-Jun upregulation decreasing from layer I of motor cortex to layer V. Fig. 3.14c is a magnified view of neurons in layer V of Fig. 3.14a; Fig. 3.14d is a magnified view of neurons in layer V of Fig. 3.14b, demonstrating increased levels of c-Jun in layer V of motor cortex following LPS injection into this layer, compared to control cortex. Scale bar in Fig. 3.14a = 200μm and also applies to Fig. 3.14b; scale bar in Fig. 3.14c = 100μm and also applies to Fig. 3.14d.

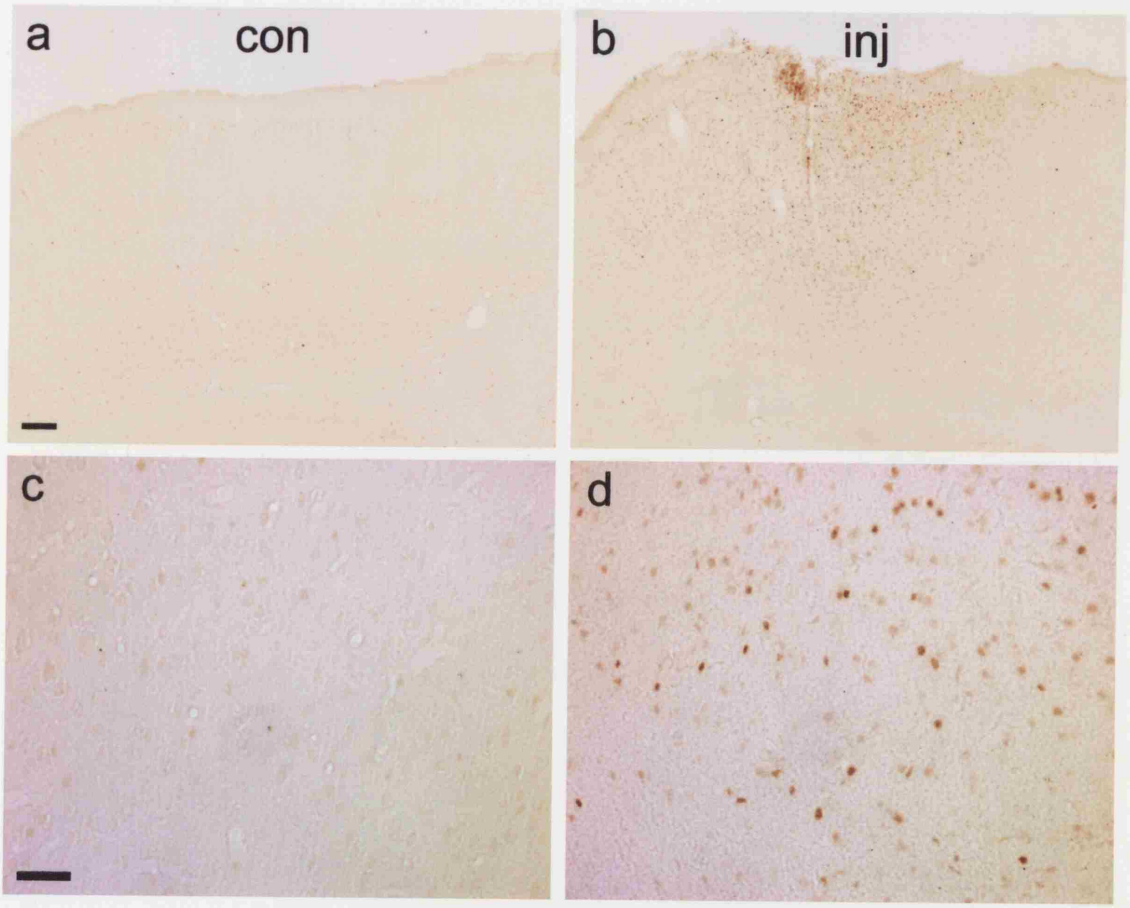
a
con
b
inj
c
d

Figure 3-15 Expression of ATF3 after intracortical LPS injection.

Coronal sections from motor cortex of adult rats 3 days after unilateral injection (inj) of LPS into the motor cortex with no operation on the contralateral, control side (not shown), immunoreacted with ATF3 antibody.

Fig. 3.15a shows the damage done to cortex at the injection site, with very localised upregulation of ATF3 immunoreactivity around the injection tract, at the site of LPS release in layer V of cortex and below the site of injectate release in the corpus callosum. Fig. 3.15b shows cortex damaged by the injection needle and, in this animal, ATF3 upregulation is mainly in the areas of cortex immediately adjacent to damaged cortex. Fig. 3.15c is an enlargement of the inset box in Fig. 3.15b demonstrating increased levels of ATF3 localised to areas inflamed / damaged by LPS. Scale bars in Fig. 3.15a and Fig. 3.15b = 200μm; scale bar in Fig. 3.15c = 100μm.

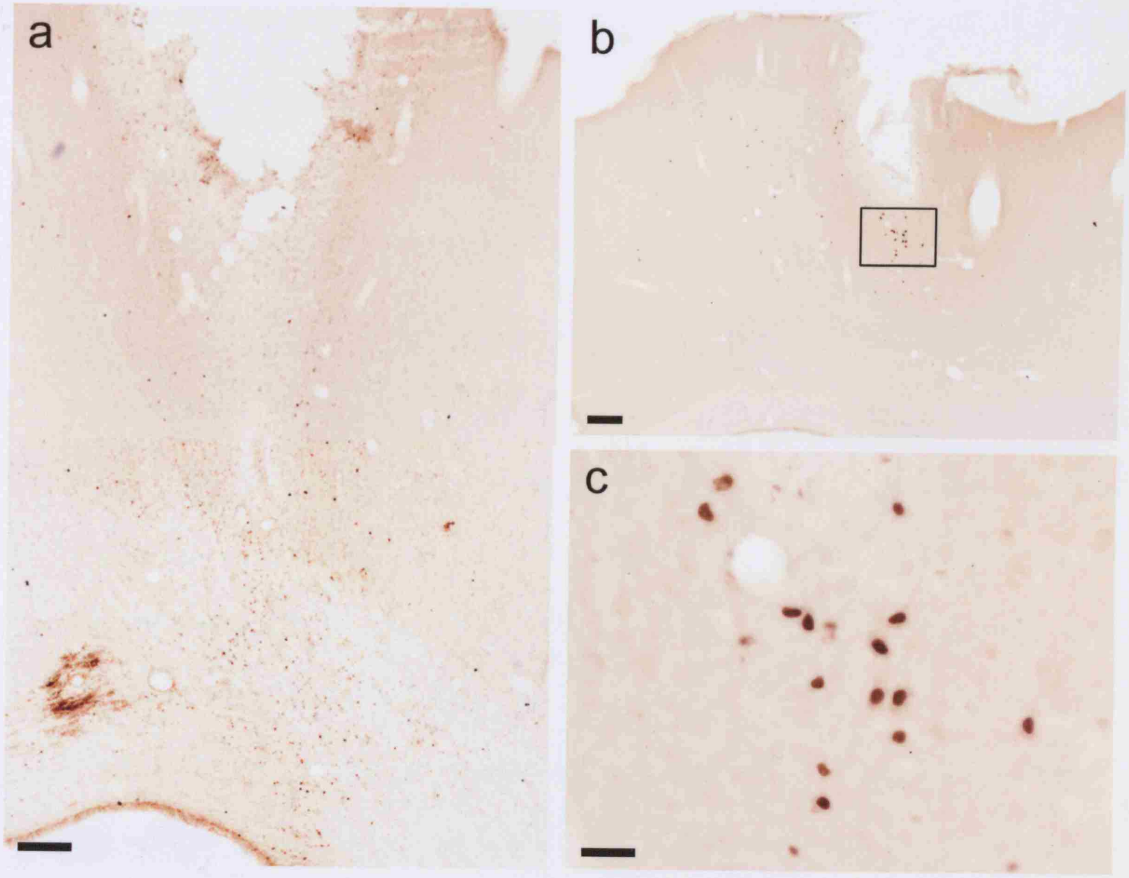
a
b
c

Figure 3-16 Expression of SCG10 after intracortical LPS injection

Coronal sections from motor cortex of adult rats 3 days after unilateral injection of LPS into the motor cortex (Figs. 3.16b and d) with no operation on the contralateral (con), control side (Figs. 3.16a and c), immunoreacted with SCG10 antibody.

In Fig. 3.16a, the control cortex demonstrates a background level of SCG10 immunoreactivity, maximal in layer V neurons. Fig. 3.16b shows the damage done to the cortical surface by the needle injection (inj), with upregulation of SCG10 immunoreactivity around the site of needle entry in the superficial layers of cortex, but also spreading laterally in layer V of cortex. Figs. 3.16c and 3.16d illustrate at higher magnification the boxes in Figs 3.16a and b respectively, and demonstrate increased levels of SCG10 in layer V of motor cortex following LPS injection into this layer, compared to control cortex. Scale bar in Fig. 3.16a = 200μm and also applies to Fig. 3.16b; scale bar in Fig. 3.16c = 50μm and also applies to Fig. 3.16d.

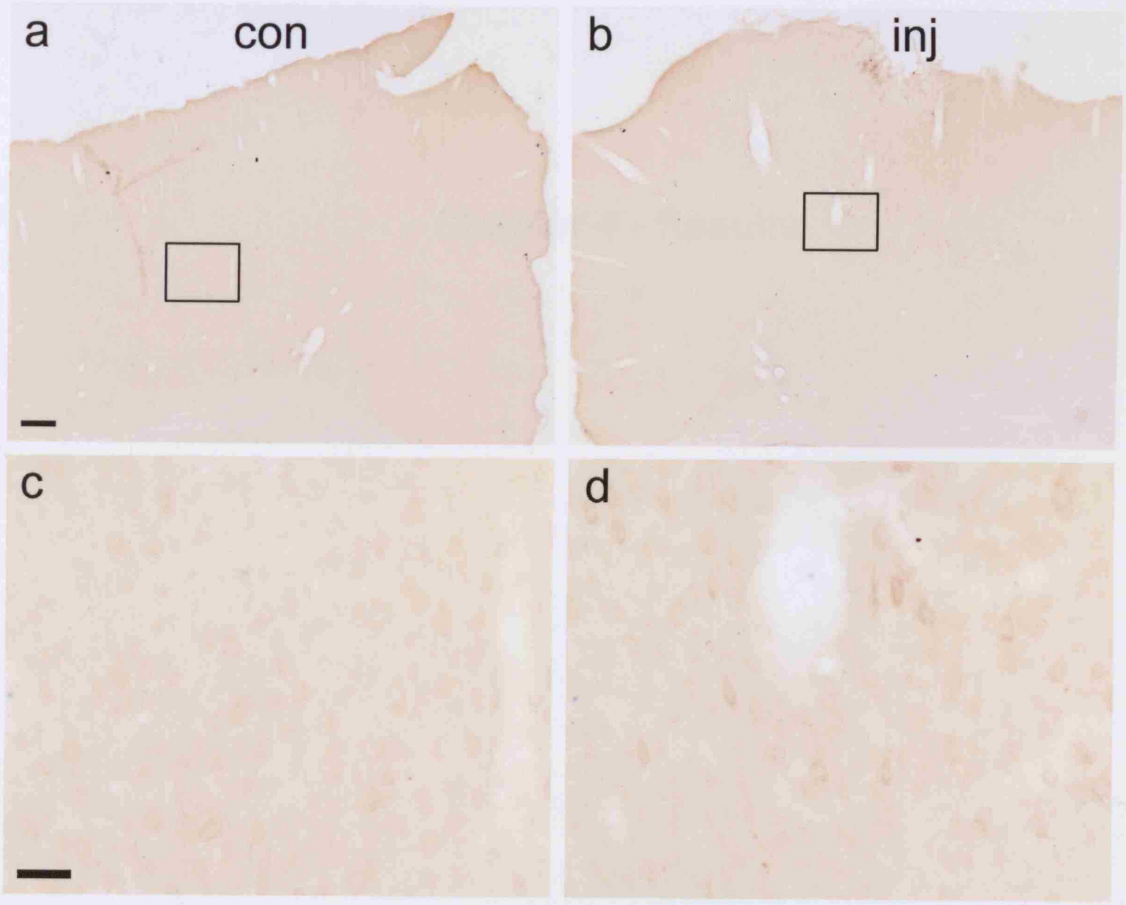
a
con
b
inj
c
d

Chapter 4 - Results

4.1 Effects of zymosan-induced inflammation on glial cells, Nogo-A and expression of growth-associated genes by corticospinal neurons

Background

Following the results of our experiments in which LPS application onto the pial surface of the motor cortex of adult rats enhanced expression of neuronal growth-associated genes but did not stimulate axonal regeneration, I repeated these experiments using zymosan on the pial surface instead. Zymosan is more potent an inflammatory agent than LPS, and I hypothesised that it may stimulate a greater response from neuronal growth-associated genes.

Results

4.1.1 Assessing zymosan-induced inflammation in motor cortex

4.1.1.1 Zymosan application

Different methods of applying zymosan were tested. Placing 500μg of zymosan on top of intact dura, as opposed to the pial surface (survival 3 days) did not reveal any discernable changes from unoperated cortex (unoperated animals included with LPS experiments), with no alteration of OX42, GFAP, NG2, c-Jun, ATF3 and SCG10 immunohistochemistry (no Nogo-A immunohistochemistry was undertaken in these 2

control animals). Zymosan solution soaked in Gelfoam placed on the cortical surface (survival 2 days) caused increased c-Jun immunoreactivity in a few cells in layers I and II only, similar to that seen in the sham-operated animals (see below).

4.1.1.2 Control experiments

Positive controls: ATF3-positive nuclei were identified in the ipsilateral facial nucleus, one week after facial nerve crush. c-Jun+ nuclei and SCG10+ cells were found in both facial nuclei, but immunoreactivity was greater in the facial nucleus ipsilateral to the crushed facial nerve (Figs. 4.8 c - h). These results were consistent for all animals. No positive control tissue was used in the Nogo-A/NG2 and Nogo-A/GFAP experiments.

Negative controls: The contralateral, unoperated cortex was used as a control in all experiments. When the primary antibody was omitted, no cells displayed immunoreactivity for c-Jun, ATF3 or SCG10 in either cortex of brain (e.g. Fig. 4.6h) and facial nucleus (see Fig. 3.1a and b), or brain alone for OX42, GFAP, NG2 or Nogo-A

4.1.1.3 Localisation of CST neurons

Placing Fluorogold (FG) into the spinal cord at C4 of animals surviving for a total of 7 days, 17 days and 1 month after zymosan application invariably labelled layer V pyramidal cell bodies in the contralateral motor cortex, allowing identification of the analysed growth-associated proteins and CST neurons in the same sections. Once excited by UV light, the emission wavelength of FG is 565nm (yellow; see Figs. 4.1 – 4.3). In Figs. 4.5 and 4.7, the appearance of retrogradely labelled CST neurons were

digitally altered to appear red. This allowed any cells in these images that were immunopositive for both FG (red) and c-Jun or SCG10 (green) to appear yellow/orange.

4.1.2 Effects of zymosan-induced inflammation in motor cortex on glial cells and Nogo-A

4.1.2.1 OX42 immunohistochemistry

Coronal sections through the motor cortex were immunostained with OX42, an antibody which binds to the complement type 3 receptor on microglia and macrophages (Aldskogius and Kozlova, 1998). On the side opposite to zymosan application, i.e. sham-operated (dura opened; no zymosan applied + Gelfoam), highly ramified (presumably resting) microglia were present throughout the cortex (Figs. 4.1a, c, e, g, i and k), although there was accumulation of some rounded OX42-positive cells at the pial surface between 3 and 7 days (Fig. 4.1e). This is more likely to represent inflammation from the zymosan placed on the opposite cortex having an effect on the exposed control cortex, rather than the trauma of opening dura alone.

In zymosan-treated cortex, microglial morphology was altered from the ramified form typical of the quiescent state, to a rounded amoeboid shape, with thicker proximal processes, loss of distal ramification and increased OX42 immunofluorescence typical of the activated state (Figs. 4.1b, d, f and h) in layers I – III after 1 day. There was a gradient of microglial activation seen in all layers of motor cortex at 3 and 7 days, maximal in layer I, with quiescent microglia seen in the subcortical white matter. At 3

days after zymosan application, the number of rounded OX42+ glia in the top layers of cortex was increased (Fig. 4.1f compared to Fig. 4.1e). These may have included peripheral macrophages infiltrating the CNS. In the animals in which Fluorogold was used to retrogradely label corticospinal tract (CST) neurons, activated OX42-positive microglia were closely associated with the cell bodies of identified CST neurons in layer V (Fig. 4.1i and j). However, in 50% of the animals tested from 3 days to 1 month, zymosan application resulted in extensive damage to cortex, with loss of tissue, usually down to (and including) layer IV of cortex, and in two animals reaching down to the corpus callosum (See Fig. 4.1j and Fig 4.2g and i). The lateral extent of OX42 upregulation / microglial activation was up to 1mm on either side of the site of zymosan application, for up to one week. Inflammation around layer V pyramidal neurons was always apparent beneath the site of zymosan application. Seventeen days after application, rounded, amoeboid microglia were rare and microglia with a ramified morphology predominated in both the ipsilateral and contralateral cortex except for those animals with cortical damage, which had a rim of activated microglia along the wound edge (Fig. 4.1i and j). At one month, the ipsilateral and contralateral cortex appeared identical in all animals, with only ramified microglial cells apparent, apart from a very few rounded cells along the upper edge of the wound of those animals with a cavity induced by zymosan application. Thus, 500μg of zymosan was sufficient to produce inflammation around layer V pyramidal neurons in all animals by 1 day, which was maximal at 3 days and had subsided by 17 days after application. However, zymosan often produced damage to the upper layers of cortex and destroyed some neurons in layer V of cortex in 2 of the 18 animals tested.

Figure 4-1 Microglial / macrophage response to zymosan application.

Coronal sections from motor cortex of adult rats 1 day, 3 days, 17 days and 1 month after unilateral placement of zymosan on the pial surface of motor cortex (zym: Figs. 4.1b, d, f, h, j and l) with no operation on the contralateral, control (con) side (Figs. 4.1a, c, e, g, i and k), immunoreacted with OX42 antibody to visualise microglia / macrophages.

In Fig. 4.1a, microglia in control cortex are ramified after 1 day. In Fig. 4.1b, microglia in superficial cortex have retracted cell processes and enlarged cell bodies (indicating their activation). Fig. 4.1c and d are magnified images of layer V from Figs. 4.1a and b respectively and demonstrate increased OX42 signal and microglial activation in layer V of zymosan-treated cortex compared to the control cortex. Fig. 4.1c shows layer V of Fig. 4.1a at greater magnification and shows quiescent microglia in control cortex.. Fig. 4.1e (3 days) demonstrates some amoeboid cells on the contralateral cortical surface under the site of sham operation. Fig. 4.1f shows that the greatest microglial activation occurs after 3 days, with a vastly increased number of rounded, amoeboid OX42+ cells seen. Figs. 4.1g and h show enlarged images from layer V of Figs. 4.1e and f respectively, to demonstrate zymosan-induced changes of microglial activation. Fig. 4.1i shows, at 17 days, normal OX42 immunoreactivity in the control cortex after 17 days. Fig. 4.1j shows zymosan-induced tissue destruction (*), with a rim of macrophages / activated microglia around its edges, but resting microglia elsewhere. Retrogradely-labelled pyramidal neurons are seen in yellow in both images. Inset images of Figs. 4.1i and j show magnified areas of layer V, with microglia (red) in close association with corticospinal neurons (yellow). Figs. 4.1k and l demonstrate no difference in OX42 immunoreactivity between control and zymosan-treated cortex in layer V at 1 month. Scale bar in Fig. 4.1a = 200μm and also applies to Fig. 4.1b; bar in Fig. 4.1c = 50μm and also applies to Figs. 4.1d, g and h; bars in Fig. 4.1e and i= 200μm and also apply to Figs. 4.1f and j respectively; bar in Fig. 4.1i inset = 20μm and also applies to Fig. 4.1j inset; bar in Fig. 4.1k = 20μm and also applies to Fig. 4.1l.

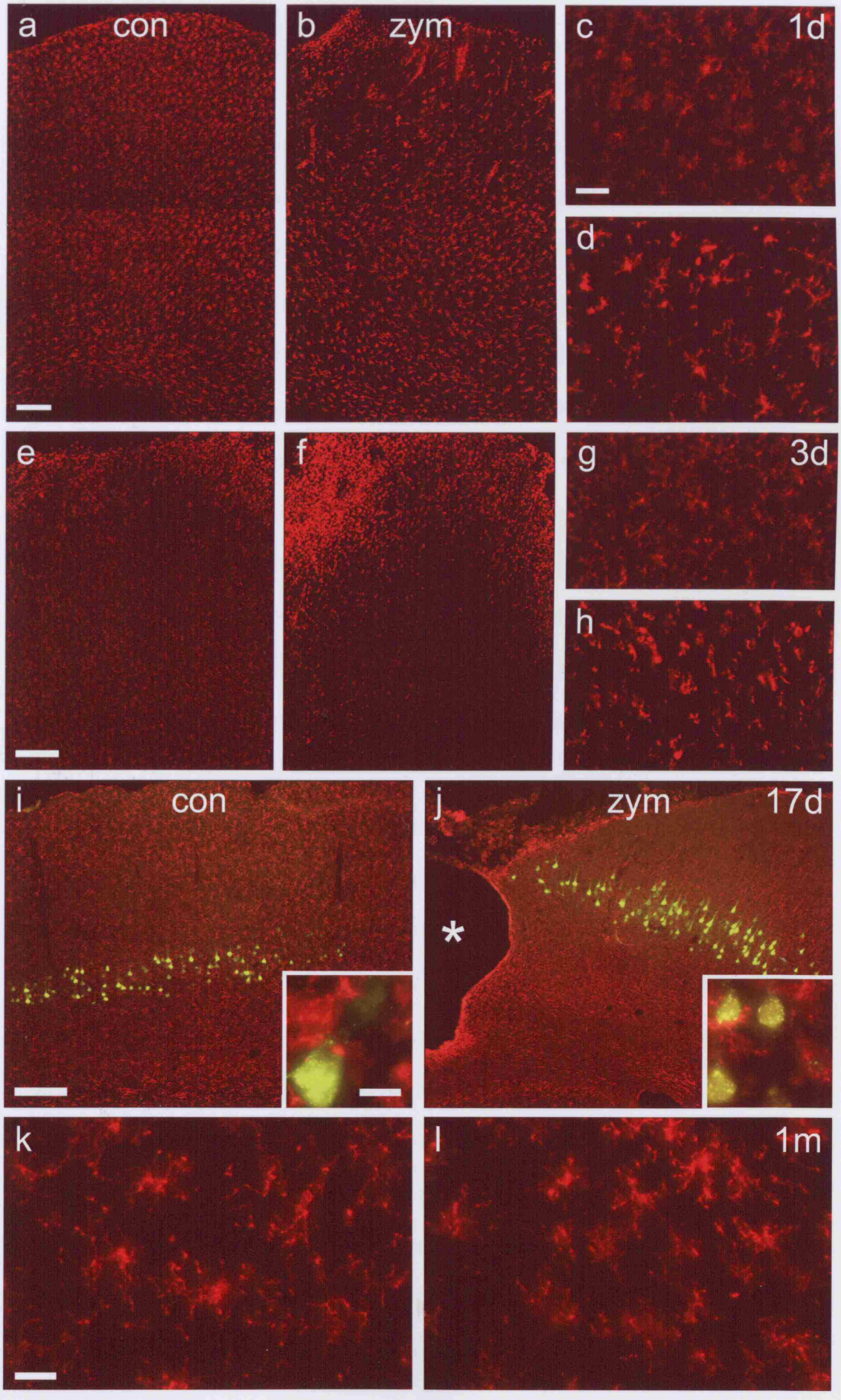
a
con
b
zym
c
1d
d
e
f
g
3d
h
i
con
j
zym
17d
*
k
l
1m

4.1.2.2 GFAP immunohistochemistry

1 day after the application of zymosan, GFAP+ astrocytes in the zymosan-treated cortex showed hypertrophy and retraction of their processes and enlargement of their cell bodies with greater immunofluorescence near the inflamed pial surface (Fig. 4.2b) than in the contralateral cortex (Fig. 4.2a). Astrogliosis was less marked in deeper layers of cortex. After 3 days, the superficial 500μm of cortex directly under the site of zymosan application (i.e. no lateral extension) lost all immunoreactivity for GFAP. The right side of Fig. 4.2c shows the appearance of this area with DAPI staining all cell nuclei, and demonstrates that there is either a selective loss of astrocytes or the astrocytes in this area have become GFAP-ve with other, unidentified GFAP-ve cells being present. The remainder of the entire hemicortex showed upregulation of GFAP compared to the contralateral cortex (not illustrated). A similar focal loss of GFAP immunoreactivity was present in one of the animals tested at 7 days, and to a lesser extent in the other (Fig. 4.2e), but at both time points, the entire hemicortex on the zymosan-treated side showed more intense GFAP immunoreactivity than the control cortex. At 17days and one month, the ipsilateral and contralateral cortex appeared identical in all animals, unless cortical damage had occurred, in which case astrogliosis was apparent for 20 – 80μm around the edges of the zymosan-induced cavity. Astrocytes in layer V of motor cortex that were not immediately adjacent to a lesion cavity were not affected by the astrogliosis. Thus, 500μg of zymosan resulted in astrogliosis from 1 day to 7 days, maximal at 3 days, but with an area devoid of GFAP expression directly under the site of application to the pial surface of motor cortex between 3 and 7 days. When cortex was not damaged, astrocytes regained normal morphology and GFAP immunoreactivity by 17 days. Whether the absence of GFAP reflected a loss of astrocytes or a loss of GFAP immunoreactivity from astrocytes is unclear.

Figure 4-2 Astrocytic response to zymosan application.

Coronal sections of motor cortex below the area of zymosan application (zym; Figs. 4.2b, e, g and i) or sham operation on the contralateral, control side (con; Figs. 4.2a, d, f and h), 1 day, 3 days, 7 days, 17 days and 1 month after application of zymosan, immunostained with GFAP antibody to visualise astrocytes (green). Fig. 4.2c shows bisbenzimide (DAPI) staining of nuclei in blue. Retrogradely labelled Fluorogold in corticospinal neurons is shown in yellow. Figs. 4.2a and b show that after 1 day, astrocytes are more brightly fluorescent in superficial cortex only, directly under the site of zymosan application, with retracted, thicker processes and enlarged cell bodies compared to control cortex, as demonstrated in the inset images, which are magnified areas from the top of Figs. 4.2a and b. Note the absence of tissue on the superficial part of the zymosan-treated section, which is most likely because the oedematous nature of inflamed cortex made the tissue friable, and therefore prone to loss during histological processing. Fig. 4.2c shows that after 3 days, the area directly underneath zymosan application shows absence of GFAP immunoreactivity to a depth of 500μm, although DAPI staining reveals that cells were present in this area. Figs. 4.2d and e show that after 7 days, in less swollen cortex, GFAP immunoreactivity is increased in all layers of cortex compared to the contralateral cortex. (The other animal examined at 7 days had more cortical swelling and loss of superficial GFAP staining, suggesting that maximal cortical inflammation downregulates GFAP. Figs. 4.2f and g show that after 17 days, GFAP immunoreactivity is equal in both cortices, unless tissue damage occurs (Fig. 4.2g), resulting in a rim of brighter GFAP+ astrocytes around the lesion edge. Inset images of Figs. 4.2f and g demonstrate that astrocytes distant to the lesion site in layer V (localised by Fluorogold (yellow) in corticospinal neurons) have similar form and GFAP signal in control and zymosan-treated cortex. Immunohistochemistry for GFAP in control and Zymosan-treated cortex was similar at 1 month, but Figs. 4.2h and i show that, if tissue damage occurred, astrogliosis is seen close to the lesion site that extended down to Layer V of cortex, as highlighted in the magnified images of the insets. Scale bar in Fig. 4.2a = 500μm and also applies to Figs. 4.2b, h and i; bar in Fig. 4.2c = 500μm; bar in Fig. 4.2d = 200μm and also applies to e; bar in Fig. 4.2f = 500μm and also applies to g; bar in Fig. 4.2a inset = 20μm and applies to b inset; bar in Fig. 4.2f inset = 20μm and applies to insets of Figs. 4.2g, h and i.

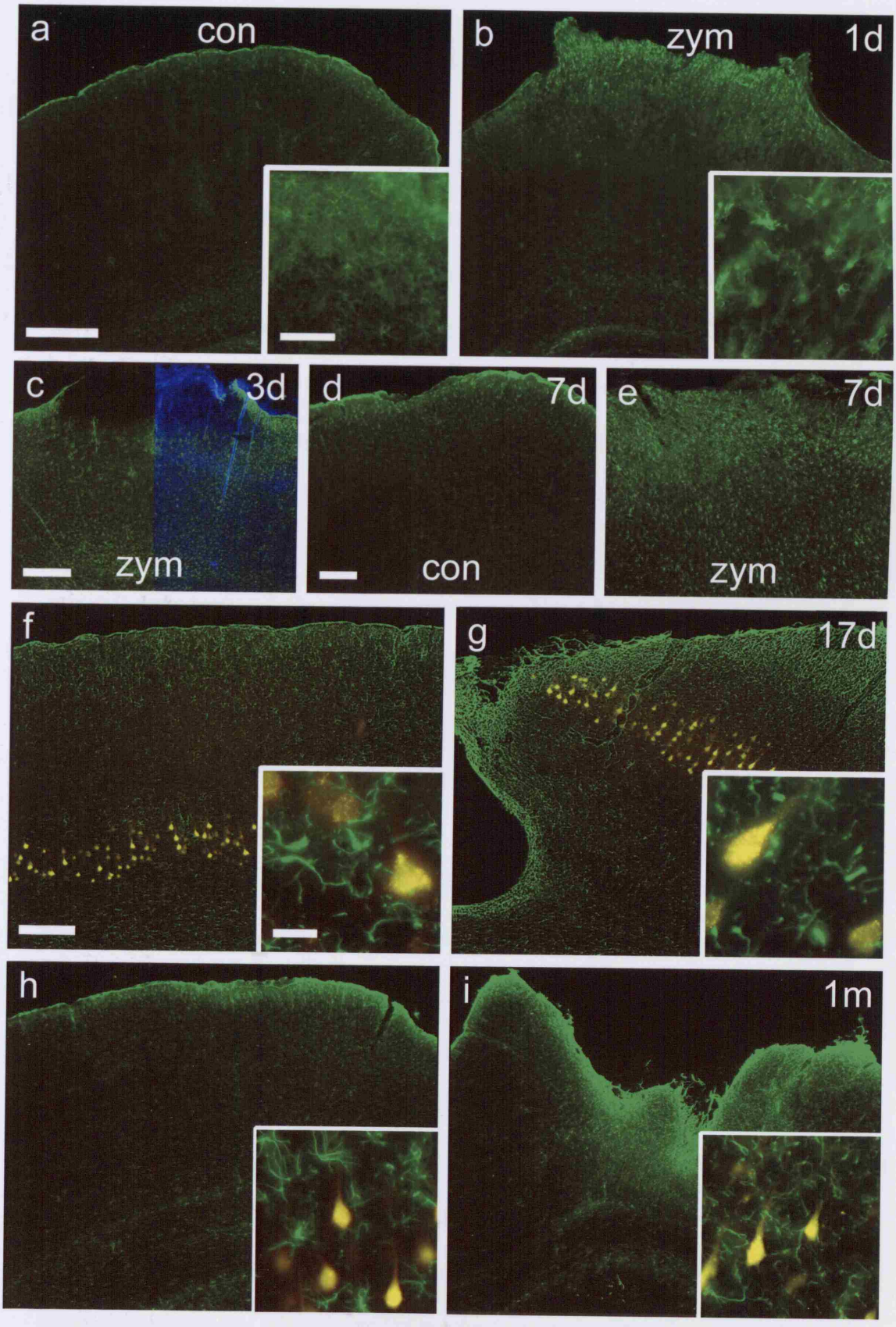
a
con
b
zym
1d
c
3d
zym
d
7d
con
e
7d
zym
f
g
17d
h
i
1m

4.1.2.3 NG2 immunohistochemistry

NG2 cells reacted in a similar manner to the astrocytes under the site of zymosan application. After 1 day, there was increased intensity of NG2 staining in layers I – III of cortex directly under the site of zymosan application (Fig. 4.3b), with enlargement of the cell body and retraction of some processes of NG2 cells (Fig. 4.3b top inset), with a gradual reduction through the depth of cortex (Fig. 4.3b bottom inset; layer V) until normal NG2 cells were seen in subcortical white matter. After 3 days, in animals with no gross cortical damage, NG2+ cells were absent at the site of maximal inflammation, directly under the site of zymosan application, for a depth of 500μm, but blood vessels showed marked upregulation of NG2 in this area (Fig. 4.3d top inset), presumably from NG2+ pericytes (Ozerdem et al., 2002). Whether the glial cells were no longer present or had lost their NG2 immunoreactivity is not clear. Below and on either side of this area, there was a penumbra of NG2 upregulation in glia compared to the control cortex, extending for up to 2mm in all directions, and NG2+ cells in layer V of inflamed cortex had shortened, fatter processes and more intense immunostaining (Fig. 4.3d bottom inset) compared to control cortex (Fig. 4.3c inset). Absence of NG2+ staining in areas of greatest inflammation and upregulation with moderate inflammation (surrounding penumbra) was similar to the pattern of GFAP immunoreactivity. These changes were greatest at 3 days (reflecting the time of maximal inflammation, as seen with OX42 immunohistochemistry), were still present at 7 days and had returned to control levels at 17 days (Figs. 4.3d - f). At 1 month, the ipsilateral and contralateral cortex appeared identical in all animals. When cortical damage occurred (seen between 3 days and 1 month), there was loss of NG2 immunoreactivity in glial cells at the lesion edge, with

upregulation of NG2 in blood vessels for 50-80μm – i.e. there was no rim of gliotic NG2+ cells.

Figure 4-3 NG2-cell response to zymosan application.

Coronal sections of motor cortex below the area of zymosan application (Figs. 4.3b, d and f) or sham operation (Figs. 4.3a, c and f) on the contralateral, control side (con), 1 day, 3 days and 17 days after application of zymosan, immunoreacted with NG2 antibody. Retrogradely labelled Fluorogold in corticospinal neurons (yellow) is shown in Figs. 4.3e and f.

Fig. 4.3a shows control cortex and Fig. 4.3b shows zymosan-treated cortex 1 day after application, demonstrating that NG2+ cells are more brightly fluorescent in the 1.5mm of cortex directly under the site of zymosan application. The top insets of Figs. 4.4a and b show magnified views of layer I of cortex and the bottom insets show layer V of cortex, which demonstrate that NG2+ cells have retracted, thicker processes and enlarged cell bodies compared to control cortex in the superficial layer of inflamed cortex, but the difference is less marked in layer V. Fig 4.3c shows control cortex after 3 days, in which NG2+ cells are quiescent, whereas in Fig. 4.3d NG2+ immunoreactivity is predominantly in blood vessels with very few NG2+ cells in the top 400μm of cortex (arrow = Gelfoam on cortical surface). The top inset to Fig. 4.3d shows that the area directly underneath zymosan application is markedly swollen and the lower insets show magnified images of layer V of cortex, showing that NG2+ cells are present deeper in cortex, but there is still increased NG2 immunoreactivity in blood vessels (e.g. arrowheads) compared to control cortex. Figs. 4.3e and f show that after 17 days, NG2 immunoreactivity is equal in both zymosan-treated and control cortex; inset images demonstrate that NG2+ cells in layer V of both cortices show similar shape and signal intensity. Scale bar in Fig. 4.3a = 200μm and also applies to b; Fig. 4.3a inset bar = 20μm and applies to other insets in Figs. 4.3a and b; bar in Fig. 4.3c = 200μm and also applies to d; Fig. 4.3c inset bar = 50μm and also applies to lower inset of Figs. 4.3d, e and f; bar in upper inset of Fig. 4.3d = 100μm.

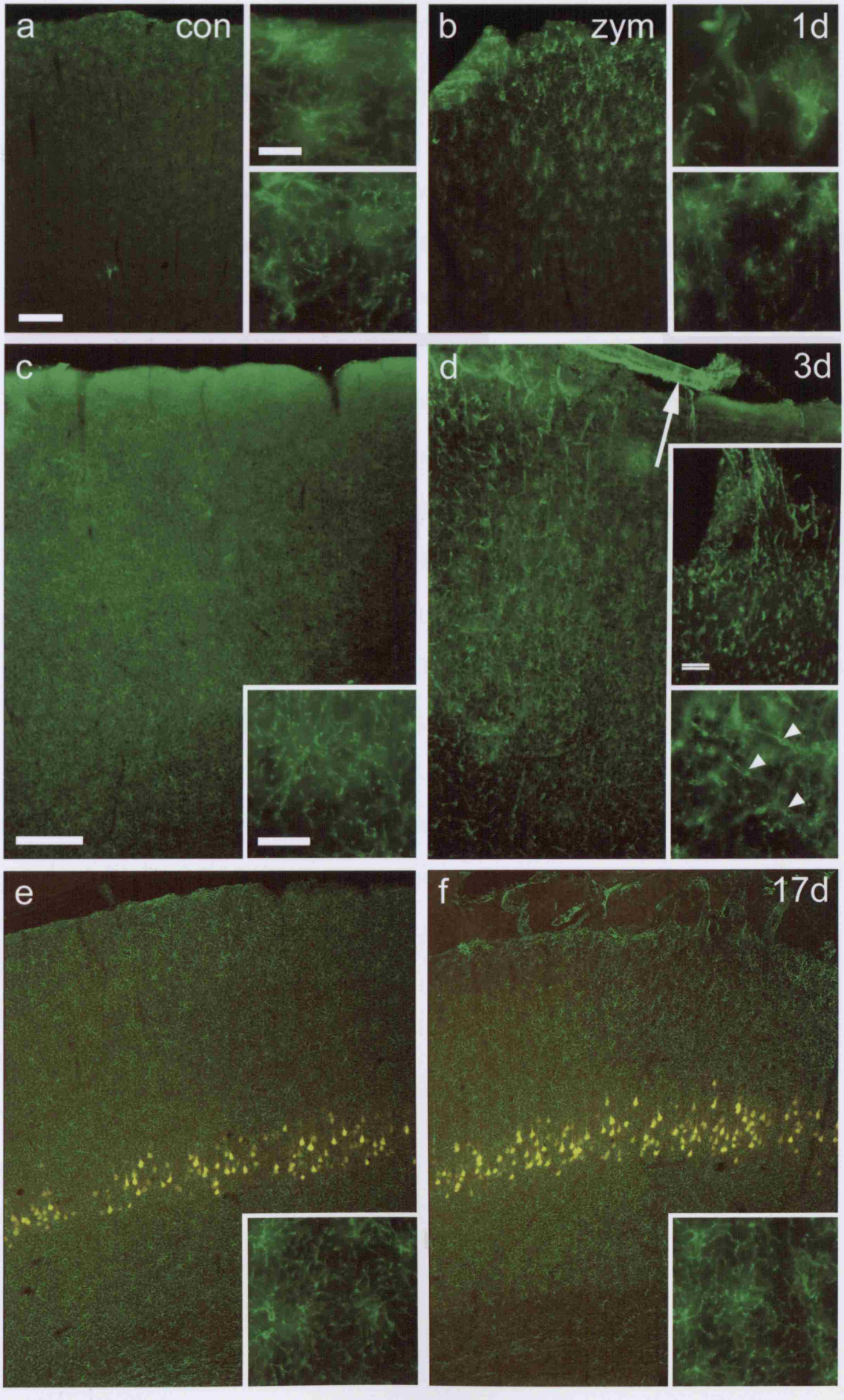
a
con
b
zym
1d
c
d
3d
e
f
17d

4.1.2.4 Nogo-A immunohistochemistry

Nogo-A was upregulated from 1 day to 1 month, in Layers I and II of cortex directly under the site of zymosan application, in the cytoplasm of cells consistent with the size and morphology of small oligodendrocytes (Figs. 4.4b, c, e and f). Very few cells were as strongly Nogo-A+ in the corresponding control cortex (Figs. 4.4a and d). This increased immunoreactivity was most marked when cortex was very swollen (Fig. 4.4f), suggesting that the degree of upregulation of Nogo-A is related to the degree of inflammation produced by zymosan application. Animals with damaged cortex (seen between 3 days and 1 month) not only had similarly increased Nogo-A immunostaining in presumed oligodendrocytes, but also in neurons at the lesion edge (Figs. 4.4k and m), with one animal demonstrating increased Nogo-A immunoreactivity in a neuron in layer III of cortex (Figs. 4.4k and l arrowhead) , which may reflect the degree of trauma to cortex. There was a variable response in Layer V, with limited upregulation of Nogo-A in cells with neuronal and oligodendrocyte-like morphology between 3 days and 1 month in some animals (Fig. 4.4d compared to e and Fig 4.4g compared to h), but not in others (Fig. 4.4n compared to o).

Figure 4-4 Response of Nogo-A to zymosan application.

Coronal sections of motor cortex below the area of zymosan application (zym; Figs. 4.4b, d, f, h, i – k and m) or sham operation on the contralateral, control side (con; Figs. 4.4a, c, e, g l), 1 day, 3 days, 17 days and 1 month after application of zymosan, immunostained for Nogo-A (red). In Figs. 4.4a, b, e and f, cell nuclei are labelled in blue with bisbenzimide (DAPI); in Figs. 4.4e - h astrocytes are labelled in green with GFAP, and CST neurons that have taken up Fluorogold (yellow) in Figs. 4.4g and h.

Fig. 4.4a shows no Nogo-A immunoreactive cells in control cortex 1 day after zymosan application. Fig. 4.4b (1 day) shows Nogo-A staining in cells with the size and shape of small oligodendrocytes in layers I and II of cortex swollen by zymosan application (arrows) and demonstrates nuclear labelling of almost all Nogo-A+ cells with DAPI. Fig. 4.4c (layer V of control cortex at 3 days), shows low levels of Nogo-A. Fig. 4.4d, demonstrates enhanced Nogo-A immunoreactivity in a larger number of (presumed) oligodendrocytes in layer V of the corresponding zymosan-treated cortex directly under the area of zymosan application. Fig. 4.4e (control layer V at 3 days) shows Nogo-A in the cytoplasm of pyramidal neurons and Fig. 4.4f, from the corresponding zymosan-treated cortex, illustrates mild upregulation of Nogo-A in layer V neurons. DAPI staining shows nuclei in this layer and GFAP staining highlights astrocytes activated by inflammation. Fig. 4.4g shows layer V (localised by Fluorogold) of control cortex and Fig. 4.4h shows zymosan-treated cortex, after 17 days: few neurons upregulate Nogo-A in layer V of inflamed cortex (arrow) compared to control cortex. There is no obvious difference in GFAP immunoreactivity between control and inflamed cortex in this animal. Fig. 4.4i shows cortical damage (*) 1 month after zymosan treatment. Nogo-A is upregulated in neurons along the cortical lesion edge (box), and in cells underneath. Nogo-A immunoreactivity was seen in Layer III in only one animal (arrowhead), that had sustained maximal damage to cortex. Fig. 4.4j illustrates this neuron at a greater magnification with smaller Nogo-A+ cells around it. Fig.4.4k shows the area boxed in Fig.4.4l at greater magnification. Fig. 4.4l shows layer V of control cortex after 1 month, in which there is no marked difference in Nogo-A immunoreactivity compared to zymosan-treated cortex (Fig. 4.4m). Scale bar in Fig. 4.4a = 100μm and also applies to b; bar in Fig. 4c = 50μm and also applies to Fig. 4.4d; bar in Fig. 4.4e = 20μm and also applies to f – h; bar in Fig. 4.4i = 200μm; bars in Figs. 4.4j and l = 50μm and also apply to Figs. 4.4k and m respectively.

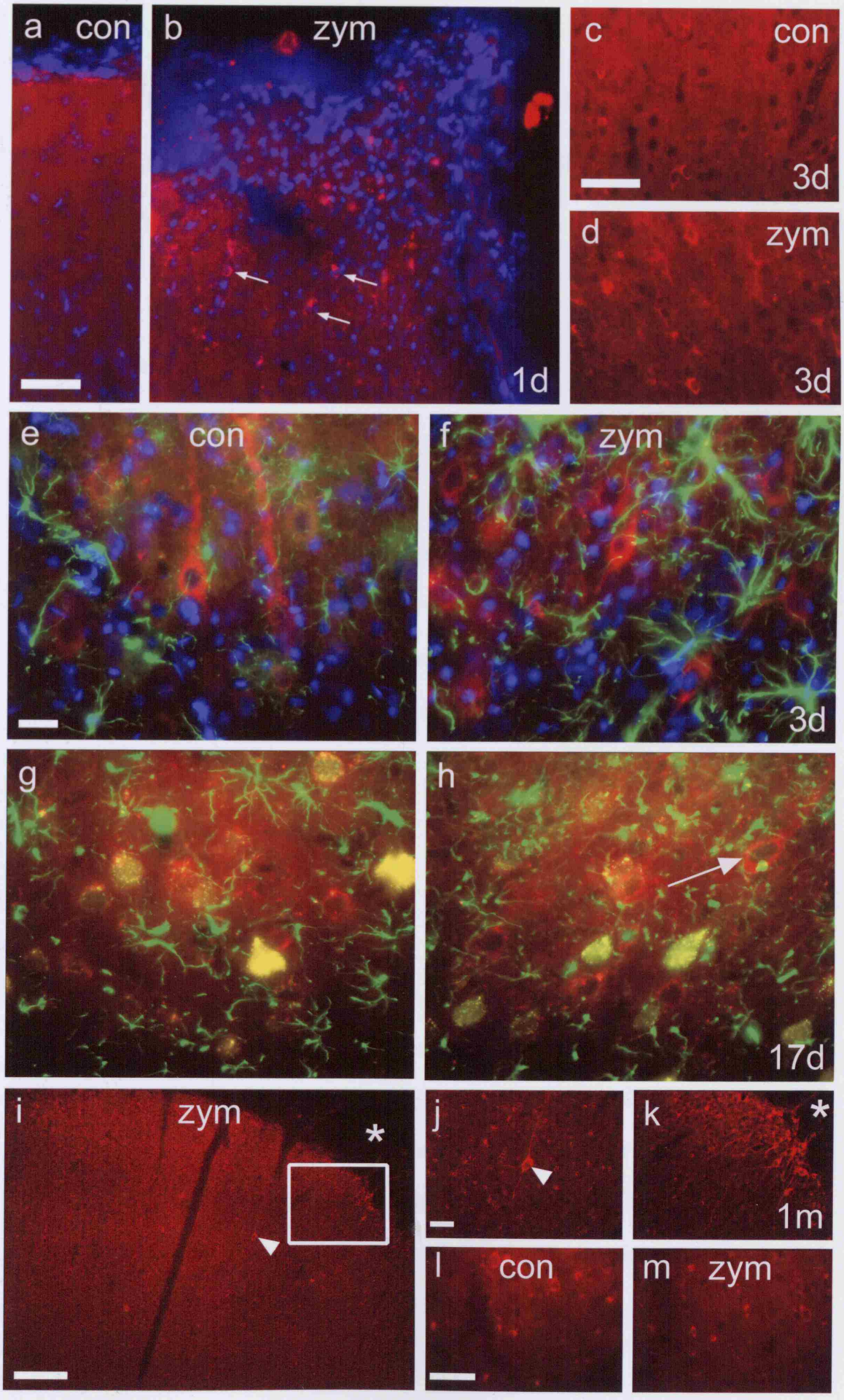
a con
b zym
1d
c con
3d
d zym
3d
e con
f zym
3d
g
h
17d
i zym
*
j
k
*
1m
l con
m zym

4.1.3 Effects of zymosan-induced inflammation on expression of growth-associated proteins by corticospinal tract neurons

4.1.3.1 c-Jun

From 1 day to 17 days after zymosan application c-Jun was markedly upregulated in most neurons of layers I, II, III and V of the zymosan-treated motor cortex (Figs. 4.5b, d and f). At 1 month, although more cells upregulated c-Jun in these layers of cortex compared to the control cortex, the effect was less marked (Figs. 4.5g and h). Retrograde labelling with Fluorogold combined with immunohistochemistry for c-Jun (Figs. 4.5e - h) showed that CST neurons in layer V were among cells upregulating c-Jun in response to zymosan application.

4.1.3.2 ATF3

By 24 hours after application of zymosan, ATF3 was upregulated in neurons, confined to the region under the burr hole. After 3 days, there were slightly fewer ATF3-positive nuclei in layer II than that seen after 1 day, and they were often abnormally shaped. ATF3-positive neurons in layers II to VI were extremely sparse (<5 per section on the treated side; none on the contralateral side), but retained a normal morphology, with very few in layer V. Expression of ATF3 in subcortical white matter glia was seen in 1 animal at 3 days, extending up to the midline (not illustrated) in a similar pattern, but

weaker to that seen 3 days after LPS application to cortex (see Results section 3.1.3.2, page 185) and with none in the contralateral hemisphere (not illustrated). ATF3 expression had disappeared by 7 days (not shown). When cortex was damaged by zymosan application, ATF3 was upregulated in the nuclei of some cells lining the edge of the lesion cavity between 3 and 17 days (Fig. 4.6f), but whether they were neurons or glia was not ascertained. Moreover, ATF3+ nuclei were seen in a very few cells located in layer V of cortex in the animals with a lesion (Fig. 4.6g arrows) at 17 days, though they were not double-labelled with Fluorogold seen in CST neurons. In one animal surviving for 3 days, ATF3 was seen in the nuclei of flattened cells in the corpus callosum (similar to the result seen with topical LPS application to cortex). Thus, ATF3 immunoreactivity was seen in very few layer V pyramidal neurons 3 days after zymosan application in undamaged cortex, and at 17 days in animals with zymosan-induced cortical lesions.

4.1.3.3 SCG10

SCG10 was weakly upregulated by layer V pyramidal neurons and by no other cells. This effect was seen from 24 hours to 17 days after zymosan application (Figs. 4.7b, d, h and j). Most of the cell bodies displaying upregulation of SCG10 were identified as CST neurons (orange/yellow double-labelled cells in Fig. 4.7i). At 1 month, SCG10 immunoreactivity was back to background levels in zymosan-treated and control cortex. However, if the cortex was lesioned by zymosan, strongly SCG10+ neurons were visible along the wound edges between 3 days and 1 month (Figs. 4.7l and m).

Figure 4-5 Expression of c-Jun after zymosan application.

Coronal sections of motor cortex 1 day, 3 days and 1 month after unilateral application of zymosan (zym; Figs. 4.5b, d, f and h), or sham operation control (con; Figs. 4.5a, c, e and g), immunoreacted for c-Jun. Fig. 4.5a shows that after 1 day, there are only background levels of c-Jun in the sham-operated cortex, and Fig. 4.5b demonstrates c-Jun upregulation predominantly in layers II, III and V under the site of zymosan application. Insets in Figs. 4.5a and b are magnified images of layer V, demonstrating the increased c-Jun signal in the zymosan-treated cortex. Figs. 4.5c and d show that, at 3 days, c-Jun is upregulated at low levels in layers I - III immediately below the craniectomy on the control side, but is almost undetectable more medially and laterally, and that c-Jun immunoreactivity is much stronger in all layers on the treated side below the site of zymosan application. Inset in Figs. 4.5c and d are magnified images of layer V, demonstrating marked upregulation of c-Jun in nuclei of zymosan-treated cortex. Fig.4.5e shows that, at 1 month, c-Jun immunoreactivity is almost back to normal levels in sham-operated cortex, compared to Fig. 4.5f where there is an increase in c-Jun immunoreactivity in all layers of cortex below the burr hole and site of zymosan application, although the increase in c-Jun expression is not as marked as that seen at 3 days or 17 days (see appendix). Layer V of Figs. 4.5e and f is identified by the presence of FG-containing CST neurons retrogradely labelled from the spinal cord and demonstrates that almost all retrogradely labelled CST neurons display c-Jun expression. Figs. 4. 5g and h show some of the retrogradely labelled cells in Figs. 4.5e and f at greater magnification in Figs to illustrate the immunostained nuclei. Scale bar in Fig. 4.5a = 200μm and applies to Figs. 4.5b, e and f; bar in Fig. 4.5c = 500μm and also applies to d; bar in Fig. 4.5g = 50μm and also applies to h; bar in Fig. 4.5a inset = 20μm and applies to all 4 insets.

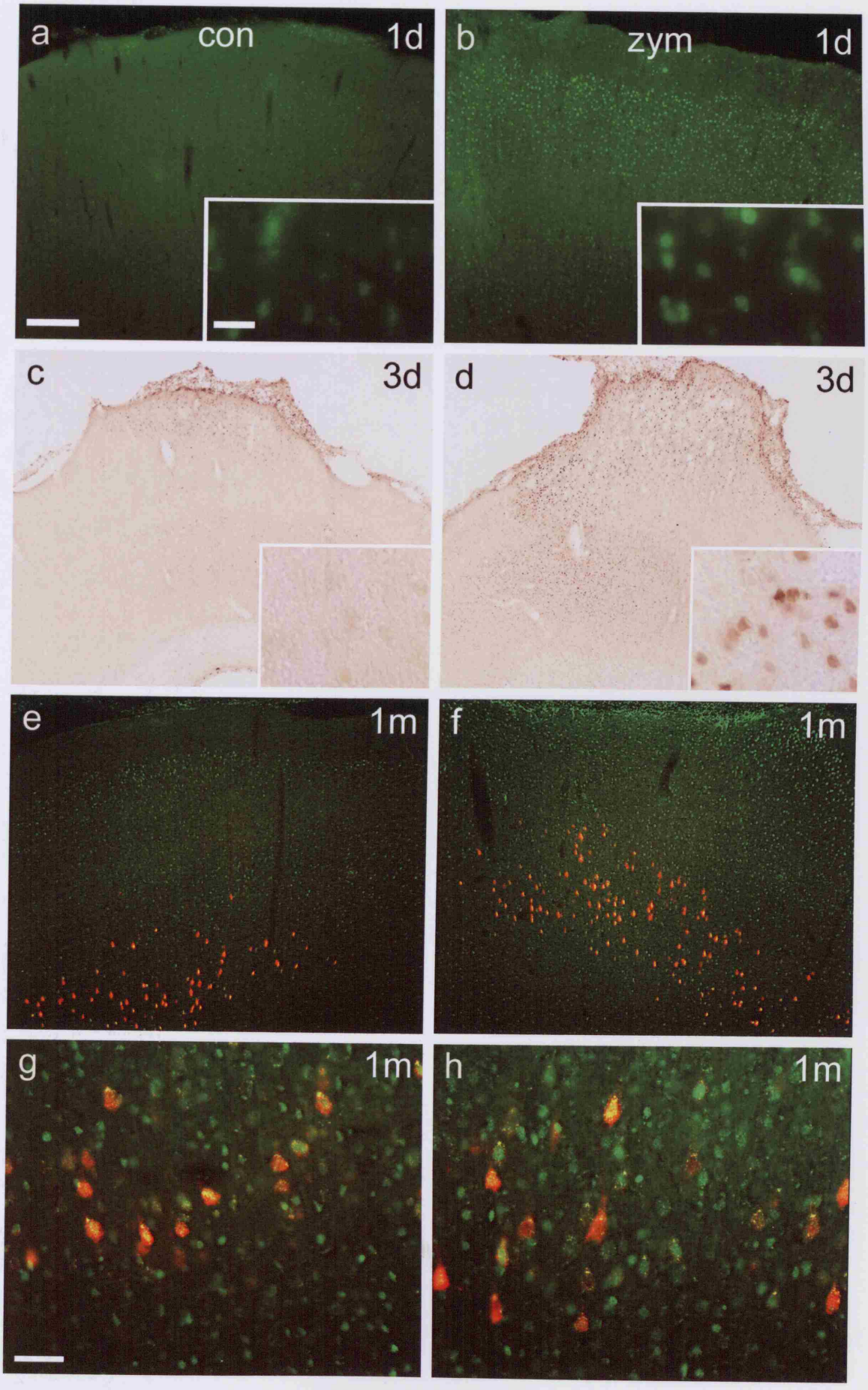
a
con
1d
b
zym
1d
c
3d
d
3d
e
1m
f
1m
g
1m
h
1m

Figure 4-6 Expression of ATF3 after zymosan application.

Coronal sections of motor cortex 1 day, 3 days, and 17 days after zymosan (zym; Figs. 4.6b - h) application or sham operation on the contralateral cortex (con; Fig. 4.6a), immunoreacted for ATF3. Corticospinal neurons in layer V of cortex, retrogradely-labelled with Fluorogold (FG) are demonstrated in Figs. 4.6f and g (yellow).

Fig. 4.6a (control cortex) shows that there is no ATF3 immunoreactivity in cortical neurons at one day. In Figs. 4.6a, b and d, arrows refer to neurons in Layer V of cortex, which do not contain ATF3+ nuclei, and show background staining in zymosan-treated and control cortex. Fig. 4.6b demonstrates upregulation ATF3 in to the superficial cortex directly under the area of zymosan application after 1 day. Fig. 4.6c is enlarged from the boxed area in Fig. 4.6b and shows ATF3+ nuclei in cortex that appears to have been damaged during histological processing. Fig. 4.6d shows zymosan-treated cortex 3 days after zymosan application, demonstrating limited ATF3 immunoreactivity under the zymosan application site. Fig. 4.6e is enlarged from the boxed area in Fig. 6d: note the irregular shape of ATF3+ nuclei, suggesting possible damage or apoptosis. Images taken 17 days (Fig. 4.6f) and 1 month (Fig. 4.6g) after zymosan application, show cortex damaged by zymosan application with loss of tissue down to layer IV of motor cortex. There is focal upregulation of ATF3 in cells along the edge of the damaged cortex, as demonstrated at increased magnification in the inset image of Fig. 4.6f. No ATF3 immunoreactivity was seen in any FG-labelled CST neurons, although a very few ATF3+ neurons are located in layer V in Fig. g (white arrows). Fig. 4.6h is a negative control, in which ATF3 primary antibody was not used, from the section adjacent to Fig. 4.6g, demonstrating that the ATF3+ nuclei seen in Fig. 4.6g are genuine. Scale bar in Fig. 4.6a = 500μm and also applies to b and d; bar in Figs. 4.6c and g = 100μm; bar in Figs. 4.6e and h = 50μm; bar in Fig. 4.6f = 200μm (inset bar = 20μm).

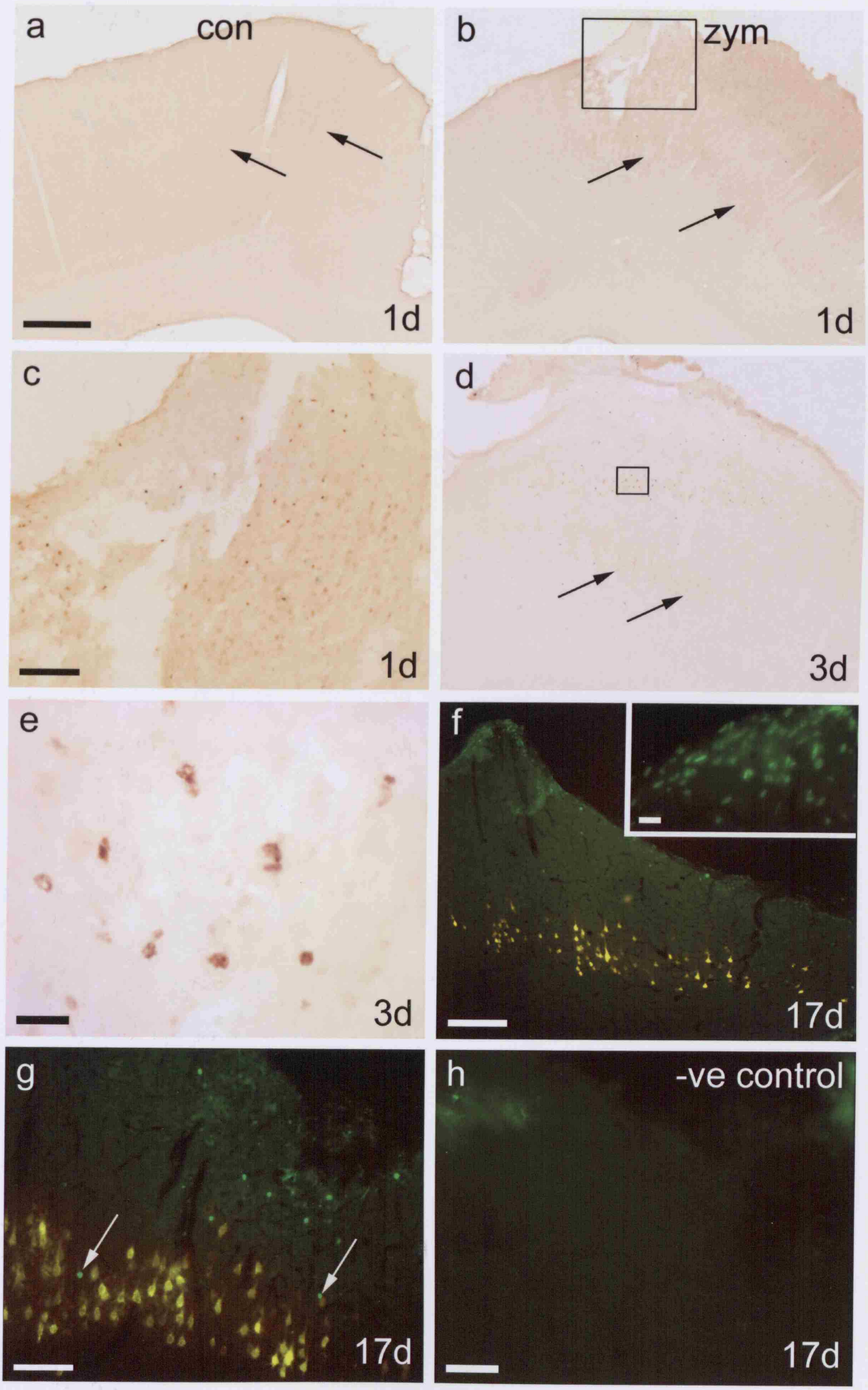
a
con
1d
b
zym
1d
c
1d
d
3d
e
3d
f
17d
g
17d
h
-ve control
17d

Figure 4-7 Expression of SCG10 after zymosan application.

Coronal sections of motor cortex, 1 day, 3 days, 17 days and 1 month after unilateral application of zymosan to cortex, immunoreacted for SCG10. Control, contralateral (con) cortex is shown in Figs. 4.7a, c, e, g and j. Zymosan-treated cortex is shown in Figs. 4.7b, d, f, h, i, k and l. Corticospinal pyramidal cells in layer V of cortex are seen in animals surviving for 17 days and 1 month, following retrograde labelling with Fluorogold (red) placed in the corticospinal tract.

Fig. 4.7a shows low background levels of SCG10 in pyramidal neurons of layer V control cortex, compared to Fig. 4.7b, which demonstrates increased SCG10 immunoreactivity in layer V cells at 1 day. The immunoreactivity seen in more superficial cortex in Fig. 4.7b is non-neuronal and non-specific. Inset images show magnified views of the boxed areas of layer V neurons, detailing greater cytoplasmic staining of SCG10 in zymosan-treated cortex. Figs. 4.7c and d, 3 days after zymosan application, also demonstrate SCG10 upregulation in layer V neurons of zymosan-treated cortex. Fig. 4.7e (control cortex) and Fig. 4.7f (zymosan-treated cortex) are magnified images from the boxes in layer V of Fig. 4.7c and Fig. 4.7d respectively, showing SCG10 in pyramidal neurons in greater detail.

Fig 4.7g shows that control cortex 17 days after zymosan application is unchanged from earlier and Fig. 4.7h that is still increased SCG10 immunoreactivity in layer V cells, but to a lesser degree than earlier and localised to the area under zymosan application. Fig. 4.7i is enlarged from the boxed area of Fig. 4.7h, and shows neuronal SCG10 immunoreactivity in layer V of cortex (yellow/orange cells are double labelled with SCG10 and Fluorogold), but the 2 neurons that show marked SCG10 upregulation are not double-labelled. Figs. 4.7j and k illustrate that in both contralateral cortex and ipsilateral cortex, one month after zymosan application, there are only background levels of SCG10 immunoreactivity in layer V neurons.

When there is damage to cortex, a few cells at the edge of the lesion cavity have increased SCG10 immunoreactivity (arrow in Fig. 4.7h and Fig. 4.7k). Fig. 4.7l is from the immediately adjacent section to Fig. 4.7k and shows neurons at the zymosan-induced lesion edge that have upregulated SCG10. Bar in Fig. 4.7a = 200μm and also applies to b; bar in inset = 20μm and also applies to inset in b; bar in Fig. 4.7c = 500μm and also applies to d; bar in Fig. 4.7e = 20μm and also applies to Figs. 4.7f, i and l; bar in 4.7g = 100μm and also applies to Figs. 4.7h, i, and k.

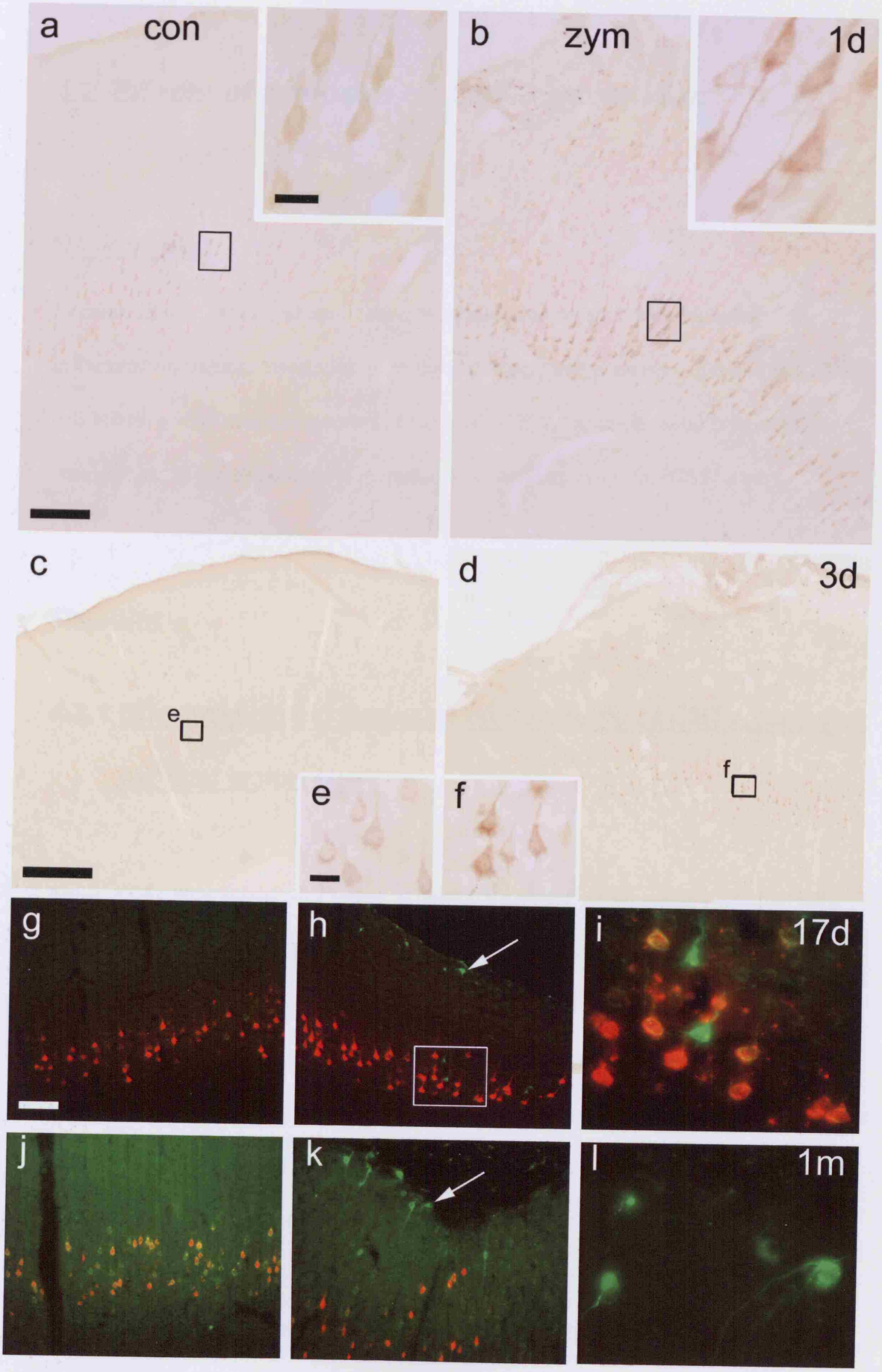
a
con
b
zym
1d
c
d
3d
e
f
g
h
i
17d
j
k
l
1m

4.2 Effects of zymosan on CST regeneration

Background

I demonstrated that topical application of zymosan to motor cortex stimulated an inflammation-induced upregulation of the growth-related proteins c-Jun and SCG10 in cell bodies of corticospinal neurons. I have asked if zymosan-induced inflammation would enhance any regenerative response to a corticospinal tract (CST) injury.

Results

4.2.1 Effect of cortical zymosan on sprouting of CST axons at a cervical lesion site

Three weeks after spinal cord lesion, injured CST axons, anterogradely labelled with BDA, terminated proximal to the lesion site, many with swollen axonal tips, in both zymosan-treated and control animals (Fig 4.2). No axons were seen to grow into or distal to the lesion cavity or to bypass the lesion site, or send branches around it. In some animals, axons were seen skirting the edge of the lesion and stopped in the 2-3mm of CST distal to the lesion. These probably represented axons that were damaged, but not completely axotomised by the edge of the lesion, and made a limited attempt at regeneration. Other axons were seen distal to the lesion site but were not in continuity with axons proximal to the lesion site, did not end in terminal bulbs of abortive regeneration or growth-cones and could be followed for 2cm caudally. When followed

in serial sections, they were seen to be uninjured axons that originated from the uninjured lateral CST. In one animal, axons were seen to have originated from the injured CST rostral to the lesion site, following incomplete lesion, and the animal was excluded from the study.

Thus, application of zymosan to the cortex appeared to produce no marked enhancement of axon regeneration into or around the lesion site. There was no statistically significant difference between control and zymosan-treated animals in either the 'total sprouting ratios' ($p = 0.26$; Mann-Whitney test, n.s.) or the 'lesion site sprouting ratios' (t-test, $p = 0.35$; Mann-Whitney test, n.s.) – see Table 4.1 notes for definition of ratios. These data, summarised in Table 4.1, suggest that application of zymosan to motor cortex has no effect on the sprouting response or regeneration of CST axons across a lesion. The application of zymosan to cortex did not cause a reduction of labelled CST axons in the medulla ($p = 0.76$, Mann-Whitney test, n.s.; Figure 4.8d), demonstrating that the uptake and anterograde transport of BDA by CST neurons was unaffected by zymosan-induced inflammation.

Figure 4-8 Anterograde labelling of CST axons after spinal cord injury and zymosan application.

Horizontal sections through spinal cord injury sites (Figs. 4.8a - c), and a transverse section through the medulla (Fig. d) 21 days after lesion of the CST at C4 with either simultaneous injection of BDA into contralateral motor cortex (con) or injection of BDA into and application of zymosan onto motor cortex (zym). In both the zymosan-treated (Fig. 4.8b) and control tissue (Fig. 4.8a), end bulbs are seen at the tips of large numbers of axons. There is little sign of axon branching into the contralateral CST (bottom of each image). No axons appear to circumnavigate or regenerate beyond the lesion site. The white box in Fig. 4.8a corresponds to the counting frame used to quantify BDA-labelled axons; the arrow in the inset box points to the same axon highlighted in fig. 4.8a and shows axons stopping at a strand of scar tissue(s) within the lesion site. The increased contrast of Figs. 4.8a and d show the settings that were used for counting axons, whereas Figs. 4.8a inset, 4.8b and c are shown with a reduced threshold setting (less bright colours are visualised), allowing observation of unlabelled background tissue and the cavity (black) of the lesion site.

Fig. 4.8b has arrows pointing to an injured CST axon that has turned 180° at the lesion edge. Fig. 4.8c shows two branches (arrowheads) of axons that have passed medially and crossed into the opposite side of spinal cord from the same animal as Fig. 4.8a. Note that the contralateral CST has two labelled axons that are presumably fibres that did not cross at the pyramid. Fig. d shows BDA-labelled CST axons in the pyramid of the medulla from the same animal as Fig. 4.8b. All images are confocal; * = lesion site; c = caudal; l = lateral; scale bar in Fig. 4.8a = 100μm and also applies to Figs. 4.8b and c; bar in Fig. 4.8d = 100μm.

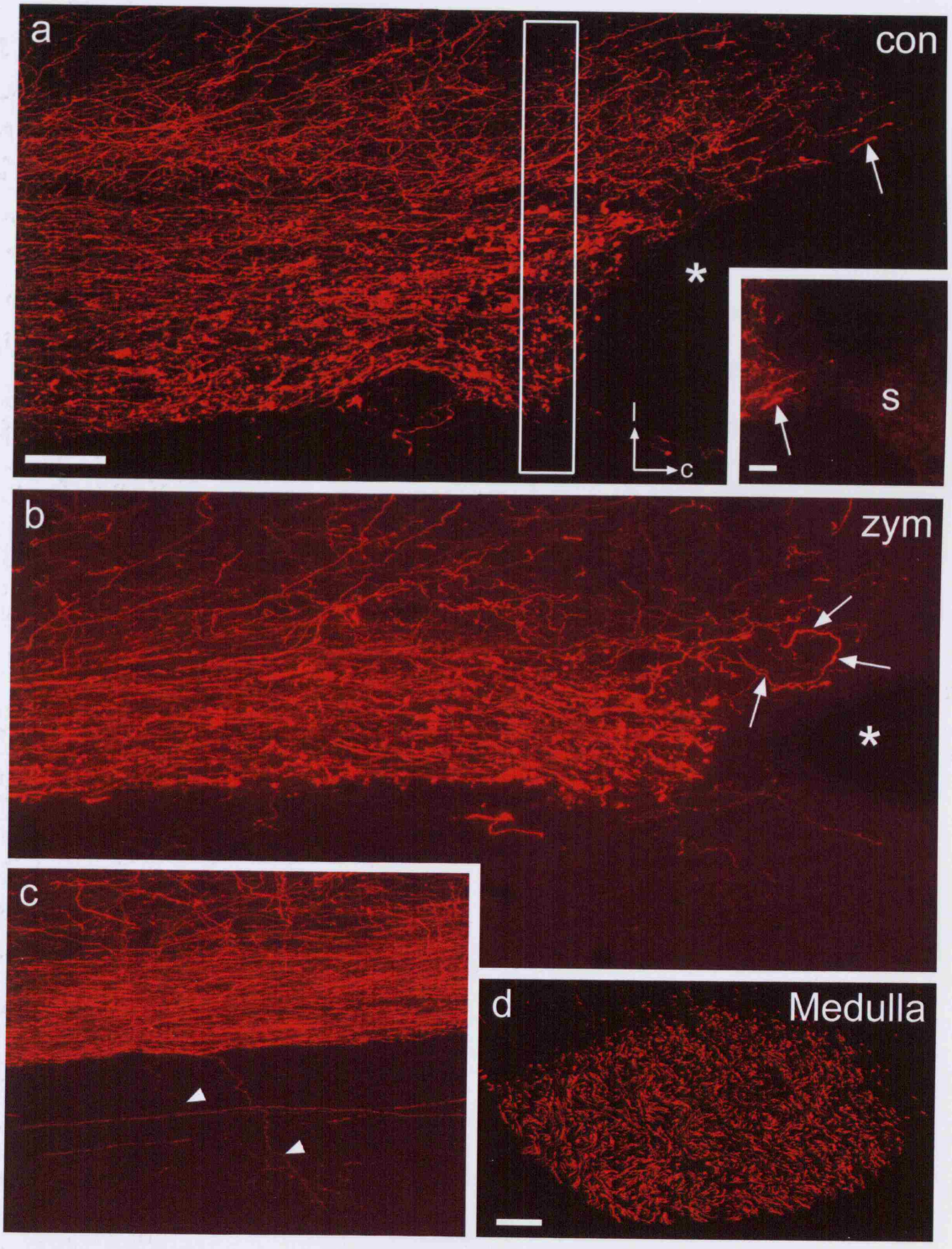
a
con
*
l
c
s
b
zym
*
c
d
Medulla

4.2.2 Effect of cortical zymosan on branching of CST axons across the midline proximal to a cervical lesion

The mean percentage of BDA-labelled axons that gave branches that crossed the midline was 0.26% in the zymosan-treated group, compared to 0.19% in the control group ($p = 0.29$; Mann-Whitney test, n.s.; see Fig. 4.8c). The finding of $p = 0.29$ is not statistically significant and suggests that the application of zymosan on the motor cortex does not affect the ability of injured CST axons to sprout axons across the midline proximal to the lesion site (and potentially grow down the intact opposite CST to bypass the lesion).

Table 4-1 Quantification of CST axons

	Axons	Branches	Medulla count	Branches crossing midline	Total branching ratio	Lesion branching ratio	Midline branching percentage
Control	126	22	2318	6	0.01	0.17	0.25
	730	225	3258	11	0.07	0.31	0.33
	129	23	2621	0	0.01	0.18	0
	317	51	1742	3	0.03	0.16	0.17
Mean					**0.03**	**0.21**	**0.19**
Zymosan	408	150	3432	12	0.04	0.37	0.35
	319	73	2480	1	0.03	0.23	0.04
	252	43	1098	0	0.04	0.17	0
	484	137	2979	15	0.05	0.28	0.50
	353	90	2547	9	0.04	0.26	0.35
	490	127	2913	10	0.04	0.26	0.34
Mean					**0.04**	**0.26**	**0.26**

Notes to Table 4.1: BDA-labelled axons (and branch points) in 6 zymosan-treated animals and 4 control animals (zymosan not applied) were counted in 9 horizontal sections through the cervical spinal cord 0.4mm rostral to the lesion site, in a 60μm wide counting frame and in transverse sections through the medulla (number of labelled axons in pyramid). Total sprouting ratio is the ratio between the number of branch points and the total number of labelled CST axons at the level of the medulla. Lesion site sprouting ratio is the ratio between branch points and labelled axons at the same level (0.4mm rostral to the lesion site). The number of branches given off by axons that crossed the midline (in the 15mm of tissue rostral to the lesion site) were counted and divided by the number of axons at the level of the medulla to calculate the 'midline branching percentage'.

Figure 4-9 Histograms comparing sprouting of BDA-labelled CST axons 21 days after cervical injury.

Anterogradely-labelled CST axons (and branch points) were counted in 4 control animals (CST injury and simultaneous injection of BDA into contralateral motor cortex) and 6 zymosan-treated animals (CST injury, BDA injection and zymosan application to cortex). See Table 4.1 notes for definition of total sprouting ratio, lesion site sprouting and midline branching percentage.

Fig. 4.9a demonstrates that the mean total sprouting ratio increases with zymosan application compared to controls, but not with statistical significance ($p = 0.25$; Mann-Whitney test). Fig. 4.9b shows no statistically significant difference in the lesion site branching ratio between control and zymosan-treated groups ($p = 0.35$; Mann-Whitney test). Fig. 4.9c shows no difference in the percentage of labelled axons giving off branches that cross the midline between control and zymosan groups ($p = 0.29$ Mann-Whitney test).

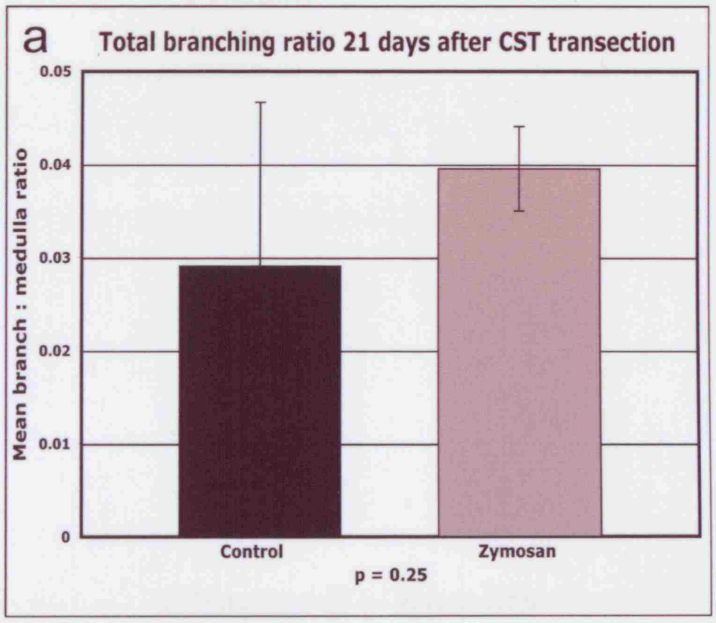
a
Total branching ratio 21 days after CST transection
Mean branch : medulla ratio
0.05
0.04
0.03
0.02
0.01
0
Control
Zymosan
p = 0.25

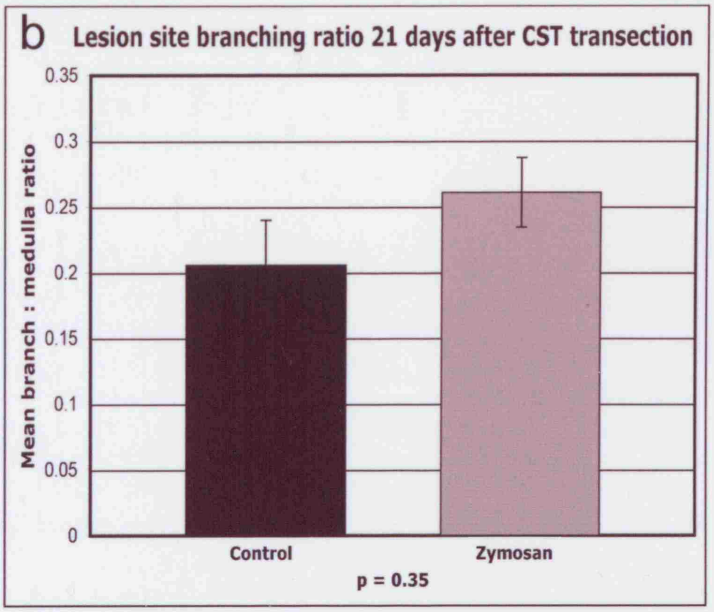
b
Lesion site branching ratio 21 days after CST transection
Mean branch : medulla ratio
0.35
0.3
0.25
0.2
0.15
0.1
0.05
0
Control
Zymosan
p = 0.35

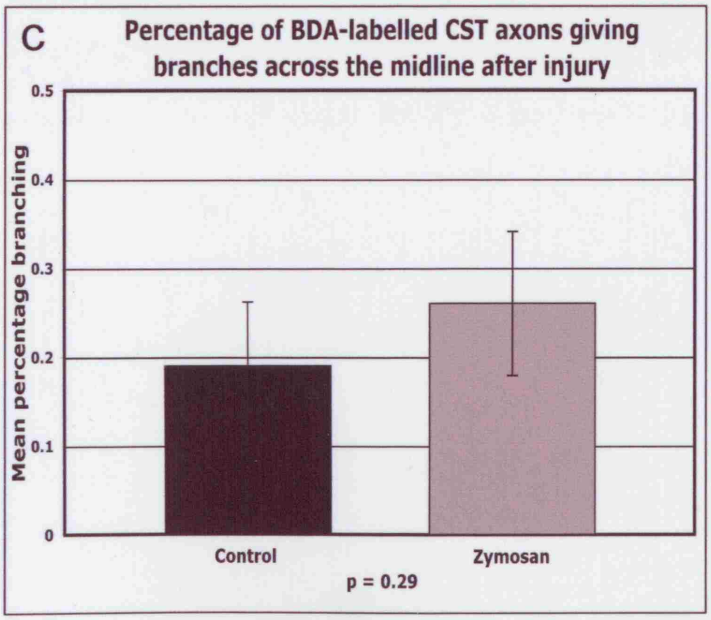
c
Percentage of BDA-labelled CST axons giving branches across the midline after injury
Mean percentage branching
0.5
0.4
0.3
0.2
0.1
0
Control
Zymosan
p = 0.29

Chapter 5 – Results

5 ATF3 expression in glia during Wallerian degeneration in peripheral nerves and CNS white matter

Background

Many changes in gene expression occur in distal stumps of injured nerves but the transcriptional control of these events is poorly understood. I have examined the expression of the transcription factors ATF3 and c-jun by non-neuronal cells during Wallerian degeneration following injury to sciatic nerves, dorsal roots of rats and mice, using immunohistochemistry and *in situ* hybridisation.

The original observation regarding ATF3 expression in injured sciatic nerves was made independently and contemporaneously by chance, by David Hunt and myself, whilst working on separate projects. When we became aware of each other's work, the study was completed as a collaboration and a single paper has been published from our observations (Hunt et al., 2004).

Results

5.1 ATF3 expression in peripheral glia

5.1.1 Sciatic nerve resection

Sciatic nerve resection in adult rats created a 2-3mm gap between the proximal and distal stumps. By 1 day post operatively (dpo) some cell nuclei in the endoneurium of the distal stump were ATF3+. In contrast, there were no ATF3+ cell nuclei in the proximal stumps of the injured nerves at 1dpo and very few at 4 dpo (Fig. 5.1a). By 4 dpo large numbers of strongly AFT3+ nuclei were present in all parts of the endoneurium of the distal stump of the injured nerves (Fig. 5.1b). ATF3+ cells were of different sizes and shapes, suggesting that a mixed population of cells were ATF3+. They were rarely found in the perineurium but a few were present in the epineurium of the nerve, often associated with the adventitia of blood vessels. 51% of the cell nuclei in the endoneurium were ATF3+ at 4 dpo (Fig. 5.2b).

By 8 dpo, and at 16 or more dpo, a thin strand of regenerating tissue connected the two stumps in most animals. Bisbenzimide staining of cell nuclei showed that numerical density of cells in the endoneurium of the distal stump increased 2 or 3 fold between 4dpo and 16dpo and remained high at 30dpo. At 8dpo, the number of ATF3+ cells in the distal stump had increased (Figs. 5.1d) and the percentage of cell nuclei in the distal stumps and their outgrowths that were ATF3+ had increased from 51% to 64%. The situation remained similar at 16dpo (Figs. 5.1e, f and 5.2b). ATF3 expression by cells within the proximal stump was quite different, with <1% of cells being ATF3+ at 4dpo and a much more substantial peak of expression at 16dpo (Figs. 5.1e and Fig.5.2a).

Additionally, in comparison to the distal stump, ATF3 immunoreactivity in the proximal stump was weaker at any given timepoint (Fig.5.1).

At 30dpo the number of ATF3+ cells in the endoneurium of the distal stumps depended upon the extent of axonal regeneration that had occurred. When the proximal stump was ligated to prevent regeneration of axons distally, the percentage of ATF3+ nuclei in the distal stump remained high (Fig. 5.1h), similar to the counts at 16 dpo. However, when the sciatic nerve was transected without ligation, the percentage of ATF3+ endoneurial cells in the distal stump varied from 10-56%. ATF3+ nuclei were found in cells that appeared to be in contact with regenerating axons (Figs. 5.3a and b). This infers that ATF3 is not immediately downregulated by Schwann cells on contact with axons, though it appears that there were fewer ATF3+ endoneurial cells when regeneration was extensive (Fig. 5.3d). The percentage of cells in the endoneurium of the proximal stump that were ATF3+ dropped between 16 and 30 dpo (almost to the low levels seen at 1 – 8dpo).

Figure 5-1 Sciatic nerve resection

Horizontal sections of proximal (Figs. 5.1a, c, e and g) and distal (Figs. 5.1b, d, f and h) stumps of severed sciatic nerves in adult rats at 4 days (Figs. 5.1a and b), 8 days (Figs. 5.1c and d), 16 days (Figs. 5.1e and f) and 30 days (Figs. 5.1g and h) after resection, immunoreacted for ATF3. Many cells express ATF3 in the distal stumps at all times after injury whereas ATF3 is more weakly expressed and by fewer cells in the proximal stumps - the inset in Fig. 5.1c shows part of a distal stump photographed at the same exposure, gain and offset settings as the main panel. Note that there is no ATF3 immunoreactivity in the perineurium (P in Fig. 5.1d) or in uninjured sciatic nerve (not shown). Scale bar in Figs. 5.1a = 200μm and also applies to b; bar in Fig. 5.1c = 50μm and applies to Figs. 5.1d - h.

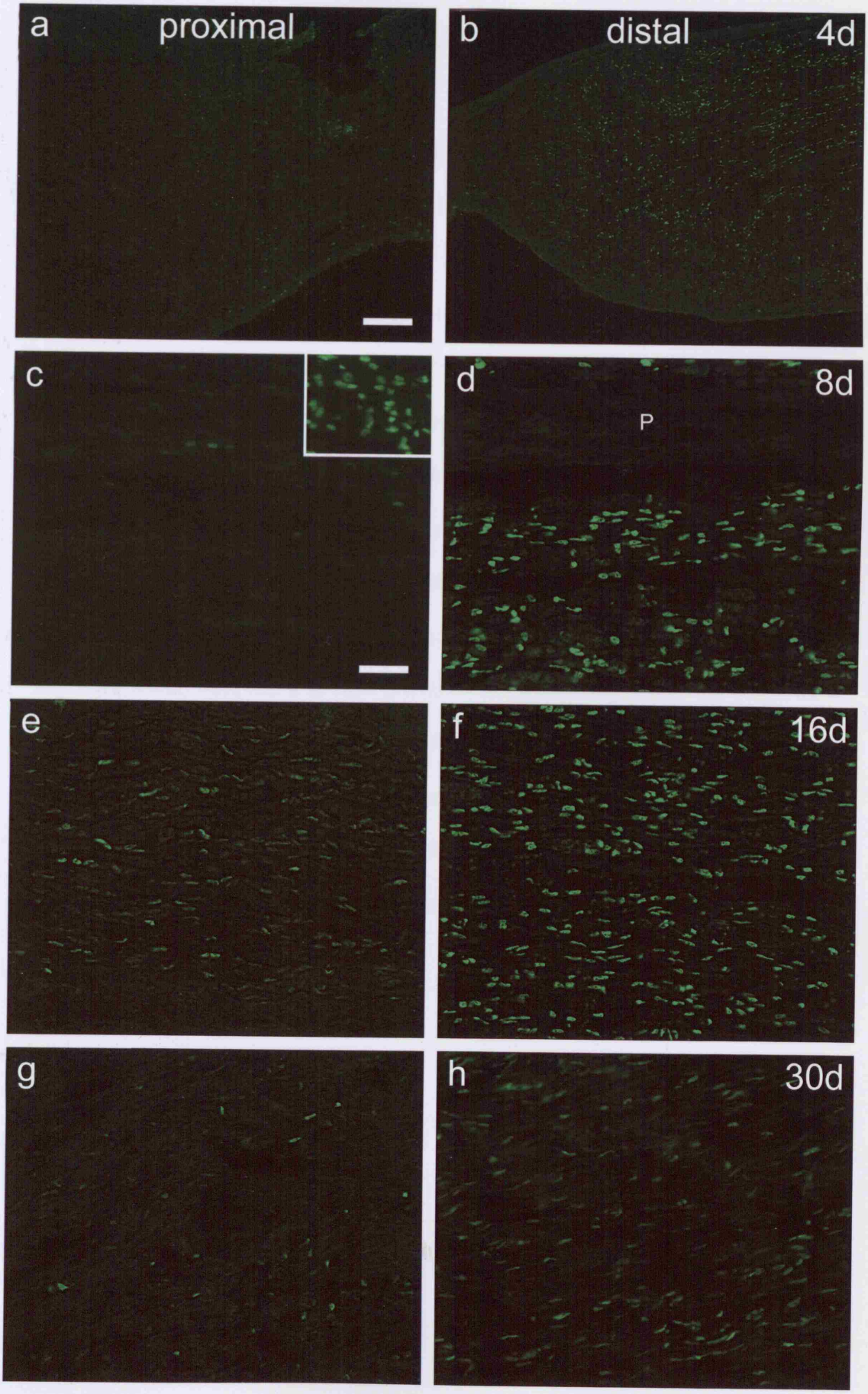
a
proximal
b
distal
4d
c
d
8d
P
e
f
16d
g
h
30d

5.1.2 Sciatic nerve transection and reanastomosis .

This procedure in adult rats allowed the regeneration of axons from the proximal stump into the distal stump of the injured nerve. Even at 4dpo regenerating axons, identifiable as thin, continuous neurofilament+ fibres, were present in parts of the distal stump within a few millimetres of the anastomosis, although a large amount of more particulate neurofilament immunoreactivity remained in the degenerating nerve fibres of the distal stump. By 16dpo there was extensive regeneration of axons into the distal stump. Large numbers of ATF3+ cell nuclei were present in all parts of the endoneurium of the distal stump by 4dpo and constituted 35 % of the total population of nuclei (Fig. 5.2c). By 16dpo the number of ATF3+ endoneurial cells remained similar but the frequency of ATF3+ cell nuclei had fallen to about 20%. Some ATF3+ cells in the distal stump were found in close proximity to regenerating axons. By 30dpo most ATF3 immunoreactivity had disappeared from the distal stump (Fig. 5.3d) and most of the cells which retained ATF3 immunoreactivity (< 5% of the endoneurial cells) were much less strongly stained than at earlier times. The proximal stumps only contained a few ATF3+ cells, very close to the site of reanastomosis.

Figure 5-2 Counts of ATF3+ nuclei in proximal and distal nerve stumps.

Histograms showing the percentage of ATF3+ nuclei in the proximal (Fig. 5.2a) and distal (Fig. 5.2b and c) stumps of injured sciatic nerves in adult rats. The animals used in Fig. 5.2a and Fig. 5.2b had sciatic nerves cut and a segment resected (restricted regeneration). The percentages of ATF3+ nuclei in the proximal stumps were lower than in the distal stumps. The bar for 4 dpo in the proximal stumps is not visible because < 1% of nuclei were AFT3 immunoreactive at this time.

Fig. 5.2c compares the percentage of ATF3+ nuclei in the distal stumps of nerves that were cut and reanastamosed (C&R; rapid regeneration) with nerves which were cut and ligated (C&L; prevents regeneration - far right column). The greatest percentage of ATF3+ nuclei were seen when regeneration was prevented. When rapid regeneration occurred, ATF3 became downregulated with time in a linear manner.

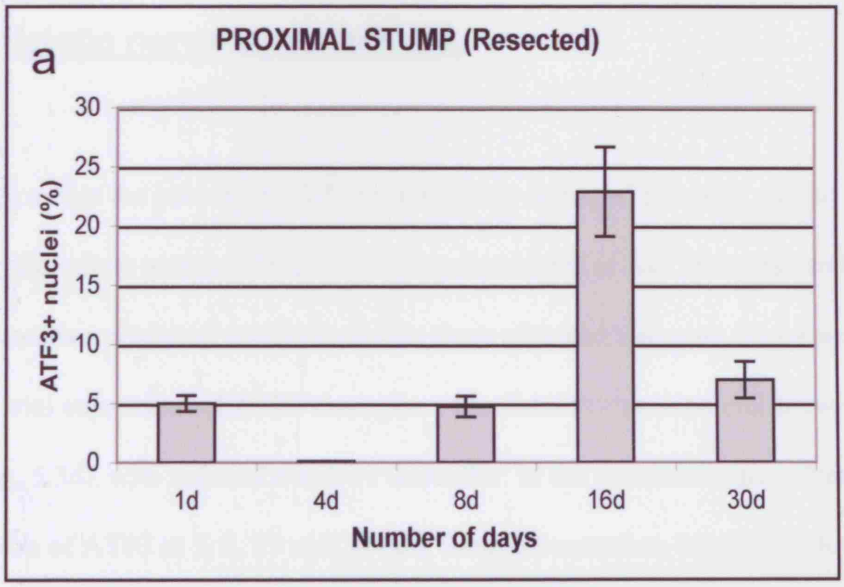
a
PROXIMAL STUMP (Resected)
ATF3+ nuclei (%)
30
25
20
15
10
5
0
1d
4d
8d
16d
30d
Number of days

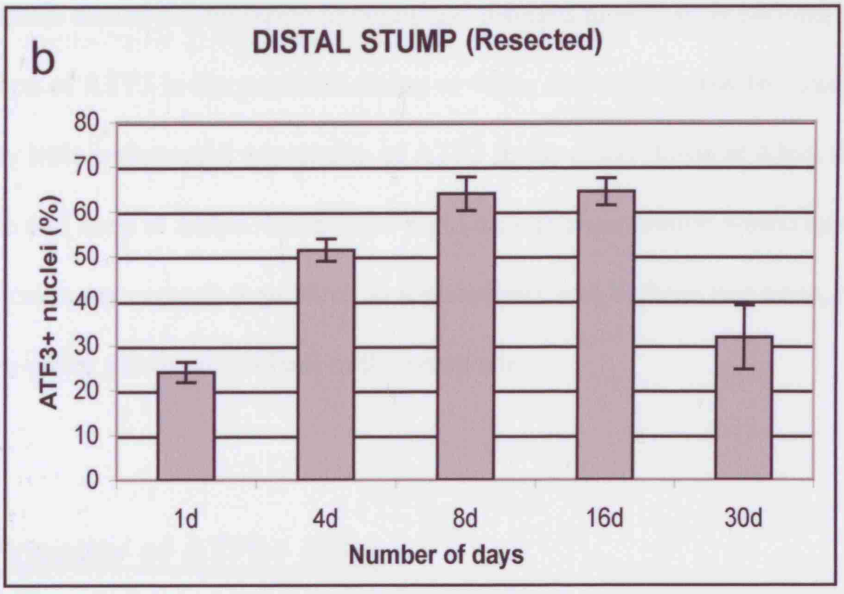
b
DISTAL STUMP (Resected)
ATF3+ nuclei (%)
80
70
60
50
40
30
20
10
0
1d
4d
8d
16d
30d
Number of days

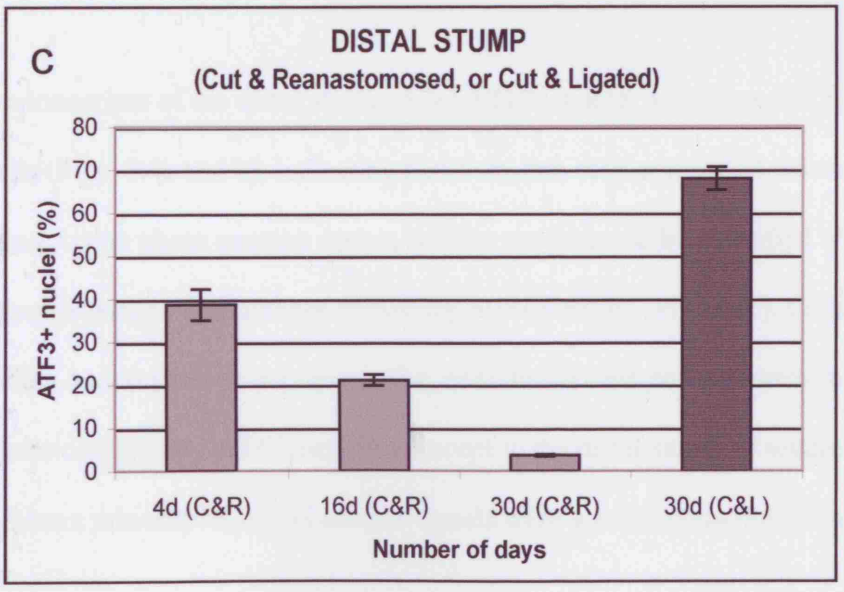
c
DISTAL STUMP
(Cut & Reanastomosed, or Cut & Ligated)
ATF3+ nuclei (%)
80
70
60
50
40
30
20
10
0
4d (C&R)
16d (C&R)
30d (C&R)
30d (C&L)
Number of days

5.1.3 Sciatic nerve injury in mice.

To confirm that the pattern of ATF3 expression in damaged nerves is similar in other species, the sciatic nerves of adult mice were transected or had 3mm resected. Sciatic nerve resection produced results similar to those obtained with rats. There was endoneurial expression of ATF3 throughout the distal stump, maximal between 5 and 8 dpo (Fig. 5.3d), with reduced numbers thereafter. In the proximal stump, there was little expression of ATF3 at 5, 8, 17 and 30 dpo. Simple transection of nerves allowed considerable axonal regeneration to occur and resulted in very little endoneurial expression of ATF3 in the proximal stump at 4dpo, and none thereafter. Similarly, there was very little endoneurial expression of ATF3 in the distal stump at 4dpo, decreasing by 8 dpo and none at 20dpo. Even more rapid axonal regeneration would have occurred after a sciatic nerve crush (compared to transection), and in these two mice, no ATF3 was seen either proximal or distal to the crush site.

5.1.4 Identity of ATF3+ cells

In the endoneurium of the distal stump, most ATF3+ nuclei were found in S100+ and p75+ cells (Figs. 5.4a and b), indicating that Schwann cells comprised the major ATF3+ population. Using phase contrast optics, ATF3+ nuclei could be identified within bands of Büngner between macrophages containing myelin debris (Fig. 5.4c). Cells surrounding endoneurial blood vessels (i.e. endothelial cells and pericytes) in the distal stump were consistently ATF3-negative, except in the distal stump of severed nerves at 1dpo, where a minority of nuclei around vessels were weakly immunoreactive. The

ATF3+ cells at the periphery of epineurial blood vessels in injured nerves were S100+ and most likely to be Schwann cells.

5.1.5 Controls

In the sciatic nerve contralateral to injury and in unoperated control rats and mice, no expression of ATF3 was observed (not illustrated). There was no fluorescence in sections of nerve reacted without primary antibody, except for some autofluorescent cells found near the cut ends (Fig. 5.4f).

Figure 5-3 ATF3 in distal nerve stumps

Distal stumps of rat sciatic nerves 30 days after resection (Figs. 5.3a, b and c) or resection and ligation (Fig. 5.3d) and proximal stump of mouse sciatic nerve 5 days after resection (Fig. 5.3e) compared to distal stump of mouse sciatic nerve 8 days after resection (Fig. 5.3f), immunoreacted for ATF3 using fluorescence (Figs. 5.3a – d) or the ABC technique (Figs. 5.3e and f).

Figs. 5.3a - c show the variation in ATF3 staining (green) and axonal regeneration (neurofilament immunoreactivity- red) in the distal stumps of resected sciatic nerves at 30 dpo. Some nuclei are closely related to regenerating axons, the presence of which does not result in immediate downregulation of ATF3. In Fig. 5.3d, axonal regeneration is extensive in the distal stump after cut and reanastamosis, and there are fewer and less intensely fluorescent ATF3+ nuclei.

In Fig. 5.3e, the proximal stump of a resected sciatic nerve from an adult mouse shows little ATF3 immunoreactivity at the end of the cut nerve, with no ATF3+ nuclei in the distal outgrowth from the stump (note the orientation: distal is to the bottom of the image, as opposed to the right in all other images). At 8 dpo the endoneurium of the distal stump contains many ATF3+ nuclei.

Scale bar in Fig. 5.3a = 50μm and also applies to Figs. 5.3b – d. Bar in Fig. 5.3e = 100μm; bar in Fig. 5.3f = 50μm.

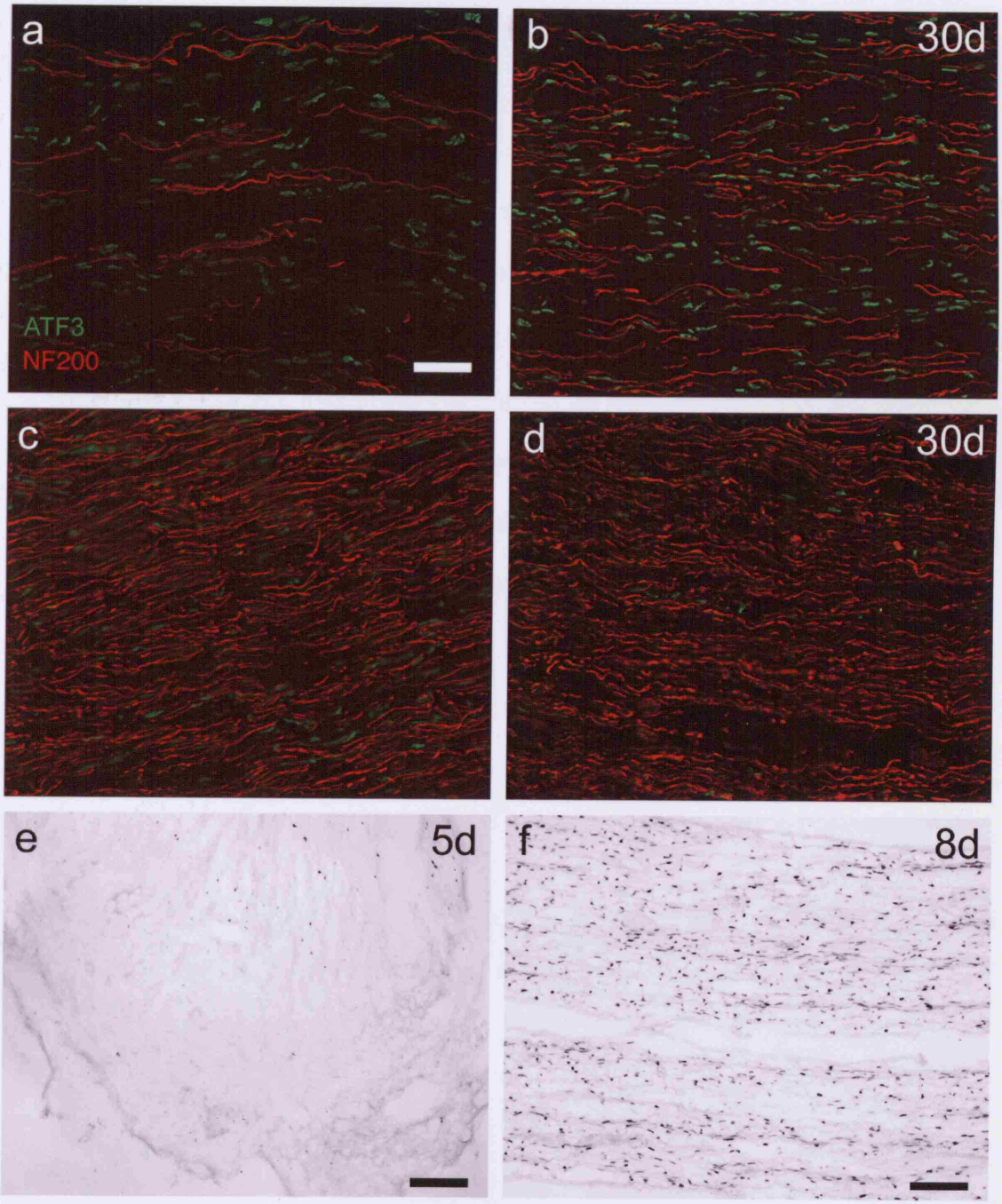
a
ATF3
NF200
b
30d
c
d
30d
e
5d
f
8d

5.2 *ATF3 expression in CNS glia*

5.2.1 Dorsal root transection.

At 1,4 and 8 dpo ATF3+ cell nuclei were present in the dorsal roots and rootlets, central to the transection site and peripheral to the DREZ (Figs. 5.4d and e). At 1dpo, more ATF3+ nuclei were present near to the injury site than were present near to the DREZ, but at later stages they were present throughout the area between lesion and spinal cord. No strongly ATF3+ cells were found in the DREZ, in the adjacent grey matter or in the dorsal column, which was undergoing Wallerian degeneration. However, some ATF3+ nuclei were found at the CNS/PNS interface.

Figure 5-4 Localisation of ATF3 in distal stumps and CNS.

Horizontal sections of the distal stump of sciatic nerves (Figs. 5.4a – c and f) and DREZ (Figs 5.4d and e), 30 days (Fig. 5.4a), 8 days (Figs. b and d- f) and 4 days (Fig. 5.4c) after resection, immunoreacted for ATF3 (green), S100 (red in Fig. a), p75 (red in Fig. 5.4b) and GFAP (red in Figs. 5.4d and e) or no primary antibody (Fig. 5.4f). ATF3+ nuclei are present in cells that express the Schwann cell markers S100 and p75. Fig. 5.4c is a double exposure showing a phase contrast image and ATF3 immunofluorescence. The AFT3+ nuclei are found between debris-laden macrophages (*) inside bands of Büngner (arrowheads). Figs. 5.4d and e show sciatic nerve dorsal rootlets; the DREZ and spinal cord (d) can be identified by the presence of GFAP+ astrocytes which extend processes into the peripheral part of the rootlets (*). ATF3 expression is largely confined to the peripheral rootlet where Schwann cells are found. Fig. 5.4f shows only very few auto fluorescent cells at the proximal end (left of image) of the distal stump of a (mouse) resected sciatic nerve, when the anti-ATF3 primary antibody was omitted. Scale bar in 5.4a = 25μm and also applies to 5.4b and c; bars in 5.4d and f = 100μm; bar in 5.4e = 50μm.

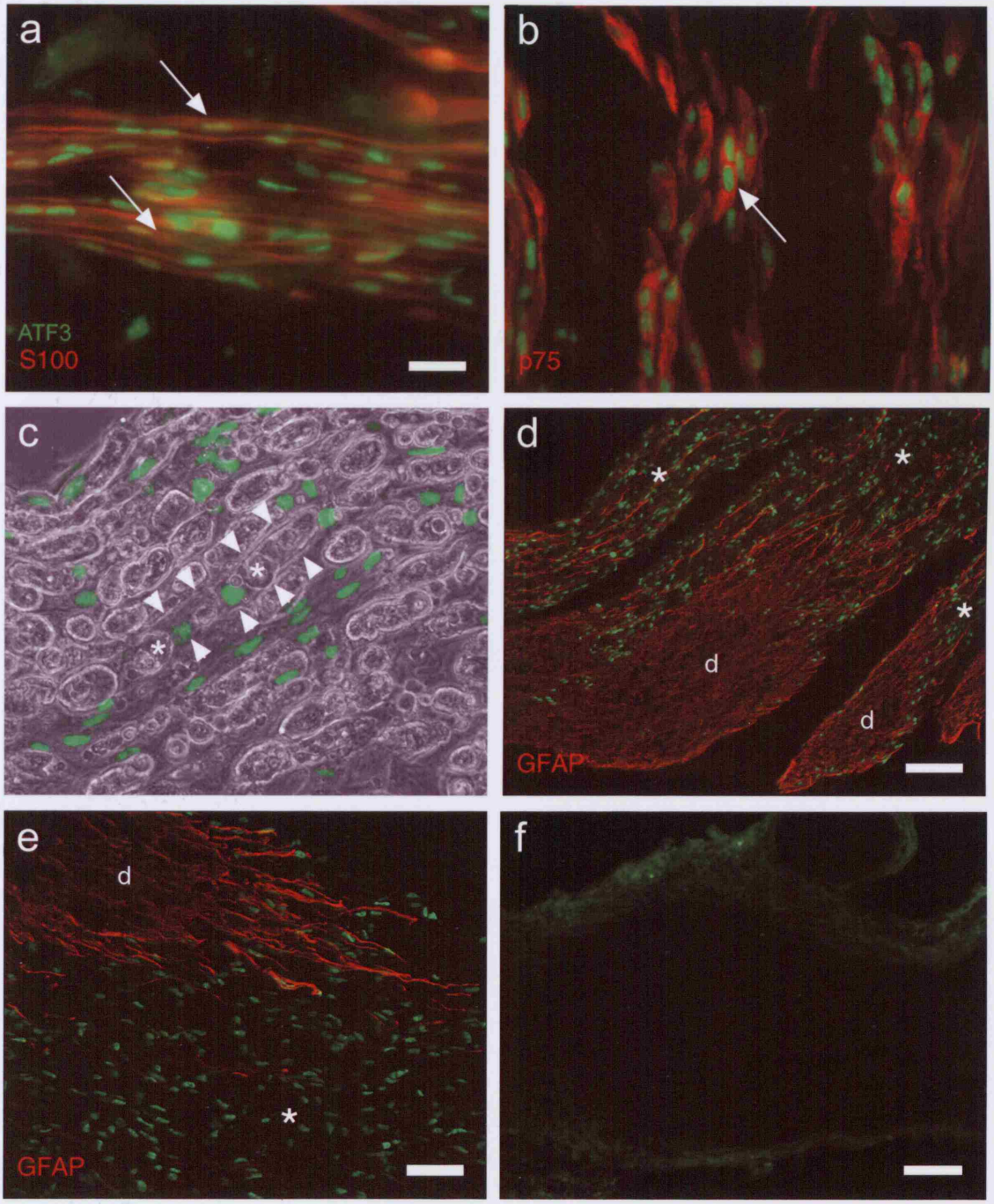
a
ATF3
S100
b
p75
c
d
GFAP
d
d
e
d
GFAP
f

Chapter 6 – Results

6 .1 Axonal regeneration in the NG2 deficient mouse

Background

The chondroitin sulphate proteoglycan NG2 blocks neurite outgrowth *in vitro* and has been proposed as a major inhibitor of axonal regeneration in the CNS. Although a substantial body of evidence underpins this hypothesis, it is challenged by recent findings including strong expression of NG2 in regenerating peripheral nerve. A study of axonal regeneration in the PNS and CNS of genetically engineered mice that do not express NG2 was performed, compared to sex and age matched wild-type controls.

Results

6.1.1 Analysis of phenotype

For all of the studies reported below, identification of knockout and wild-type mice was based on immunohistochemical phenotyping of tail snips with anti-NG2 antibody, which provided unequivocal evidence for the absence or presence of NG2 (see Fig. 6.1). No differences were apparent between knockout and wild-type mice with respect to appearance, behaviour, weight or gross features of brain and spinal cord.

6.1.2 NG2 in injured sciatic nerve

Analysis of sciatic nerve 7 days after excision of a 3mm segment confirmed previous findings from our laboratory of NG2 immunoreactivity in the perineurium and in cells with varying shapes, but not the elongated profile of Schwann cells (see Rezajooi et al., 2004). In wild-type mice, NG2 was strongly upregulated in the cells that capped the proximal stump. There was no co-localisation with neurofilament, which stained the many axons seen regenerating out of the proximal stump in close association with NG2+ cells (Fig. 6.1c). In the distal stump, NG2+ cells were noted to be less fluorescent than those in the proximal stump and appeared to be perineurial cells of various shapes. In knockout mice, no NG2 immunoreactivity was seen and there was no obvious difference in neurofilament immunohistochemistry, compared to wild-type mice.

6.1.3 NG2 in skin of plantar hindpaw

In wild-type uninjured mice, NG2 immunoreactivity was seen predominantly in the blood vessel walls, presumably in pericytes (Ozerdem et al., 2001; 2002) rather than endothelial cells, although this distinction was not easy to make. The basal lamina of the epidermis was also strongly positive for NG2, with no NG2+ cells superficial to this (Fig. 6.1d). This suggests that, if NG2 is inhibitory to regenerating axons in this area, then one may have expected to see aberrant sprouting of regenerating PGP+ axons in the experiments described below (see Results section 6.5.3). There was no NG2 immunoreactivity in NG2 knockout mice (not illustrated).

Figure 6-1 Phenotyping of tailsnips and NG2 expression in injured sciatic nerve and hindpaw

Longitudinal sections of tail snips from a wild-type mouse (a) and a knockout mouse (b), wild-type sciatic nerve one week after transection (c) and transverse section of glabrous hindpaw (d), immunoreacted with anti-NG2 antibody. In Fig. 6.1a, strong NG2 immunofluorescence is apparent in hair follicles (h), sebaceous glands (s) and bone marrow (bm) and other structures, but no NG2 fluorescence is detectable in Fig. 6.1b. Arrowheads delineate the edges of the tail snip sections. Fig. 6.1c shows that NG2+ cells are present in the proximal stump of sciatic nerve from which 3mm was sectioned, in cells of varying shapes, including Schwann cells, although staining is brightest in the perineurium. NG2 appears upregulated at the site of cellular outgrowth from the proximal stump, through which neurofilament+ axons (red) are regenerating. Fig. 6.1d (cut perpendicular to the surface of the skin) shows that NG2 is present in the basal layer of the epidermis (b) and blood vessel wall (v) of the glabrous skin of hindpaw. Bar = 100μm. Scale bar in Fig. 6.1a = 200μm and also applies to b; bar in Fig. 6.1c = 25μm; bar in Fig. 6.1d = 100μm.

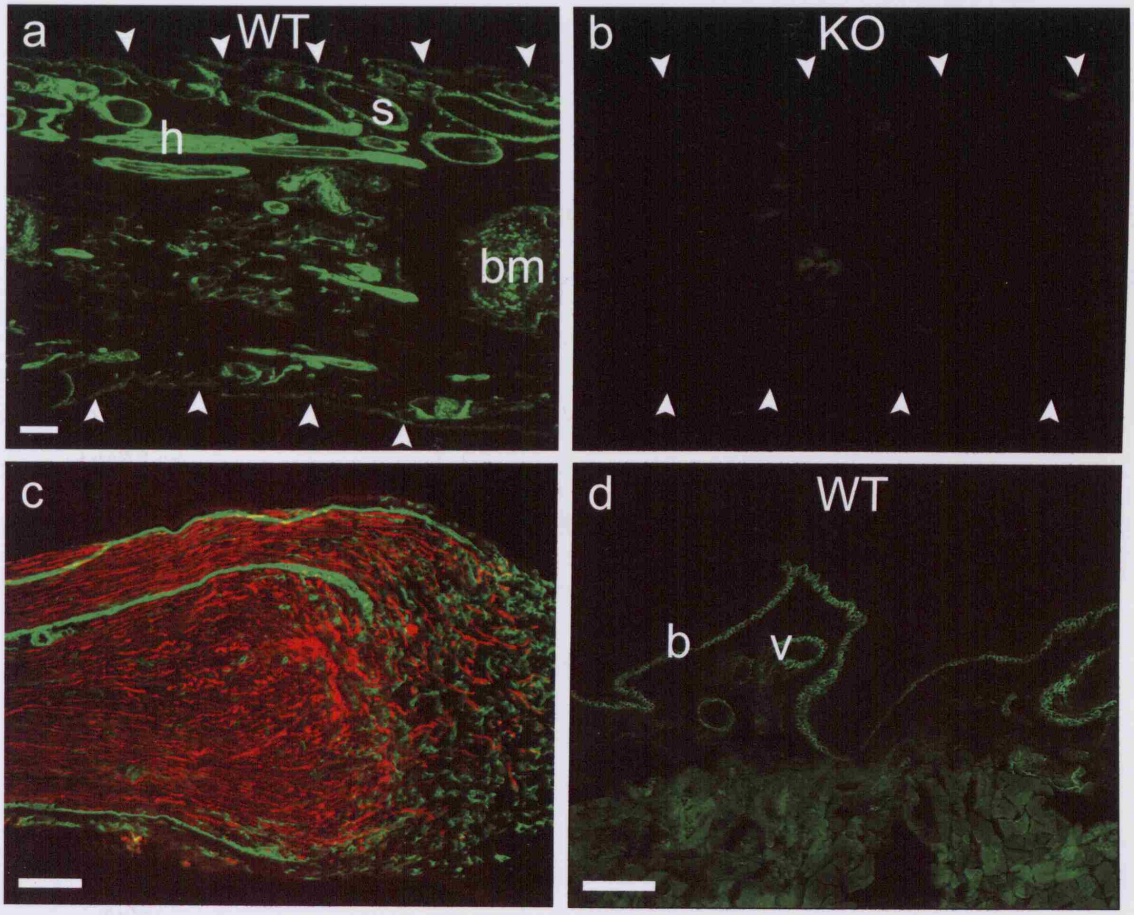
a
WT
h
s
bm
b
KO
c
d
WT
b
v

6.2 CNS injury models

6.2.1 Dorsal column injury

Following dorsal column lesions (and all other types of experimental injury) no differences were apparent at autopsy or in overall histological appearance of the lesion site or other areas of CNS tissue, between knockout and wild-type mice. In all cases the dorsal column above and below the lesion site was separated by a zone of collagenous connective tissue (scar tissue) which was adherent to the overlying meningeal tissue and was often lost during tissue processing, leaving a cyst-like cavity.

In both knockout and wild-type mice surviving 28 days after transection of the dorsal column at T8 (and sciatic conditioning lesion), axons labelled transganglionically with CT-HRP were present in the dorsal column below the level of the lesion (Figs. 6.2a, b), but with the exception of a small number of axons which appeared to penetrate into the most caudal region of the lesion (Figs. 6.2c, d), labelled axons were not detected at more rostral levels (Figs. 6.2e, f). Furthermore, most of the labelled axons at the caudal margin of the lesion displayed enlarged end-bulbs suggesting arrested regeneration at this level. Systematic examination of serial sections showed no labelled axons growing around the lesion or bypassing it ventrally.

Figure 6-2 Transganglionic labelling with CT-HRP of dorsal column axons after spinal cord injury.

Horizontal sections through the dorsal columns of the spinal cord of wild-type (Figs. 6.2a, c and e) and knockout (Figs. 6.2b, d and f) mice 28 days after unilateral transection of the dorsal column and ipsilateral sciatic nerve crush, and 3 days after injection of CT-HRP proximal to the sciatic nerve crush site. All sections were reacted for HRP. In Figs. 6.2a and b at the lesion site (lesion marked with an asterisk and adjacent area enlarged in Figs. 6.2c and d), there is no indication of more extensive labelling or increased sprouting into or around the lesion site in the knockout relative to the wild-type control, and in both many axons displayed enlarged end bulbs (e.g. at arrows). Figs. 6.2e and f are taken approximately 2mm rostral to the lesion site. There are no regenerating or spared axons in the injured dorsal column in either. The dotted lines mark the midline; the injured dorsal column is below (to the left of) the midline in both figures. The orientation markers in Figs. 6.2a and b show medial (m) and caudal (c) for the left (injured) dorsal column. Scale bars = 100μm; the bar in Fig. 6.2a also applies to 6.2b; the bar in Fig. 6.2c also applies to 6.2d – f.

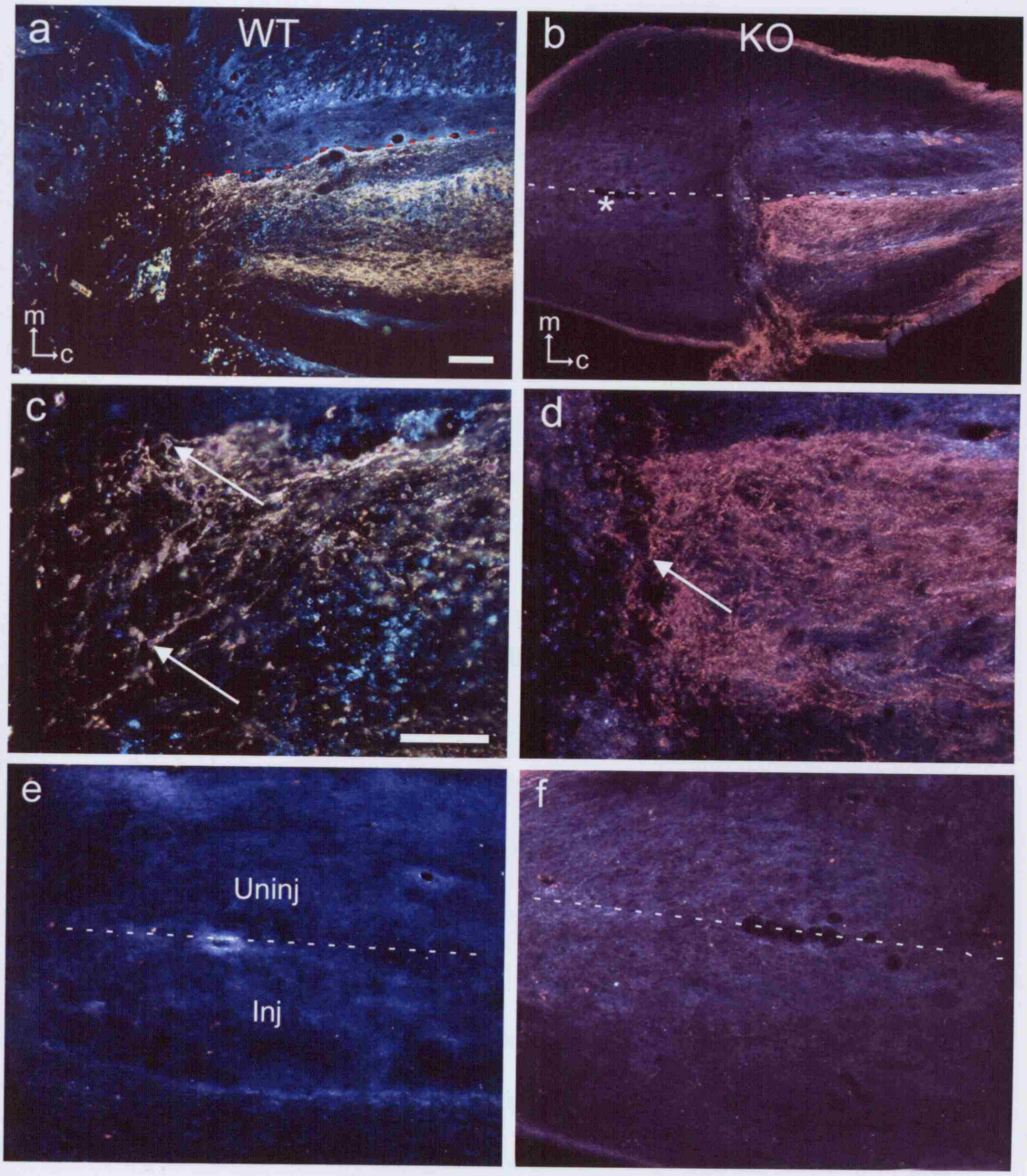
a
WT
m
c
b
KO
*
m
c
c
d
e
Uninj
Inj
f

6.2.2 Dorsal root injury

In both knockout and wild-type mice 28 days after L5 dorsal root transection (and sciatic nerve conditioning lesion) labelled axons (transganglionic CT-HRP) were present in the dorsal root central to the injury site. However, the great majority appeared to be arrested at the DREZ where some formed end-bulbs (Figs. 6.3a, b) and some appeared to turn back into the root (Fig. 6.3a). No labelled axons were detected in the dorsal column or dorsal column nuclei (Fig. 6.3c) in either knockout or wild-type animals.

6.2.3 Corticospinal tract injury

Twenty-one days after transection of the dorsal column (incorporating the corticospinal tract, CST) at C6 and anterograde labelling of CST axons with BDA injected into the contralateral sensorimotor cortex, labelled axons were abundant in the CST rostral to the injury site but appeared to be arrested at the rostral border of the latter in both wild-type (Figs. 6.4a and b) and knockout mice (Figs. 6.4c and d). Many of the labelled axons displayed terminal end-bulbs in this area. No labelled axons penetrated the lesion site, none was observed bypassing the lesion site laterally or ventrally, none was found in the dorsal part of CST caudal to the lesion site, and there was no evidence to suggest that axons in the injured CST had grown or sent branches into the intact contralateral CST in either group. Fine lateral branches were observed to emerge from labelled CST axons rostral to the lesion site (not illustrated) but these were as likely to have been

normal collateral branches as regenerative sprouts and no difference in the distribution or frequency of such side branches was detected between knockout and wild-type mice.

Figure 6-3 Transganglionic labelling with CT-HRP of dorsal roots after transection and conditioning lesion.

The dorsal root entry zone (DREZ) of a wild-type (Fig. 6.3a) and knockout mouse (Fig. 3b) in horizontal sections and the dorsal column nucleus (DCN) in transverse section 28 days after transection and reapposition of the cut ends of the L5 dorsal root and crush of the ipsilateral sciatic nerve and 3 days after injection of CT-HRP into the sciatic nerve proximal to the crush site. All sections were reacted for HRP. In both the wild-type and knockout almost all labelled axons (e.g. at arrows) stopped at the DREZ or turned back towards the dorsal root. The dorsal columns (DC) are devoid of labelled axons in both. The area indicated by the large arrowhead in Fig. 6.3a is enlarged in the inset, and illustrates a regenerating axon (indicated by small arrowheads) that turns back at the DREZ and displays a large terminal end bulb. Fig. 6.3c shows absence of labelled (spared) axons at the level of the DCN in a wild-type mouse. Scale bar = 100μm and applies also to 6.3b and c; inset scale bar = 50μm.

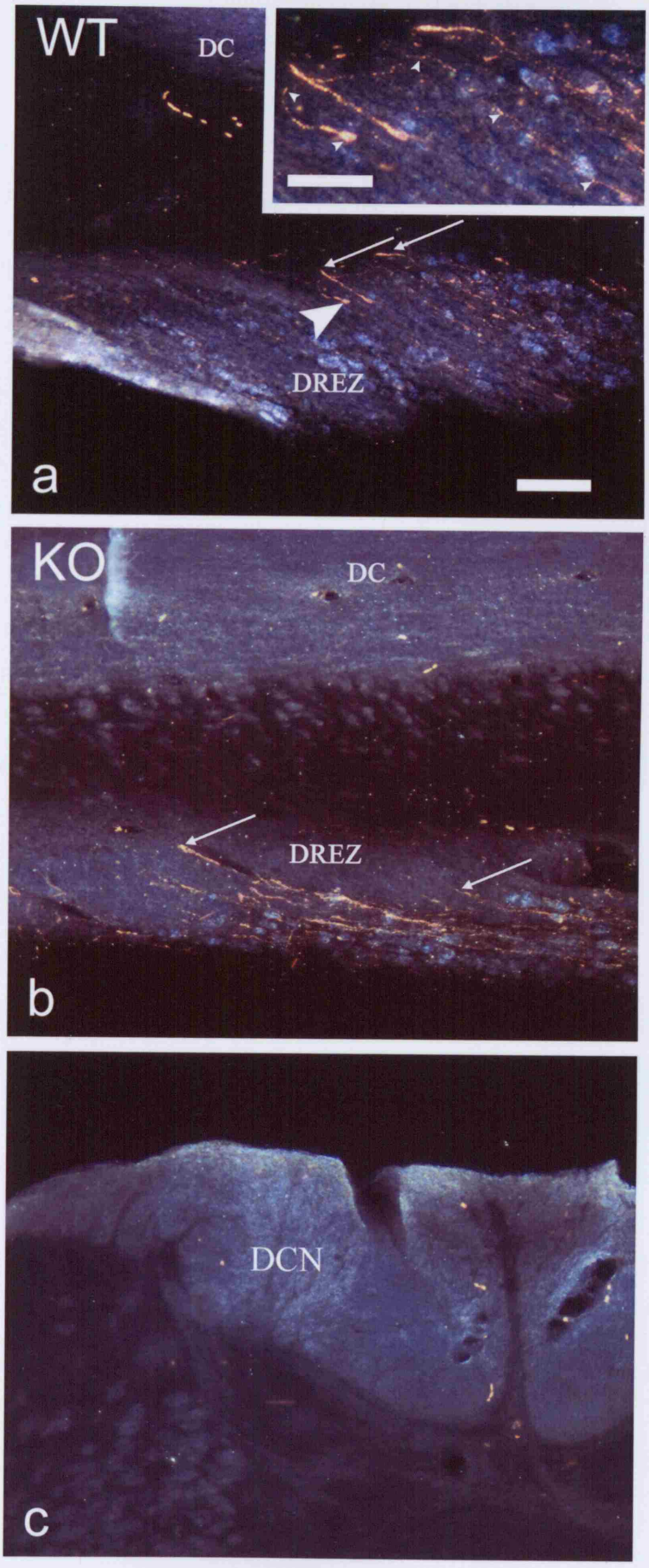
WT
DC
DREZ
a
KO
DC
DREZ
b
DCN
c

Figure 6-4 Anterograde labelling with BDA of the CST after spinal cord injury.

Horizontal sections of the deep dorsal columns of low cervical spinal cord at and immediately rostral to the site of a unilateral transection of the dorsal column (including the CST) 21 days after the lesion and simultaneous anterograde labelling of the CST by application of BDA to the contralateral sensory-motor cortex, in a wild-type mouse (Fig. 6.4a, enlarged in Fig. 6.4b) and a knockout mouse (Fig. 6.4c, enlarged in Fig. 6.4d). There is no apparent enhancement of labelling in the knockout mouse relative to the wild-type, and in both examples CST axons terminate just rostral to the lesion cavity (asterisk in Figs. 6.4a and b), some with large end bulbs (e.g. arrows in Figs. 6.4b and d). The apparent labelling medial to the injury site in Fig. 4c is actually non-specific autofluorescence. The orientation markers on Figs. 6.4b and d show medial (m) and caudal (c). Scale bars in Figs. 6.4a and b = 100μm and also apply to 6.4c and d.

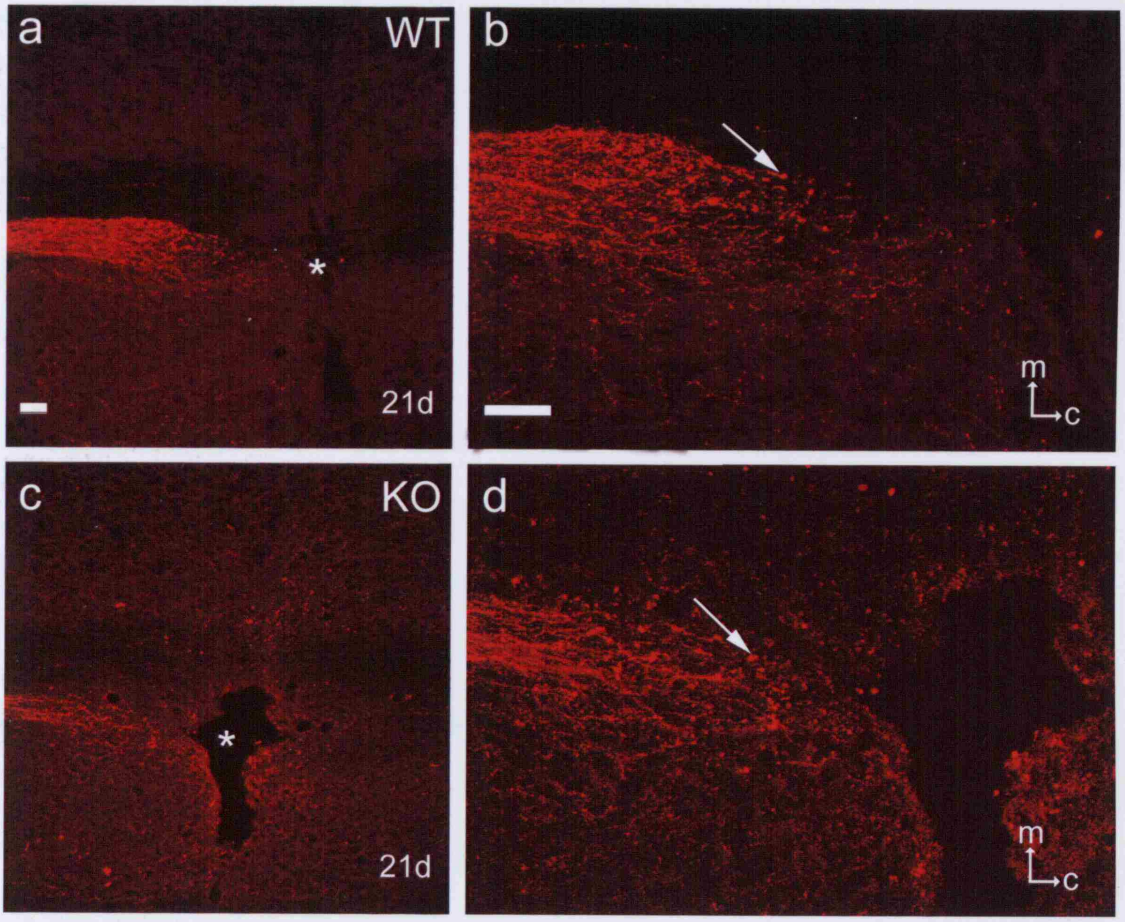
a
WT
*
21d
b
m
c
c
KO
*
21d
d
m
c

6.3 *Functional recovery after peripheral nerve injury*

6.3.1 Sciatic nerve crush and transection

Recovery of sensory function, as a measure of the rate and extent of regeneration of sensory axons in the injured sciatic nerve, was assessed by twice-daily monitoring of the withdrawal reflex in response to stimulation of the lateral hindpaw with Von Frey hairs from 1 day following nerve injury to 2 days after full recovery was first observed. The threshold stimulus for eliciting withdrawal was identical for both hindpaws preoperatively and for the control hindpaw postoperatively in both wild-type and knockout mice. After sciatic nerve crush, wild-type mice recovered the preoperative withdrawal reflex threshold after a mean of 10.2 days and knockout mice after a mean of 9.8 days ($p = 0.63$ n.s.; Fig. 6.5a). After simultaneous excision of 3 mm of the saphenous nerve, recovery times were not significantly different: the withdrawal reflex was restored by 10.3 days in wild-type mice and by 11.0 days in knockout mice ($p=1.0$, n.s. (calculated using a two tailed Fisher exact test because all 6 NG2 knockout mice recovered on the same day); Fig. 6.5b). These results confirm that recovery times after sciatic nerve injury alone could not be due to reinnervation as a result of sprouting from branches of the saphenous nerve, which, if it occurred, might give rise to false positive results. After sciatic nerve section and reanastamosis, which presents a greater barrier to regeneration than crush injury, recovery times were 16.7 days on average for wild-type and 15.3 days for knockout mice ($p = 0.18$ n.s.; Fig. 6.5c).

Recovery of motor function, as a measure of the rate and extent of regeneration of motor axons in the injured sciatic nerve, was assessed at the same time that sensory function was tested, by recording the toe spreading reflex when the hindpaw is raised above the supporting surface (this test is dependent on motor innervation of hindpaw muscles and is lost after sciatic nerve injury). The mean time for the toe-spreading reflex to be restored was 8.5 days in wild-type and 9.2 days in knockout mice after sciatic nerve crush ($p = 0.36$ n.s.; Fig. 6.5a). The mean time to recovery increased to 10.7 days versus 10.3 days after simultaneous sciatic nerve crush and saphenous nerve resection ($p = 0.50$ n.s.; Fig. 5b). After sciatic nerve transection and reanastamosis, the toe-spreading reflex recovered after a mean of 17.4 days in the wild-type versus 20.8 days in the knockout mice, but this apparent 3-day lag in recovery of knockout mice was not statistically significant ($p = 0.06$; Fig. 6.5c).

6.3.2 Facial nerve crush

Recovery of motor function after facial nerve crush was assessed twice daily, from 1 to 14 days postoperatively, by monitoring spontaneous whisker twitching and the corneal blink reflex. Whisker twitch took, on average, 9.3 days to recover in the 4 wild-type animals and 9.7 days in the 4 knockout animals ($p = 0.65$, n.s.; Mann-Whitney), with the corneal reflex recovering in 9.3 days versus 9.7 days ($p = 0.65$, n.s.; Mann-Whitney). Thus there was no significant difference between wild-type and knockout mice with respect to regeneration of facial nerve axons (Fig. 6.6d).

Figure 6-5 Functional recovery after sciatic nerve injury.

Histograms illustrating the time taken for the recovery of motor function (assayed by toe spreading reflex) and sensory function (assayed by sensitivity to Von Frey hairs) after peripheral nerve injury in wild-type (black columns) versus knockout mice (grey columns). Group size was N = 6 wild-type and N = 6 knockout for Fig. 6.5a and b and N = 9 wild-type and N = 9 knockout for Fig. 6.5c. Standard error of the mean is indicated for each column. The differences between wild-type and knockout mice in time taken to recover sensory and motor function were not significant for any of the lesion groups (sciatic nerve crush, Fig. 6.5a; sciatic nerve crush and saphenous nerve excision, Fig. 6.5b; sciatic nerve transection and reanastamosis, Fig. 6.5c).

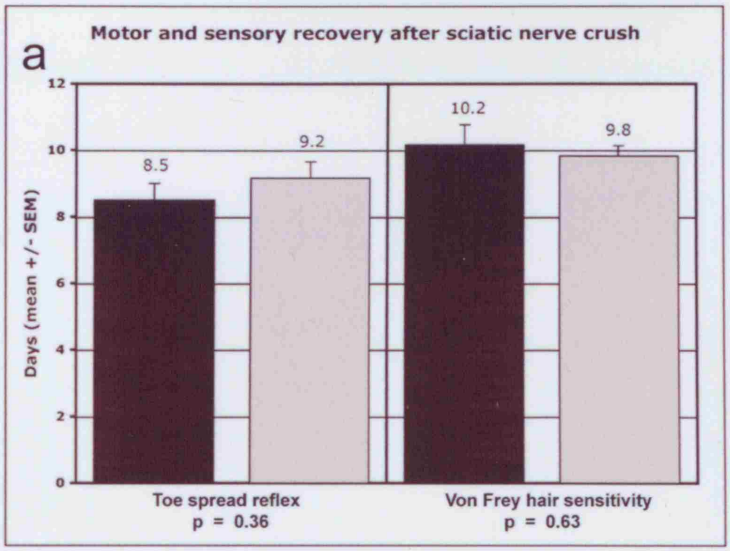
a
Motor and sensory recovery after sciatic nerve crush
Days (mean +/- SEM)
12
10
8
6
4
2
0
8.5
9.2
10.2
9.8
Toe spread reflex
p = 0.36
Von Frey hair sensitivity
p = 0.63

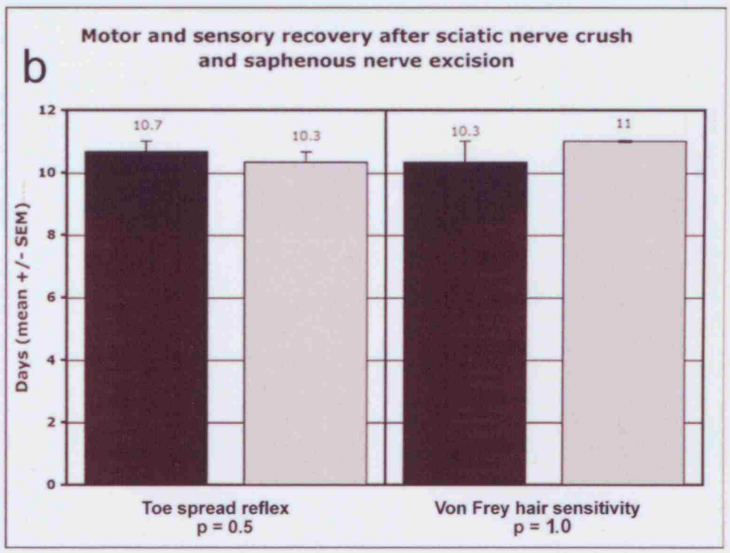
b
Motor and sensory recovery after sciatic nerve crush
and saphenous nerve excision
Days (mean +/- SEM)
12
10
8
6
4
2
0
10.7
10.3
10.3
11
Toe spread reflex
p = 0.5
Von Frey hair sensitivity
p = 1.0

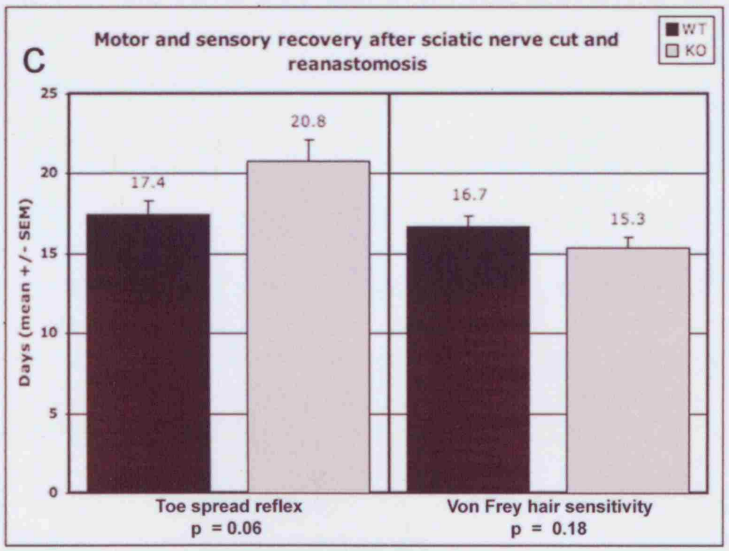
c
Motor and sensory recovery after sciatic nerve cut and
reanastomosis
WT
KO
Days (mean +/- SEM)
25
20
15
10
5
0
17.4
20.8
16.7
15.3
Toe spread reflex
p = 0.06
Von Frey hair sensitivity
p = 0.18

Figure 6-6 Anatomical and functional correlates of regeneration after facial nerve injury

Analyses of facial nerve regeneration in wild-type versus knockout mice after crush or transection of the facial nerve. Fig. 6.6a illustrates DiAsp-labelled neurons in the ipsilateral facial nucleus of a knockout mouse 14 days after facial nerve crush; scale bar = 100μm. Fig. 6.6b shows Fluorogold (FG)-labelled neurons in the facial nucleus of a wild-type mouse in a coronal section of the ipsilateral pons 28 days after facial nerve transection; scale bar = 100μm and applies to Fig. 6.6c also. Fig. 6.6c shows FG-labelled neurons in the contralateral (uninjured) facial nucleus of the same mouse as Fig. 6b. Note that some injured neurons are larger and that they are distributed throughout the facial nucleus rather than being clustered at its lateral edge, as in the uninjured facial nucleus. Fig. 6.6d shows histograms of the time taken for the blink reflex and spontaneous whisker twitching to reappear after facial nerve crush in 4 wild-type (black columns) versus 4 knockout (grey columns) mice. The means and standard errors of the means are shown at the top of each column. No differences were apparent between the wild-type and knockout groups for either test ($p = 0.65$; Mann-Whitney). Retrogradely labelled neurons were counted in the facial nucleus of 3 wild-type versus 2 knockout mice 14 days after facial nerve crush (DiAsp labelling; Fig. 6.6e), in 8 wild-type versus 8 knockout mice 30 days after facial nerve transection (FG labelling; Fig. 6.6f) and in 4 wild-type versus 4 knockout mice 40days after facial nerve transection (DiAsp labelling; Fig. 6.6g). Differences between wild-type and knockout mice do not reach significance, at 28 days or 40 days survival and with either retrograde label (numbers not sufficient at 14 days for statistical analysis).

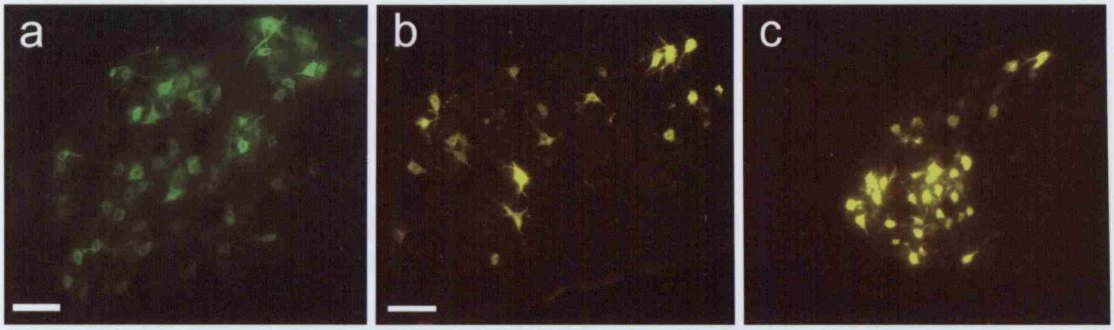
a
b
c

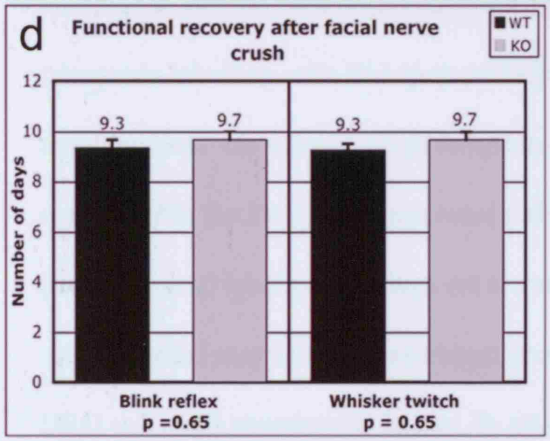
d
Functional recovery after facial nerve crush
WT
KO
Number of days
12
10
8
6
4
2
0
9.3
9.7
9.3
9.7
Blink reflex
p =0.65
Whisker twitch
p = 0.65

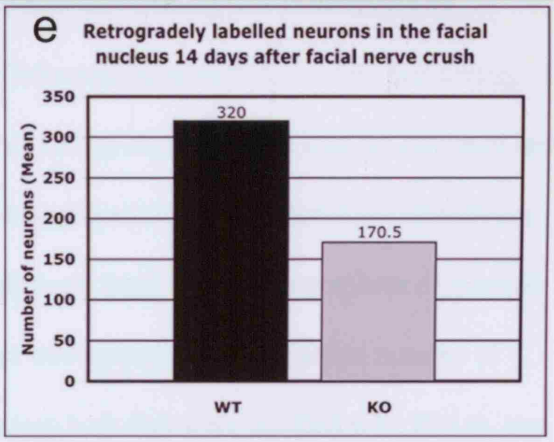
e
Retrogradely labelled neurons in the facial nucleus 14 days after facial nerve crush
Number of neurons (Mean)
350
300
250
200
150
100
50
0
320
170.5
WT
KO

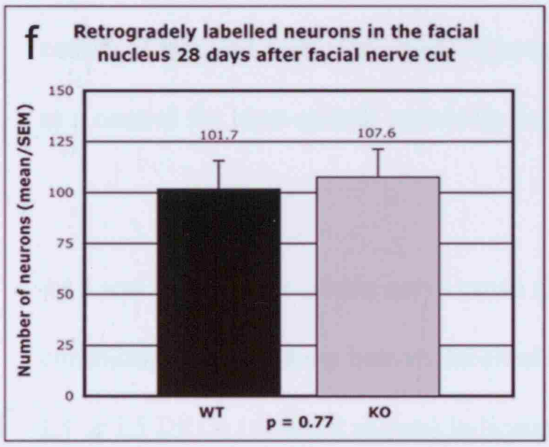
f
Retrogradely labelled neurons in the facial nucleus 28 days after facial nerve cut
Number of neurons (mean/SEM)
150
125
100
75
50
25
0
101.7
107.6
WT
p = 0.77
KO

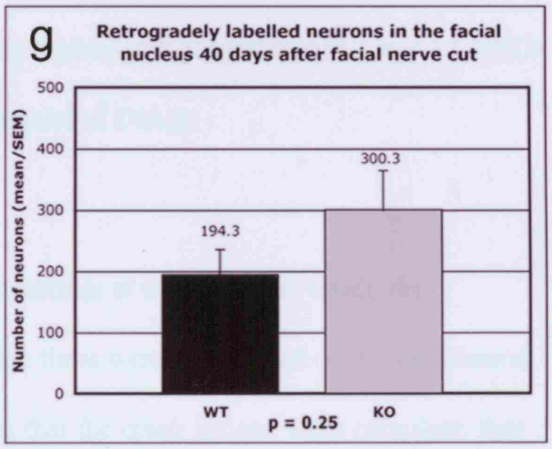
g
Retrogradely labelled neurons in the facial nucleus 40 days after facial nerve cut
Number of neurons (mean/SEM)
500
400
300
200
100
0
194.3
300.3
WT
p = 0.25
KO

6.4 Anatomical studies after peripheral nerve injury

6.4.1 Retrograde labelling of DRG cells

The number of DRG cells with axons that had regenerated into the glabrous skin of the hindpaw at various time points following sciatic nerve crush was determined by retrograde labelling with DiAsp to provide information on both the extent and timing of reinnervation. Because of variable uptake of DiAsp after injection into the hindpaw and variability in the intensity of neuronal cell body labelling, the threshold for identifying (and counting) labelled cells was set at a relatively high level. The numbers of labelled cells recorded may therefore represent gross underestimates of the actual number of DRG cells with regenerated axons. In all cases both feet were injected with DiAsp, and counts of labelled cells were made in both ipsilateral and contralateral L4 and L5 DRGs as a control for inter-animal variability in uptake of DiAsp.

At 5 and 9 days after sciatic nerve crush (2 animals at each survival time), the contralateral DRGs were heavily labelled but there were no labelled cells in ipsilateral L4 or L5 DRGs (data not shown) indicating that the crush lesions were complete, that L4 and L5 DRG are not labelled via routes other than injured sciatic nerve, and that regenerating sensory axons had not reached the hindpaw at these survival times. Very few labelled neurons were present in the ipsilateral DRG 13 days after sciatic nerve crush (i.e. 11 days after DiAsp injection into hindpaw) in either wild-type or knockout mice, with a mean of 28 labelled neurons per DRG in wild-type mice compared to 14 in

knockout mice ($p = 0.18$ n.s.; Figs. 6.7a, b and f). The appearance of retrograde label in injured DRG neurons 13 days after sciatic nerve crush, but not before, correlates with the onset of functional recovery being 9-10 days after sciatic nerve crush in our other experiments (see Figure 6.5a and b).

Much larger numbers of labelled DRG cells were present 90 days after injury, averaging 424 per DRG in the wild-type mice and 677 in the knockout mice ($p = 0.27$ n.s.; Figs. 6.7d, e and g). Thus, differences between wild-type and knockout mice groups were not significant at either 13 or 90 days after injury. There were also no significant differences in the numbers of retrogradely labelled DRG cells in the L4/5 DRGs on the control side between wild-type and knockout mice at either 13 days (see Fig. 6.7c for example); on average 138 labelled neurons in the wild-type and 135 in the knockout; $p = 0.96$) or at 90 days (on average 489 labelled cells in the wild-type and 627 in the knockout mice; $p = 0.21$). The marked phenotype-independent difference in the number of labelled neurons in the contralateral (control) L4 and L5 DRGs at 13 days versus 90 days was, however, a consistent and unexpected finding. A possible explanation for this may be that DiAsp is a more effective retrograde label for DRG cells in mature animals than in young ones.

Figure 6-7 Retrograde labelling of DRGs after sciatic nerve injury

Anatomical analyses of regeneration of sensory axons after sciatic nerve injuries in wild-type versus knockout mice. Figs. 6.7a-c show composite images made up by merging the entire z-series of optical sections through L5 DRG in wild-type (Fig. 6.7a) and knockout mice (Fig. 6.7b) 13 days after sciatic nerve crush and 2 days after injection of DiAsp into the skin of the hindpaw. Fig. 6.7c shows the control DRG (no sciatic nerve injury) from the same animal as Fig. 6.7b. Figs. 6.7d and e show a similar comparison of labelling in wild-type and knockout mice 90 days after sciatic nerve crush. Scale bar = 200μm and applies to Figs. 6.7a-e. Figs. 6.7f and g compare the numbers of labelled cells in L5 DRG 13 days (Fig. 6.7f) and 90 days (Fig. 6.7g) after sciatic nerve crush in wild-type (N = 8 + 8; black columns) versus knockout mice (N = 8 + 8; grey columns). The quantitative analyses show that there are no statistically significant differences in the numbers of retrogradely labelled DRG cells (and thus in the extent of sensory axon regeneration) between wild-type and knockout mice at either short or long postoperative survival times.

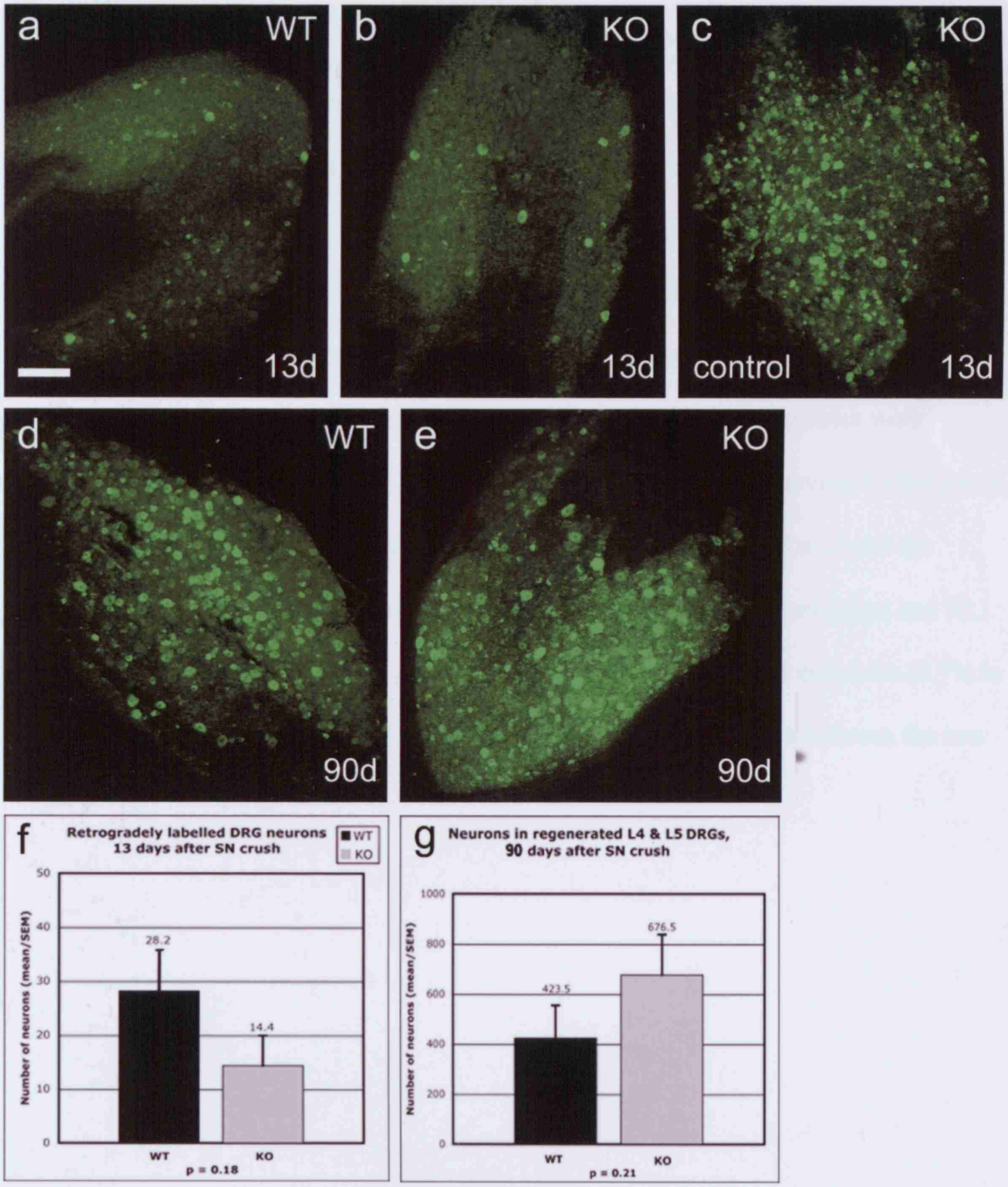
a
WT
13d
b
KO
13d
c
KO
control
13d
d
WT
90d
e
KO
90d
f
Retrogradely labelled DRG neurons
13 days after SN crush
WT
KO
Number of neurons (mean/SEM)
50
40
30
20
10
0
28.2
14.4
WT
KO
p = 0.18
g
Neurons in regenerated L4 & L5 DRGs,
90 days after SN crush
Number of neurons (mean/SEM)
1000
800
600
400
200
0
423.5
676.5
WT
KO
p = 0.21

6.4.2 Reinnervation of denervated endplates in the soleus muscle

The progress and extent of muscle reinnervation 7 and 10 days after sciatic nerve crush was examined by light microscopy, using silver-cholinesterase histochemistry. Endplates in control soleus muscle from both wild-type and knockout mice were almost all innervated by a single axon (data not shown). At 7 days after injury no endplates had been reinnervated in either group (Fig. 6.8a). At 10 days, however, there was extensive reinnervation of endplates in both wild-type (Fig. 6.8c) and knockout mice (Fig. 6.8b) and no consistent differences in the appearance of the endplates were observed between the two groups. The mean percentage of non-innervated endplates at 10 days was 2.1% in wild-type and 3.1% in knockout mice ($p = 0.18$ n.s.) and the proportion of endplates reinnervated by a single axon was 91.3% in wild-type and 92.1 % in knockout mice ($p = 0.57$ n.s.), the proportion of polyinnervated endplates (2.7% in wild-type and 2.2% in knockout mice) was not significantly different between the two groups ($p = 0.51$; Fig. 6.8d).

Figure 6-8 Silver-cholinesterase stained motor end plates after sciatic nerve injury.

Longitudinal sections of soleus muscle 7 days (Fig. 6.8a) and 10 days (Figs. 6.8b and c) after sciatic nerve crush showing that regenerating axons have not reached/reinnervated end-plates at 7 days but extensive reinnervation has occurred by 10 days in both wild-type (Fig. 6.8c) and knockout (Fig. 6.8b) mice. Some endplates were apparently not reinnervated at 10 days (e.g. at arrowhead in Fig. 6.8c) and a few appeared to be innervated by more than one axon (e.g. at arrow in Fig. 6.8c). Bar = 100μm in 6.8a and applies to c; bar = 50μm in 6.8b. Fig. 6.8d shows quantitative data on the extent of reinnervation of end-plates 10 days after sciatic nerve crush, expressed as the percentages of end-plates without axons, with a single reinnervating axon and with more than one reinnervating axon for wild-type (N = 6; black columns) and knockout mice (N = 6; grey columns). No significant differences in the timing, extent or type of reinnervation were detected.

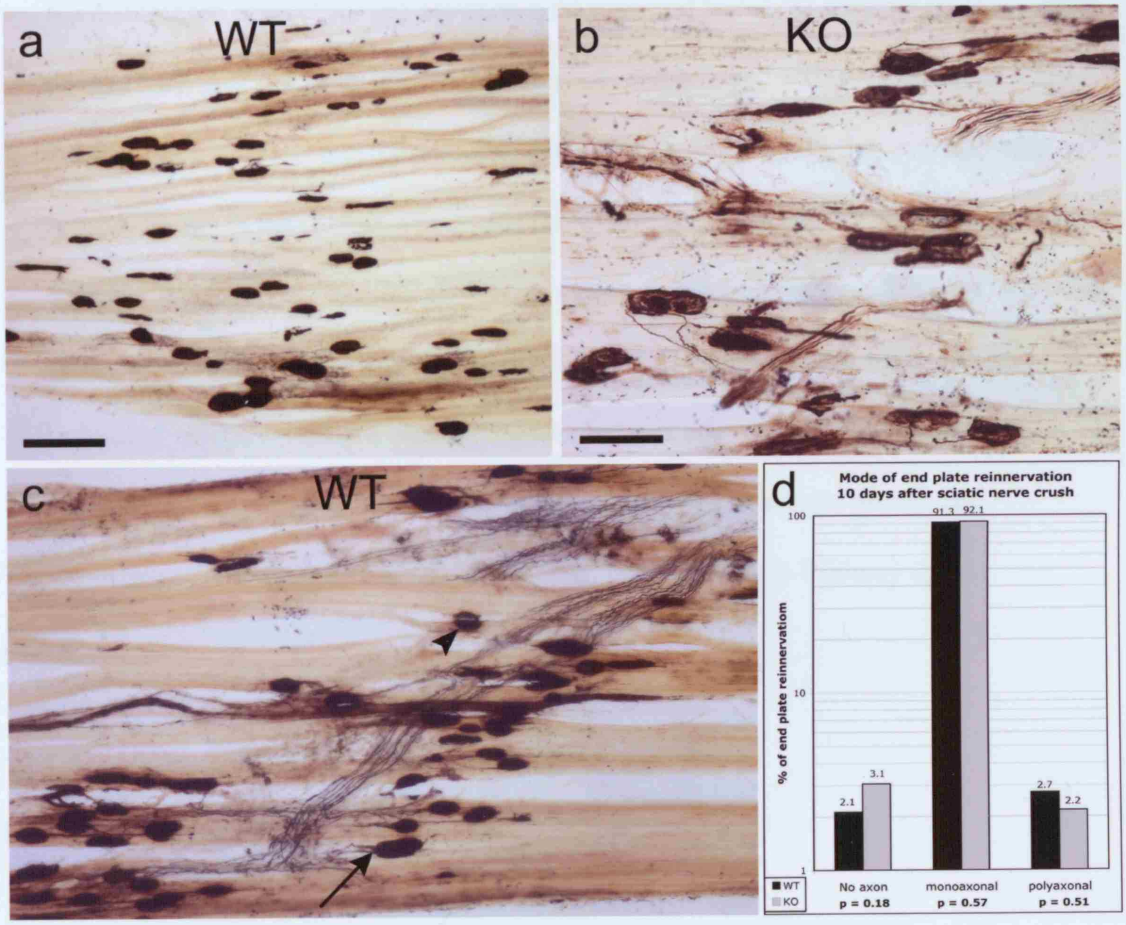
a
WT
b
KO
c
WT
d
Mode of end plate reinnervation
10 days after sciatic nerve crush
% of end plate reinnervation
100
10
1
91.3
92.1
2.1
3.1
2.7
2.2
WT
KO
No axon
p = 0.18
monoaxonal
p = 0.57
polyaxonal
p = 0.51

6.4.3 Sensory reinnervation of hindpaw glabrous skin

The extent of sensory reinnervation of the glabrous skin of the hindpaw was assessed at 17 days after sciatic nerve crush by light microscopy after immunostaining for PGP 9.5. No differences were observed between wild-type and knockout animals on the control or injured side (Figs. 6.9a - f). In the sampled microscope fields (see Methods section 2.8.5.3, page 157) the mean number of immunostained (presumptive regenerated) sensory axons in the dermis was 33 for the wild-type group and 35 for the knockout animals ($p = 0.78$ n.s.; Fig. 6.9g). There was an apparent difference between the wild-type and knockout animals with respect to PGP 9.5-positive nerve fibres in the uninjured hindpaw where a mean of 120 axons was counted in the wild-type versus 72 in the knockout, but this finding was based on only 3 animals per group, and significance could not be reliably established ($p = 0.1$, Mann-Whitney test).

Figure 6-9 PGP 9.5 immunohistochemistry for axons in plantar hindpaw skin after sciatic nerve injury.

Sections of glabrous hindpaw skin in wild-type (Figs. 6.9a, c and e) and knockout mice (Figs. 6.9 b and d) illustrating the extent of sensory reinnervation (PGP 9.5 immunopositive axons) after sciatic nerve crush. Figs. 6.9a and b show sections from normal (uninjured) wild-type and knockout mice, and Figs. 6.9c and d show similar areas of wild-type and knockout mouse skin 17 days after sciatic nerve crush. In the control material the sensory axons are concentrated in the superficial dermis (D) but are not present in the epidermis (E) or in subdermal musculature (M) and their distribution and extent is comparable in both wild-type and knockout mice. Seventeen days after nerve crush a few sensory axons have regenerated into the dermis to about the same extent in both wild-type and knockout animals. Figs. 6.9e and f are enlargements of the boxed areas in Figs. 6.9b and 9d, and illustrate the relative poverty of regenerating PGP 9.5-positive axons in the dermis 17 days after sciatic nerve section (e.g. at arrow in Fig. 6.9f) compared with the dense innervation in control skin (e.g. at arrowheads in Fig. 6.9e). Fig. 6.9g compares counts of PGP 9.5-positive axons in glabrous hindpaw skin 17 days after sciatic nerve crush, in wild-type (N = 6) versus knockout mice (N = 6). There is no significant difference. Bar in Fig. 9a = 100μm and also applies to b – d; bar in Fig. 9e = 20μm and applies to f also.

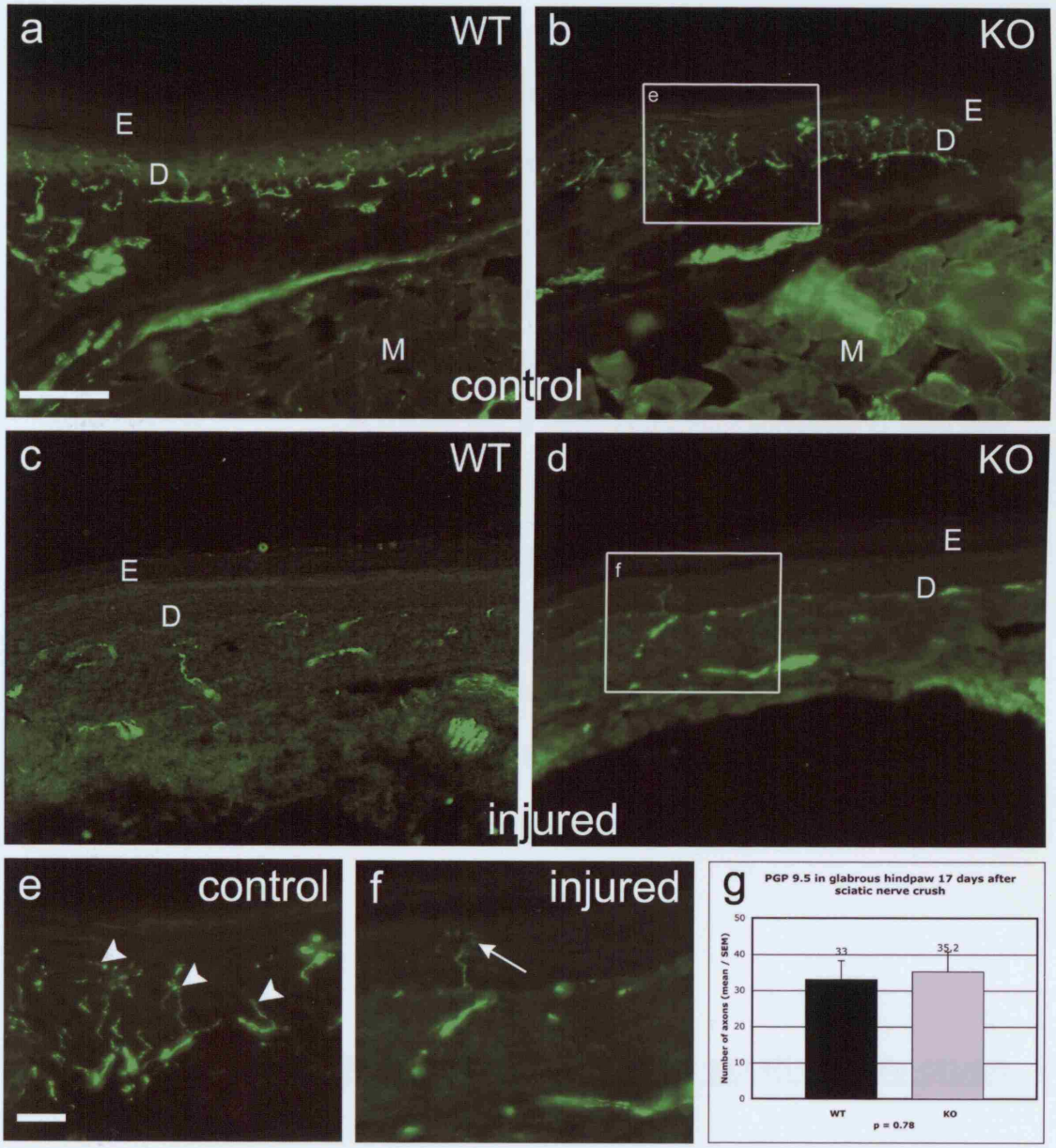
a
WT
E
D
M
control
b
KO
e
E
D
M
c
WT
E
D
injured
d
KO
f
E
D
e
control
f
injured
g
PGP 9.5 in glabrous hindpaw 17 days after sciatic nerve crush
Number of axons (mean / SEM)
50
40
30
20
10
0
33
35.2
WT
KO
p = 0.78

6.4.4 Axon counts in digital nerves after sciatic nerve crush

Ultrathin sections of the digital nerves in the fourth toe distal to a sciatic nerve crush were analysed by electron microscopy 17 and 21 days after a sciatic nerve crush to compare numbers of regenerating unmyelinated and myelinated axons (e.g. Fig. 6.10a). There were no gross morphological differences in the ultrastructure of the digital nerves of wild-type and knockout mice 17 days after a sciatic nerve crush. All axons were unmyelinated and the mean number counted in the dorsal digital nerves of wild-type mice was 78.3 (median 75.5; SD 38) compared to a mean of 90.3 axons in the knockout mice (median 93; SD 45) ($p = 0.63$; Fig. 6.10e). In the mice surviving 21 days after sciatic nerve crush, premyelinating axons (Fig. 6.10b) and remyelinating axons (Fig. 6.10c) were counted in all digital nerves (Fig. 6.10a) of the ipsilateral fourth toe. Wild-type mice had a mean of 12.3 (partially) myelinated axons in the 4^{th} toe digital nerve (median 11.5; SD 7.71) compared to a mean of 12.8 axons (median 12.5; SD 6.37) in the knockout mice ($p = 0.91$; Fig. 6.10f). In summary, the regenerative growth of sensory axons into digital nerves after sciatic nerve crush appears to be unaffected by the NG2 null mutation.

6.4.5 Axon counts in the tibial nerve after sciatic nerve crush

Transverse sections of the tibial nerve 5mm distal to a sciatic nerve crush injury site were analysed 15 days after injury. The mean number of myelinated axons in wild-type mice was 2375, compared to 3087 in knockout mice. Estimates of the surface area of the wild-type and knockout tibial nerve cross sections were sufficiently similar to

suggest that overall size differences in the nerve cross sections were unlikely to be a confounding factor in the numerical estimates. The difference in the number of regenerating myelinated axons between wild-type and knockout animals was not statistically significant ($p = 0.164$; Fig. 6.10g).

Figure 6-10 Electron microscopy of regenerating axons in the digital and tibial nerves.

Figs. 6.10a – d show transverse sections of digital nerves of the fourth toe 21 days after sciatic nerve crush. In Fig. 6.10a an entire nerve is shown at low magnification (bar = 10μm). Fig. 6.10b shows a regenerating axon (AX) with 2-3 wrappings of Schwann cell processes ('premyelinated' axon; bar = 200nm), and Fig. 6.10c shows a large regenerating axon with a thin semi-compacted myelin sheath and satellite Schwann cell (SC) (remyelinating axon; bar = 200nm). Both of these axons would have been counted in the analysis for Fig. 6.10f. Fig. 6.10d shows unmyelinated regenerating axons, some surrounded by a thin layer of Schwann cell cytoplasm (at arrowhead) and others embedded within Schwann cell cytoplasm (e.g. at arrow), neither of which would have been counted. Bar = 500nm. Figs. 6.10 e-f show counts of all axons and of remyelinating axons only in the digital nerves of the fourth toe of wild-type (N = 6; black columns) and knockout mice (N = 6; grey columns) 17 days (Fig. 6.10e) and 21 days (Fig. 6.10f) after sciatic nerve crush. Difference between axon counts in wild-type and knockout mice are insignificant. Fig. 6.10g shows counts of myelinated and remyelinating axons in the tibial nerve 15days after, and about 5mm distal to, a crush lesion of the sciatic nerve in 8 wild-type (black column) and 6 knockout mice (grey column). Although the mean fibre count was 3087 in the knockout and 2375 in the wild-type mice these differences were not statistically significant.

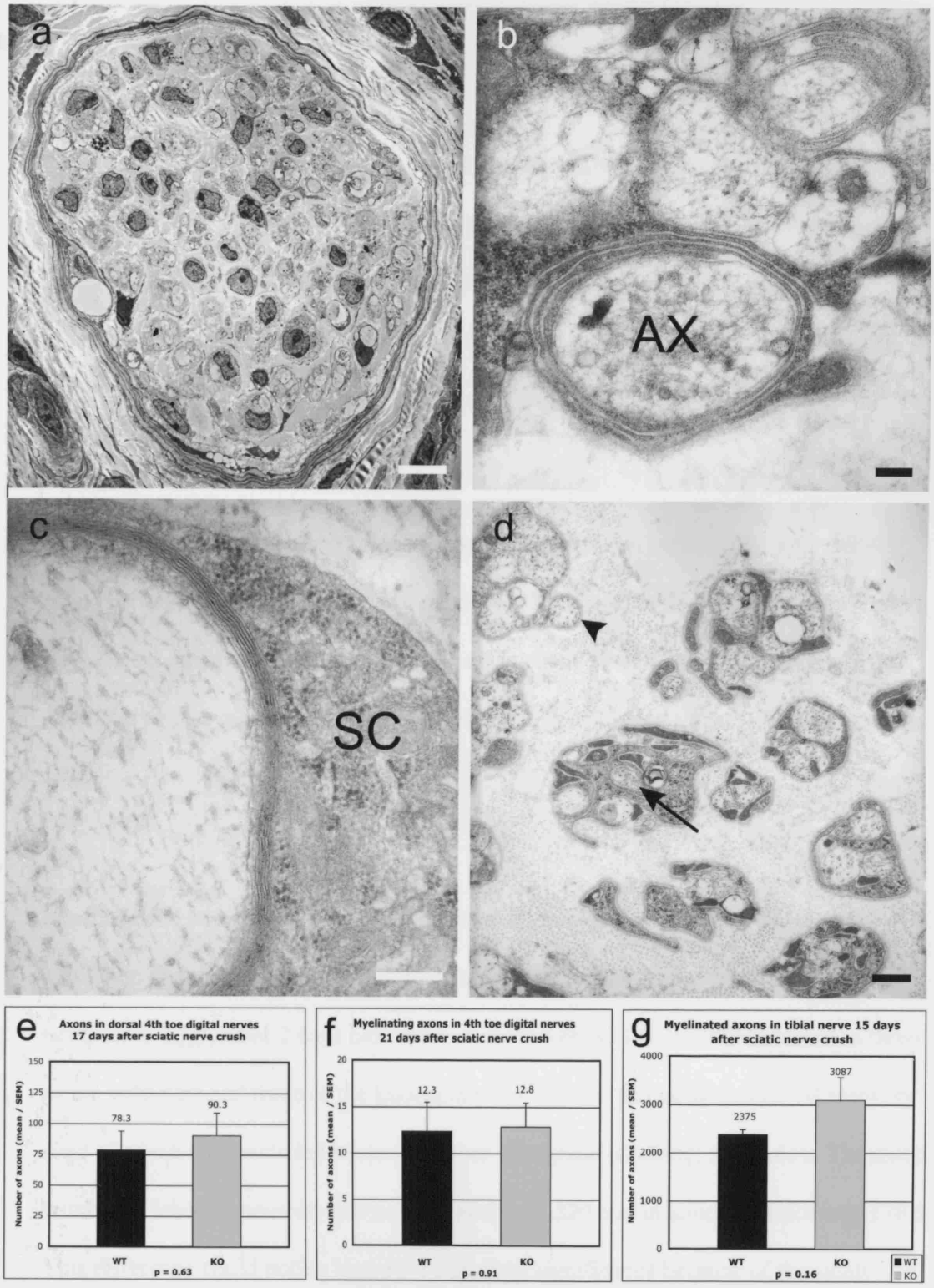
a
b
AX
c
SC
d
e
Axons in dorsal 4th toe digital nerves
17 days after sciatic nerve crush
Number of axons (mean / SEM)
150
125
100
75
50
25
0
78.3
90.3
WT
KO
p = 0.63
f
Myelinating axons in 4th toe digital nerves
21 days after sciatic nerve crush
Number of axons (mean / SEM)
20
15
10
5
0
12.3
12.8
WT
KO
p = 0.91
g
Myelinated axons in tibial nerve 15 days
after sciatic nerve crush
Number of axons (mean / SEM)
4000
3000
2000
1000
0
2375
3087
WT
KO
p = 0.16
WT
KO

6.4.6 Facial motor nucleus neuron counts after facial nerve injury

The numbers of facial nucleus neurons retrogradely labelled with Fluorogold (FG) applied to the whisker pad 27 days after facial nerve transection and 3 days before the animals were killed, were determined in 8 wild-type and 8 knockout mice (Fig. 6.6b). The mean number of labelled neurons in the wild-type mice was 101.7 and in knockout mice was 107.6 ($p = 0.77$ n.s.; Student's t-test; Fig. 6.6f).

In order to confirm that retrograde label was being uptaken sufficiently, a further 4 wild-type and 4 knockout mice received DiAsp 37 days after facial nerve transection (3 days before sacrifice). Wild-type mice had a mean of 194.3 labelled neurons and the knockout mice a mean of 300.3 labelled neurons ($p = 0.25$ n.s.; Mann-Whitney test; Fig. 6.6g).

Similarly, the numbers of facial nucleus neurons retrogradely labelled with DiAsp applied to the whisker pad 12 days after facial nerve *crush* (at the same level as transection injury) and 2 days before the animals were killed, were determined in three of the wild-type and three of the knockout mice used for assessing functional recovery (one of which was excluded because of poor retrograde labelling; Fig. 6.6a). The mean number of labelled neurons in wild-type mice was 320 and in knockout mice was 170.5. This difference could not be tested for statistical significance because of the small number of animals included in these groups (Fig. 6.6e).

The fact that there were apparently more DiAsp-labelled neurons in the knockout mice than in the wild-type mice after facial nerve transection, but more in the wild-type than in the knockout mice in the facial nerve crush group further suggests that the difference between wild-type and knockout animals in the crush group was not significant and reinforces the conclusion that the absence of NG2 in the knockout mice has no detectable effect on the regeneration of axotomised facial nerve axons.

These findings are entirely consistent with those obtained with FG, thus strengthening confidence in DiAsp-based results. The control side facial nucleus had a mean of 305.4 neurons labelled with FG in the wild-type mice and 279 neurons labelled in the knockout mice ($p = 0.3$ n.s.; Student's t-test; Fig. 6.6c), suggesting that there was very little variability in FG uptake or retrograde transport of FG (data not shown).

Chapter 7 - Discussion

7.1 LPS-induced inflammation around corticospinal neuron cell bodies results in their expression of growth-associated proteins, but does not stimulate axonal regeneration

Inflammation around neuronal perikarya has been shown to stimulate axonal regeneration, but has not been examined in the CST

Two experimental models provide evidence that inflammation around neuronal perikarya can stimulate axonal regeneration *in vivo*. Injection of Corynebacterium extracts into the DRG both enhances the ability of the central axons of DRG cells to regenerate after injury (Lu and Richardson, 1991) and stimulates upregulation of GAP-43 and c-jun in their cell bodies (Lu and Richardson, 1995), thus mimicking some of the effects of a conditioning peripheral nerve lesion. Similarly, Leon et al. (2000) have shown that zymosan injected into the vitreous body of the eye in adult rats, produces inflammation in the retina, upregulation of GAP-43 expression by RGCs and enhanced regeneration of RGC axons following optic nerve injury. The interpretation of these experiments has been questioned by Fischer et al. (2001) who suggested that zymosan may injure the lens, releasing factors that stimulate axonal regeneration. However, it has been shown recently that activated macrophages secrete a protein, oncomodulin, that, acts as a powerful promoter of neurite outgrowth in conjunction with cAMP (Yin et al., 2003; Yin et al., 2006).

The inability of axotomised CST neurons to upregulate growth-associated gene expression is believed to be one cause of their failure to regenerate axons (Anderson et al., 1998; Anderson and Lieberman, 1999). I have shown that application of LPS onto the pial surface of motor cortex produced inflammation - demonstrated by activation of microglia - in most cases throughout the entire depth of cortex and also increased expression of growth-associated genes in some CST neurons. ATF3 expression was upregulated for 1 day (but in very few cells), GAP-43 for 3 days, c-Jun for 2 weeks and SCG10 for 2 weeks in neurons within the inflamed cortex. However, in animals treated with LPS on cortex and having a concomitant C4 CST injury, there was neither an obvious increase in CST axon sprouting nor any regeneration across or around the lesion site. Causes of this failure may be due to lack of a sufficient inflammatory stimulus or injury to CST axons from the LPS, the refractory nature of CNS axons or effects at the lesion site.

LPS on cortex induces inflammation

LPS applied to the cortical surface in this study markedly increased the number of rounded OX42-positive cells at the surface of the brain and in the meninges (which were most likely to be peripheral macrophages – see Fig. 3.2), and activated microglia, increasing their number throughout the motor cortex (Table 3.1; Figs. 3.2 and 3.3). In most animals, there was a clear gradient of activation from superficial to deep, suggesting that LPS activated microglia in a concentration-dependent manner. LPS may also alter the properties of the blood-brain barrier in such a way that circulating monocytes can gain access into the brain (Persidsky et al., 1997; Weiss et al., 1998). However, it is not clear to what extent circulating monocytes entered the cortex in my experiments, as there are no reliable cell markers that distinguish macrophages from microglia. Furthermore, the astrogliosis shown by GFAP immunofluorescence in the

cortex to which LPS was applied confirms the inflammatory effect of the LPS (Fig. 3.4). The amount of swelling of cortex under the site of LPS application, together with the OX42 and GFAP immunostaining (Eng et al., 2000) demonstrated that the amount of inflammation produced was variable, with a standard dose of 500μg of LPS.

LPS placed on or injected into cortex did not produce significant axonal damage to CST neurons

Although the effects of applying LPS to the surface of the cerebral cortex have not been studied previously, it has been shown that injection of LPS into the cortex results in recruitment of macrophages, activation of local microglia and, later, activation of astrocytes (Perry et al., 1995a; Montero-Menei et al., 1996), with no significant cavitation. Only chronic infusions of LPS caused significant cavitation (in hippocampus), with a surrounding region showing activation of astrocytes and macrophages (Szczepanik et al., 1996). Aiming to cause no damage to the CST cell bodies or their axons within the cortex, LPS was applied to the pial surface of the cortex. When this was found not to enhance CST regeneration, the experiments were repeated using injections of LPS solution into layer V of motor cortex, in an attempt to cause even greater inflammation around corticospinal cell bodies. There was no sign of necrosis either when LPS was applied to the pial surface or when using up to four injections of LPS solution into motor cortex. Damage from the needle used for injections was mostly in the superficial part of cortex, with very small cystic areas in layer V in some animals, neither of which caused substantial axonal injury to CST neurons. (As the LPS injection experiment was a pilot study, control saline injections to look for the effects of needle injury were not performed).

If LPS application had resulted in axonal injury, there would have been reductions in the numbers of BDA-labelled axons in the medulla of animals in which BDA was injected into motor cortex. There were no significant differences between the counts of labelled CST axons in LPS-treated versus control animals (Table 3.3), which suggests that direct axonal injury did not occur. Furthermore, CST neurons showing upregulation of SCG10 and c-Jun were retrogradely labelled from the spinal cord after LPS application on the pial surface of motor cortex, demonstrating that their axons were intact (Fig. 3.8).

Growth-associated protein expression without regeneration

Despite stimulating inflammation around CST cell bodies, LPS did not enhance CST axonal regeneration, possibly because of local inhibitors at the injury site. The estimated number of cells that upregulated c-Jun, SCG10 and GAP-43 after LPS application was far greater than the number of BDA-labelled fibres in the spinal cord injury experiments, suggesting that the cell bodies of the BDA-labelled axons had probably upregulated growth-associated genes.

It is possible that CST axotomy interrupts target derived regeneration-suppressing signals, and this may potentiate the effects of LPS in promoting growth-associated gene expression. However, there was no difference in growth associated protein expression between axotomised and intact CST neurons. Previous work in this laboratory has demonstrated that cervical axotomy is insufficient to induce upregulation of growth associated genes, although axotomy within the cortex (close to the cell body) does so (Mason et al., 2002). However, promoting enhanced cell body responses by proximal

axotomy is unlikely to be of practical value because of the very large distance over which the CST axons would have to regrow to effect functional reconnection.

The growth-associated proteins that I have studied are only examples of a large range of neuronal molecules that may be required for regeneration of axons. Tetzlaff et al. (1991) showed that although cut rubrospinal axons do not regenerate; the injury results in prolonged increased levels of GAP-43 in their cell bodies, from which they concluded that it is their failure to maintain tubulin and actin synthesis that prevents regeneration. Since individual growth-associated genes are unlikely to greatly stimulate axonal regeneration, finding a mechanism whereby a whole cascade of such molecules could be upregulated may be necessary to bring about axonal regeneration in otherwise refractory CNS neurons. It seems clear that further studies are needed into the mechanisms of upregulating transcription factors that control growth associated proteins.

LPS injections into cortex compared to LPS placement on the pial surface of cortex

An intracortical injection of a solution of LPS might have been expected to induce a stronger inflammation closer to the cell bodies of CST neurons, but such an approach is problematic because direct tissue damage may elicit responses which mask/confound those due to the induction of an inflammatory response by cortical application of LPS. Injections of LPS into deep cortex resulted in neither a detectably greater inflammatory response nor greater upregulation of growth-associated proteins in layer V, with the possible exception of ATF3. It was surprising that c-Jun immunoreactivity was not maximal in layer V of cortex after LPS injection, and suggests that the trauma of injection was a greater stimulus to c-Jun upregulation than the LPS-induced inflammation.

The greater inflammatory response and greater c-Jun immunoreactivity seen in Layer V of cortex with application of LPS onto the pial surface compared to LPS injections may be dose-related. A 1μl injection of 20mg/ml LPS equates to 20μg of LPS within cortex. This is the maximum concentration of LPS that can be dissolved in LPS without it precipitating out (which would block fine-bore needles used for injection). The animals given 4 injections therefore received a dose of 80μg of LPS, compared to other animals receiving 500μg of topical LPS powder on top of cortex. ATF3 showed almost no upregulation with topical LPS application and very little upregulation around the site of LPS injection. This modest increase in ATF3 expression after LPS injections compared to topical LPS may reflect the fact that the injected LPS was more concentrated within layer V compared to its topical application. However, one would have expected more c-Jun expression in Layer V after LPS injection if this were the case, as these experiments have demonstrated that c-Jun expression increases with inflammation. Therefore, it is more likely that the increased ATF3 seen is a reflection of the greater trauma produced by a needle being pushed down to layer V of cortex.

Further experiments

It remains to be seen whether other approaches to inducing a more prolonged cortical inflammation in layer V of cortex would promote a more effective and longer-lasting expression of growth-associated proteins, with the effect of stimulating CST axon regeneration. Furthermore, examining the effects of the individual downstream products of LPS- or zymosan-induced inflammation, such as complement factors and cytokines, on growth-associated gene / protein expression may stimulate their upregulation without excessive cortical damage.

7.2 Local and systemic LPS-induced inflammation does not stimulate dorsal root regeneration

Inflammation without regeneration

LPS-induced inflammation around the DREZ did not increase regeneration of injured dorsal root axons into the CNS. Inflammation was achieved by either placing LPS onto the DREZ, systemic injections of LPS or a combination of the two. Injured dorsal roots were transganglionically labelled with CT-HRP and they almost all stopped regenerating at the DREZ. There was no difference in regeneration if the LPS was placed on the DREZ at the time of dorsal root injury, or 1 week after injury (i.e. when regenerating axons would have reached the DREZ), or by additional I-P LPS injections after injury.

LPS-induced microglial activation in injured dorsal roots

7 days after injury, OX42 immunohistochemistry showed that dorsal root transection alone caused accumulation of some macrophages in the injured dorsal root, with minimal microglial activation in the ipsilateral spinal cord. The contralateral dorsal root and spinal cord were unaffected by injury. However, the addition of intra-peritoneal LPS caused marked accumulation of macrophages in the injured dorsal root and a massive activation and accumulation of microglia in the DREZ and spinal cord on the injured side, with a similar but much smaller effect on the contralateral side (Fig. 3.11). Whether some of the rounded OX42+ cells seen in the DREZ and spinal cord were actually blood-borne monocytes cannot be excluded.

Dorsal root injury, with or without additional I-P LPS, had no effect on the resting microglial profile in the ipsilateral and contralateral cervical DREZ, and minor activation of microglia in the area postrema which has a deficient blood-brain barrier. This finding and the difference between injured and uninjured lumbar DREZ microglia suggest that LPS does not activate all microglia indiscriminately, but rather it primes microglia to become activated in the presence of degenerating axons. Further studies would be required to ascertain whether LPS acted directly on microglia, indirectly via secretion of cytokines to activate microglia, or via disruption of the blood-brain barrier to allow migration of circulating monocytes into the DREZ and spinal cord.

Microglia and axonal regeneration

Axonal regeneration in the injured spinal cord has been claimed after implantation of autologous activated microglia into the lesion site (Rabchevsky et al., 1997; Prewitt et al., 1997; Rapalino et al., 1998), although these experiments have proven difficult to replicate. Presumably, these grafts would be having local effects at the inhibitory glial scar via an immune-modulatory mechanism. The DREZ is also a barrier to regeneration in the CNS (Carlstedt et al., 1988), but injured dorsal roots can regenerate through it given a strong enough stimulus, such as a conditioning lesion (Chong et al., 1999). Lazar et al., (1999) speculated that 'priming' macrophages and microglia with systemic LPS resulted in an enhanced response to degenerating axons in the CNS, that might promote axonal regeneration. However, despite the aims stated in its conclusion, a regeneration study has not followed this paper. Macrophages clear a path for axonal regeneration in the PNS, and there is a delay in debris clearance in the injured CNS by microglia. However, it has been shown that, despite their importance, neither macrophages nor microglia are vital for axonal regeneration (see Introduction sections 1.1.1 and 1.2.5)

The results of this study confirm that enhanced macrophage/microglial activation along the path needed for CNS regeneration was insufficient to stimulate regeneration. It would seem that other factors are required for this to occur. It was surprising how few axons crossed the DREZ in my experiments, as all animals had a conditioning lesion at the time of dorsal root transection. However, this finding was consistent between control and LPS-treated animals, and is more likely to represent the severity of injury than an effect of activated microglia.

LPS and astrocytes

Although the astrocytic response to LPS at the DREZ was not investigated, it is worth mentioning that the functional properties of reactive astrocytes are not completely understood. Their presence in the DREZ and glial scar has led to a widespread belief that they are inhibitory to axon growth. However, given the correct stimulus, dorsal roots and axons in the dorsal columns are able to regenerate through these barriers. The inhibitory astrocyte cell line that was used in an *in vitro* study concluding that NG2 was the main inhibitor in the glial scar was from a tumour cell line, not from normal, native astrocytic spinal cord tissue (Fidler et al., 1999). 3 week old cultures of neonatal astrocytes can be stimulated to increase their ability to support the growth of long neurites by treatment with LPS macrophage conditioned medium (or db-cAMP) (Miller et al., 1994). However, the results of my experiment suggest that LPS treatment *in vivo* does not alter the astrocytes of the DREZ in a manner that allows neurite extension.

Further experiments

Following dorsal root injury, ATF3 is strongly upregulated in Schwann cells around degenerating axons in the dorsal root, but not in the CNS glial cells around the degenerating axons in the dorsal column (Hunt et al., 2004)(see Chapter 5). It is not known what role this may play in axonal regeneration. Topical LPS on motor cortex resulted in more extensive upregulation of ATF3 in subcortical glia than in neurons (see Chapter 3 and Fig. 3.5). It would be interesting to see if LPS upregulates ATF3 expression in CNS glia of the injured DREZ and dorsal columns which would mimic ATF3 expression in Schwann cells and hence see if ATF3 expression is related to the lack of regeneration of injured dorsal root axons through the inflamed DREZ.

7.3 Effects of zymosan-induced inflammation on motor cortex

Application of 500μg of zymosan powder onto the pial surface of motor cortex resulted in almost identical expression patterns of OX42 and growth-associated proteins to those seen in LPS-treated rats at corresponding time points. However, half of the animals thus treated developed cortical damage, often severe, in layers I to IV, that made it impossible to distinguish the effect of inflammation from other destructive processes.

OX42 expression

OX42 immunostaining of microglia showed them to be upregulated from 1 day to 17 days after zymosan application, with an amoeboid shape and increased intensity of staining compared to the contralateral cortex, which contained ramified microglia. Inflammation, as demonstrated by OX42+ microglial activation, reached through the full depth of cortex. It was not greater than inflammation produced by 500μg of LPS application onto cortex, despite zymosan being a more potent inflammogen. This suggests that LPS may have stimulated a maximal inflammatory response in microglia, although this does not correlate with the toxic effects and cavity formation of zymosan injections into corpus callosum compared to LPS injections (Fitch et al., 1999).

Growth associated protein expression

c-Jun was markedly upregulated through the full depth of motor cortex for up to 17 days and upregulated to a lesser extent after 1 month. There was very limited upregulation of

ATF-3 expression for up to 17 days, by cortical cells along the edges of the inflammation-induced cavity, or, in those animals with no cavity, in layers I and II of cortex. SCG10 was upregulated immediately adjacent to damaged cortex and to a lesser extent in Layer V of all animals, maximally at 3 days but still minimally upregulated thereafter until 17 days after zymosan application. As zymosan is more potent an inflammogen than LPS, it is possible that LPS stimulated a maximal expression of growth-associated proteins in CST cell bodies without causing overt damage.

Cortical damage resulted in upregulation of c-Jun, ATF3, SCG10 and and Nogo-A along the lesion edge, but no appreciable increase in their expression in layer V corticospinal neurons, although it is not possible to distinguish the effects of cortical damage from cortical inflammation. It is unlikely that any greater inflammation can be achieved with the application of zymosan on the pial surface of motor cortex without causing significant cortical damage.

Zymosan acts on several receptors, TLR-2 being the main one. TLR-2 and dectin-1, activation together by zymosan is thought to act synergistically to produce more TNF-α and more of an oxidative burst than is induced by LPS, which in turn may cause greater cortical damage. IL-10 signalling - which can mediate a feedback inhibition loop that limits inflammatory cytokine production (Moore et al., 2001) - was inhibited in human macrophages in vitro by zymosan, but not by LPS (Du et al., 2006). TLR-4 is an LPS receptor and is found on microglia (Laflamme and Rivest, 2001; Rivest, 2003), but not cortical neurons (Lehnardt et al., 2003). It is possible that TLR-4 activation, and other pathways of LPS-induced activity, may have more effect on corticospinal neuronal gene expression whilst being less inflammatory than zymosan. The amount of LPS that was applied to cortex in my experiments was limited by the volume of LPS that could physically be placed in a 4 x 3mm craniectomy defect but, in theory, greater doses of

LPS, rather than zymosan, could provide a greater stimulus to CST neuronal gene expression without cortical damage.

GFAP and NG2 expression

It is interesting that both GFAP and NG2 expression was decreased from 3 days to 7 days in the most superficial 500μm of cortex directly under the site of zymosan application (Figs. 4.2 and 4.3). This only occurred in the animals with the greatest amount of inflammation (as gauged by the degree and depth of microglial activation and by the amount of gross swelling evident in the treated cortex). Surrounding this area was a penumbra of increased GFAP and NG2 immunoreactivity with enlargement of the cell bodies of the glia and retraction of their processes, consistent with previous reports of their response to injury (Fitch et al., 1999; Kloss et al., 2001; Rhodes et al., 2006). However, there have been no reports suppression of GFAP and NG2 expression in response to inflammation. There was no suppression of GFAP and NG2 immunoreactivity after 1 day, but it was a consistent finding at 3 days, with one animal exhibiting this phenomenon after 7 days and it was not seen thereafter. Whether it represents a loss of astrocytes and NG2 cells, which correlates with the extreme toxicity of zymosan, or it is due to astrocytes and NG2 cells completely downregulating GFAP and NG2 respectively is not known. DAPI staining of nuclei showed that cells were present in this GFAP- / NG2- inflamed cortex, but their origin is unknown. GFAP- astrocytes are discussed in a review by Kimelberg, (2004), who suggests that they are actually OPCs, but others have found them to be a discrete group of S100β+ cells with different structural and membrane properties from normal astrocytes (Walz and Lang, 1998; Walz, 2000). Neither of these descriptions correlate with the appearance of GFAP downregulation seen in this experiment. Animals with less swollen / inflamed cortex after zymosan application, and most of the LPS-treated animals demonstrated

upregulation of GFAP and NG2 under the site of zymosan application, similar to that seen in the less inflamed penumbra. This suggests that the reaction of GFAP and NG2 expression to inflammation is graded, with maximal inflammation causing cell death or their downregulation and moderate inflammation causing upregulation of these two molecules. Growth-associated proteins were upregulated in these maximally inflamed areas, but it is interesting to note that ATF3 expression in these areas was in abnormal, unhealthy looking nuclei (Fig. 4.6). Furthermore, NG2 was upregulated in blood vessel walls, where it has been shown to be present in pericytes (Ozerdem et al., 2001). Whether this NG2 upregulation plays a role in the increased vascular permeability of inflamed blood vessel walls (which correlates with the oedema seen in the inflamed brains) is unknown.

Nogo-A expression

Nogo-A was upregulated from 1 day to 1 month, in Layers I and II of cortex directly under zymosan application. In Layer V, some animals had limited upregulation of Nogo-A between 3 days and 1 month (Fig. 4.4). Expression was noted in neurons in layer V and in smaller cells that could have been oligodendrocytes in all layers of cortex. Animals with maximal Nogo-A upregulation had cavitation of their cortex, and it is possible that the upregulation of Noga-A was a response to factors relating to this damage. The very few neurons seen to express Nogo-A in superficial cortex were present only when cortex was damaged.

It appears that inflammation upregulates Nogo-A expression in cortex. It is not possible to comment on whether maximal inflammation (indicated by cavitation of cortex), or processes involved in cortical tissue destruction resulted in even greater expression of

Nogo-A in both neuronal and non-neuronal cells. One can conclude from these findings that Nogo-A is a stress-related molecule, akin to ATF3 (Hai et al., 1999). However, it is not a general marker of inflammation-induced stress, as double-labelling with GFAP and NG2 showed that it was not expressed in astrocytes and NG2 glia.

Future experiments

It is unlikely that one could ameliorate the expression of growth-associated proteins to any greater degree using zymosan applied to the cortical surface. Injecting zymosan into cortex causes cavitation (Fitch et al., 1999), and would therefore damage too many CST neurons for successful regeneration after concomitant spinal cord injury to occur. However, the interesting novel finding of decreased GFAP and NG2 immunoreactivity with maximal inflammation (but no tissue loss) warrants further investigation. Using other markers of astrocytes, such as S100β or PGDFα to label NG2 cells in inflamed cortex would help establish if these cells are actually present or have been killed by the intense inflammation. Nogo-A was upregulated with inflammation and even more so after cortical damage; the small cells in which it was predominantly upregulated in may be oligodendrocytes. It would be useful to repeat the experiments using LPS to induce inflammation and double labelling with a marker for oligodendrocytes to confirm the identity of cells upregulating Nogo-A. It was not possible to determine if Nogo-A may be used as marker for regeneration (like ATF3) and it would be interesting to see if it is upregulated in proven models of regeneration. It has been shown to be upregulated after sciatic nerve injury *in axons,* and it would therefore be of interest to compare its expression in DRG neurons after peripheral branch injury, central branch injury and central branch injury plus conditioning lesion. Similarly, Nogo-A is upregulated in the borders of optic nerve crush lesions, but not in RGCs. It would be of interest see if its

expression could be induced in injured RGCs after injection of zymosan into the eye or lens injury.

7.4 Effects of cortical zymosan application on regeneration of injured CST axons

Application of zymosan to the cortical surface induced inflammation and upregulated c-Jun and SCG10 in corticospinal cell bodies (with ATF3 upregulated in very few layer V neurons only if there was substantial tissue damage in cortex). Neither animals receiving zymosan treatment, nor control animals (CST injury alone) showed any difference in the amount of axon sprouting rostral to the lesion site. There was no difference in the number of branches crossing the midline and no regeneration of injured CST axons across the lesion site, compared to controls. Up to twelve axons in white matter distal to the lesion were seen in a minority of animals. However, their straight course, thick diameter and distance up to 15mm caudal to the lesion site suggests that they were either spared fibres from the edges of the lesion, or branches of the uninjured DLCST. There were numerous branches from the DLCST into grey matter rostral and caudal to the lesion. However, in no animal were axons seen traversing the lesion site in continuity with axons labelled distally.

Taken with the results discussed above, these results suggest that zymosan-induced upregulation of growth associated proteins around CST cell bodies is insufficient to stimulate axonal sprouting or regeneration after cervical injury

Further experiments

It is likely that any increase in the inflammatory stimulus above that produced zymosan would cause cell damage in motor cortex to such an extent that it would counteract any increase in CST regenerative potential. Driving the cell body response towards successful regeneration would therefore have to be achieved using other agents, such as rolipram or dibutyrl cAMP (db-cAMP). Overexpression of the anti-apoptotic Bcl-2 gene in postnatal CNS neurons leads to robust optic nerve regeneration (Chen et al., 1997; Cho et al., 2005) by enhancing intracellular Ca^{2+} signalling and activating CREB (which mediates the effects of cAMP transcription) (Jiao et al., 2005). However, no studies have shown enhanced CST regeneration following elevation of cAMP. Pearse et al. (2004) injected db-cAMP directly into the spinal cord, as exogenous cAMP has been shown to influence growth cone turning and affect guidance towards chemoattractant cues (Ming et al., 1997; Song et al., 1997), but this resulted in CST fibres entering the rostral edge of the lesion only. Further studies of the effect of cAMP on descending axon tracts are certainly warranted, especially with the combinatorial approach of db-cAMP in cord, subcutaneous rolipram and a Schwann cell bridge in the lesion used by Pearse et al. (2004) that addresses intrinsic and extrinsic causes of CNS regeneration failure (assuming that rolipram acted on the CST cell bodies). The cell body response could be enhanced by repeating this experiment with inflammation in cortex. Alternatively, it would be interesting to analyse the axonal response to CST injuries performed in the mice that constitutively express neuronal Bcl-2 (with and without graft transplantation into the lesion, db-cAMP and rolipram).

However, directly injecting db-cAMP around corticospinal cell bodies would not be safe, as there is ample evidence that intracortical cAMP injection is epileptogenic (Ludvig and Moshe, 1987; Ludvig et al., 1992) and not controllable by even diazepam (Morishita et al., 1984). A series of experiments that I performed, aimed at comparing

CST regeneration in rats treated with topical cortical zymosan or with zymosan plus db-cAMP injections into motor cortex resulted in intractable seizures in the db-cAMP group (and the rats were culled with an overdose of CO_2) – data not shown.

7.5 ATF3 upregulation in glia during Wallerian degeneration: differential expression in peripheral nerves and CNS white matter

Following sciatic nerve transection or transection and reanastomosis, there was strong ATF3 upregulation by endoneurial, but not perineneurial cells in the distal sciatic nerve stumps beginning at 1 dpo. Most ATF3+ cells were S100+ and p75+ (both Schwann cell markers). When nerves were transected and reanastomosed, allowing rapid regeneration, most ATF3 had been downregulated by 30 days (3.6% of DAPI labelled cells were ATF3+ at 30dpo). Transection without anastomosis, forcing slower regeneration, resulted in an increase of labelled cells being ATF3+ to 31.8% at 30dpo. Transection with ligation of the proximal stump, to stop axonal regeneration, increased ATF3+ expression in distal stumps still further to 67.9% at 30 dpo. ATF3 expression in mice was similar to that in rats.

Following dorsal root injury, ATF3 was upregulated in the part of the root between the lesion and the spinal cord containing Schwann cells (i.e. the PNS), beginning at 1dpo, but not in the dorsal root entry zone or the degenerating dorsal column of the spinal cord (i.e. the CNS portion of the same bipolar axons).

Regulation of ATF3 in peripheral nerve glia

ATF3 expression in endoneurial cells (including many Schwann cells) after sciatic nerve injury, is eventually downregulated following axonal regeneration into the distal

stump, but its expression remains high if nerve regeneration is delayed or prevented. The upregulation of ATF3 may be due to the death of injured neurons, with downregulation correlating with axonal regeneration. However, this negative regulation of ATF3 by axons seemed to be from unspecified axonal signals, rather than from direct axonal contact, as downregulation did not occur as soon as they entered the distal stump. This is demonstrated by transected and reanastomosed nerves. Between 16dpo and 30dpo, there was no obvious increase in the numbers of these axons in distal stumps, yet the proportion of ATF3+ nuclei dropped markedly from 21.1% to 3.6%. Correspondingly, when axonal regeneration was delayed, there was more ATF3 expression in the distal stump at 30 days (31.8%).

The expression of ATF3 appears to be specific to endoneurial cells, and so is unlikely to be a general stress response; it was not upregulated by perineurial cells or by most endothelial cells in the distal stump. Although S100+ and p75+ Schwann cells principally expressed ATF3, the variety in the size and shape of ATF3+ nuclei may be a result of other cell types also expressing ATF3. The mechanisms underlying the upregulation are unknown, but the pro-inflammatory cytokine TNFα is a positive regulator of ATF3 (Inoue et al., 2004; Hartman et al., 2004) and is upregulated after nerve injury.

ATF3 expression in CNS glia differs from that in PNS glia

The experiments detailed in this thesis have shown that following injury of the peripheral branch of bipolar DRG cells, AFT3 is upregulated in glia during Wallerian degeneration. However, injury to their central branch does not cause upregulation of ATF3 in CNS glia around the central branches of the same degenerating axons. ATF3

has been seen in optic nerve glia following injury (Hunt et al., 2004), but this was a direct injury to the CNS, as opposed to the injury site being in the PNS in my experiments. It appears that ATF3 expression in CNS glia after injury, like that of c-jun, is not downregulated by signals from axons, and that the transcriptional regulation of Wallerian degeneration in the CNS is very different from that in peripheral nerves.

ATF3 and c-Jun: a joint role in axonal regeneration?

The pattern of expression of c-Jun in injured peripheral nerves and degenerating dorsal column after dorsal root injury strongly resembles that of ATF3 (Stewart, 1995; Soares et al., 2001; Hunt et al., 2004). The functional activity of ATF3 depends on dimerisation with other transcription factors. ATF3 and c-Jun share a similar pattern of expression in injured RGCs (Takeda et al., 2000). Neuronal dimerisation with c-Jun regulates the activity of regeneration associated genes such as *gadd153/Chop10, HSP27* and *Gadd45* (Hai and Hartman, 2001; Nakagomi et al., 2003; Befort et al., 2003), and ATF3 enhances c-Jun-mediated neurite outgrowth in neuronal cell lines (Pearson et al., 2003). It is possible that ATF3 forms heterodimers with c-Jun in glia as well, which would result in transcriptional activation (ATF3 homodimers are transcriptional repressors) (Hai and Hartman, 2001). This could potentially regulate the numerous changes in gene expression by Schwann cells that aid successful peripheral nerve regeneration, such as upregulation of NGF, BDNF, NCAM, L1, CHL1 and laminin, along with downregulation of markers of the myelinated state including MAG and P0 (see Introduction section 1.1.1). The target genes of ATF3 homo- and hetero-dimers in peripheral glia remain to be identified.

It is also possible that ATF3 may control changes in injured neurons as they come into contact with the Schwann cells in which it is expressed. Both Schwann cells and neurons upregulate CHL1, GAP-43 and $p75^{NTR}$ (Verge et al., 1990; Hall et al., 1992; Chong et al., 1994; Zhang et al., 2000; Gschwendtner et al., 2003). However, this may not be via heterodimeric binding with c-Jun in the case of GAP-43, as overexpression of c-Jun does not drive transcription of GAP-43 (Carulli et al., 2002), despite its promoter containing an AP-1 transcription factor binding site (Weber and Skene, 1998).

Finally, HSP27 is induced in Schwann cells after sciatic nerve injury, accompanied by the re-expression of the intermediate filament protein of the cytoskeleton, suggesting a role in cytoskeletal dynamics (Hirata et al., 2003). HSP27 is also expressed in neurons and is thought to be correlated with the survival of axotomised sensory neurons (Lewis et al., 1999). ATF3 has been reported to be anti-apoptotic and a promoter of neurite outgrowth acting through HSP27 *in vitro* (Nakagomi et al., 2003). The novel finding of ATF3 expression in peripheral nerve glia raises the possibility that ATF3 has regulatory effects on both Schwann cells and neurons that promote neuronal survival and regeneration after injury, possibly via HSP27.

In the CNS, reactive astrocytes are thought to be an impediment to axonal regeneration. The experiments described in this thesis raise the hypothesis that one reason for the failure of axonal regeneration in the CNS may be that the glia do not react sufficiently strongly to axotomy, by failing to express ATF3.

Future experiments

I looked at the functional effect of ATF3 expression in the PNS, by comparing rates of functional recovery after sciatic nerve injury in wild-type mice to ATF3 knockouts. Although there was no significant difference in the time taken to recover their toe-spreading reflex and sensitivity to Von Frey hairs, this result was inconclusive, as it was not possible to ascertain whether they were genuine knockout mice (data not shown).

Until the ATF3 knockout mice are conclusively shown to not express ATF3, or a non-functional stub of ATF3 in nervous tissue, an interesting follow-up to these studies would be to double label peripheral nerves with polyclonal ATF3 and monoclonal c-Jun antibody to look for co-expression of these transcription factors in peripheral glia. Further studies into the molecular mechanisms underlying glial cell responses to neuronal injury will no doubt aid our understanding of both PNS and CNS regeneration.

The principal observation reported in Chapter 5, that ATF3 is upregulated in the endoneurial cells of axotomised peripheral nerve, was also independently discovered by D. Hunt. Figures 5.1 – 5.4 incorporate our collective data on the expression profile of ATF3 in various models of peripheral nerve injury.

7.6 Axonal regeneration in the NG2 deficient mouse

The role of NG2 in the injured nervous system is controversial. Although NG2, a molecule widely regarded as a potent inhibitor of axonal regeneration, is strongly expressed at injury sites in the CNS, where regeneration is abortive, it is also strongly expressed in injured peripheral nerves, where axonal regeneration is vigorous (e.g. (Levine, 1994; Zhang et al., 2001; Tang et al., 2003; Rezajooi et al., 2004); and see review by Butt et al., (2002b)). It might have been expected, therefore, that the absence of NG2 would enhance axonal regeneration in the CNS and/or reduce regeneration in peripheral nerves. The findings in this thesis are consistent and in some respects surprising: the absence of NG2 had no effect on axonal regeneration *in vivo*. Specifically, there was no evidence that regenerative growth of dorsal root axons into the spinal cord after dorsal root injury, or of ascending (sensory) axons within the spinal cord following dorsal column injury, was enhanced in the NG2 knockout mice. Similarly, descending corticospinal tract axons failed to show enhanced regeneration in NG2 knockout mice following spinal cord injury. In addition, I have shown, by quantitative methods, that motor and sensory sciatic nerve fibres, and motor facial nerve fibres, regenerated and re-established functional innervation of target tissues to the same extent and at the same speed in the NG2 knockout and wild-type groups.

The response to the inhibitory molecule Nogo may be dependent on the expression of NgR by different classes of neuron (see Introduction section 1.2.7), and there is evidence that neurons may vary in their sensitivity to NG2 (see below) - although the NG2 receptor has not been isolated. It was therefore important that regeneration in the

NG2 knockout mouse was examined in a number of models. Two different populations of projection axons within the spinal cord (dorsal column sensory axons and CST axons), dorsal root axons at the PNS/CNS interface, and motor and sensory axons of two peripheral nerves (sciatic and facial) were all tested for possible effects of the absence of NG2 on regeneration after axotomy. Furthermore, in the case of the injured peripheral nerve, different types of lesion were examined, and both functional and multiple types of anatomical analyses of regeneration were carried out. In all of the systems and experimental conditions tested, no statistically significant differences between NG2-deficient and normal animals were found. One can therefore conclude that:

NG2, on its own, does not exert a profound influence on the regenerative growth of peripheral nerve fibres; and absence of NG2 from the microenvironment of the CNS does not enhance the regenerative growth of injured axons or facilitate the entry of regenerating dorsal root axons into the CNS, even when the regenerative potential of the DRG cells is enhanced by a conditioning lesion.

In other words, NG2 cannot be viewed as a major cause of failure of axonal regeneration within or into the CNS. The latter conclusion is in keeping with the recent findings of de Castro *et al.* (2005), who carried out closely related studies on NG2 knockout mice. They transected the spinal cord at vertebral level T9/10 and found that the penetration of immunohistochemically visualised CGRP-containing (presumptive sensory axons) into the NG2-rich scar tissue at the transection site was no more extensive in the knockout mice than in the wild-type controls, and that penetration into the scar tissue of serotoninergic (5HT-immunopositive) axons was *greater* in the wild-type than in the knockout mice.

The findings and conclusions in this thesis are also in line with other evidence that NG2 is neither a major inhibitor of axonal regeneration in the CNS nor a promoter of longitudinal regeneration in peripheral nerves. This includes the recent work of Yang *et al.* (2006) which provides some of the strongest and most direct *in vitro* evidence that NG2+ cells do not inhibit or repel growing/regenerating neurites. Indeed, their paper provides both *in vitro* and *in vivo* data suggesting the opposite, albeit based heavily on CNS neurons derived from neonatal rather than mature animals (discussed below).

7.6.1 NG2 as a facilitator of regeneration in peripheral nerves

Whether or not NG2 has an insignificant role in preventing axonal regeneration in the CNS – as my findings suggest – or is a contributory factor in this process, NG2 is upregulated in vigorously regenerating peripheral nerves. Hence it may be that NG2 has facilitatory roles with respect to axonal regeneration, especially in the PNS where it has been suggested that NG2 may promote enhanced mobility of non-neuronal cells after injury, thereby aiding the formation of cellular (Schwann cell) bridges to act as a supportive substrate for regenerating axons (Rezajooi et al., 2004; Makagiansar et al., 2004; Karram et al., 2005). It has also previously been suggested (based on its distribution within normal and injured peripheral nerve) that a plausible role for NG2 might be to facilitate regeneration by helping to confine regenerating axons within the endoneurial compartment and/or within the bands of Von Büngner of the distal stump (Rezajooi et al., 2004) and see Raisman's comments on Nogo (Raisman, 2004). However, the finding that regeneration of sensory and motor axons in peripheral nerves

is not reduced or delayed in NG2 knockout mice suggests that any such effects are of very minor significance for peripheral nerve regeneration.

Schwann cells in the distal stump of injured peripheral nerves upregulate molecules other than NG2 that are believed to be inhibitory to axonal regeneration. These include Nogo and Semaphorin-3A (Hunt et al., 2002b; Scarlato et al., 2003). Counter to their putative role in the CNS, these do not appear to be detrimental to regeneration within the PNS. This may be because they are overriden by the plethora of growth-promoting substances in the PNS, which are not upregulated in the CNS, rendering the latter environment inhibitory to axonal regeneration.

7.6.2 Potential confounding factors

It is pertinent to consider why the absence from the transgenic mice of NG2, a molecule with powerful effects *in vitro*, had so little effect on axonal regeneration *in vivo*. First, it is possible that NG2 has a redundant role in this process since NG2 is only one of a number of potential growth inhibitory or repulsive molecules at injury sites in the nervous system. For example, NG2, tenascin-C and CSPGs other than NG2 are expressed in similar regions of lesion sites in spinal cord (e.g. the meningeal scar) and peripheral nerves (the perineurium and the surface of bands of Von Bungner) (Martini et al., 1990; Martini, 1994; Zhang et al., 1995a; Zhang et al., 1995b; Tang et al., 2003). Second, elimination of the NG2 gene may have induced upregulation of other molecules with similar functions during development, thus further compensating for any effects of the absence of NG2 in the knockout animals. Conditional knockout and/or knockdown experiments (e.g. with siRNA) would be necessary to test this hypothesis.

Third, it is also possible that the neuronal populations investigated in this study were particularly insensitive to NG2. It is known that neuronal populations differ in their responsiveness to NG2 *in vitro* (Dou and Levine, 1994; Niehaus et al., 1999; Schneider et al., 2001) and *in vivo* (de Castro, Jr. et al., 2005), and it is conceivable that (some of) the neuronal populations examined do not normally express receptors for NG2 and are thus intrinsically less responsive to NG2 than other populations. However, the types of neuron that have been reported to show inhibition of neurite growth in the presence of NG2 include DRG cells (Dou and Levine, 1994; Fidler et al., 1999) and neocortical neurons (albeit not specifically CST neurons (Fidler et al., 1999)). Furthermore, I tested several types of neurons, so it is extremely unlikely that my findings are not generally applicable. It is also possible that age is a relevant factor when considering the negative findings in the current study. Thus adult animals were used in my experiments and regeneration was studied *in vivo*, whereas much of the data suggesting inhibitory effects of NG2 on axonal growth derive from *in vitro* studies using embryonic or neonatal neurons: for example, embryonic or neonatal rat (or chick) DRG neurons (Dou and Levine, 1994; Fidler et al., 1999; Snow et al., 2001); rat E17 cortical neurons (Fidler et al., 1999); E24-25 chick retinal ganglion cells (Canning et al., 1996); and early postnatal rat cerebellar granule cells (Dou and Levine, 1994; Chen et al., 2002b). Inhibition by NG2 of regenerative axonal growth from adult neurons has not been directly demonstrated, and it would not be surprising if developing neurons differed significantly from their adult counterparts with respect to their responsiveness to NG2. However, in view of the body of (largely indirect) evidence favouring a role for NG2 in inhibiting axonal regeneration in the adult CNS (see Introduction and further discussion below), the failure to find evidence for such a role of NG2 is unlikely to be explicable solely in terms of the age/maturity of my experimental animals.

Part of the lack of effect of knocking out NG2 may have been due to the genetic background of the mice studied- C57BL/6. Genetic background can have considerable effects on axonal regeneration in strains of transgenic mice. Recently Dimou et al. (2006) showed that corticospinal axons regenerated less well in Nogo-A knockout mice with a C57BL/6 background (as used in the present study) than in knockout mice with a 129X1/SvJ background, a finding that may be produced by a weaker intrinsic regenerative response by neurons from the C57BL/6 strain. However, C57BL/6 mice can regenerate axons vigorously following peripheral nerve injury and intrinsic CNS neurons from such animals can regenerate axons into peripheral nerve implants in the brain (P.Anderson, unpublished observations). If NG2 was the major factor preventing axonal regeneration in the spinal cord of C57BL/6 mice, some enhancement of regeneration in the knockout animals would have been expected.

7.6.3 Other roles of NG2

In the PNS, as well as a possible role in axon guidance, it has also been speculated that the presence of NG2 on satellite cells of DRG neurons may be involved in keeping the underlying somal surface free of synaptic input (Rezajooi et al., 2004). As to possible roles within the adult CNS, the presence of NG2-positive cell processes around some synaptic complexes (Ong and Levine, 1999; Butt et al., 2002a) and at nodes of Ranvier (Butt et al., 2002a) and the presence of synaptic contacts and neurotransmitter receptors on NG2+ cells (Bergles et al., 2000; Lin and Bergles, 2002) suggest that NG2 may be involved in functional interactions between neurons and glia (Wigley et al., 2007). The presence of NG2 in the glial scar that forms around CNS lesions is well established, but

its inhibitory role is now under question. *In vitro*, injury to astrocytes by placing zymosan particles on plated astrocytes resulted in astrocytic migration away from the inflammatory stimulus to form a cavity along with upregulation of CSPGs (Fitch et al., 1999). It is possible that the CSPG (and presumably NG2) upregulation plays as much a process in astrocyte migration – as is seen after spinal cord injuries – as it does in the formation of an inhibitory barrier to regeneration. This would correlate with the findings of Fang et al., (1999) that NG2 was involved in cell spreading and rearrangement of the cytoskeleton. The possible cleavage of the extracellular domain of NG2 to release fragments into the extracellular environment (Morgenstern et al., 2003) raises further functional possibilities. Other data suggest that NG2+ cells function as precursors for oligodendrocytes and possibly other cell lineages under both normal conditions and after injury (Karram et al., 2005) and studies on NG2 knockout mice suggest no role for NG2 in CNS (hippocampal) neurogenesis (Thallmair et al., 2006), but a possible role in angiogenesis (Ozerdem and Stallcup, 2004).

7.7 Concluding remarks

The main points that I would like to make in this thesis relate to:

1. The effect of inflammation around the cell bodies of corticospinal neurons on their expression of growth-associated proteins and ability to regenerate after injury
2. Axonal regeneration in mice lacking the putative inhibitory molecule NG2

7.7.1 Inflammation-induced expression of growth-associated proteins in motor cortex, and the effect on injured CST regeneration

Inflammation of the motor cortex was found to upregulate c-Jun, SCG10 and GAP-43 in some neurons. However, the response was generally greatest in superficial layers, as was the degree of inflammation, even when the stronger inflammogen zymosan was used. The level of upregulation of growth-associated proteins seemed to be related to the degree of inflammation. The injection of LPS solution into motor cortex resulted in almost as much upregulation of growth-associated proteins, but the duration of this upregulation was not studied.

However, the number of cells which responded in this way was limited and the effects most obvious in the first few days after application. Axonal regeneration was not enhanced. The failure of CST neurons to show enhanced axon regeneration may be due to the inflammatory stimulus not being strong enough or not lasting long enough. There was variation between animals in the extent of inflammation / microglial activation produced by the standard dose (500μg) of LPS or zymosan applied to the cortical surface. The cortical damage sustained in half of the animals treated with zymosan suggests that the maximal inflammation-inducing dose of zymosan was reached, although perhaps not with LPS. The absence of a widespread upregulation of ATF3 in CST neurons may have been the result of insufficient inflammation within layer V, which may have limited the expression of the full repertoire of downstream genes necessary for regeneration. Direct injections of LPS into layer V of cortex resulted in possibly a very minor increase in ATF3 expression compared to LPS application on the cortical surface. Sustained inflammation deeper in the cortex may be necessary to induce a sufficiently strong and prolonged upregulation of growth-associated genes, without excessive cortical damage, that would lead to a vigorous regenerative response to injury by CST neurons.

7.7.2 Axonal Regeneration in the NG2 deficient mouse

The studies described in this thesis suggest that NG2 is not a major inhibitory molecule preventing regeneration in the CNS and, further, that it is not essential for successful axonal pathfinding, regeneration and functional reinnervation in injured peripheral nerves. It is conceivable that if CNS regeneration-promoting interventions such as enhancing the intrinsic regenerative ability of CNS neurons, expressing neurotrophic molecules to support regenerating axons and neutralising other putative inhibitory molecules were to be applied, NG2 knockout mice would show enhanced regeneration relative to wild-type mice. However, such studies have not yet been carried out and for the moment the evidence that NG2 is not a key inhibitor of axon regeneration appears to be very strong.

Appendix

Figure A-1 Course of descending corticospinal axons,

Descending fibres split into the dorsal and dorsolateral CST at the spinomedullary junction in the C57Bl mouse, *taken with permission from Steward et al., J. Comp. Neurol.* 472: *463-477, 2004.*

The sections are from a mouse in which BDA injections had been made into the sensorimotor cortex on the left. **Fig. A1a:** BDA-labelled axons are evident in the pyramidal tract (PT) ipsilateral to the injection; no labelled axons are seen in the pyramid on the contralateral side. **Fig. A1b:** at the spinomedullary junction, CST axons decussate in the pyramidal decussation (Dec). Most labelled axons join the main tract at the base of the dorsal column, but a contingent of axons projects laterally (arrow), collecting into fascicles in the dorsomedial and sometimes dorsolateral gray matter. **Fig. A1c:** just below the pyramidal decussation, BDA-labelled axons are present in the main tract and in fascicles in the gray matter (arrow). Collaterals extend into and arborise within the grey matter. **Fig. A1d:** horizontal section through the most rostral portion of thoracic spinal cord showing BDA-labelled fibres in the dorsal CST (DCST) and dorsolateral CTS (DLCST). Note that axons in both fibre tracts are present in the same horizontal plane. Scale bar in c = 500μm and also applies to Figs. a and b; bar in d = 500μm.

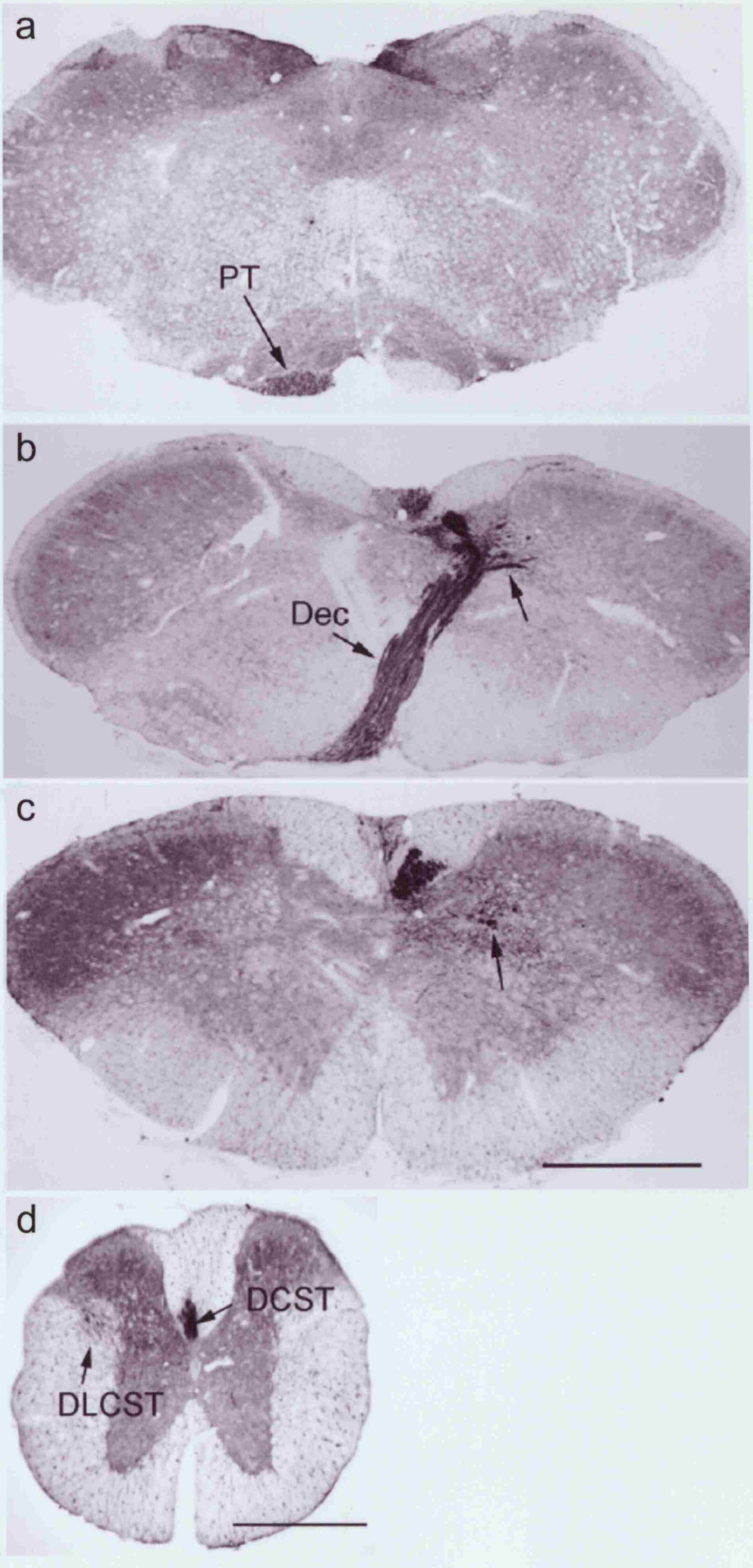
a
PT
b
Dec
c
d
DCST
DLCST

Figure A-2 Expression of c-Jun and variable tissue damage after zymosan application to cortex.

Coronal sections of motor cortex 17 days (Figs. A2a - f) and 3 days (Fig. A2g) after unilateral application of zymosan, or sham operation (Figs. A2a, c and e), immunoreacted for c-Jun. After 17 days, there are only background levels of c-Jun in the sham-operated, control (con) cortex, but c-Jun is upregulated in all cortical layers under the site of zymosan application (zym). Boxed areas of layer V in Figs. A2a and b are shown at greater magnification in Figs. A2c and d, demonstrating double-labelling of corticospinal cells with c-Jun and retrogradely transported Fluourogold. They show upregulation of c-Jun in layer V neurons, including corticospinal neurons, in zymosan-treated cortex.

Note the variability in injury to the cortex following zymosan application. Fig. A2b shows damage in layers I and II only, with a mass of immunoreactive cells, that is more likely to represent non-specific peroxidase activity of macrophages, rather than neuronal c-Jun expression, whereas Fig. A2f shows damage down to layer IV under the site of zymosan application (*), with cystic changes below that, medially (arrow). This damage has not had an effect on the degree of c-Jun immunoreactivity in remaining cortex, which is still significantly greater than the corresponding contralateral, sham operated cortex (Fig. A2e). Damage to cortex is variable in its severity: the degree of tissue injury (*) seen in the animal analysed in Fig. A2g, 3 days after zymosan application, is more localised than in the animal depicted in Fig. A2f, for example. Scale bar in Fig. A2a = 200μm and applies to b; bar in Fig. A2c = 20μm and also applies to d; bar in Fig. A2e = 20μm and also applies to f and g.

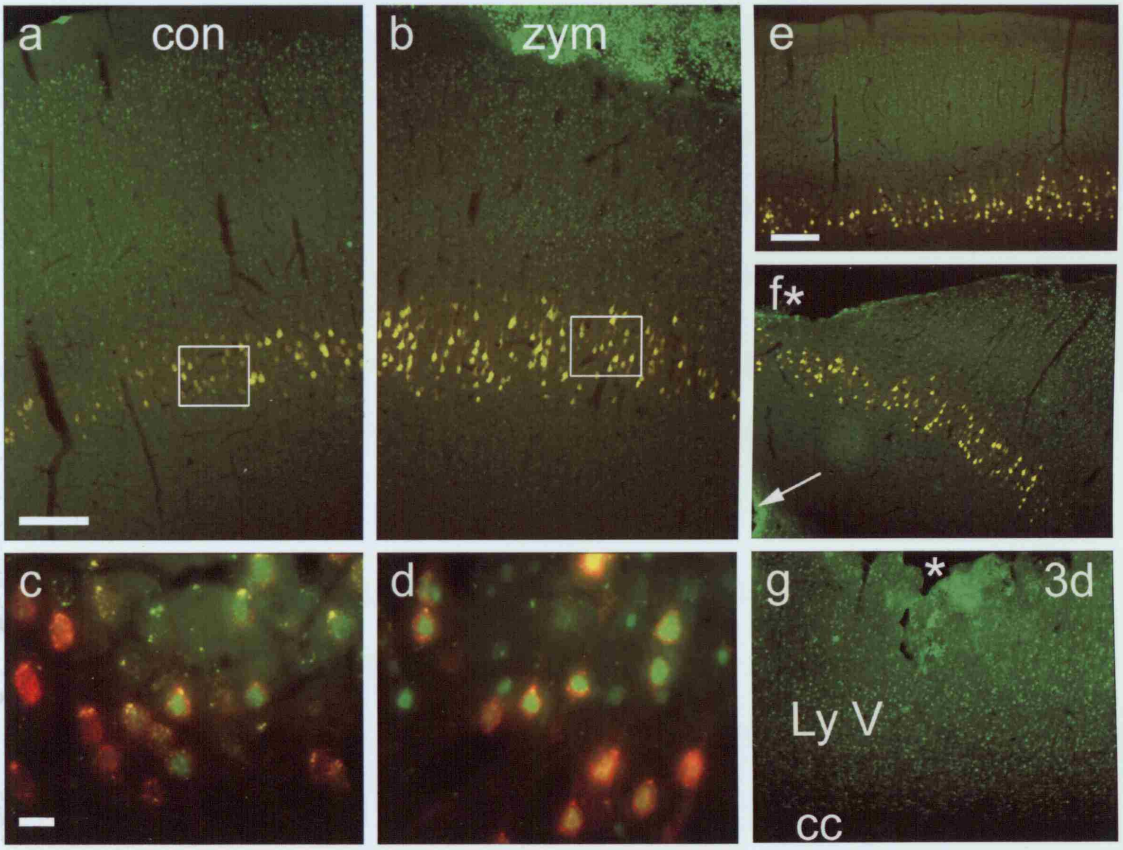
a
con
b
zym
e
f*
c
d
g
*
3d
Ly V
cc

8 Bibliography

Abercrombie,M. (1946) Estimation of nuclear population from microtome sections. *Anatomical Record*, **94**, 239-247.

Abernethy,D.A., Rud,A. & Thomas,P.K. (1992) Neurotropic influence of the distal stump of transected peripheral nerve on axonal regeneration: absence of topographic specificity in adult nerve. *J.Anat.*, **180**, 395-400.

Acheson,A., Conover,J.C., Fandl,J.P., DeChiara,T.M., Russell,M., Thadani,A., Squinto,S.P., Yancopoulos,G.D. & Lindsay,R.M. (1995) A BDNF autocrine loop in adult sensory neurons prevents cell death. *Nature*, **374**, 450-453.

Aguayo,A.J. (1985) Axonal regeneration from injured neurons in the adult mammalian central nervous system. In Cotman,C.W. (ed), *Synaptic Plasticity*. The Guilford Press, New York, pp. 457-484.

Ahmed,Z., Dent,R.G., Suggate,E.L., Barrett,L.B., Seabright,R.J., Berry,M. & Logan,A. (2005) Disinhibition of neurotrophin-induced dorsal root ganglion cell neurite outgrowth on CNS myelin by siRNA-mediated knockdown of NgR, p75NTR and Rho-A. *Mol.Cell Neurosci.*, **28**, 509-523.

Ahmed,Z., Suggate,E.L., Brown,E.R., Dent,R.G., Armstrong,S.J., Barrett,L.B., Berry,M. & Logan,A. (2006) Schwann cell-derived factor-induced modulation of the NgR/p75NTR/EGFR axis disinhibits axon growth through CNS myelin in vivo and in vitro. *Brain.*, **129**, 1517-1533.

Aigner,L., Arber,S., Kaphammer,J.P., Laus,T., Schneider,C., Botteri,F., Brenner,H.-R. & Caroni,P. (1995) Overexpression of the neural growth-associated protein GAP-43

induces nerve sprouting in the adult nervous system of transgenic mice. *Cell*, **83**, 269-278.

Akira,S. (1999) Functional roles of STAT family proteins: lessons from knockout mice. *Stem Cells*, **17**, 138-146.

Aldskogius,H. (2001) Microglia in neuroregeneration. *Microsc.Res.Tech.*, **54**, 40-46.

Aldskogius,H. & Kozlova,E.N. (1998) Central neuron-glial and glial-glial interactions following axon injury. *Prog.Neurobiol.*, **55**, 1-26.

Aloisi,F. (2001) Immune function of microglia. *Glia*, **36**, 165-179.

Anderson,P.N., Campbell,G., Zhang,Y. & Lieberman,A.R. (1998) Cellular and molecular correlates of the regeneration of adult mammalian CNS axons into peripheral nerve grafts. *Prog.Brain Res.*, **117**, 211-232.

Anderson,P.N., Fabes,J. & Hunt,D. (2007) The Role Of Inhibitory Molecules In Limiting Axonal Regeneration In The Mammalian Spinal Cord. In Becker,C.G. & Becker,T. (eds), *Model Organisms in Spinal Cord Regeneration*. Wiley-VCH, (Ch.1).

Anderson,P.N. & Lieberman,A.R. (1999) Intrinsic determinants of differential axonal regeneration by adult mammalian CNS neurons. In Saunders,N.R. & Dziegielewska,K.M. (eds), *Degeneration and regeneration in the nervous system*. Harwood Academic Press, pp. 53-75.

Anderson,P.N. & Turmaine,M. (1986) Axonal regeneration through arterial grafts. *.J.Anat.*, **147**, 73-82.

Andersson,P.B., Perry,V.H. & Gordon,S. (1992) The acute inflammatory response to lipopolysaccharide in CNS parenchyma differs from that in other body tissues. *Neuroreport.*, **48**, 169-186.

Angelov,D.N., Walther,M., Streppel,M., Guntinas Lichius,O., Neiss,W.F., Probstmeier,R. & Pesheva,P. (1998) Tenascin-R is antiadhesive for activated microglia that induce downregulation of the protein after peripheral nerve injury: a new role in neuronal protection. *J.Neurosci.*, **18**, 6218-6229.

Ashwell,K. (1990) Microglia and cell death in the developing mouse cerebellum. *Brain Res.Dev.Brain Res.*, **55**, 219-230.

Ashwell,K. (1991) The distribution of microglia and cell death in the fetal rat forebrain. *Brain Res.Dev.Brain Res.*, **58**, 1-12.

Atwal,J.K., Singh,K.K., Tessier-Lavigne,M., Miller,F.D. & Kaplan,D.R. (2003) Semaphorin 3F antagonizes neurotrophin-induced phosphatidylinositol 3-kinase and mitogen-activated protein kinase kinase signaling: a mechanism for growth cone collapse. *J.Neurosci.*, **23**, 7602-7609.

Bamburg,J.R., Bray,D. & Chapman,K. (1986) Assembly of microtubules at the tip of growing axons. Nature, 321, 788-790.

Banati,R.B., Gehrmann,J., Schubert,P. & Kreutzberg,G.W. (1993) Cytotoxicity of microglia. *Glia*, **7**, 111-118.

Bareyre,F.M., Haudenschild,B. & Schwab,M.E. (2002) Long-lasting sprouting and gene expression changes induced by the monoclonal antibody IN-1 in the adult spinal cord. *J.Neurosci.*, **22**, 7097-7110.

Bareyre,F.M., Kerschensteiner,M., Raineteau,O., Mettenleiter,T.C., Weinmann,O. & Schwab,M.E. (2004) The injured spinal cord spontaneously forms a new intraspinal circuit in adult rats. *Nat.Neurosci.*, **7**, 269-277.

Barritt,A.W., Davies,M., Marchand,F., Hartley,R., Grist,J., Yip,P., McMahon,S.B. & Bradbury,E.J. (2006) Chondroitinase ABC promotes sprouting of intact and injured spinal systems after spinal cord injury. *J.Neurosci.*, **26**, 10856-10867.

Barron,K.D., Marciano,F.F., Amundson,R. & Mankes,R. (1990) Perineuronal glial responses after axotomy of central and peripheral axons. A comparison. *Brain Res.*, **523**, 219-229.

Barton,W.A., Liu,B.P., Tzvetkova,D., Jeffrey,P.D., Fournier,A.E., Sah,D., Cate,R., Strittmatter,S.M. & Nikolov,D.B. (2003) Structure and axon outgrowth inhibitor binding of the Nogo-66 receptor and related proteins. *EMBO J.*, **22**, 3291-3302.

Bartsch,U., Bandtlow,C.E., Schnell,L., Bartsch,S., Spillmann,A.A., Rubin,B.P., Hillenbrand,R., Montag,D., Schwab,M.E. & Schachner,M. (1995) Lack of evidence that myelin-associated glycoprotein is a major inhibitor of axonal regeneration in the CNS. .*Neuron*, **15**, 1375-1381.

Bavetta,S., Hamlyn,P.J., Burnstock,G., Lieberman,A.R. & Anderson,P.N. (1999) The effects of FK506 on dorsal column axons following spinal cord injury in adult rats: neuroprotection and local regeneration. *Exp.Neurol.*, **158**, 382-393.

Beattie,M.S., Li,Q. & Bresnahan,J.C. (2000) Cell death and plasticity after experimental spinal cord injury. *Prog.Brain Res.*, **128:9-21.**, 9-21.

Becker,C.G., Schweitzer,J., Feldner,J., Schachner,M. & Becker,T. (2004) Tenascin-R as a repellent guidance molecule for newly growing and regenerating optic axons in adult zebrafish. *Mol.Cell Neurosci.*, **26**, 376-389.

Becker,T., Anliker,B., Becker,C.G., Taylor,J., Schachner,M., Meyer,R.L. & Bartsch,U. (2000) Tenascin-R inhibits regrowth of optic fibers in vitro and persists in the optic nerve of mice after injury. *Glia*, **29**, 330-346.

Befort,K., Karchewski,L., Lanoue,C. & Woolf,C.J. (2003) Selective up-regulation of the growth arrest DNA damage-inducible gene Gadd45 alpha in sensory and motor neurons after peripheral nerve injury. *Eur.J.Neurosci.*, **18**, 911-922.

Behrens,A., Sibilia,M. & Wagner,E.F. (1999) Amino-terminal phosphorylation of c-Jun regulates stress-induced apoptosis and cellular proliferation. *Nat.Genet.*, **21**, 326-329.

Benfey,M. & Aguayo,A.J. (1982) Extensive elongation of axons from rat brain into peripheral nerve grafts. *Nature*, **296**, 150-152.

Benfey,M., Bunger,U.R., Vidal Sanz,M., Bray,G.M. & Aguayo,A.J. (1985) Axonal regeneration from GABAergic neurons in the adult rat thalamus. *J.Neurocytol.*, **14**, 279-296.

Benowitz,L.I. & Routtenberg,A. (1997) GAP-43: an intrinsic determinant of neuronal development and plasticity. *Trends.Neurosci.*, **20**, 84-91.

Benson,M.D., Romero,M.I., Lush,M.E., Lu,Q.R., Henkemeyer,M. & Parada,L.F. (2005) Ephrin-B3 is a myelin-based inhibitor of neurite outgrowth. *Proc.Natl.Acad.Sci.U.S.A.*, **102**, 10694-10699.

Bergles,D.E., Roberts,J.D., Somogyi,P. & Jahr,C.E. (2000) Glutamatergic synapses on oligodendrocyte precursor cells in the hippocampus. *Nature*, **405**, 187-191.

Berry,M. (1982) Post-injury myelin-breakdown products inhibit axonal growth: an hypothesis to explain the failure of axonal regeneration in the mammalian central nervous system. *Bibl.Anat.*, **23**, 1-11.

Berry,M., Carlile,J. & Hunter,A. (1996) Peripheral nerve explants grafted into the vitreous body of the eye promote the regeneration of retinal ganglion cell axons severed in the optic nerve. *J.Neurocytol.*, **25**, 147-170.

Berry,M., Rees,L., Hall,S., Yiu,P. & Sievers,J. (1988) Optic axons regenerate into sciatic nerve isografts only in the presence of Schwann cells. *Brain Res.Bull.*, **20**, 223-231.

Berry,M., Rees,L. & Sievers,J. (1986) Unequivocal regeneration of rat optic nerve axons into sciatic nerve isografts. In Das,G.D. & Wallace,R.B. (eds), *Neural transplantation and regeneration*. Springer-Verlag, New York, pp. 63-79.

Bertrand,J., Winton,M.J., Rodriguez-Hernandez,N., Campenot,R.B. & McKerracher,L. (2005) Application of Rho antagonist to neuronal cell bodies promotes neurite growth in compartmented cultures and regeneration of retinal ganglion cell axons in the optic nerve of adult rats. *J.Neurosci.*, **25**, 1113-1121.

Beuche,W. & Friede,R.L. (1984) The role of non-resident cells in Wallerian degeneration. *J.Neurocytol.*, **13**, 767-796.

Bianco,J.I., Perry,C., Harkin,D.G., kay-Sim,A. & Feron,F. (2004) Neurotrophin 3 promotes purification and proliferation of olfactory ensheathing cells from human nose. *Glia*, **45**, 111-123.

Black,M.M. & Lasek,R.J. (1979) Slowing of the rate of axonal regeneration during growth and maturation. *Exp.Neurol.*, **63**, 108-119.

Blits,B., Dijkhuizen,P.A., Boer,G.J. & Verhaagen,J. (2000) Intercostal nerve implants transduced with an adenoviral vector encoding neurotrophin-3 promote regrowth of injured rat corticospinal tract fibers and improve hindlimb function. *Exp.Neurol.*, **164**, 25-37.

Blondet,B., Carpentier,G., Lafdil,F. & Courty,J. (2005) Pleiotrophin cellular localization in nerve regeneration after peripheral nerve injury. *J.Histochem.Cytochem.*, **53**, 971-977.

Boeshore,K.L., Schreiber,R.C., Vaccariello,S.A., Sachs,H.H., Salazar,R., Lee,J., Ratan,R.R., Leahy,P. & Zigmond,R.E. (2004) Novel changes in gene expression following axotomy of a sympathetic ganglion: a microarray analysis. *J.Neurobiol.*, **59**, 216-235.

Bohatschek,M., Werner,A. & Raivich,G. (2001) Systemic LPS injection leads to granulocyte influx into normal and injured brain: effects of ICAM-1 deficiency. *Exp.Neurol.*, **172**, 137-152.

Bolton,S.J. & Perry,V.H. (1997) Histone H1; a neuronal protein that binds bacterial lipopolysaccharide. *J.Neurocytol.*, **26**, 823-831.

Bomze,H.M., Bulsara,K.R., Iskandar,B.J., Caroni,P. & Pate Skene,J.H. (2001) Spinal axon regeneration evoked by replacing two growth cone proteins in adult neurons. *Nat.Neurosci.*, **4**, 38-43.

Boos,L., Szalai,A.J. & Barnum,S.R. (2005) C3a expressed in the central nervous system protects against LPS-induced shock. *Neurosci.Lett.*, **387**, 68-71.

Boruch,A.V., Conners,J.J., Pipitone,M., Deadwyler,G., Storer,P.D., DeVries,G.H. & Jones,K.J. (2001) Neurotrophic and migratory properties of an olfactory ensheathing cell line. *Glia*, **33**, 225-229.

Bovolenta,P., Fernaud Espinosa,I., Mendez Otero,R. & Nieto Sampedro,M. (1997) Neurite outgrowth inhibitor of gliotic brain tissue. Mode of action and cellular localization, studied with specific monoclonal antibodies. *Eur.J.Neurosci.*, **9**, 977-989.

Boyd,J.G. & Gordon,T. (2001) The neurotrophin receptors, trkB and p75, differentially regulate motor axonal regeneration. *J.Neurobiol.*, **49**, 314-325.

Boyd,J.G. & Gordon,T. (2003) Glial cell line-derived neurotrophic factor and brain-derived neurotrophic factor sustain the axonal regeneration of chronically axotomized motoneurons in vivo. *Exp.Neurol.*, **183**, 610-619.

Bradbury,E.J. & McMahon,S.B. (2006) Spinal cord repair strategies: why do they work? *Nat.Rev.Neurosci.*, **7**, 644-653.

Bradbury,E.J., Moon,L.D., Popat,R.J., King,V.R., Bennett,G.S., Patel,P.N., Fawcett,J.W. & McMahon,S.B. (2002) Chondroitinase ABC promotes functional recovery after spinal cord injury. *Nature*, **416**, 636-640.

Bregman,B.S., Kunkel-Bagden,E., Schnell,L., Ning Dai,H., Gao,D. & Schwab,M.E. (1995) Recovery from spinal cord injury mediated by antibodies to neurite growth inhibitors. *Nature*, **378**, 498-501.

Bresnahan,J.C., Beattie,M.S., Stokes,B.T. & Conway,K.M. (1991) Three-dimensional computer-assisted analysis of graded contusion lesions in the spinal cord of the rat. *J.Neurotrauma*, **8**, 91-101.

Bronfman,F.C. & Fainzilber,M. (2004) Multi-tasking by the p75 neurotrophin receptor: sortilin things out? *EMBO Rep.*, **5**, 867-871.

Brosamle,C., Huber,A.B., Fiedler,M., Skerra,A. & Schwab,M.E. (2000) Regeneration of lesioned corticospinal tract fibers in the adult rat induced by a recombinant, humanized IN-1 antibody fragment. *J.Neurosci.*, **20**, 8061-8068.

Broude,E., McAtee,M., Kelley,M.S. & Bregman,B.S. (1997) c-Jun expression in adult rat dorsal root ganglion neurons: differential response after central or peripheral axotomy. *Exp.Neurol.*, **148**, 367-377.

Brown,M.C., Perry,V.H., Lunn,E.R., Gordon,S. & Heumann,R. (1991) Macrophage dependence of peripheral sensory nerve regeneration: possible involvement of nerve growth factor. *Neuron*, **6**, 359-370.

Brummendorf,T., Hubert,M., Treubert,U., Leuschner,R., Tarnok,A. & Rathjen,F.G. (1993) The axonal recognition molecule F11 is a multifunctional protein: specific domains mediate interactions with Ng-CAM and restrictin. *Neuron*, **10**, 711-727.

Brushart,T.M. (1993) Motor axons preferentially reinnervate motor pathways. *J.Neurosci.*, **13**, 2730-2738.

Brushart,T.M., Mathur,V., Sood,R. & Koschorke,G.M. (1995) Joseph H. Boyes Award. Dispersion of regenerating axons across enclosed neural gaps. *J.Hand Surg.[Am.]*., **20**, 557-564.

Buffo,A., Holtmaat,A.J., Savio,T., Verbeek,J.S., Oberdick,J., Oestreicher,A.B., Gispen,W.H., Verhaagen,J., Rossi,F. & Strata,P. (1997) Targeted overexpression of the neurite growth-associated protein B-50/GAP-43 in cerebellar Purkinje cells induces sprouting after axotomy but not axon regeneration into growth-permissive transplants. *J.Neurosci.*, **17**, 8778-8791.

Buffo,A., Zagrebelsky,M., Huber,A.B., Skerra,A., Schwab,M.E., Strata,P. & Rossi,F. (2000) Application of neutralizing antibodies against NI-35/250 myelin- associated neurite growth inhibitory proteins to the adult rat cerebellum induces sprouting of uninjured purkinje cell axons. *J.Neurosci.*, **20**, 2275-2286.

Bundesen,L.Q., Scheel,T.A., Bregman,B.S. & Kromer,L.F. (2003) Ephrin-B2 and EphB2 regulation of astrocyte-meningeal fibroblast interactions in response to spinal cord lesions in adult rats. *J.Neurosci.*, **23**, 7789-7800.

Bunge,M.B., Holets,V.R., Bates,M.L., Clarke,T.S. & Watson,B.D. (1994) Characterization of photochemically induced spinal cord injury in the rat by light and electron microscopy. *Exp.Neurol.*, **127**, 76-93.

Bunge,M.B. & Pearse,D.D. (2003) Transplantation strategies to promote repair of the injured spinal cord. *J.Rehabil.Res.Dev.*, **40**, 55-62.

Burrell,R. (1990) Immunomodulation by bacterial endotoxin. *Crit Rev.Microbiol.*, **17**, 189-208.

Butt,A., Kirvell,S. & Ibrahim,M. (2002a) NG2 glia (oligodendrocyte progenitor cells) and sodium channel clustering at developing nodes of Ranvier in the rat brain. *J.Anat.*, **200**, 206.

Butt,A.M., Kiff,J., Hubbard,P. & Berry,M. (2002b) Synantocytes: new functions for novel NG2 expressing glia. *J.Neurocytol.*, **31**, 551-565.

Cafferty,W.B., Gardiner,N.J., Das,P., Qiu,J., McMahon,S.B. & Thompson,S.W. (2004) Conditioning injury-induced spinal axon regeneration fails in interleukin-6 knock-out mice. *J.Neurosci.*, **24**, 4432-4443.

Cafferty,W.B., Gardiner,N.J., Gavazzi,I., Powell,J., McMahon,S.B., Heath,J.K., Munson,J., Cohen,J. & Thompson,S.W. (2001) Leukemia inhibitory factor determines the growth status of injured adult sensory neurons. *J.Neurosci.*, **21**, 7161-7170.

Cafferty,W.B., Yang,S.H., Duffy,P.J., Li,S. & Strittmatter,S.M. (2007) Functional axonal regeneration through astrocytic scar genetically modified to digest chondroitin sulfate proteoglycans. *J.Neurosci.*, **27**, 2176-2185.

Caggiano,A.O., Zimber,M.P., Ganguly,A., Blight,A.R. & Gruskin,E.A. (2005) Chondroitinase ABCI improves locomotion and bladder function following contusion injury of the rat spinal cord. *J.Neurotrauma.*, **22**, 226-239.

Cai,D., Deng,K., Mellado,W., Lee,J., Ratan,R.R. & Filbin,M.T. (2002) Arginase I and polyamines act downstream from cyclic AMP in overcoming inhibition of axonal growth MAG and myelin in vitro. *Neuron*, **35**, 711-719.

Cai,D., Shen,Y., De Bellard,M., Tang,S. & Filbin,M.T. (1999) Prior exposure to neurotrophins blocks inhibition of axonal regeneration by MAG and myelin via a cAMP-dependent mechanism. *Neuron*, **22**, 89-101.

Cai,Z., Pang,Y., Lin,S. & Rhodes,P.G. (2003) Differential roles of tumor necrosis factor-alpha and interleukin-1 beta in lipopolysaccharide-induced brain injury in the neonatal rat. *Brain Res.*, **975**, 37-47.

Cajal (1991) *Cajal's Degneration and Regeneration of the Nervous System* OUP, New York.

Cajal,S.R. (1928) *Cajal's Degneration and Regeneration of the Nervous System* OUP, London.

Calderon,R.O., Attema,B. & DeVries,G.H. (1995) Lipid composition of neuronal cell bodies and neurites from cultured dorsal root ganglia. *J.Neurochem.*, **64**, 424-429.

Campbell,G., Anderson,P.N., Turmaine,M. & Lieberman,A.R. (1991) GAP-43 in the axons of mammalian CNS neurons regenerating into peripheral nerve grafts. *Exp.Brain Res.*, **87**, 67-74.

Campbell,G., Hutchins,K., Winterbottom,J., Grenningloh,G., Lieberman,A.R. & Anderson,P.N. (2005) Upregulation of activating transcription factor 3 (ATF3) by intrinsic CNS neurons regenerating axons into peripheral nerve grafts. *Exp.Neurol.*, **192**, 340-347.

Canning,D.R., Hoke,A., Malemud,C.J. & Silver,J. (1996) A potent inhibitor of neurite outgrowth that predominates in the extracellular matrix of reactive astrocytes. *Int.J.Dev.Neurosci.*, **14**, 153-175.

Cao,Z., Gao,Y., Bryson,J.B., Hou,J., Chaudhry,N., Siddiq,M., Martinez,J., Spencer,T., Carmel,J., Hart,R.B. & Filbin,M.T. (2006) The cytokine interleukin-6 is sufficient but not necessary to mimic the peripheral conditioning lesion effect on axonal growth. *J.Neurosci.*, **26**, 5565-5573.

Carim-Todd,L., Escarceller,M., Estivill,X. & Sumoy,L. (2003) LRRN6A/LERN1 (leucine-rich repeat neuronal protein 1), a novel gene with enriched expression in limbic system and neocortex. *Eur.J.Neurosci.*, **18**, 3167-3182.

Carlstedt,T., Cullheim,S., Risling,M. & Ulfhake,B. (1988) Mammalian root-spinal cord regeneration. *Prog.Brain Res.*, **78**, 225-229.

Caroni,P. (1997) Intrinsic neuronal determinants that promote axonal sprouting and elongation. *Bioessays*, **19**, 767-775.

Caroni,P. & Schwab,M.E. (1988a) Antibody against myelin-associated inhibitor of neurite growth neutralizes nonpermissive substrate properties of CNS white matter. *Neuron*, **1**, 85-96.

Caroni,P. & Schwab,M.E. (1988b) Two membrane proteins fractions from rat central myelin with inhibitory properties for neurite outgrowth. *J.Cell Biol.*, **106**, 1281-1288.

Carulli,D., Buffo,A., Botta,C., Altruda,F. & Strata,P. (2002) Regenerative and survival capabilities of Purkinje cells overexpressing c-Jun. *Eur.J.Neurosci.*, **16**, 105-118.

Carulli,D., Laabs,T., Geller,H.M. & Fawcett,J.W. (2005) Chondroitin sulfate proteoglycans in neural development and regeneration. Curr.Opin.Neurobiol., 15, 116-120.

Chaisuksunt,V., Campbell,G., Zhang,Y., Schachner,M., Lieberman,A.R. & Anderson,P.N. (2003) Expression of regeneration-related molecules in injured and regenerating striatal and nigral neurons. *J.Neurocytol.*, **32**, 161-183.

Chaisuksunt,V., Zhang,Y., Anderson,P.N., Campbell,G., Vaudano,E., Schachner,M. & Lieberman,A.R. (2000) Patterns of expression and distribution of mRNAs for L1, CHL1, c-jun and GAP-43 in identified regenerating neurons of the cerebellum and brainstem of the adult rat. *Neuroscience.*, **100**, 87-108.

Challacombe,J.F., Snow,D.M. & Letourneau,P.C. (1997) Dynamic microtubule ends are required for growth cone turning to avoid an inhibitory guidance cue. J.Neurosci., 17, 3085-3095.

Chamak,B., Morandi,V. & Mallat,M. (1994) Brain macrophages stimulate neurite growth and regeneration by secreting thrombospondin. *J.Neurosci.Res.*, **38**, 221-233.

Charbaut,E., Chauvin,S., Enslen,H., Zamaroczy,S. & Sobel,A. (2005) Two separate motifs cooperate to target stathmin-related proteins to the Golgi complex. *J.Cell Sci.*, **118**, 2313-2323.

Chaudhry,N., de,S.U. & Smith,G.M. (2006) Cell adhesion molecule L1 modulates nerve-growth-factor-induced CGRP-IR fiber sprouting. *Exp.Neurol.*, **202**, 238-249.

Chen,J., Bernreuther,C., Dihne,M. & Schachner,M. (2005) Cell adhesion molecule l1-transfected embryonic stem cells with enhanced survival support regrowth of corticospinal tract axons in mice after spinal cord injury. *J.Neurotrauma.*, **22**, 896-906.

Chen,D.F., Schneider,G.E., Martinou, J.C. & Tonegawa,S. (1997) Bcl-2 promotes regeneration of severed axons in mammalian CNS. *Nature,* **385**, 434-439.

Chen,J., Wu,J., Apostolova,I., Skup,M., Irintchev,A., Kugler,S. & Schachner,M. (2007) Adeno-associated virus-mediated L1 expression promotes functional recovery after spinal cord injury. *Brain*, **130**, 954-969.

Chen,M.S., Huber,A.B., van der Haar,M.E., Frank,M., Schnell,L., Spillmann,A.A., Christ,F. & Schwab,M.E. (2000) Nogo-A is a myelin-associated neurite outgrowth inhibitor and an antigen for monoclonal antibody IN-1. *Nature*, **403**, 434-439.

Chen,Z.J., Negra,M., Levine,A., Ughrin,Y. & Levine,J.M. (2002a) Oligodendrocyte precursor cells: reactive cells that inhibit axon growth and regeneration. *J.Neurocytol.*, **31**, 481-495.

Chen,Z.J., Ughrin,Y. & Levine (2002b) Inhibition of axon growth by oligodendrocyte precursor cells. *Mol.Cell Neurosci.*, **20**, 125-139.

Chen,Z.L. & Strickland,S. (2003) Laminin gamma1 is critical for Schwann cell differentiation, axon myelination, and regeneration in the peripheral nerve. *J.Cell Biol.*, **163**, 889-899.

Cheng,H., Cao,Y. & Olson,L. (1996a) Spinal cord repair in adult paraplegic rats: partial restoration of hind limb function. *Science*, **273**, 510-513.

Cheng,H.L., Randolph,A., Yee,D., Delafontaine,P., Tennekoon,G. & Feldman,E.L. (1996b) Characterization of insulin-like growth factor-I and its receptor and binding proteins in transected nerves and cultured Schwann cells. *J.Neurochem.*, **66**, 525-536.

Cho,K-S., Yang,L., Lu,B.,Ma,H.F., Huang,X., Pekny,M. & Chen.D.F. (2005) Re-establishing the regenerative potential of central nervous system axons in postnatal mice. *J.Cell Sci.*, **118 (5)**, 863-872.

Chong,M.S., Woolf,C.J., Turmaine,M., Emson,P.C. & Anderson,P.N. (1996) Intrinsic versus extrinsic factors in determining the regeneration of the central processes of rat

dorsal root ganglion neurons: the influence of a peripheral nerve graft. *J.Comp Neurol.*, **370**, 97-104.

Chong,M.-S., Fitzgerald,M., Winter,J., Hu-Tsai,M., Emson,P.C., Weise,U. & Woolf,C.J. (1992) GAP-43 mRNA in rat spinal cord and dorsal root ganglia neurons: developmental changes and re-expression following peripheral nerve injury. *Eur.J.Neurosci.*, **4**, 883-895.

Chong,M.-S., Reynolds,M.L., Irwin,N., Coggeshall,R.E., Emson,P.C., Benowitz,L.I. & Woolf,C.J. (1994) GAP-43 expression in primary sensory neurons following central axotomy. *J.Neurosci.*, **14(7)**, 4375-4384.

Chong,M.-S., Woolf,C.J., Haque,N.S.K. & Anderson,P.N. (1999) Regeneration of axons from injured dorsal roots into the spinal cord in adult rats. *J.Comp.Neurol.*, **410**, 42-54.

Cohen,R.I., Rottkamp,D.M., Maric,D., Barker,J.L. & Hudson,L.D. (2003) A role for semaphorins and neuropilins in oligodendrocyte guidance. *J.Neurochem.*, **85**, 1262-1278.

Corness,J., Shi,T.J., Xu,Z.Q., Brulet,P. & Hokfelt,T. (1996) Influence of leukemia inhibitory factor on galanin/GMAP and neuropeptide Y expression in mouse primary sensory neurons after axotomy. *Exp.Brain Res.*, **112**, 79-88.

Corvetti,L. & Rossi,F. (2005) Degradation of chondroitin sulfate proteoglycans induces sprouting of intact purkinje axons in the cerebellum of the adult rat. *J.Neurosci.*, **25**, 7150-7158.

Cosgaya,J.M., Chan,J.R. & Shooter,E.M. (2002) The neurotrophin receptor p75NTR as a positive modulator of myelination. *Science*, **298**, 1245-1248.

Costigan,M., Befort,K., Karchewski,L., Griffin,R.S., D'Urso,D., Allchorne,A., Sitarski,J., Mannion,J.W., Pratt,R.E. & Woolf,C.J. (2002) Replicate high-density rat genome oligonucleotide microarrays reveal hundreds of regulated genes in the dorsal root ganglion after peripheral nerve injury. *BMC.Neurosci.*, **3**, 16.

Csordas,G., Santra,M., Reed,C.C., Eichstetter,I., McQuillan,D.J., Gross,D., Nugent,M.A., Hajnoczky,G. & Iozzo,R.V. (2000) Sustained down-regulation of the epidermal growth factor receptor by decorin. A mechanism for controlling tumor growth in vivo. *J.Biol.Chem.*, **275**, 32879-32887.

Cui,Q., Pollett,M.A., Symons,N.A., Plant,G.W. & Harvey,A.R. (2003) A new approach to CNS repair using chimeric peripheral nerve grafts. J.Neurotrauma, 20, 17-31.

Di Carlo,F.J. & Fiore,J.V. (1958) On the composition of zymosan. Science, 127, 756-757.

Davalos,D., Grutzendler,J., Yang,G., Kim,J.V., Zuo,Y., Jung,S., Littman,D.R., Dustin,M.L. & Gan,W.B. (2005) ATP mediates rapid microglial response to local brain injury in vivo. *Nat.Neurosci.*, **8**, 752-758.

David,S. & Aguayo,A.J. (1981) Axonal elongation into peripheral nervous system "bridges" after central nervous system injury in adult rats. *Science*, **214**, 931-933.

Davies,J.E., Tang,X., Denning,J.W., Archibald,S.J. & Davies,S.J. (2004) Decorin suppresses neurocan, brevican, phosphacan and NG2 expression and promotes axon growth across adult rat spinal cord injuries. *Eur.J.Neurosci.*, **19**, 1226-1242.

Davies,S.J., Fitch,M.T., Memberg,S.P., Hall,A.K., Raisman,G. & Silver,J. (1997) Regeneration of adult axons in white matter tracts of the central nervous system. *Nature*, **390**, 680-683.

Davies,S.J.A., Goucher,D.R., Doller,C. & Silver,J. (1999) Robust regeneration of adult sensory axons in degenerating white matter of the adult rat spinal cord. *J.Neurosci.*, **19**, 5810-5822.

Dawson,M.R., Polito,A., Levine,J.M. & Reynolds,R. (2003) NG2-expressing glial progenitor cells: an abundant and widespread population of cycling cells in the adult rat CNS. *Mol.Cell Neurosci.*, **24**, 476-488.

De Castro,R., Jr., Tajrishi,R., Claros,J. & Stallcup,W.B. (2005) Differential responses of spinal axons to transection: influence of the NG2 proteoglycan. *Exp.Neurol.*, **192**, 299-309.

De Angelis.E., Brummendorf,T., Cheng,L., Lemmon,V. & Kenwrick,S. (2001) Alternative use of a mini exon of the L1 gene affects L1 binding to neural ligands. *J.Biol.Chem.*, **276**, 32738-32742.

De Leon.M., Nahin,R.L., Molina,C.A., De Leon,D.D. & Ruda,M.A. (1995) Comparison of c-jun, junB, and junD mRNA expression and protein in the rat dorsal root ganglia following sciatic nerve transection. *J.Neurosci.Res.*, **42**, 391-401.

De Winter,F, Oudega,M., Lankhorst,A.J., Hamers,F.P., Blits,B., Ruitenberg,M.J., Pasterkamp,R.J., Gispen,W.H. & Verhaagen,J. (2002) Injury-induced class 3 semaphorin expression in the rat spinal cord. *Exp.Neurol.*, **175**, 61-75.

De Wit,J, De,W.F., Klooster,J. & Verhaagen,J. (2005) Semaphorin 3A displays a punctate distribution on the surface of neuronal cells and interacts with proteoglycans in the extracellular matrix. *Mol.Cell Neurosci.*, **29**, 40-55.

Deller,T., Haas,C.A., Naumann,T., Joester,A., Faissner,A. & Frotscher,M. (1997) Up-regulation of astrocyte-derived tenascin-C correlates with neurite outgrowth in the rat dentate gyrus after unilateral entorhinal cortex lesion. *Neuroreport.*, **81**, 829-846.

Dergham,P., Ellezam,B., Essagian,C., Avedissian,H., Lubell,W.D. & McKerracher,L. (2002) Rho signaling pathway targeted to promote spinal cord repair. *J.Neurosci.*, **22**, 6570-6577.

Devor,M., Schonfield,D., Seltzer,Z. & Wall,P.D. (1979) Two modes of cutaneous reinnervation following peripheral nerve injury. *J.Comp.Neurol.*, **185**, 211-220.

Diamond,J., Foerster,A., Holmes,M. & Coughlin,M.D. (1992) Sensory nerves in adult rat regenerate and restore sensory function to the skin independently of endogenous NGF. *J.Neurosci.*, **12**, 1467-1476.

Dimou,L., Schnell,L., Montani,L., Duncan,C., Simonen,M., Schneider,R., Liebscher,T., Gullo,M. & Schwab,M.E. (2006) Nogo-A-deficient mice reveal strain-dependent differences in axonal regeneration. *J.Neurosci.*, **26**, 5591-5603.

DiStefano,P.S., Friedman,B., Radziejewesk,C., Alexander,C., Boland,P., Schieck,C.M., Lindsay,R.M. & Wiegand,S.J. (1992) The neurotrophins BDNF, NT-3 and NGF display distinct patterns of retrograde axonal transport in peripheral and central neurons. *Neuron*, **8**, 983-993.

Dodd,D.A., Niederoest,B., Bloechlinger,S., Dupuis,L., Loeffler,J.P. & Schwab,M.E. (2005) Nogo-A, -B, and -C are found on the cell surface and interact together in many different cell types. *J.Biol.Chem.*, **280**, 12494-12502.

Domeniconi,M., Cao,Z., Spencer,T., Sivasankaran,R., Wang,K., Nikulina,E., Kimura,N., Cai,H., Deng,K., Gao,Y., He,Z. & Filbin,M. (2002) Myelin-associated glycoprotein interacts with the nogo66 receptor to inhibit neurite outgrowth. *Neuron*, **35**, 283-290.

Domeniconi,M., Zampieri,N., Spencer,T., Hilaire,M., Mellado,W., Chao,M.V. & Filbin,M.T. (2005) MAG induces regulated intramembrane proteolysis of the p75 neurotrophin receptor to inhibit neurite outgrowth. *Neuron*, **46**, 849-855.

Donovan,M.J., Hahn,R., Tessarollo,L. & Hempstead,B.L. (1996) Identification of an essential nonneuronal function of neurotrophin 3 in mammalian cardiac development. *Nat.Genet.*, **14**, 210-213.

Dontchev,V.D. & Letourneau,P.C. (2002) Nerve growth factor and semaphorin 3A signaling pathways interact in regulating sensory neuronal growth cone motility. *J.Neurosci.*, **22**, 6659-6669.

Dooley, J. M. and Aguayo, A. J. Axonal elongation from cerebellum into peripheral nervous system grafts in the adult rat. Annals of Neurology 12, 221. 1982.

Doster,S.K., Lozano,A.M., Aguayo,A.J. & Willard,M.B. (1991) Expression of the growth-associated protein GAP-43 in adult rat retinal ganglion cells following axon injury. *Neuron*, **6**, 635-647.

Dottori,M., Hartley,L., Galea,M., Paxinos,G., Polizzotto,M., Kilpatrick,T., Bartlett,P.F., Murphy,M., Kontgen,F. & Boyd,A.W. (1998) EphA4 (Sek1) receptor tyrosine kinase is required for the development of the corticospinal tract. *Proc.Natl.Acad.Sci.U.S.A*, **95**, 13248-13253.

Dou,C.L. & Levine,J.M. (1994) Inhibition of neurite growth by the NG2 chondroitin sulfate proteoglycan. *J.Neurosci.*, **14**, 7616-7628.

Driessens,M.H., Hu,H., Nobes,C.D., Self,A., Jordens,I., Goodman,C.S. & Hall,A. (2001) Plexin-B semaphorin receptors interact directly with active Rac and regulate the actin cytoskeleton by activating Rho. *Curr.Biol.*, **11**, 339-344.

Du,Z., Kelly,E., Mecklenbrauker,I., Agle,L., Herrero,C., Paik,P. & Ivashkiv,L.B. (2006) Selective regulation of IL-10 signaling and function by zymosan. *J.Immunol.*, **176**, 4785-4792.

Eberhart,J., Swartz,M., Koblar,S.A., Pasquale,E.B., Tanaka,H. & Krull,C.E. (2000) Expression of EphA4, ephrin-A2 and ephrin-A5 during axon outgrowth to the hindlimb indicates potential roles in pathfinding. *Dev.Neurosci.*, **22**, 237-250.

Elkabes,S., DiCicco-Bloom,E.M. & Black,I.B. (1996) Brain microglia/macrophages express neurotrophins that selectively regulate microglial proliferation and function. *J.Neurosci.*, **16**, 2508-2521.

Elkabes,S., Peng,L. & Black,I.B. (1998) Lipopolysaccharide differentially regulates microglial trk receptor and neurotrophin expression. *J.Neurosci.Res.*, **54**, 117-122.

Eng,L.F., Ghirnikar,R.S. & Lee,Y.L. (2000) Glial fibrillary acidic protein: GFAP-thirty-one years (1969-2000). *Neurochem.Res.*, **25**, 1439-1451.

English,A.W., Meador,W. & Carrasco,D.I. (2005) Neurotrophin-4/5 is required for the early growth of regenerating axons in peripheral nerves. *Eur.J.Neurosci.*, **21**, 2624-2634.

Erickson,J.T., Conover,J.C., Borday,V., Champagnat,J., Barbacid,M., Yancopoulos,G. & Katz,D.M. (1996) Mice lacking brain-derived neurotrophic factor exhibit visceral sensory neuron losses distinct from mice lacking NT4 and display a severe developmental deficit in control of breathing. *J.Neurosci.*, **16**, 5361-5371.

Ernfors,P., Wetmore,C., Olsson,L. & Persson,H. (1990) Identification of cells in rat brain and peripheral tissues expressing mRNA for members of the nerve growth factor family. *Neuron*, **5**, 511-526.

Estus,S., Zaks,W.J., Freeman,R.S., Gruda,M., Bravo,R. & Johnson,E.M., Jr. (1994) Altered gene expression in neurons during programmed cell death: identification of c-jun as necessary for neuronal apoptosis. *J.Cell Biol.*, **127**, 1717-1727.

Faissner,A. & Kruse,J. (1990) J1/tenascin is a repulsive substrate for central nervous system neurons. *Neuron*, **5**, 627-637.

Fang,X., Burg,M.A., Barritt,D., Dahlin Huppe,K., Nishiyama,A. & Stallcup,W.B. (1999) Cytoskeletal reorganization induced by engagement of the NG2 proteoglycan leads to cell spreading and migration. *Mol.Biol.Cell*, **10**, 3373-3387.

Farooque,M., Badonic,T., Olsson,Y. & Holtz,A. (1995) Astrocytic reaction after graded spinal cord compression in rats: immunohistochemical studies on glial fibrillary acidic protein and vimentin. *J.Neurotrauma.*, **12**, 41-52.

Fawcett,J.W. & Asher,R.A. (1999) The glial scar and central nervous system repair. *Brain Res.Bull.*, **49**, 377-391.

Fawcett,J.W. & Keynes,R.J. (1990) Peripheral nerve regeneration. *Ann.Rev.Neurosci.*, **13**, 43-60.

Fernandes,K.J., Fan,D.P., Tsui,B.J., Cassar,S.L. & Tetzlaff,W. (1999) Influence of the axotomy to cell body distance in rat rubrospinal and spinal motoneurons: differential regulation of GAP-43, tubulins, and neurofilament-M. *J.Comp Neurol.*, **414**, 495-510.

Fernandez Valle,C., Bunge,R.P. & Bunge,M.B. (1995) Schwann cells degrade myelin and proliferate in the absence of macrophages: evidence from in vitro studies of Wallerian degeneration. .*J.Neurocytol.*, **24**, 667-679.

Feron,F., Perry,C., Cochrane,J., Licina,P., Nowitzke,A., Urquhart,S., Geraghty,T. & kay-Sim,A. (2005) Autologous olfactory ensheathing cell transplantation in human spinal cord injury. *Brain.*, **128**, 2951-2960.

Feron,F., Perry,C., McGrath,J.J. & kay-Sim,A. (1998) New techniques for biopsy and culture of human olfactory epithelial neurons. *Arch.Otolaryngol.Head Neck Surg.*, **124**, 861-866.

Fidler,P.S., Schuette,K., Asher,R.A., Dobbertin,A., Thornton,S.R., Calle Patino,Y., Muir,E., Levine,J.M., Geller,H.M., Rogers,J.H., Faissner,A. & Fawcett,J.W. (1999) Comparing astrocytic cell lines that are inhibitory or permissive for axon growth: the major axon-inhibitory proteoglycan is NG2. *J.Neurosci.*, **19**, 8778-8788.

Fischer,D., Heiduschka,P. & Thanos,S. (2001) Lens-injury-stimulated axonal regeneration throughout the optic pathway of adult rats. *Exp.Neurol.*, **172**, 257-272.

Fischer,D., Pavlidis,M. & Thanos,S. (2000) Cataractogenic lens injury prevents traumatic ganglion cell death and promotes axonal regeneration both In vivo and in culture [In Process Citation]. *Invest Ophthalmol.Vis.Sci.*, **41**, 3943-3954.

Fitch,M.T., Doller,C., Combs,C.K., Landreth,G.E. & Silver,J. (1999) Cellular and molecular mechanisms of glial scarring and progressive cavitation: in vivo and in vitro analysis of inflammation-induced secondary injury after CNS trauma. *J.Neurosci.*, **19**, 8182-8198.

Fitch,M.T. & Silver,J. (1997) Glial cell extracellular matrix: boundaries for axon growth in development and regeneration. .*Cell Tissue Res.*, **290**, 379-384.

Fouad,K., Schnell,L., Bunge,M.B., Schwab,M.E., Liebscher,T. & Pearse,D.D. (2005) Combining Schwann cell bridges and olfactory-ensheathing glia grafts with chondroitinase promotes locomotor recovery after complete transection of the spinal cord. *J.Neurosci.*, **25**, 1169-1178.

Fournier,A.E., Gould,G.C., Liu,B.P. & Strittmatter,S.M. (2002) Truncated soluble Nogo receptor binds Nogo-66 and blocks inhibition of axon growth by myelin. *J.Neurosci.*, **22**, 8876-8883.

Fournier,A.E., GrandPre,T. & Strittmatter,S.M. (2001) Identification of a receptor mediating Nogo-66 inhibition of axonal regeneration. *Nature*, **409**, 341-346.

Fournier,A.E., Takizawa,B.T. & Strittmatter,S.M. (2003) Rho kinase inhibition enhances axonal regeneration in the injured CNS. *J.Neurosci.*, **23**, 1416-1423.

Franz,C.K., Rutishauser,U. & Rafuse,V.F. (2005) Polysialylated neural cell adhesion molecule is necessary for selective targeting of regenerating motor neurons. *J.Neurosci.*, **25**, 2081-2091.

Freeman,L.W. (1954) Injuries of the spinal cord. *Surg.Clin.North Am.*, 1131-1146.

Frey,D., Laux,T., Xu,L., Schneider,C. & Caroni,P. (2000) Shared and unique roles of CAP23 and GAP43 in actin regulation, neurite outgrowth, and anatomical plasticity. *J.Cell Biol.*, **149**, 1443-1454.

Friedlander,D.R., Milev,P., Karthikeyan,L., Margolis,R.K., Margolis,R.U. & Grumet,M. (1994) The neuronal chondroitin sulfate proteoglycan neurocan binds to the neural cell adhesion molecules Ng-CAM/L1/NILE and N-CAM, and inhibits neuronal adhesion and neurite outgrowth. *.J.Cell Biol.*, **125**, 669-680.

Fujitani,M., Kawai,H., Proia,R.L., Kashiwagi,A., Yasuda,H. & Yamashita,T. (2005) Binding of soluble myelin-associated glycoprotein to specific gangliosides induces the association of p75NTR to lipid rafts and signal transduction. *J.Neurochem.*, **94**, 15-21.

Funakoshi,H., Frisen,J., Barbany,G., Timmusk,T., Zachrisson,O., Verge,V.M.K. & Persson,H. (1993) Differential expression of mRNAs for neurotrophins and their receptors after axotomy of the sciatic nerve. *J.Cell Biol.*, **123**, 455-465.

Fuss,B., Bartsch,U., Wintergerst,E.S., Pesheva,P. & Schachner,M. (1993) Characterization of the neural recognition molecule janusin (J1- 160/180). *.Schweiz.Arch.Neurol.Psychiatr.*, **144**, 197-198.

Galtrey,C.M., Asher,R.A., Nothias,F. & Fawcett,J.W. (2007) Promoting plasticity in the spinal cord with chondroitinase improves functional recovery after peripheral nerve repair. *Brain.*, **130**, 926-939.

Gantner,B.N., Simmons,R.M., Canavera,S.J., Akira,S. & Underhill,D.M. (2003) Collaborative induction of inflammatory responses by dectin-1 and Toll-like receptor 2. J.Exp.Med., 197, 1107-1117.

Gao,Y., Deng,K., Hou,J., Bryson,J.B., Barco,A., Nikulina,E., Spencer,T., Mellado,W., Kandel,E.R. & Filbin,M.T. (2004) Activated CREB is sufficient to overcome inhibitors in myelin and promote spinal axon regeneration in vivo. *Neuron.*, **44**, 609-621.

Gard,A.L., Maughon,R.H. & Schachner,M. (1996) In vitro oligodendrogliotrophic properties of cell adhesion molecules in the immunoglobulin superfamily: myelin-associated glycoprotein and N- CAM. *J.Neurosci.Res.*, **46**, 415-426.

Gavazzi,I., Stonehouse,J., Sandvig,A., Reza,J.N., ppiah-Kubi,L.S., Keynes,R. & Cohen,J. (2000) Peripheral, but not central, axotomy induces neuropilin-1 mRNA expression in adult large diameter primary sensory neurons. *J.Comp Neurol.*, **423**, 492-499.

George,R. & Griffin,J.W. (1994) Delayed macrophage responses and myelin clearance during Wallerian degeneration in the central nervous system: the dorsal radiculotomy model. *Exp.Neurol.*, **129**, 225-236.

Giehl,K.M. (2001) Trophic dependencies of rodent corticospinal neurons. *Rev.Neurosci.*, **12**, 79-94.

Gilbert,R.J., McKeon,R.J., Darr,A., Calabro,A., Hascall,V.C. & Bellamkonda,R.V. (2005) CS-4,6 is differentially upregulated in glial scar and is a potent inhibitor of neurite extension. *Mol.Cell Neurosci.*, **29**, 545-558.

Goldberg,J.L., Vargas,M.E., Wang,J.T., Mandemakers,W., Oster,S.F., Sretavan,D.W. & Barres,B.A. (2004) An oligodendrocyte lineage-specific semaphorin, Sema5A, inhibits axon growth by retinal ganglion cells. *J.Neurosci.*, **24**, 4989-4999.

Goldshmit,Y., Galea,M.P., Wise,G., Bartlett,P.F. & Turnley,A.M. (2004) Axonal regeneration and lack of astrocytic gliosis in EphA4-deficient mice. *J.Neurosci.*, **24**, 10064-10073.

Gomez,V.M., Averill,S., King,V., Yang,Q., Perez,E.D., Chacon,S.C., Ward,R., Nieto-Sampedro,M., Priestley,J. & Taylor,J. (2003) Transplantation of olfactory ensheathing cells fails to promote significant axonal regeneration from dorsal roots into the rat cervical cord. *J.Neurocytol.*, **32**, 53-70.

Goodman,C.S. (1996) Mechanisms and molecules that control growth cone guidance. *Annu.Rev.Neurosci.*, **19**, 341-377.

Gotz,B., Scholze,A., Clement,A., Joester,A., Schutte,K., Wigger,F., Frank,R., Spiess,E., Ekblom,P. & Faissner,A. (1996) Tenascin-C contains distinct adhesive, anti-adhesive, and neurite outgrowth promoting sites for neurons. *J.Cell Biol.*, **132**, 681-699.

Graeber,M.B., Streit,W.J. & Kreutzberg,G.W. (1988) Axotomy of the rat facial nerve leads to increased CR3 complement receptor expression by activated microglial cells. *J.Neurosci.Res.*, **21**, 18-24.

GrandPre,T., Li,S. & Strittmatter,S.M. (2002) Nogo-66 receptor antagonist peptide promotes axonal regeneration. *Nature*, **417**, 547-551.

GrandPre,T., Nakamura,F., Vartanian,T. & Strittmatter,S.M. (2000) Identification of the Nogo inhibitor of axon regeneration as a Reticulon protein. *Nature*, **403**, 439-444.

Greenberg,S.G. & Lasek,R.J. (1988) Neurofilament protein synthesis in DRG neurons decreases more after peripheral axotomy than after central axotomy. *J.Neurosci.*, **8**, 1739-1746.

Greene,L.A. & Shooter,E.M. (1980) The nerve growth factor: biochemistry, synthesis, and mechanism of action. *Annu.Rev.Neurosci.*, **3**, 353-402.

Grill,R., Murai,K., Blesch,A., Gage,F.H. & Tuszynski,M.H. (1997) Cellular delivery of neurotrophin-3 promotes corticospinal axonal growth and partial functional recovery after spinal cord injury. *J.Neurosci.*, **17**, 5560-5572.

Gross,P.M. (1992) Circumventricular organ capillaries. *Prog.Brain Res.*, **91**, 219-233.

Grumet,M., Flaccus,A. & Margolis,R.U. (1993) Functional characterization of chondroitin sulfate proteoglycans of brain: interactions with neurons and neural cell adhesion molecules. *.J.Cell Biol.*, **120**, 815-824.

Gschwendtner,A., Liu,Z., Hucho,T., Bohatschek,M., Kalla,R., Dechant,G. & Raivich,G. (2003) Regulation, cellular localization, and function of the p75 neurotrophin receptor (p75NTR) during the regeneration of facial motoneurons. *Mol.Cell Neurosci.*, **24**, 307-322.

Guan,K.L. & Rao,Y. (2003) Signalling mechanisms mediating neuronal responses to guidance cues. *Nat.Rev.Neurosci.*, **4**, 941-956.

Habib,A.A., Marton,L.S., Allwardt,B., Gulcher,J.R., Mikol,D.D., Hognason,T., Chattopadhyay,N. & Stefansson,K. (1998) Expression of the oligodendrocyte-myelin glycoprotein by neurons in the mouse central nervous system. *J.Neurochem.*, **70**, 1704-1711.

Hafner,C., Schmitz,G., Meyer,S., Bataille,F., Hau,P., Langmann,T., Dietmaier,W., Landthaler,M. & Vogt,T. (2004) Differential gene expression of Eph receptors and ephrins in benign human tissues and cancers. *Clin.Chem.*, **50**, 490-499.

Hagg,T., Baker,K.A., Emsley,J.G. & Tetzlaff,W. (2005) Prolonged local neurotrophin-3 infusion reduces ipsilateral collateral sprouting of spared corticospinal axons in adult rats. *Neuroscience.*, **130**, 875-887.

Hai,T. & Hartman,M.G. (2001) The molecular biology and nomenclature of the activating transcription factor/cAMP responsive element binding family of transcription factors: activating transcription factor proteins and homeostasis. *Gene*, **273**, 1-11.

Hai,T., Wolfgang,C.D., Marsee,D.K., Allen,A.E. & Sivaprasad,U. (1999) ATF3 and stress responses. *Gene Expr.*, **7**, 321-335.

Hall,H., Liu,L., Schachner,M. & Schmitz,B. (1993) The L2/HNK-1 carbohydrate mediates adhesion of neural cells to laminin. *Eur.J.Neurosci.*, **5**, 34-42.

Hall,S.M., Kent,A.P., Curtis,R. & Robertson,D. (1992) Electron microscopic immunocytochemistry of GAP-43 within proximal and chronically denervated distal stumps of transected peripheral nerve. *J.Neurocytol.*, **21**, 820-831.

Ham,J., Babij,C., Whitfield,J., Pfarr,C.M., Lallemand,D., Yaniv,M. & Rubin,L.L. (1995) A c-Jun dominant negative mutant protects sympathetic neurons against programmed cell death. *Neuron*, **14**, 927-939.

Han,P.J., Shukla,S., Subramanian,P.S. & Hoffman,P.N. (2004) Cyclic AMP elevates tubulin expression without increasing intrinsic axon growth capacity. *Exp.Neurol.*, **189**, 293-302.

Hanisch,U. (2002) Microglia as a source of cytokines. *Glia*, **40**, 140-155.

Harada,F., Hoshino,N., Hanada,K., Kawano,Y., Atsumi,Y., Wakisaka,S. & Maeda,T. (2003) The involvement of brain-derived neurotrophic factor (BDNF) in the regeneration of periodontal Ruffini endings following transection of the inferior alveolar nerve. *Arch.Histol.Cytol.*, **66**, 183-194.

Harel,N.Y. & Strittmatter,S.M. (2006) Can regenerating axons recapitulate developmental guidance during recovery from spinal cord injury? *Nat.Rev.Neurosci.*, **7**, 603-616.

Hartman,M.G., Lu,D., Kim,M.L., Kociba,G.J., Shukri,T., Buteau,J., Wang,X., Frankel,W.L., Guttridge,D., Prentki,M., Grey,S.T., Ron,D. & Hai,T. (2004) Role for activating transcription factor 3 in stress-induced beta-cell apoptosis. *Mol.Cell Biol.*, **24**, 5721-5732.

Hartmann,U. & Maurer,P. (2001) Proteoglycans in the nervous system--the quest for functional roles in vivo. *Matrix Biol.*, **20**, 23-35.

Hashimoto,M., Ino,H., Koda,M., Murakami,M., Yoshinaga,K., Yamazaki,M. & Moriya,H. (2004) Regulation of semaphorin 3A expression in neurons of the rat spinal cord and cerebral cortex after transection injury. *Acta Neuropathol.(Berl).*, **107**, 250-256.

He,Q., Dent,E.W. & Meiri,K.F. (1997) Modulation of actin filament behavior by GAP-43 (neuromodulin) is dependent on the phosphorylation status of serine 41, the protein kinase C site. *J.Neurosci.*, **17** 3515-24.

Heimburger,R.F. (2005) Return of function after spinal cord transection. *Spinal Cord.*, **43**, 438-440.

Herdegen,T., Blume,A., Buschmann,T., Georgakopoulos,E., Winter,C., Schmid,W., Hsieh,T.F., Zimmermann,M. & Gass,P. (1997a) Expression of activating transcription factor-2, serum response factor and cAMP/Ca response element binding protein in the

adult rat brain following generalized seizures, nerve fibre lesion and ultraviolet irradiation. *Neuroreport.*, **81**, 199-212.

Herdegen,T., Kovary,K., Leah,J.D. & Bravo,R. (1991) Specific temporal and spatial distribution of Jun, Fos, and Krox-24 proteins in spinal neurons following noxious transsynaptic stimulation. *J.Comp.Neurol.*, **313**, 178-191.

Herdegen,T. & Leah,J.D. (1998) Inducible and constitutive transcription factors in the mammalian nervous system: control of gene expression by Jun, Fos and Krox, and CREB/ATF proteins. .*Brain Res.Brain Res.Rev.*, **28**, 370-490.

Herdegen,T., Skene,P. & Bahr,M. (1997b) The c-Jun transcription factor--bipotential mediator of neuronal death, survival and regeneration. *Trends Neurosci.*, **20**, 227-231.

Hermanns,S. & Werner,M.H. (2001) Preservation and detection of lesion-induced collagenous scar in the CNS depend on the method of tissue processing. *Brain Res.Brain Res.Protoc.*, **7**, 162-167.

Heumann,R., Korsching,S., Bandtlow,C. & Thoenen,H. (1987) Changes of nerve growth factor synthesis in nonneuronal cells in response to sciatic nerve transection. *J.Cell Biol.*, **104**, 1623-1631.

Hiebert,G.W., Khodarahmi,K., McGraw,J., Steeves,J.D. & Tetzlaff,W. (2002) Brain-derived neurotrophic factor applied to the motor cortex promotes sprouting of corticospinal fibers but not regeneration into a peripheral nerve transplant. *J.Neurosci.Res.*, **69**, 160-168.

Hikawa,N. & Takenaka,T. (1996) Myelin-stimulated macrophages release neurotrophic factors for adult dorsal root ganglion neurons in culture. *Cell Mol.Neurobiol.*, **16**, 517-528.

Himi,T., Okazaki,T., Wang,H., McNeill,T.H. & Mori,N. (1994) Differential localization of SCG10 and p19/stathmin messenger RNAs in adult rat brain indicates distinct roles for these growth- associated proteins. *Neuroreport.*, **60**, 907-926.

Hirata,K., He,J., Hirakawa,Y., Liu,W., Wang,S. & Kawabuchi,M. (2003) HSP27 is markedly induced in Schwann cell columns and associated regenerating axons. *Glia.*, **42**, 1-11.

Hirsch,S. & Bahr,M. (1999) Immunocytochemical characterization of reactive optic nerve astrocytes and meningeal cells. *Glia*, **26**, 36-46.

Hirsch,S., Labes,M. & Bahr,M. (2000) Changes in BDNF and neurotrophin receptor expression in degenerating and regenerating rat retinal ganglion cells. *Restor.Neurol.Neurosci.*, **17**, 125-134.

Hoffman,P.N., Cleveland,D.W., Griffin,J.W., Landes,P.W., Cowan,N.J. & Price,D.L. (1987) Neurofilament gene expression: a major determinant of axonal caliber. *Proc.Natl.Acad.Sci.U.S.A*, **84**, 3472-3476.

Hoffman,P.N., Kosik,K.S., Orecchio,L.D., Bruns,G.A., Benowitz,L.I., MacDonald,G.P., Cox,D.R. & Neve,R.L. (1988) Expression of GAP-43, a rapidly transported growth-associated protein, and class II beta tubulin, a slowly transported cytoskeletal protein, are coordinated in regenerating neurons Human GAP-43: its deduced amino acid sequence and chromosomal localization in mouse and human. *J.Neurosci.*, **1**, 127-132.

Hoke,A. (2006) Mechanisms of Disease: what factors limit the success of peripheral nerve regeneration in humans? *Nat.Clin.Pract.Neurol.*, **2**, 448-454.

Hoke,A., Ho,T., Crawford,T.O., LeBel,C., Hilt,D. & Griffin,J.W. (2003) Glial cell line-derived neurotrophic factor alters axon schwann cell units and promotes myelination in unmyelinated nerve fibers. *J.Neurosci.*, **23**, 561-567.

Horie,H., Inagaki,Y., Sohma,Y., Nozawa,R., Okawa,K., Hasegawa,M., Muramatsu,N., Kawano,H., Horie,M., Koyama,H., Sakai,I., Takeshita,K., Kowada,Y., Takano,M. & Kadoya,T. (1999) Galectin-1 regulates initial axonal growth in peripheral nerves after axotomy. *J.Neurosci.*, **19**, 9964-9974.

Horie,H., Kadoya,T., Hikawa,N., Sango,K., Inoue,H., Takeshita,K., Asawa,R., Hiroi,T., Sato,M., Yoshioka,T. & Ishikawa,Y. (2004) Oxidized galectin-1 stimulates macrophages to promote axonal regeneration in peripheral nerves after axotomy. *J.Neurosci.*, **24**, 1873-1880.

Horner,P.J., Power,A.E., Kempermann,G., Kuhn,H.G., Palmer,T.D., Winkler,J., Thal,L.J. & Gage,F.H. (2000) Proliferation and differentiation of progenitor cells throughout the intact adult rat spinal cord. *J.Neurosci.*, **20**, 2218-2228.

Houle,J.D., Tom,V.J., Mayes,D., Wagoner,G., Phillips,N. & Silver,J. (2006) Combining an autologous peripheral nervous system "bridge" and matrix modification by chondroitinase allows robust, functional regeneration beyond a hemisection lesion of the adult rat spinal cord. *J.Neurosci.*, **26**, 7405-7415.

Hu,B., Yip,H.K. & So,K.F. (1999) Expression of p75 neurotrophin receptor in the injured and regenerating rat retina. *Neurorep.*, **10**, 1293-1297.

Hu,P. & McLachlan,E.M. (2002) Macrophage and lymphocyte invasion of dorsal root ganglia after peripheral nerve lesions in the rat. *Neuroreport.*, **112**, 23-38.

Hu,Y., Cui,Q. & Harvey,A.R. (2007) Interactive effects of C3, cyclic AMP and ciliary neurotrophic factor on adult retinal ganglion cell survival and axonal regeneration. *Mol.Cell Neurosci.*, **34**, 88-98.

Huang,H., Chen,L., Wang,H., Xiu,B., Li,B., Wang,R., Zhang,J., Zhang,F., Gu,Z., Li,Y., Song,Y., Hao,W., Pang,S. & Sun,J. (2003) Influence of patients' age on functional

recovery after transplantation of olfactory ensheathing cells into injured spinal cord injury. *Chin Med.J.(Engl.)*, **116**, 1488-1491.

Huang,J.K., Phillips,G.R., Roth,A.D., Pedraza,L., Shan,W., Belkaid,W., Mi,S., Fex-Svenningsen,A., Florens,L., Yates,J.R., III & Colman,D.R. (2005) Glial membranes at the node of Ranvier prevent neurite outgrowth. *Science*, **310**, 1813-1817.

Huang,Z.J., Kirkwood,A., Pizzorusso,T., Porciatti,V., Morales,B., Bear,M.F., Maffei,L. & Tonegawa,S. (1999) BDNF regulates the maturation of inhibition and the critical period of plasticity in mouse visual cortex. *Cell*, **98**, 739-755.

Huber,A.B., Kolodkin,A.L., Ginty,D.D. & Cloutier,J.F. (2003) Signaling at the growth cone: ligand-receptor complexes and the control of axon growth and guidance. *Annu.Rev.Neurosci.*, **26**, 509-563.

Huber,A.B., Weinmann,O., Brosamle,C., Oertle,T. & Schwab,M.E. (2002) Patterns of Nogo mRNA and protein expression in the developing and adult rat and after CNS lesions. *J.Neurosci.*, **22**, 3553-3567.

Hull,M. & Bahr,M. (1994) Regulation of immediate-early gene expression in rat retinal ganglion cells after axotomy and during regeneration through a peripheral nerve graft. *J.Neurobiol.*, **25**, 92-105.

Hunt, D., Coffin, R., and Anderson, P. N. (2002a) The Nogo receptor, its ligands and axonal regeneration in the spinal cord: a review. Journal of Neurocytology 31, 93-120..

Hunt,D., Mason,M.R.J., Campbell,G., Coffin,R. & Anderson,P.N. (2002b) Nogo receptor mRNA expression in intact and regenerating CNS neurons. *Mol.Cell Neurosci.*, **20**, 537-552.

Hunt, D., Coffin, R. S., Prinjha, R. K., Campbell, G., and Anderson, P. N. (2003) Nogo-A expression in the intact and injured nervous system. Molecular and Cellular Neuroscience **24** (4), 1083-10102.

Hunt,D., Hossain-Ibrahim,K., Mason,M.R., Coffin,R.S., Lieberman,A.R., Winterbottom,J. & Anderson,P.N. (2004) ATF3 upregulation in glia during Wallerian degeneration: differential expression in peripheral nerves and CNS white matter. *BMC.Neurosci.*, **5**, 9.

Inoue,K., Zama,T., Kamimoto,T., Aoki,R., Ikeda,Y., Kimura,H. & Hagiwara,M. (2004) TNFalpha-induced ATF3 expression is bidirectionally regulated by the JNK and ERK pathways in vascular endothelial cells. *Genes Cells.*, **9**, 59-70.

Itoh,K., Fushiki,S., Kamiguchi,H., Arnold,B., Altevogt,P. & Lemmon,V. (2005) Disrupted Schwann cell-axon interactions in peripheral nerves of mice with altered L1-integrin interactions. *Mol.Cell Neurosci.*, **30**, 624-629.

Iwamasa,H., Ohta,K., Yamada,T., Ushijima,K., Terasaki,H. & Tanaka,H. (1999) Expression of Eph receptor tyrosine kinases and their ligands in chick embryonic motor neurons and hindlimb muscles. *Dev.Growth Differ.*, **41**, 685-698.

Jabbar,S., Harada,F., Aita,M., Ohishi,M., Saito,I., Kawano,Y., Suzuki,A., Nozawa-Inoue,K. & Maeda,T. (2007) Involvement of neurotrophin-4/5 in regeneration of the periodontal Ruffini endings at the early stage. *J.Comp Neurol.*, **501** (3), 400-412.

Jacob,J., Haspel,J., Kane-Goldsmith,N. & Grumet,M. (2002) L1 mediated homophilic binding and neurite outgrowth are modulated by alternative splicing of exon 2. *J.Neurobiol.*, **51**, 177-189.

Jain,A., Brady-Kalnay,S.M. & Bellamkonda,R.V. (2004) Modulation of Rho GTPase activity alleviates chondroitin sulfate proteoglycan-dependent inhibition of neurite extension. *J.Neurosci.Res.*, **77**, 299-307.

Jakeman,L.B., Chen,Y., Lucin,K.M. & McTigue,D.M. (2006) Mice lacking L1 cell adhesion molecule have deficits in locomotion and exhibit enhanced corticospinal tract sprouting following mild contusion injury to the spinal cord. *Eur.J.Neurosci.*, **23**, 1997-2011.

James H.Breasted (1930) *The Edwin Smith Surgical Papyrus. Published in Facsimile and Hieroglyphic Transliteration with Translation and Commentary in Two Volumes* University of Chicago Press, Chicago.

Jenkins,R. & Hunt,S.P. (1991) Long-term increase in the levels of c-jun mRNA and jun protein-like immunoreactivity in motor and sensory neurons following axon damage. *Neurosci.Lett.*, **129**, 107-110.

Jenkins,R., McMahon,S.B., Bond,A.B. & Hunt,S.P. (1993a) Expression of c-Jun as a response to dorsal root and peripheral nerve section in damaged and adjacent intact primary sensory neurons in the rat. *Eur.J.Neurosci.*, **5**, 751-759.

Jenkins,R., Tetzlaff,W. & Hunt,S.P. (1993b) Differential expression of immediate early genes in rubrospinal neurons following axotomy in rat. *Eur.J.Neurosci.*, **5**, 203-209.

Ji,B., Li,M., Wu,W.T., Yick,L.W., Lee,X., Shao,Z., Wang,J., So,K.F., McCoy,J.M., Pepinsky,R.B., Mi,S. & Relton,J.K. (2006) LINGO-1 antagonist promotes functional recovery and axonal sprouting after spinal cord injury. *Mol.Cell Neurosci.*, **33**, 311-320.

Jiao,J., Huang,X., Feit-Leithman,R.A., Neve,R.L., Snider,W., Dartt,D.A. & Chen,D.F. (2005) Bcl-2 enhances Ca(2+) signaling to support the intrinsic regenerative capacity of CNS axons. *EMBO J.*, **24**, 1068-1078.

Jin,S.L., Richard,F.J., Kuo,W.P., D'Ercole,A.J. & Conti,M. (1999) Impaired growth and fertility of cAMP-specific phosphodiesterase PDE4D-deficient mice. *Proc.Natl.Acad.Sci.U.S.A.*, **96**, 11998-12003.

Johnson,P.W., bramow-Newerly,W., Seilheimer,B., Sadoul,R., Tropak,M.B., Arquint,M., Dunn,R.J., Schachner,M. & Roder,J.C. (1989) Recombinant myelin-associated glycoprotein confers neural adhesion and neurite outgrowth function. *Neuron*, **3**, 377-385.

Jonakait,G.M., Luskin,M.B., Wei,R., Tian,X.F. & Ni,L. (1996) Conditioned medium from activated microglia promotes cholinergic differentiation in the basal forebrain in vitro. *Dev.Biol.*, **177**, 85-95.

Jones,K.R. & Reichardt,L.F. (1990) Molecular cloning of a human gene that is a member of the nerve growth factor family. *Proc.Natl.Acad.Sci.U.S.A*, **87**, 8060-8064.

Jones,L.L., Sajed,D. & Tuszynski,M.H. (2003) Axonal regeneration through regions of chondroitin sulfate proteoglycan deposition after spinal cord injury: a balance of permissiveness and inhibition. *J.Neurosci.*, **23**, 9276-9288.

Jones,L.L., Yamaguchi,Y., Stallcup,W.B. & Tuszynski,M.H. (2002) NG2 is a major chondroitin sulfate proteoglycan produced after spinal cord injury and is expressed by macrophages and oligodendrocyte progenitors. *J.Neurosci.*, **22**, 2792-2803.

Josephson,A., Widenfalk,J., Widmer,H.W., Olson,L. & Spenger,C. (2001) NOGO mRNA expression in adult and fetal human and rat nervous tissue and in weight drop injury. *Exp.Neurol.*, **169**, 319-328.

Jung,M., Pesheva,P., Schachner,M. & Trotter,J. (1993) Astrocytes and neurons regulate the expression of the neural recognition molecule janusin by cultured oligodendrocytes. *Glia*, **9**, 163-175.

Kalcheim,C., Carmeli,C. & Rosenthal,A. (1992) Neurotrophin 3 is a mitogen for cultured neural crest cells. *Proc.Natl.Acad.Sci.U.S.A.*, **89**, 1661-1665.

Kalla,R., Liu,Z., Xu,S., Koppius,A., Imai,Y., Kloss,C.U., Kohsaka,S., Gschwendtner,A., Moller,J.C., Werner,A. & Raivich,G. (2001) Microglia and the early phase of immune surveillance in the axotomized facial motor nucleus: impaired microglial activation and lymphocyte recruitment but no effect on neuronal survival or axonal regeneration in macrophage-colony stimulating factor-deficient mice. *J.Comp Neurol.*, **436**, 182-201.

Kaneko,S., Iwanami,A., Nakamura,M., Kishino,A., Kikuchi,K., Shibata,S., Okano,H.J., Ikegami,T., Moriya,A., Konishi,O., Nakayama,C., Kumagai,K., Kimura,T., Sato,Y., Goshima,Y., Taniguchi,M., Ito,M., He,Z., Toyama,Y. & Okano,H. (2006) A selective Sema3A inhibitor enhances regenerative responses and functional recovery of the injured spinal cord. *Nat.Med.*, **12**, 1380-1389.

Kantor,D.B., Chivatakarn,O., Peer,K.L., Oster,S.F., Inatani,M., Hansen,M.J., Flanagan,J.G., Yamaguchi,Y., Sretavan,D.W., Giger,R.J. & Kolodkin,A.L. (2004) Semaphorin 5A is a bifunctional axon guidance cue regulated by heparan and chondroitin sulfate proteoglycans. *Neuron*, **44**, 961-975.

Karram,K., Chatterjee,N. & Trotter,J. (2005) NG2-expressing cells in the nervous system: role of the proteoglycan in migration and glial-neuron interaction. *J.Anat.*, **207**, 735-744.

Kartje,G.L., Schulz,M.K., Lopez-Yunez,A., Schnell,L. & Schwab,M.E. (1999) Corticostriatal plasticity is restricted by myelin-associated neurite growth inhibitors in the adult rat. *Ann.Neurol.*, **45**, 778-786.

Kerjan,G., Dolan,J., Haumaitre,C., Schneider-Maunoury,S., Fujisawa,H., Mitchell,K.J. & Chedotal,A. (2005) The transmembrane semaphorin Sema6A controls cerebellar granule cell migration. *Nat.Neurosci.*, **8**, 1516-1524.

Kim,B.G., Dai,H.N., Lynskey,J.V., McAtee,M. & Bregman,B.S. (2006) Degradation of chondroitin sulfate proteoglycans potentiates transplant-mediated axonal remodeling and functional recovery after spinal cord injury in adult rats. *J.Comp Neurol.*, **497**, 182-198.

Kim,J.E., Li,S., GrandPre,T., Qiu,D. & Strittmatter,S.M. (2003) Axon regeneration in young adult mice lacking nogo-a/b. *Neuron*, **38**, 187-199.

Kim,J.E., Liu,B.P., Park,J.H. & Strittmatter,S.M. (2004) Nogo-66 receptor prevents raphespinal and rubrospinal axon regeneration and limits functional recovery from spinal cord injury. *Neuron*, **44**, 439-451.

Kimelberg,H.K. (2004) The problem of astrocyte identity. *Neurochem.Int.*, **45**, 191-202.

Kinnman,E. & Aldskogius,H. (1986) Collateral sprouting of sensory axons in the glabrous skin of the hindpaw after chronic sciatic lesion in adult and neonatal rats: a morphological study. *Brain Res.*, **377**, 73-82.

Kinnman,E., Aldskogius,H., Johansson,O. & Wiesenfeld-Hallin,Z. (1992) Collateral reinnervation and expansive regenerative reinnervation by sensory axons into "foreign" denervated skin: an immunohistochemical study in the rat. *Exp.Brain Res.*, **91**, 61-72.

Kiryushko,D., Berezin,V. & Bock,E. (2004) Regulators of neurite outgrowth: role of cell adhesion molecules. *Ann.N.Y.Acad.Sci.*, **1014**, 140-154.

Klein,M.A., Moller,J.C., Jones,L.L., Bluethmann,H., Kreutzberg,G.W. & Raivich,G. (1997) Impaired neuroglial activation in interleukin-6 deficient mice. *Glia*, **19**, 227-233.

Kloss,C.U., Bohatschek,M., Kreutzberg,G.W. & Raivich,G. (2001) Effect of lipopolysaccharide on the morphology and integrin immunoreactivity of ramified microglia in the mouse brain and in cell culture. *Exp.Neurol.*, **168**, 32-46.

Knoller,N., Auerbach,G., Fulga,V., Zelig,G., Attias,J., Bakimer,R., Marder,J.B., Yoles,E., Belkin,M., Schwartz,M. & Hadani,M. (2005) Clinical experience using incubated autologous macrophages as a treatment for complete spinal cord injury: phase I study results. *J.Neurosurg.Spine*, **3**, 173-181.

Koeberle,P.D. & Bahr,M. (2004) Growth and guidance cues for regenerating axons: where have they gone? *J.Neurobiol.*, **59**, 162-180.

Koprivica,V., Cho,K.S., Park,J.B., Yiu,G., Atwal,J., Gore,B., Kim,J.A., Lin,E., Tessier-Lavigne,M., Chen,D.F. & He,Z. (2005) EGFR activation mediates inhibition of axon regeneration by myelin and chondroitin sulfate proteoglycans. *Science*, **310**, 106-110.

Korsching,S. & Thoenen,H. (1983) Quantitative demonstration of the retrograde axonal transport of endogenous nerve growth factor. *Neurosci.Lett.*, **30**, 1-4.

Korsching,S. & Thoenen,H. (1985) Nerve growth factor supply for sensory neurons: site of origin and competition with the sympathetic nervous system. *Neurosci.Lett.*, **54**, 201-205.

Kottis,V., Thibault,P., Mikol,D., Xiao,Z.C., Zhang,R., Dergham,P. & Braun,P.E. (2002) Oligodendrocyte-myelin glycoprotein (OMgp) is an inhibitor of neurite outgrowth. *J.Neurochem.*, **82**, 1566-1569.

Kovalchuk,Y., Hanse,E., Kafitz,K.W. & Konnerth,A. (2002) Postsynaptic Induction of BDNF-Mediated Long-Term Potentiation. *Science*, **295**, 1729-1734.

Krause,W. & Kuhne,G. (1988) Pharmacokinetics of rolipram in the rhesus and cynomolgus monkeys, the rat and the rabbit. Studies on species differences. *Xenobiotica.*, **18**, 561-571.

Kreutzberg,G.W. (1996) Microglia: a sensor for pathological events in the CNS. *Trends Neurosci.*, **19**, 312-318.

Kreutzberg,G.W. & Barron,K.D. (1978) 5'-Nucleotidase of microglial cells in the facial nucleus during axonal reaction. *J.Neurocytol.*, **7**, 601-610.

Krikorian,J.G., Guth,L. & Donati,E.J. (1981) Origin of the connective tissue scar in the transected rat spinal cord. *Exp.Neurol.*, **72**, 698-707.

Kullander,K., Croll,S.D., Zimmer,M., Pan,L., McClain,J., Hughes,V., Zabski,S., DeChiara,T.M., Klein,R., Yancopoulos,G.D. & Gale,N.W. (2001) Ephrin-B3 is the midline barrier that prevents corticospinal tract axons from recrossing, allowing for unilateral motor control. *Genes Dev.*, **15**, 877-888.

Kullander,K. & Klein,R. (2002) Mechanisms and functions of Eph and ephrin signalling. *Nat.Rev.Mol.Cell Biol.*, **3**, 475-486.

Kwon,B.K., Liu,J., Lam,C., Plunet,W., Oschipok,L.W., Hauswirth,W., Di,P.A., Blesch,A. & Tetzlaff,W. (2007) Brain-derived neurotrophic factor gene transfer with adeno-associated viral and lentiviral vectors prevents rubrospinal neuronal atrophy and stimulates regeneration-associated gene expression after acute cervical spinal cord injury. *Spine.*, **32**, 1164-1173.

Kwon,B.K., Liu,J., Messerer,C., Kobayashi,N.R., McGraw,J., Oschipok,L. & Tetzlaff,W. (2002) Survival and regeneration of rubrospinal neurons 1 year after spinal cord injury. *Proc.Natl.Acad.Sci.U.S.A.*, **99**, 3246-3251.

Kwon,B.K., Liu,J., Oschipok,L., Teh,J., Liu,Z.W. & Tetzlaff,W. (2004) Rubrospinal neurons fail to respond to brain-derived neurotrophic factor applied to the spinal cord injury site 2 months after cervical axotomy. *Exp.Neurol.*, **189**, 45-57.

Laflamme,N. & Rivest,S. (2001) Toll-like receptor 4: the missing link of the cerebral innate immune response triggered by circulating gram-negative bacterial cell wall components. *FASEB J.*, **15**, 155-163.

Landolt,R.M., Vaughan,L., Winterhalter,K.H. & Zimmermann,D.R. (1995) Versican is selectively expressed in embryonic tissues that act as barriers to neural crest cell migration and axon outgrowth. *Development*, **121**, 2303-2312.

Lauren,J., Airaksinen,M.S., Saarma,M. & Timmusk,T. (2003) Two novel mammalian Nogo receptor homologs differentially expressed in the central and peripheral nervous systems. *Mol.Cell Neurosci.*, **24**, 581-594.

Laux,T., Fukami,K., Thelen,M., Golub,T., Frey,D. & Caroni,P. (2000) GAP43, MARCKS, and CAP23 modulate PI(4,5)P(2) at plasmalemmal rafts, and regulate cell cortex actin dynamics through a common mechanism. *J.Cell Biol.*, **149**, 1455-1472.

Laywell,E.D., Dorries,U., Bartsch,U., Faissner,A., Schachner,M. & Steindler,D.A. (1992) Enhanced expression of the developmentally regulated extracellular matrix molecule tenascin following adult brain injury. *Proc.Natl.Acad.Sci.U.S.A.*, **89**, 2634-2638.

Lazar,D.A., Ellegala,D.B., Avellino,A.M., Dailey,A.T., Andrus,K. & Kliot,M. (1999) Modulation of macrophage and microglial responses to axonal injury in the peripheral and central nervous systems. *Neurosurgery*, **45**, 593-600.

Lazarov Spiegler,O., Solomon,A.S., Zeev Brann,A.B., Hirschberg,D.L., Lavie,V. & Schwartz,M. (1996) Transplantation of activated macrophages overcomes central nervous system regrowth failure. *FASEB J.*, **10**, 1296-1302.

Lee,J.K., Kim,J.E., Sivula,M. & Strittmatter,S.M. (2004) Nogo receptor antagonism promotes stroke recovery by enhancing axonal plasticity. *J.Neurosci.*, **24**, 6209-6217.

Lee,Y.B., Nagai,A. & Kim,S.U. (2002) Cytokines, chemokines, and cytokine receptors in human microglia. *J.Neurosci.Res.*, **69**, 94-103.

Lehmann,M., Fournier,A., Selles-Navarro,I., Dergham,P., Sebok,A., Leclerc,N., Tigyi,G. & McKerracher,L. (1999) Inactivation of Rho signaling pathway promotes CNS axon regeneration. *J.Neurosci.*, **19**, 7537-7547.

Lehnardt,S., Massillon,L., Follett,P., Jensen,F.E., Ratan,R., Rosenberg,P.A., Volpe,J.J. & Vartanian,T. (2003) Activation of innate immunity in the CNS triggers neurodegeneration through a Toll-like receptor 4-dependent pathway. *Proc.Natl.Acad.Sci.U.S.A*, **100**, 8514-8519.

Leon,S., Yin,Y., Nguyen,J., Irwin,N. & Benowitz,L.I. (2000) Lens injury stimulates axon regeneration in the mature rat optic nerve. *J.Neuroscience*, **20**, 4615-4626.

Letourneau,P.C. & Ressler,A.H. (1984) Inhibition of neurite initiation and growth by taxol. *J.Cell Biol.*, **98**, 1355-1362.

Levi-Montalcini,R. & Hamburger,V. (1951) Selective growth stimulating effects of mouse sarcoma on the sensory and sympathetic nervous system of the chick embryo. *J.Exp.Zool.*, **116**, 321-361.

Levine,J.M. (1994) Increased expression of the NG2 chondroitin-sulfate proteoglycan after brain injury. *J.Neurosci.*, **14**, 4716-4730.

Levine,J.M., Reynolds,R. & Fawcett,J.W. (2001) The oligodendrocyte precursor cell in health and disease. *Trends Neurosci.*, **24**, 39-47.

Lewis,S.E., Mannion,R.J., White,F.A., Coggeshall,R.E., Beggs,S., Costigan,M., Martin,J.L., Dillmann,W.H. & Woolf,C.J. (1999) A role for HSP27 in sensory neuron survival. *J.Neurosci.*, **19**, 8945-8953.

Li,M., Shibata,A., Li,C., Braun,P.E., McKerracher,L., Roder,J., Kater,S.B. & David,S. (1996) Myelin-associated glycoprotein inhibits neurite/axon growth and causes growth cone collapse. *J.Neurosci.Res.*, **46**, 404-414.

Li,S., Liu,B.P., Budel,S., Li,M., Ji,B., Walus,L., Li,W., Jirik,A., Rabacchi,S., Choi,E., Worley,D., Sah,D.W., Pepinsky,B., Lee,D., Relton,J. & Strittmatter,S.M. (2004) Blockade of Nogo-66, myelin-associated glycoprotein, and oligodendrocyte myelin glycoprotein by soluble Nogo-66 receptor promotes axonal sprouting and recovery after spinal injury. *J.Neurosci.*, **24**, 10511-10520.

Li,Y., Decherchi,P. & Raisman,G. (2003) Transplantation of olfactory ensheathing cells into spinal cord lesions restores breathing and climbing. *J.Neurosci.*, **23**, 727-731.

Li,Y., Field,P.M. & Raisman,G. (1997) Repair of adult rat corticospinal tract by transplants of olfactory ensheathing cells. *Science*, **277**, 2000-2002.

Li,Y., Field,P.M. & Raisman,G. (1999) Death of oligodendrocytes and microglial phagocytosis of myelin precede immigration of Schwann cells into the spinal cord. *J.Neurocytol.*, **28**, 417-427.

Li,Y., Field,P.M. & Raisman,G. (2005) Olfactory ensheathing cells and olfactory nerve fibroblasts maintain continuous open channels for regrowth of olfactory nerve fibres. *Glia.*, **52**, 245-251.

Li,Y. & Raisman,G. (1995) Sprouts from cut corticospinal axons persist in the presence of astrocytic scarring in long-term lesions of the adult rat spinal cord. *Exp.Neurol.*, **134**, 102-111.

Lieberman,A.R. (1971) The axon reaction: a review of the principal features of perikaryal responses to axon injury. *Int.Rev.Neurobiol.*, **14**, 49-124.

Liebl,D.J., Morris,C.J., Henkemeyer,M. & Parada,L.F. (2003) mRNA expression of ephrins and Eph receptor tyrosine kinases in the neonatal and adult mouse central nervous system. *J.Neurosci.Res.*, **71**, 7-22.

Liebscher,T., Schnell,L., Schnell,D., Scholl,J., Schneider,R., Gullo,M., Fouad,K., Mir,A., Rausch,M., Kindler,D., Hamers,F.P. & Schwab,M.E. (2005) Nogo-A antibody improves regeneration and locomotion of spinal cord-injured rats. *Ann.Neurol.*, **58**, 706-719.

Lima,C., Pratas-Vital,J., Escada,P., Hasse-Ferreira,A., Capucho,C. & Peduzzi,J.D. (2006) Olfactory mucosa autografts in human spinal cord injury: a pilot clinical study. *J.Spinal Cord.Med.*, **29**, 191-203.

Lin,S.C. & Bergles,D.E. (2002) Physiological characteristics of NG2-expressing glial cells. *J.Neurocytol.*, **31**, 537-549.

Lin,S.C. & Bergles,D.E. (2004) Synaptic signaling between neurons and glia. *Glia*, **47**, 290-298.

Lindholm,D., Neumann,R., Meyer,M. & Thoenen,H. (1987) Interleukin-1 regulates synthesis of nerve growth factor in non- neuronal cells of rat sciatic nerve. *Nature*, **330**, 658-659.

Lindholm,D., Neumann,R., Meyer,M. & Thoenen,H. (1987) Interleukin-1 regulates synthesis of nerve growth factor in non- neuronal cells of rat sciatic nerve. *Nature*, **330**, 658-659.

Lindholm,T., Skold,M.K., Suneson,A., Carlstedt,T., Cullheim,S. & Risling,M. (2004) Semaphorin and neuropilin expression in motoneurons after intraspinal motoneuron axotomy. *Neuroreport.*, **15**, 649-654.

Lindsay,R.M. (1988) Nerve growth factors (NGF, BDNF) enhance axonal regeneration but are not required for survival of adult sensory neurones. *J.Neurosci.*, **8**, 2394-2405.

Ling,E.A., Ng,Y.K., Wu,C.H. & Kaur,C. (2001) Microglia: its development and role as a neuropathology sensor. *Prog.Brain Res.*, **132**, 61-79.

Ling,E.A. & Wong,W.C. (1993) The origin and nature of ramified and amoeboid microglia: a historical review and current concepts. *Glia*, **7**, 9-18.

Linnarsson,S., Willson,C.A. & Ernfors,P. (2000) Cell death in regenerating populations of neurons in BDNF mutant mice. *Brain Res.Mol.Brain Res.*, **75**, 61-69.

Lips,K., Stichel,C.C. & Muller,H.W. (1995) Restricted appearance of tenascin and chondroitin sulphate proteoglycans after transection and sprouting of adult rat postcommissural fornix. *J.Neurocytol.*, **24**, 449-464.

Lipson,A.C., Widenfalk,J., Lindqvist,E., Ebendal,T. & Olson,L. (2003) Neurotrophic properties of olfactory ensheathing glia. *Exp.Neurol.*, **180**, 167-171.

Liu,Y., Kim,D., Himes,B.T., Chow,S.Y., Schallert,T., Murray,M., Tessler,A. & Fischer,I. (1999) Transplants of fibroblasts genetically modified to express BDNF promote regeneration of adult rat rubrospinal axons and recovery of forelimb function. *J.Neurosci.*, **19**, 4370-4387.

Liuzzi,F.J. & Lasek,R.J. (1987) Astrocytes block axonal regeneration in mammals by activating the physiological stop mechanism. *Science*, **237**, 642-645.

Loewy,A.D. & Schader,R.E. (1977) A quantitative study of retrograde neuronal changes in Clarke's column. *J.Comp Neurol.*, **171**, 65-81.

Logan,A., Ahmed,Z., Baird,A., Gonzalez,A.M. & Berry,M. (2006) Neurotrophic factor synergy is required for neuronal survival and disinhibited axon regeneration after CNS injury. *Brain.*, **129**, 490-502.

Logan,A., Baird,A. & Berry,M. (1999) Decorin attenuates gliotic scar formation in the rat cerebral hemisphere. *Exp.Neurol.*, **159**, 504-510.

Lorber,B., Berry,M. & Logan,A. (2005) Lens injury stimulates adult mouse retinal ganglion cell axon regeneration via both macrophage- and lens-derived factors. *Eur.J.Neurosci.*, **21**, 2029-2034.

Lorber,B., Berry,M., Logan,A. & Tonge,D. (2002) Effect of lens lesion on neurite outgrowth of retinal ganglion cells in vitro. *Mol.Cell Neurosci.*, **21**, 301-311.

Low,K., Orberger,G., Schmitz,B., Martini,R. & Schachner,M. (1994) The L2/HNK-1 carbohydrate is carried by the myelin associated glycoprotein and sulphated glucuronyl glycolipids in muscle but not cutaneous nerves of adult mice. *Eur.J.Neurosci.*, **6**, 1773-1781.

Lu,J., Feron,F., Ho,S.M., kay-Sim,A. & Waite,P.M. (2001) Transplantation of nasal olfactory tissue promotes partial recovery in paraplegic adult rats. *Brain Res.*, **889**, 344-357.

Lu,J., Feron,F., kay-Sim,A. & Waite,P.M. (2002) Olfactory ensheathing cells promote locomotor recovery after delayed transplantation into transected spinal cord. *Brain.*, **125**, 14-21.

Lu,P., Jones,L.L., Snyder,E.Y. & Tuszynski,M.H. (2003) Neural stem cells constitutively secrete neurotrophic factors and promote extensive host axonal growth after spinal cord injury. *Exp.Neurol.*, **181**, 115-129.

Lu,P., Yang,H., Jones,L.L., Filbin,M.T. & Tuszynski,M.H. (2004) Combinatorial therapy with neurotrophins and cAMP promotes axonal regeneration beyond sites of spinal cord injury. *J.Neurosci.*, **24**, 6402-6409.

Lu,X. & Richardson,P.M. (1991) Inflammation near the nerve cell body enhances axonal regeneration. *J.Neurosci.*, **11**, 972-978.

Lu,X. & Richardson,P.M. (1993) Responses of macrophages in rat dorsal root ganglia following peripheral nerve injury. *J.Neurocytol.*, **22**, 334-341.

Lu,X. & Richardson,P.M. (1995) Changes in neuronal mRNAs induced by a local inflammatory reaction. *J.Neurosci.Res.*, **41**, 8-14.

Luckenbill-Edds,L. (1997) Laminin and the mechanism of neuronal outgrowth. *Brain Res.Brain Res.Rev.*, **23**, 1-27.

Ludvig,N., Mishra,P.K. & Jobe,P.C. (1992) Dibutyryl cyclic AMP has epileptogenic potential in the hippocampus of freely behaving rats: a combined EEG-intracerebral microdialysis study. *Neurosci.Lett.*, **%20;141**, 187-191.

Ludvig,N. & Moshe,S.L. (1987) Cyclic AMP derivatives injected into the inferior colliculus induce audiogenic seizure-like phenomena in normal rats. *Brain Res.*, **437**, 193-196.

Luk,H.W., Nobe,L.J., Werb, Z.(1993) Mocrophages contribute to the maintenance of stable regenerating neurites following peripheral nerve injury. *J.Neurosci Res.* **73** (5), 644-658.

Lunn,E.R., Perry,V.H., Brown,M.C., Rosen,H. & Gordon,S. (1989) Absence of Wallerian Degeneration does not Hinder Regeneration in Peripheral Nerve. *Eur.J.Neurosci.*, **1**, 27-33.

Lutjens,R., Igarashi,M., Pellier,V., Blasey,H., Di Paolo,G., Ruchti,E., Pfulg,C., Staple,J.K., Catsicas,S. & Grenningloh,G. (2000) Localization and targeting of SCG10 to the trans-Golgi apparatus and growth cone vesicles. *Eur.J.Neurosci.*, **12**, 2224-2234.

Lyons,W.E., Mamounas,L.A., Ricaurte,G.A., Coppola,V., Reid,S.W., Bora,S.H., Wihler,C., Koliatsos,V.E. & Tessarollo,L. (1999) Brain-derived neurotrophic factor-

deficient mice develop aggressiveness and hyperphagia in conjunction with brain serotonergic abnormalities. *Proc.Natl.Acad.Sci.U.S.A*, **96**, 15239-15244.

Ma,M., Basso,D.M., Walters,P., Stokes,B.T. & Jakeman,L.B. (2001) Behavioral and histological outcomes following graded spinal cord contusion injury in the C57Bl/6 mouse. *Exp.Neurol.*, **169**, 239-254.

Makagiansar,I.T., Williams,S., Dahlin-Huppe,K., Fukushi,J.I., Mustelin,T. & Stallcup,W.B. (2004) Phosphorylation of NG2 proteoglycan by PKC-alpha regulates polarized membrane distribution and cell motility. *J.Biol.Chem.*, **279**, 55262-55270.

Makwana,M. & Raivich,G. (2005) Molecular mechanisms in successful peripheral regeneration. *FEBS J.*, **272**, 2628-2638.

Martin,S., Levine,A.K., Chen,Z.J., Ughrin,Y. & Levine,J.M. (2001) Deposition of the NG2 proteoglycan at nodes of Ranvier in the peripheral nervous system. *J.Neurosci.*, **21**, 8119-8128.

Martin-Villalba,A., Winter,C., Brecht,S., Buschmann,T., Zimmermann,M. & Herdegen,T. (1998) Rapid and long-lasting suppression of the ATF-2 transcription factor is a common response to neuronal injury. *Brain Res.Mol.Brain Res.*, **62**, 158-166.

Martini,R. (1994) Expression and functional roles of neural cell surface molecules and extracellular matrix components during development and regeneration of peripheral nerves. *J.Neurocytol.*, **23**, 1-28.

Martini,R. & Schachner,M. (1988) Immunoelectron microscopic localization of neural cell adhesion molecules (L1, NCAM and myelin-associated glycoprotein) in regenerating adult mouse sciatic nerves. *J.Cell Biol.*, **106**, 1735-1746.

Martini,R., Schachner,M. & Brushart,T.M. (1994) The L2/HNK-1 carbohydrate is preferentially expressed by previously motor axon-associated Schwann cells in reinnervated peripheral nerves. *J.Neurosci.*, **14**, 7180-7191.

Martini,R., Schachner,M. & Faissner,A. (1990) Enhanced expression of the extracellular matrix molecule J1/tenascin in the regenerating adult mouse sciatic nerve. *J.Neurocytol.*, **19**, 601-616.

Mashima,T., Udagawa,S. & Tsuruo,T. (2001) Involvement of transcriptional repressor ATF3 in acceleration of caspase protease activation during DNA damaging agent-induced apoptosis. *J.Cell Physiol*, **188**, 352-358.

Mason,M.R.J., Campbell,G., Caroni,P., Anderson,P.N. & Lieberman,A.R. (2000) Overexpression of GAP-43 in thalamic projection neurons does not enable them to regenerate into peripheral nerve grafts. *Exp.Neurol.*, **165**, 143-152.

Mason,M.R.J., Lieberman,A.R. & Anderson,P.N. (2003) Corticospinal neurons upregulate a range of growth-associated genes following intracortical, but not spinal, axotomy. *Eur.J.Neurosci.*, **18**, 789-802.

Mason,M.R.J., Lieberman,A.R., Grenningloh,G. & Anderson,P.N. (2002) Transcriptional upregulation of SCG10 and CAP-23 is correlated with regeneration of the axons of peripheral and central neurons in vivo. *Mol.Cell Neurosci.*, **20**, 595-615.

Massey,J.M., Hubscher,C.H., Wagoner,M.R., Decker,J.A., Amps,J., Silver,J. & Onifer,S.M. (2006) Chondroitinase ABC digestion of the perineuronal net promotes functional collateral sprouting in the cuneate nucleus after cervical spinal cord injury. *J.Neurosci.*, **26**, 4406-4414.

Matsui,F., Nishizuka,M., Yasuda,Y., Aono,S., Watanabe,E. & Oohira,A. (1998) Occurrence of a N-terminal proteolytic fragment of neurocan, not a C-terminal half, in a perineuronal net in the adult rat cerebrum. .*Brain Res.*, **790**, 45-51.

Mazzoni,I.E. & Kenigsberg,R.L. (1997) Microglia from the developing rat medial septal area can affect cholinergic and GABAergic neuronal differentiation in vitro. *Neuroreport.*, **76**, 147-157.

McDonald,J.W. & Sadowsky,C. (2002) Spinal-cord injury. *Lancet.*, **359**, 417-425.

McGraw,J., McPhail,L.T., Oschipok,L.W., Horie,H., Poirier,F., Steeves,J.D., Ramer,M.S. & Tetzlaff,W. (2004) Galectin-1 in regenerating motoneurons. *Eur.J.Neurosci.*, **20**, 2872-2880.

McKeon,R.J., Schreiber,R.C., Rudge,J.S. & Silver,J. (1991) Reduction of neurite outgrowth in a model of glial scarring following CNS injury is correlated with the expression of inhibitory molecules on reactive astrocytes. *.J.Neurosci.*, **11**, 3398-3411.

McKerracher,L. (2002) Ganglioside rafts as MAG receptors that mediate blockade of axon growth. *Proc.Natl.Acad.Sci.U.S.A*, **99**, 7811-7813.

McKerracher,L., David,S., Jackson,D.L., Kottis,V., Dunn,R.J. & Braun,P.E. (1994) Identification of myelin-associated glycoprotein as a major myelin- derived inhibitor of neurite growth. *Neuron*, **13**, 805-811.

McQuarrie,I.G. (1978) The effect of a conditioning lesion on the regeneration of motor axons. *Brain Res.*, **152**, 597-602.

McTigue,D.M., Tripathi,R. & Wei,P. (2006) NG2 colocalizes with axons and is expressed by a mixed cell population in spinal cord lesions. *J.Neuropathol.Exp.Neurol.*, **65**, 406-420.

Meiners,S., Mercado,M.L., Nur-e-Kamal MS & Geller,H.M. Tenascin-C contains domains that independently regulate neurite outgrowth and neurite guidance. (1999) *J.Neurosci.* **19** (19), 8443-53.

Mesulam,M.M. & Brushart,T.M. (1979) Transganglionic and anterograde transport of horseradish peroxidase across dorsal root ganglia, a tetramethylbenzidine method for tracing central sensory connections of muscles and peripheral nerves. *Neurosci.Lett.*, **4**, 1107-1117.

Meyer,M., Matsuoka,I., Wetmore,C., Olson,L. & Thoenen,H. (1992) Enhanced synthesis of brain-derived neurotrophic factor in the lesioned peripheral nerve: different mechanisms are responsible for the regulation of BDNF and NGF mRNA. *J.Cell Biol.*, **119**, 45-54.

Mi,S., Lee,X., Shao,Z., Thill,G., Ji,B., Relton,J., Levesque,M., Allaire,N., Perrin,S., Sands,B., Crowell,T., Cate,R.L., McCoy,J.M. & Pepinsky,R.B. (2004) LINGO-1 is a component of the Nogo-66 receptor/p75 signaling complex. *Nat.Neurosci.*. **7** (3), 221-8.

Mikol,D.D., Gulcher,J.R. & Stefansson,K. (1990) The oligodendrocyte-myelin glycoprotein belongs to a distinct family of proteins and contains the HNK-1 carbohydrate. *J.Cell Biol.*, **110**, 471-479.

Miller,C., Tsatas,O. & David,S. (1994) Dibutyryl cAMP, interleukin-1 beta, and macrophage conditioned medium enhance the ability of astrocytes to promote neurite growth. *J.Neurosci.Res.*, **38**, 56-63.

Miller,F.D., Tetzlaff,W., Bisby,M.A., Fawcett,J.W. & Milner,R.J. (1989) Rapid induciton of the major embryonic α tubulin mRNA, Tα1, during nerve regeneration in adult rats. *J.Neurosci.*, **9**, 1452-1463.

Ming,G.L., Song,H.J., Berninger,B., Holt,C.E., Tessier-Lavigne,M. & Poo,M.M. (1997) cAMP-dependent growth cone guidance by netrin-1. *Neuron*, **19**, 1225-1235.

Ming,G.L., Wong,S.T., Henley,J., Yuan,X.B., Song,H.J., Spitzer,N.C. & Poo,M.M. (2002) Adaptation in the chemotactic guidance of nerve growth cones. *Nature*, **417**, 411-418.

Mingorance A, Fontana X Sole M Burgaya F Urena JM Teng FYH Tang BL Hunt D Anderson PN Bethea JR Schwab ME Soriano E del Rio JA. Regulation of Nogo and Nogo receptor during development of the entorhinal-hippocampal pathway and after adult hipocampal lesions. Mol.Cell Neurosci. [in press]. 2004.

Miranda,J.D., White,L.A., Marcillo,A.E., Willson,C.A., Jagid,J. & Whittemore,S.R. (1999) Induction of Eph B3 after spinal cord injury. *Exp.Neurol.*, **156**, 218-222.

Misantone,L.J., Gershenbaum,M. & Murray,M. (1984) Viability of retinal ganglion cells after optic nerve crush in adult rats. *J.Neurocytol.*, **13**, 449-465.

Miwa,T., Furukawa,S., Nakajima,K., Furukawa,Y. & Kohsaka,S. (1997) Lipopolysaccharide enhances synthesis of brain-derived neurotrophic factor in cultured rat microglia. *J.Neurosci.Res.*, **50**, 1023-1029.

Monnier,P.P., Sierra,A., Schwab,J.M., Henke-Fahle,S. & Mueller,B.K. (2003) The Rho/ROCK pathway mediates neurite growth-inhibitory activity associated with the chondroitin sulfate proteoglycans of the CNS glial scar. *Mol.Cell Neurosci.*, **22**, 319-330.

Montero-Menei,C.N., Sindji,L., Garcion,E., Mege,M., Couez,D., Gamelin,E. & Darcy,F. (1996) Early events of the inflammatory reaction induced in rat brain by lipopolysaccharide intracerebral injection: relative contribution of peripheral monocytes and activated microglia. *Brain Res.*, **724**, 55-66.

Montero-Menei,C.N., Sindji,L., Pouplard-Barthelaix,A., Jehan,F., Denechaud,L. & Darcy,F. (1994) Lipopolysaccharide intracerebral administration induces minimal inflammatory reaction in rat brain. *Brain Res.*, **653**, 101-111.

Moon,L.D., Asher,R.A. & Fawcett,J.W. (2003) Limited growth of severed CNS axons after treatment of adult rat brain with hyaluronidase. *J.Neurosci.Res.*, **71**, 23-37.

Moon,L.D., Asher,R.A., Rhodes,K.E. & Fawcett,J.W. (2001) Regeneration of CNS axons back to their target following treatment of adult rat brain with chondroitinase ABC. *Nat.Neurosci.*, **4**, 465-466.

Moore,K.W., de Waal,M.R., Coffman,R.L. & O'Garra,A. (2001) Interleukin-10 and the interleukin-10 receptor. *Annu.Rev.Immunol.*, **19:683-765.**, 683-765.

Moran,L.B., Duke,D.C., Turkheimer,F.E., Banati,R.B. & Graeber,M.B. (2004) Towards a transcriptome definition of microglial cells. *Neurogenetics.*, **5**, 95-108.

Moreau-Fauvarque,C., Kumanogoh,A., Camand,E., Jaillard,C., Barbin,G., Boquet,I., Love,C., Jones,E.Y., Kikutani,H., Lubetzki,C., Dusart,I. & Chedotal,A. (2003) The transmembrane semaphorin Sema4D/CD100, an inhibitor of axonal growth, is expressed on oligodendrocytes and upregulated after CNS lesion. *J.Neurosci.*, **23**, 9229-9239.

Morgenstern,D.A., Asher,R.A., Naidu,M., Carlstedt,T., Levine,J.M. & Fawcett,J.W. (2003) Expression and glycanation of the NG2 proteoglycan in developing, adult, and damaged peripheral nerve. *Mol.Cell Neurosci.*, **24**, 787-802.

Morishita,S., Goto,M. & Fukuda,H. (1984) Brain cyclic nucleotides and the development of convulsion, with reference to the anticonvulsant activity of diazepam. *Gen.Pharmacol.*, **15**, 379-383.

Morrow,D.R., Campbell,G., Lieberman,A.R. & Anderson,P.N. (1993) Differential regenerative growth of CNS axons into tibial and peroneal nerve grafts in the thalamus of adult rats. *Exp.Neurol.*, **120**, 60-69.

Mukhopadhyay,G., Doherty,P., Walsh,F.S., Crocker,P.R. & Filbin,M.T. (1994) A novel role for myelin-associated glycoprotein as an inhibitor of axonal regeneration. *Neuron*, **13**, 757-767.

Murphy,P.G., Borthwick,L.S., Johnston,R.S., Kuchel,G. & Richardson,P.M. (1999) Nature of the retrograde signal from injured nerves that induces interleukin-6 mRNA in neurons. *J.Neurosci.*, **19**, 3791-3800.

Nagata,K., Takei,N., Nakajima,K., Saito,H. & Kohsaka,S. (1993) Microglial conditioned medium promotes survival and development of cultured mesencephalic neurons from embryonic rat brain. *J.Neurosci.Res.*, **34**, 357-363.

Nakagomi,S., Suzuki,Y., Namikawa,K., Kiryu-Seo,S. & Kiyama,H. (2003) Expression of the activating transcription factor 3 prevents c-Jun N-terminal kinase-induced neuronal death by promoting heat shock protein 27 expression and Akt activation. *J.Neurosci.*, **23**, 5187-5196.

Nakajima,K., Honda,S., Tohyama,Y., Imai,Y., Kohsaka,S. & Kurihara,T. (2001) Neurotrophin secretion from cultured microglia. *J.Neurosci.Res.*, **65**, 322-331.

Namba,T., Nakamura,T. & Grob,D. (1967) Staining for nerve fiber and cholinesterase activity in fresh frozen sections. *Am.J.Clin.Pathol.*, **47**, 74-77.

Nathan,C.F. (1987) Secretory products of macrophages. *J.Clin.Invest.*, **79**, 319-326.

Navarro,X., Kamei,H. & Kennedy,W.R. (1988) Effect of age and maturation on sudomotor nerve regeneration in mice. *Brain Res.*, **447**, 133-140.

Neumann,S., Bradke,F., Tessier-Lavigne,M. & Basbaum,A.I. (2002) Regeneration of sensory axons within the injured spinal cord induced by intraganglionic cAMP elevation. *Neuron.*, **34**, 885-893.

Neumann,S. & Woolf,C.J. (1999) Regeneration of dorsal column fibres into and beyond the lesion site following adult spinal cord injury. *Neuron*, **23**, 83-91.

Niclou,S.P., Franssen,E.H., Ehlert,E.M., Taniguchi,M. & Verhaagen,J. (2003) Meningeal cell-derived semaphorin 3A inhibits neurite outgrowth. *Mol.Cell Neurosci.*, **24**, 902-912.

Niederost,B., Oertle,T., Fritsche,J., McKinney,R.A. & Bandtlow,C.E. (2002) Nogo-A and Myelin-Associated Glycoprotein Mediate Neurite Growth Inhibition by Antagonistic Regulation of RhoA and Rac1. *J.Neurosci.*, **22**, 10368-10376.

Niehaus,A., Stegmuller,J., ers-Fenger,M. & Trotter,J. (1999) Cell-surface glycoprotein of oligodendrocyte progenitors involved in migration. *J.Neurosci.*, **19**, 4948-4961.

Nieke,J. & Schachner,M. (1985) Expression of the neural cell adhesion molecules L1 and N-CAM and their common carbohydrate epitope L2/HNK-1 during development and after transection of the mouse sciatic nerve. *Differentiation.*, **30**, 141-151.

Nikulina,E., Tidwell,J.L., Dai,H.N., Bregman,B.S. & Filbin,M.T. (2004) The phosphodiesterase inhibitor rolipram delivered after a spinal cord lesion promotes axonal regeneration and functional recovery. *Proc.Natl.Acad.Sci.U.S.A.*, **101**, 8786-8790.

Nimmerjahn,A., Kirchhoff,F. & Helmchen,F. (2005) Resting microglial cells are highly dynamic surveillants of brain parenchyma in vivo. *Science*, **308**, 1314-1318.

Nishiyama,A. (2007) Polydendrocytes: NG2 cells with many roles in development and repair of the CNS. *Neuroscientist.*, **13**, 62-76.

Nishiyama,A., Chang,A. & Trapp,B.D. (1999) NG2+ glial cells: a novel glial cell population in the adult brain. *J.Neuropathol.Exp.Neurol.*, **58**, 1113-1124.

Nishiyama,A., Dahlin,K.J., Prince,J.T., Johnstone,S.R. & Stallcup,W.B. (1991) The primary structure of NG2, a novel membrane-spanning proteoglycan. *J.Cell Biol.*, **114**, 359-371.

Nitzan,A., Kermer,P., Shirvan,A., Bahr,M., Barzilai,A. & Solomon,A.S. (2006) Examination of cellular and molecular events associated with optic nerve axotomy. *Glia*, **54**, 545-556.

Norenberg,U., Hubert,M., Brummendorf,T., Tarnok,A. & Rathjen,F.G. (1995) Characterization of functional domains of the tenascin-R (restrictin) polypeptide: cell attachment site, binding with F11, and enhancement of F11-mediated neurite outgrowth by tenascin-R. *J.Cell Biol.*, **130**, 473-484.

Oblinger,M.M. & Lasek,R.J. (1988) A conditioning lesion of the peripheral axons of dorsal root ganglion cell accelerates regeneration of only their peripheral axons. *J.Neurosci.*, **4**, 1736-1744.

Oertle,T., van der Haar,M.E., Bandtlow,C.E., Robeva,A., Burfeind,P., Buss,A., Huber,A.B., Simonen,M., Schnell,L., Brosamle,C., Kaupmann,K., Vallon,R. & Schwab,M.E. (2003) Nogo-A inhibits neurite outgrowth and cell spreading with three discrete regions. *J.Neurosci.*, **23**, 5393-5406.

Ong,W.Y. & Levine,J.M. (1999) A light and electron microscopic study of NG2 chondroitin sulfate proteoglycan-positive oligodendrocyte precursor cells in the normal and kainate-lesioned rat hippocampus. *Neuroreport.*, **92**, 83-95.

Oudega,M. (2007) Schwann cell and olfactory ensheathing cell implantation for repair of the contused spinal cord. *Acta Physiol (Oxf).*, **189**, 181-189.

Oudega,M. & Hagg,T. (1996) Nerve growth factor promotes regeneration of sensory axons into adult rat spinal cord. *Exp.Neurol.*, **140**, 218-229.

Oudega,M. & Hagg,T. (1999) Neurotrophins promote regeneration of sensory axons in the adult rat spinal cord. *Brain Res.*, **818**, 431-438.

Oudega,M., Rosano,C., Sadi,D., Wood,P.M., Schwab,M.E. & Hagg,T. (2000) Neutralizing antibodies against neurite growth inhibitor NI-35/250 do not promote regeneration of sensory axons in the adult rat spinal cord. *Neuroreport.*, **100**, 873-883.

Oudega,M., Varon,S. & Hagg,T. (1994) Regeneration of adult rat sensory axons into intraspinal nerve grafts: promoting effects of conditioning lesion and graft predegeneration. *Exp.Neurol.*, **129**, 194-206.

Ozerdem,U., Grako,K.A., Dahlin-Huppe,K., Monosov,E. & Stallcup,W.B. (2001) NG2 proteoglycan is expressed exclusively by mural cells during vascular morphogenesis. *Dev.Dyn.*, **222**, 218-227.

Ozerdem,U., Monosov,E. & Stallcup,W.B. (2002) NG2 proteoglycan expression by pericytes in pathological microvasculature. *Microvasc.Res.*, **63**, 129-134.

Ozerdem,U. & Stallcup,W.B. (2004) Pathological angiogenesis is reduced by targeting pericytes via the NG2 proteoglycan. *Angiogenesis.*, **7**, 269-276.

Park,J.B., Yiu,G., Kaneko,S., Wang,J., Chang,J., He,X.L., Garcia,K.C. & He,Z. (2005) A TNF receptor family member, TROY, is a coreceptor with Nogo receptor in mediating the inhibitory activity of myelin inhibitors. *Neuron*, **45**, 345-351.

Pasquale,E.B. (2005) Eph receptor signalling casts a wide net on cell behaviour. *Nat.Rev.Mol.Cell Biol.*, **6**, 462-475.

Pasterkamp,R.J., Anderson,P.N. & Verhaagen,J. (2001) Peripheral nerve injury fails to induce growth of lesioned ascending dorsal column axons into spinal cord scar tissue expressing the axon repellent Semaphorin3A. *Eur.J.Neurosci.*, **13**, 457-471.

Pasterkamp,R.J., De Winter,F., Giger,R.J. & Verhaagen,J. (1998a) Role for semaphorin III and its receptor neuropilin-1 in neuronal regeneration and scar formation? .*Prog.Brain Res.*, **117**, 151-170.

Pasterkamp,R.J., Giger,R.J., Ruitenberg,M.J., Holtmaat,A.J., De Wit,G.M., De Winter,F. & Verhaagen,J. (1999) Expression of the gene encoding the chemorepellent semaphorin III is induced in the fibroblast component of neural scar tissue formed following injuries of adult but not neonatal CNS. *Mol.Cell Neurosci.*, **13**, 143-166.

Pasterkamp,R.J., Giger,R.J. & Verhaagen,J. (1998b) Regulation of semaphorin III/collapsin-1 gene expression during peripheral nerve regeneration. *.Exp.Neurol.*, **153**, 313-327.

Pasterkamp,R.J. & Verhaagen,J. (2006) Semaphorins in axon regeneration: developmental guidance molecules gone wrong? *Philos.Trans.R.Soc.Lond B Biol.Sci.*, **361**, 1499-1511.

Paxinos,G. & Watson,C. (1998) *The Rat Brain in Stereotaxic Coordinates* Academic Press Harcourt Brace Jovanovich, Publishers, Sydney, Australia.

Pearse,D.D., Pereira,F.C., Marcillo,A.E., Bates,M.L., Berrocal,Y.A., Filbin,M.T. & Bunge,M.B. (2004) cAMP and Schwann cells promote axonal growth and functional recovery after spinal cord injury. *Nat.Med.*, **10**, 610-616.

Pearson,A.G., Gray,C.W., Pearson,J.F., Greenwood,J.M., During,M.J. & Dragunow,M. (2003) ATF3 enhances c-Jun-mediated neurite sprouting. *Brain Res.Mol.Brain Res.*, **120**, 38-45.

Perry,V.H., Bell,M.D., Brown,H.C. & Matyszak,M.K. (1995b) Inflammation in the nervous system. *Curr.Opin.Neurobiol.*, **5**, 636-641.

Perry,V.H., Bolton,S.J., Anthony,D.C. & Betmouni,S. (1998) The contribution of inflammation to acute and chronic neurodegeneration. *Res.Immunol.*, **149**, 721-725.

Perry,V.H. & Brown,M.C. (1992) Macrophages and nerve regeneration. *Curr.Opin.Neurobiol.*, **2**, 679-682.

Perry,V.H., Brown,M.C. & Gordon,S. (1987) The macrophage response to central and peripheral nerve injury. A possible role for macrophages in regeneration. *J.Exp.Med.*, **165**, 1218-1223.

Perry,V.H. & Gordon,S. (1991) Macrophages and the nervous system. *Int.Rev.Cytol.*, **125:203-44.**, 203-244.

Perry,V.H., Tsao,J.W., Fearn,S. & Brown,M.C. (1995a) Radiation-induced reductions in macrophage recruitment have only slight effects on myelin degeneration in sectioned peripheral nerves of mice. *Eur.J.Neurosci.*, **7**, 271-280.

Persidsky,Y., Buttini,M., Limoges,J., Bock,P. & Gendelman,H.E. (1997) An analysis of HIV-1-associated inflammatory products in brain tissue of humans and SCID mice with HIV-1 encephalitis. *J.Neurovirol.*, **3**, 401-416.

Pesheva,P., Gennarini,G., Goridis,C. & Schachner,M. (1993) The F3/11 cell adhesion molecule mediates the repulsion of neurons by the extracellular matrix glycoprotein J1-160/180. *Neuron*, **10**, 69-82.

Pesheva,P. & Probstmeier,R. (2000) The yin and yan of tenascin-R in CNS development and pathology. *Prog.Neurobiol.*, **61**, 465-493.

Pesheva,P., Probstmeier,R., Skubitz,A.P., McCarthy,J.B., Furcht,L.T. & Schachner,M. (1994) Tenascin-R (J1 160/180 inhibits fibronectin-mediated cell adhesion--functional relatedness to tenascin-C. *J.Cell Sci.*, **107**, 2323-2333.

Pesheva,P., Spiess,E. & Schachner,M. (1989) J1-160 and J1-180 are oligodendrocyte-secreted nonpermissive substrates for cell adhesion. *J.Cell Biol.*, **109**, 1765-1778.

Peters,A. (2004) A fourth type of neuroglial cell in the adult central nervous system. *J.Neurocytol.*, **33**, 345-357.

Phillips,H.S., Hains,J.M., Laramee,G.R., Rosenthal,A. & Winslow,J.W. (1990) Widespread expression of BDNF but not NT3 by target areas of basal forebrain cholinergic neurons. *Science*, **250**, 290-294.

Pignot,V., Hein,A.E., Barske,C., Wiessner,C., Walmsley,A.R., Kaupmann,K., Mayeur,H., Sommer,B., Mir,A.K. & Frentzel,S. (2003) Characterization of two novel proteins, NgRH1 and NgRH2, structurally and biochemically homologous to the Nogo-66 receptor. *J.Neurochem.*, **85**, 717-728.

Pindzola,R.R., Doller,C. & Silver,J. (1993) Putative inhibitory extracellular matrix molecules at the dorsal root entry zone of the spinal cord during development and after root and sciatic nerve lesions. *Dev.Biol.*, **156**, 34-48.

Plunet,W., Kwon,B.K. & Tetzlaff,W. (2002) Promoting axonal regeneration in the central nervous system by enhancing the cell body response to axotomy. *J.Neurosci.Res.*, **68**, 1-6.

Polito,A. & Reynolds,R. (2005) NG2-expressing cells as oligodendrocyte progenitors in the normal and demyelinated adult central nervous system. *J.Anat.*, **207**, 707-716.

Prewitt,C.M., Niesman,I.R., Kane,C.J. & Houle,J.D. (1997) Activated macrophage/microglial cells can promote the regeneration of sensory axons into the injured spinal cord. *Exp.Neurol.*, **148**, 433-443.

Prinjha, R., Hill, C., Irving, E., Roberts, J., Campbell, C., Parsons, A., Morrow, R., Woodhams, P. L., Philpott, K. L., Pangalos, M., and Walsh, F. S. Mapping the functional inhibitory sites of Nogo-A. Discovery of regulated expression following neuronal injury. SFN Itinerary planner CD-ROM Program No. 333.12. (2002). Society for Neuroscience, Washington, DC.

Prinjha,R., Moore,S.E., Vinson,M., Blake,S., Morrow,R., Christie,G., Michalovich,D., Simmons,D.L. & Walsh,F.S. (2000) Inhibitor of neurite outgrowth in humans. *Nature*, **403**, 383-384.

Probstmeier,R., Michels,M., Franz,T., Chan,B.M. & Pesheva,P. (1999) Tenascin-R interferes with integrin-dependent oligodendrocyte precursor cell adhesion by a ganglioside-mediated signalling mechanism. *Eur.J.Neurosci.*, **11**, 2474-2488.

Probstmeier,R., Stichel,C.C., Muller,H.W., Asou,H. & Pesheva,P. (2000) Chondroitin sulfates expressed on oligodendrocyte-derived tenascin-R are involved in neural cell recognition. Functional implications during CNS development and regeneration. *J.Neurosci.Res.*, **60**, 21-36.

Pu,S.F., Zhuang,H.X. & Ishii,D.N. (1995) Differential spatio-temporal expression of the insulin-like growth factor genes in regenerating sciatic nerve. *Brain Res.Mol.Brain Res.*, **34**, 18-28.

Qiu,J., Cai,D., Dai,H., McAtee,M., Hoffman,P.N., Bregman,B.S. & Filbin,M.T. (2002) Spinal axon regeneration induced by elevation of cyclic AMP. *Neuron*, **34**, 895-903.

Quan,N., Sundar,S.K. & Weiss,J.M. (1994) Induction of interleukin-1 in various brain regions after peripheral and central injections of lipopolysaccharide. *J.Neuroimmunol.*, **49**, 125-134.

Quarles,R.H. (2007) Myelin-associated glycoprotein (MAG): past, present and beyond. *J.Neurochem.*, **100**, 1431-1448.

Rabchevsky,A.G. & Streit,W.J. (1997) Grafting of cultured microglial cells into the lesioned spinal cord of adult rats enhances neurite outgrowth. *J.Neurosci.Res.*, **47**, 34-48.

Rabinovsky,E.D., Smith,G.M., Browder,D.P., Shine,H.D. & McManaman,J.L. (1992) Peripheral nerve injury down-regulates CNTF expression in adult rat sciatic nerves. *J.Neurosci.Res.*, **31**, 188-192.

Raineteau,O., Z'Graggen,W.J., Thallmair,M. & Schwab,M.E. (1999) Sprouting and regeneration after pyramidotomy and blockade of the myelin-associated neurite growth inhibitors NI 35/250 in adult rats. *Eur.J.Neurosci.*, **11**, 1486-1490.

Raisman,G. (2004) Myelin inhibitors: does NO mean GO? *Nat.Rev.Neurosci.*, **5**, 157-161.

Raisman,G. & Li,Y. (2007) Repair of neural pathways by olfactory ensheathing cells. *Nat.Rev.Neurosci.*, **8**, 312-319.

Raivich,G. (2002) Microglial response in the axotomised facial motor nucleus. In Streit WJ (ed), *Microglia in the regenerating and degenerating central nervous system.* Springer-Verlag, New York, pp. 166-187.

Raivich,G. & Behrens,A. (2006) Role of the AP-1 transcription factor c-Jun in developing, adult and injured brain. *Prog.Neurobiol.*, **78**, 347-363.

Raivich,G., Bohatschek,M., Da Costa,C., Iwata,O., Galiano,M., Hristova,M., Nateri,A.S., Makwana,M., Riera-Sans,L., Wolfer,D.P., Lipp,H.P., Aguzzi,A., Wagner,E.F. & Behrens,A. (2004) The AP-1 transcription factor c-Jun is required for efficient axonal regeneration. *Neuron*, **43**, 57-67.

Raivich,G., Bohatschek,M., Kloss,C.U., Werner,A., Jones,L.L. & Kreutzberg,G.W. (1999) Neuroglial activation repertoire in the injured brain: graded response, molecular mechanisms and cues to physiological function. *Brain Res.Brain Res.Rev.*, **30**, 77-105.

Raivich,G. & Kreutzberg,G.W. (1994) Pathophysiology of glial growth factor receptors. *Glia*, **11**, 129-146.

Ramer,L.M., Au,E., Richter,M.W., Liu,J., Tetzlaff,W. & Roskams,A.J. (2004a) Peripheral olfactory ensheathing cells reduce scar and cavity formation and promote regeneration after spinal cord injury. *J.Comp Neurol.*, **473**, 1-15.

Ramer,L.M., Richter,M.W., Roskams,A.J., Tetzlaff,W. & Ramer,M.S. (2004b) Peripherally-derived olfactory ensheathing cells do not promote primary afferent regeneration following dorsal root injury. *Glia.*, **47**, 189-206.

Ramer,M.S., Priestley,J.V. & McMahon,S.B. (2000) Functional regeneration of sensory axons into the adult spinal cord. *Nature*, **403**, 312-316.

Ramon-Cueto,A., Cordero,M.I., Santos-Benito,F.F. & Avila,J. (2000) Functional recovery of paraplegic rats and motor axon regeneration in their spinal cords by olfactory ensheathing glia. *Neuron*, **25**, 425-435.

Ramon-Cueto,A. & Nieto-Sampedro,M. (1994) Regeneration into the spinal cord of transected dorsal root axons is promoted by ensheathing glia transplants. *Exp.Neurol.*, **127**, 232-244.

Rapalino,O., Lazarov Spiegler,O., Agranov,E., Velan,G.J., Yoles,E., Fraidakis,M., Solomon,A., Gepstein,R., Katz,A., Belkin,M., Hadani,M. & Schwartz,M. (1998) Implantation of stimulated homologous macrophages results in partial recovery of paraplegic rats. *Nat.Med.*, **4**, 814-821.

Raper,J.A. (2000) Semaphorins and their receptors in vertebrates and invertebrates. *Curr.Opin.Neurobiol.*, **10**, 88-94.

Rathjen,F.G. (1988) A neurite outgrowth-promoting molecule in developing fiber tracts. *Trends Neurosci.*, **11**, 183-184.

Reh,T.A., Redshaw,J.D. & Bisby,M.A. (1987) Axons of the pyramidal tract do not increase their transport of growth-associated proteins after axotomy. *Brain Res.*, **388**, 1-6.

Reier,P.J. (2004) Cellular transplantation strategies for spinal cord injury and translational neurobiology. *NeuroRx.*, **1**, 424-451.

Ren,K. (1999) An improved method for assessing mechanical allodynia in the rat. *Physiol Behav.*, **67**, 711-716.

Rezajooi,K., Pavlides,M., Winterbottom,J., Stallcup,W.B., Hamlyn,P.J., Lieberman,A.R. & Anderson,P.N. (2004) NG2 proteoglycan expression in the peripheral nervous system: upregulation following injury and comparison with CNS lesions. *Mol.Cell Neurosci.*, **25**, 572-582.

Rhodes,K.E., Raivich,G. & Fawcett,J.W. (2006) The injury response of oligodendrocyte precursor cells is induced by platelets, macrophages and inflammation-associated cytokines. *Neuroscience.*, **140 (1)**, 87-100.

Richardson,P.M., Issa,V.M. & Aguayo,A.J. (1984) Regeneration of long spinal axons in the rat. *J.Neurocytol.*, **13**, 165-182.

Richardson,P.M., Issa,V.M. & Shemie,S. (1982a) Regeneration and retrograde degeneration of axons in the rat optic nerve. *J.Neurocytol.*, **11**, 949-966.

Richardson,P.M. & Issa,V.M.K. (1984) Peripheral injury enhances central regeneration of primary sensory neurones. *Nature*, **309**, 791-793.

Richardson,P.M., McGuinness,U.M. & Aguayo,A.J. (1980) Axons from CNS neurons regenerate into PNS grafts. *Nature*, **284**, 264-265.

Richardson,P.M., McGuinness,U.M. & Aguayo,A.J. (1982b) Peripheral nerve autografts to the rat spinal cord: studies with axonal tracing methods. *Brain Res.*, **237**, 147-162.

Richardson,P.M. & Riopelle,R.J. (1984) Uptake of nerve growth factor along peripheral and spinal axons of primary sensory neurons. *J.Neurosci.*, **4**, 1683-1689.

Richardson,P.M. & Verge,V.M. (1987) Axonal regeneration in dorsal spinal roots is accelerated by peripheral axonal transection. *Brain Res.*, **411**, 406-408.

Riddell,J.S., Enriquez-Denton,M., Toft,A., Fairless,R. & Barnett,S.C. (2004) Olfactory ensheathing cell grafts have minimal influence on regeneration at the dorsal root entry zone following rhizotomy. *Glia.*, **47**, 150-167.

Riederer,B.M., Pellier,V., Antonsson,B., Di Paolo,G., Stimpson,S.A., Lutjens,R., Catsicas,S. & Grenningloh,G. (1997) Regulation of microtubule dynamics by the neuronal growth- associated protein SCG10. *Proc.Natl.Acad.Sci.U.S.A.*, **94**, 741-745.

Rio-Hortega P. (1932) Microglia. In Penfield W. (ed), *Cytology and Cellular Pathology of the Nervous System*. Paul B. Hoebeer, New York, pp. 483-534.

Rios,M., Lambe,E.K., Liu,R., Teillon,S., Liu,J., Akbarian,S., Roffler-Tarlov,S., Jaenisch,R. & Aghajanian,G.K. (2006) Severe deficits in 5-HT2A -mediated neurotransmission in BDNF conditional mutant mice. *J.Neurobiol.*, **66**, 408-420.

Rivest,S. (2003) Molecular insights on the cerebral innate immune system. *Brain Behav.Immun.*, **17**, 13-19.

Rodriguez-Tebar,A., Jeffrey,P.L., Thoenen,H. & Barde,Y.A. (1989) The survival of chick retinal ganglion cells in response to brain-derived neurotrophic factor depends on their embryonic age. *Dev.Biol.*, **136**, 296-303.

Rogers,N.C., Slack,E.C., Edwards,A.D., Nolte,M.A., Schulz,O., Schweighoffer,E., Williams,D.L., Gordon,S., Tybulewicz,V.L., Brown,G.D. & Reis e Sousa (2005) Syk-dependent cytokine induction by Dectin-1 reveals a novel pattern recognition pathway for C type lectins. *Immunity.*, **22**, 507-517.

Roosen,A., Schober,A., Strelau,J., Bottner,M., Faulhaber,J., Bendner,G., McIlwrath,S.L., Seller,H., Ehmke,H., Lewin,G.R. & Unsicker,K. (2001) Lack of neurotrophin-4 causes selective structural and chemical deficits in sympathetic ganglia and their preganglionic innervation. *J.Neurosci.*, **21**, 3073-3084.

Roskams,A.J. & Tetzlaff,W. (2005) Directing stem cells and progenitor cells on the stage of spinal cord injury. *Exp.Neurol.*, **193**, 267-272.

Rossi,F., Buffo,A. & Strata,P. (2001) Regulation of intrinsic regenerative properties and axonal plasticity in cerebellar Purkinje cells. *Restor.Neurol.Neurosci.*, **19**, 85-94.

Roux,P.P. & Barker,P.A. (2002) Neurotrophin signaling through the p75 neurotrophin receptor. *Prog.Neurobiol.*, **67**, 203-233.

Rudge,J.S. & Silver,J. (1990) Inhibition of neurite outgrowth on astroglial scars in vitro. *J.Neurosci.*, **10**, 3594-3603.

Ruijs,A.C., Jaquet,J.B., Kalmijn,S., Giele,H. & Hovius,S.E. (2005) Median and ulnar nerve injuries: a meta-analysis of predictors of motor and sensory recovery after modern microsurgical nerve repair. *Plast.Reconstr.Surg.*, **116**, 484-494.

Ruitenberg,M.J., Levison,D.B., Lee,S.V., Verhaagen,J., Harvey,A.R. & Plant,G.W. (2005) NT-3 expression from engineered olfactory ensheathing glia promotes spinal sparing and regeneration. *Brain.*, **128**, 839-853.

Ruitenberg,M.J., Plant,G.W., Hamers,F.P., Wortel,J., Blits,B., Dijkhuizen,P.A., Gispen,W.H., Boer,G.J. & Verhaagen,J. (2003) Ex vivo adenoviral vector-mediated

neurotrophin gene transfer to olfactory ensheathing glia: effects on rubrospinal tract regeneration, lesion size, and functional recovery after implantation in the injured rat spinal cord. *J.Neurosci.*, **23**, 7045-7058.

Rutishauser,U. (1985) Influences of the neural cell adhesion molecule on axon growth and guidance. *J.Neurosci.Res.*, **13**, 123-131.

Salonen,V., Peltonen,J., Roytta,M. & Virtanen,I. (1987) Laminin in traumatized peripheral nerve: basement membrane changes during degeneration and regeneration. *J.Neurocytol.*, **16**, 713-720.

Salzer,J.L., Williams,A.K., Glaser,L. & Bunge,R.P. (1980) Studies of Schwann cell proliferation. II. Characterization of the stimulation and specificity of the response to a neurite membrane fraction. *J.Cell Biol.*, **84**, 753-766.

Samii,A., Unger,J. & Lange,W. (1999) Vascular endothelial growth factor expression in peripheral nerves and dorsal root ganglia in diabetic neuropathy in rats. *Neurosci.Lett.*, **262**, 159-162.

Sandrock,A.W., Jr. & Matthew,W.D. (1987) Substrate-bound nerve growth factor promotes neurite growth in peripheral nerve. *Brain Res.*, **425**, 360-363.

Scarlato,M., Ara,J., Bannerman,P., Scherer,S. & Pleasure,D. (2003) Induction of neuropilins-1 and -2 and their ligands, Sema3A, Sema3F, and VEGF, during Wallerian degeneration in the peripheral nervous system. *Exp.Neurol.*, **183**, 489-498.

Schafer,M., Fruttiger,M., Montag,D., Schachner,M. & Martini,R. (1996) Disruption of the gene for the myelin-associated glycoprotein improves axonal regrowth along myelin in C57BL/Wlds mice. *Neuron*, **16**, 1107-1113.

Schmalbruch,H. (1987) Loss of sensory neurons after sciatic nerve section in the rat. *Anat.Rec.*, **219**, 323-329.

Schmalfeldt,M., Bandtlow,C.E., Dours-Zimmermann,M.T., Winterhalter,K.H. & Zimmermann,D.R. (2000) Brain derived versican V2 is a potent inhibitor of axonal growth. *J.Cell Sci.*, **113 (Pt 5)**, 807-816.

Schneider,S., Bosse,F., D'Urso,D., Muller,H., Sereda,M.W., Nave,K., Niehaus,A., Kempf,T., Schnolzer,M. & Trotter,J. (2001) The AN2 protein is a novel marker for the Schwann cell lineage expressed by immature and nonmyelinating Schwann cells. *J.Neurosci.*, **21**, 920-933.

Schnell,L., Schneider,R., Kolbeck,R., Barde,Y.-A. & Schwab,M.E. (1994) Neurotrophin-3 enhances sprouting of corticospinal tract during development and after adult spinal cord lesion. *Nature*, **367**, 170-173.

Schnell,L. & Schwab,M.E. (1990) Axonal regeneration in the rat spinal cord produced by an antibody against myelin-associated neurite growth inhibitors. *Nature*, **343**, 269-272.

Schnell,L. & Schwab,M.E. (1993) Sprouting and regeneration of lesioned corticospinal tract fibres in the adult rat spinal cord. *Eur.J.Neurosci.*, **5**, 1156-1171.

Schreyer,D.J. & Skene,J.H. (1993) Injury-associated induction of GAP-43 expression displays axon branch specificity in rat dorsal root ganglion neurons. *.J.Neurobiol.*, **24**, 959-970.

Schwab,M.E. & Caroni,P. (1988) Oligodendrocytes and CNS myelin are nonpermissive substrates for neurite growth and fibroblast spreading in vitro. *J.Neurosci.*, **8**, 2381-2393.

Schwartz,M., Lazarov Spiegler,O., Rapalino,O., Agranov,I., Velan,G. & Hadani,M. (1999) Potential repair of rat spinal cord injuries using stimulated homologous macrophages. *Neurosurgery*, **44**, 1041-1045.

Schwartz,M. & Yoles,E. (2006) Immune-based therapy for spinal cord repair: autologous macrophages and beyond. *J.Neurotrauma*, **23**, 360-370.

Schweigreiter,R., Walmsley,A.R., Niederost,B., Zimmermann,D.R., Oertle,T., Casademunt,E., Frentzel,S., Dechant,G., Mir,A. & Bandtlow,C.E. (2004) Versican V2 and the central inhibitory domain of Nogo-A inhibit neurite growth via p75NTR/NgR-independent pathways that converge at RhoA. *Mol.Cell Neurosci.*, **27**, 163-174.

Schweizer,U., Gunnersen,J., Karch,C., Wiese,S., Holtmann,B., Takeda,K., Akira,S. & Sendtner,M. (2002) Conditional gene ablation of Stat3 reveals differential signaling requirements for survival of motoneurons during development and after nerve injury in the adult. *J.Cell Biol.*, **156**, 287-297.

Scott,A.L., Borisoff,J.F. & Ramer,M.S. (2005) Deafferentation and neurotrophin-mediated intraspinal sprouting: a central role for the p75 neurotrophin receptor. *Eur.J.Neurosci.*, **21**, 81-92.

Sendtner,M., Kreutzberg,G.W. & Thoenen,H. (1990) Ciliary neurotrophic factor prevents the degeneration of motor neurons after axotomy. *Nature*, **345**, 440-441.

Sendtner,M., Stockli,D.A. & Thoenen,H. (1992) Synthesis and localization of ciliary neurotrophic factor in the sciatic nerve of the adult rat after lesion and during regeneration. *J.Cell Biol.*, **118**, 139-148.

Setzu,A., Lathia,J.D., Zhao,C., Wells,K., Rao,M.S., ffrench-Constant,C. & Franklin,R.J. (2006) Inflammation stimulates myelination by transplanted oligodendrocyte precursor cells. *Glia.*, **54**, 297-303.

Shao,Z., Browning,J.L., Lee,X., Scott,M.L., Shulga-Morskaya,S., Allaire,N., Thill,G., Levesque,M., Sah,D., McCoy,J.M., Murray,B., Jung,V., Pepinsky,R.B. & Mi,S. (2005) TAJ/TROY, an orphan TNF receptor family member, binds Nogo-66 receptor 1 and regulates axonal regeneration. *Neuron.*, **45**, 353-359.

Shearer,M.C. & Fawcett,J.W. (2001) The astrocyte/meningeal cell interface--a barrier to successful nerve regeneration? *Cell Tissue Res.*, **305**, 267-273.

Shearer,M.C., Niclou,S.P., Brown,D., Asher,R.A., Holtmaat,A.J., Levine,J.M., Verhaagen,J. & Fawcett,J.W. (2003) The astrocyte/meningeal cell interface is a barrier to neurite outgrowth which can be overcome by manipulation of inhibitory molecules or axonal signalling pathways. *Mol.Cell Neurosci.*, **24**, 913-925.

Shibuya,Y., Mizoguchi,A., Takeichi,M., Shimada,K. & Ide,C. (1995) Localization of N-cadherin in the normal and regenerating nerve fibers of the chicken peripheral nervous system. *Neuroreport.*, **67**, 253-261.

Shumsky,J.S., Tobias,C.A., Tumolo,M., Long,W.D., Giszter,S.F. & Murray,M. (2003) Delayed transplantation of fibroblasts genetically modified to secrete BDNF and NT-3 into a spinal cord injury site is associated with limited recovery of function. *Exp.Neurol.*, **184**, 114-130.

Sievers,J., Hausmann,B. & Berry,M. (1989) Fetal brain grafts rescue adult retinal ganglion cells from axotomy-induced cell death. *J.Comp.Neurol.*, **281**, 467-478.

Sievers,J., Hausmann,B., Unsicker,K. & Berry,M. (1987) Fibroblast growth factors promote the survival of adult rat retinal ganglion cells after transection of the optic nerve. .*Neurosci.Lett.*, **76**, 157-162.

Simonen,M., Pedersen,V., Weinmann,O., Schnell,L., Buss,A., Ledermann,B., Christ,F., Sansig,G., van der,P.H. & Schwab,M.E. (2003) Systemic deletion of the myelin-associated outgrowth inhibitor nogo-a improves regenerative and plastic responses after spinal cord injury. *Neuron*, **38**, 201-211.

Singer,M., Nordlander,R.H. & Egar,M. (1979) Axonal guidance during embryogenesis and regeneration in the spinal cord of the newt: the blueprint hypothesis of neuronal pathway patterning. *J.Comp Neurol.*, **185**, 1-21.

Sivasankaran,R., Pei,J., Wang,K.C., Zhang,Y.P., Shields,C.B., Xu,X.M. & He,Z. (2004) PKC mediates inhibitory effects of myelin and chondroitin sulfate proteoglycans on axonal regeneration. *Nat.Neurosci.*, **7**, 261-268.

Skene,J.H. & Virag,I. (1989) Posttranslational membrane attachment and dynamic fatty acylation of a neuronal growth cone protein, GAP-43. *J.Cell Biol.*, **108**, 613-624.

Skene,J.H. & Willard,M. (1981) Axonally transported proteins associated with axon growth in rabbit central and peripheral nervous systems. *J.Cell Biol.*, **89**, 96-103.

Skene,J.H.P. (1989) Axonal growth associated proteins. *Ann.Rev.Neurosci.*, **12**, 127-156.

Smith-Thomas,L.C., Fok-Seang,J., Stevens,J., Du,J.S., Muir,E., Faissner,A., Geller,H.M., Rogers,J.H. & Fawcett,J.W. (1994) An inhibitor of neurite outgrowth produced by astrocytes. *J.Cell Sci.*, **107 (Pt 6)**, 1687-1695.

Snedecor,G.W. & Cochran,W.G. (1999) *Statistical Methods* Iowa State University Press.

Snow,D.M., Lemmon,V., Carrino,D.A., Caplan,A.I. & Silver,J. (1990) Sulfated proteoglycans in astroglial barriers inhibit neurite outgrowth in vitro. .*Exp.Neurol.*, **109**, 111-130.

Snow,D.M. & Letourneau,P.C. (1992) Neurite outgrowth on a step gradient of chondroitin sulfate proteoglycan (CS-PG). *J.Neurobiol.*, **23**, 322-336.

Snow,D.M., Mullins,N. & Hynds,D.L. (2001) Nervous system-derived chondroitin sulfate proteoglycans regulate growth cone morphology and inhibit neurite outgrowth: a light, epifluorescence, and electron microscopy study. *Microsc.Res.Tech.*, **54**, 273-286.

Snow,D.M., Watanabe,M., Letourneau,P.C. & Silver,J. (1991) A chondroitin sulfate proteoglycan may influence the direction of retinal ganglion cell outgrowth. .*Development*, **113**, 1473-1485.

Soares,H.D., Chen,S.C. & Morgan,J.I. (2001) Differential and prolonged expression of Fos-lacZ and Jun-lacZ in neurons, glia, and muscle following sciatic nerve damage. *Exp.Neurol.*, **167**, 1-14.

Sobel,R.A. (2005) Ephrin A receptors and ligands in lesions and normal-appearing white matter in multiple sclerosis. *Brain Pathol.*, **15**, 35-45.

Sofroniew,M.V. & Isacson,O. (1988) Distribution of degeneration of cholinergic neurons in the septum following axotomy in different portions of the fimbria-fornix: a correlation between degree of cell loss and proximity of neuronal somata to the lesion. *J.Chem.Neuroanat.*, **1**, 327-337.

Song,H., Ming,G., He,Z., Lehmann,M., McKerracher,L., Tessier-Lavigne,M. & Poo,M. (1998) Conversion of neuronal growth cone responses from repulsion to attraction by cyclic nucleotides. *Science*, **281**, 1515-1518.

Song,H.J., Ming,G.L. & Poo,M.M. (1997) cAMP-induced switching in turning direction of nerve growth cones [published erratum appears in Nature 1997 Sep 25;389(6649):412]. *Nature*, **388**, 275-279.

Stallcup,W.B. (2002) The NG2 proteoglycan: past insights and future prospects. *J.Neurocytol.*, **31**, 423-435.

Stein,E., Lane,A.A., Cerretti,D.P., Schoecklmann,H.O., Schroff,A.D., Van Etten,R.L. & Daniel,T.O. (1998) Eph receptors discriminate specific ligand oligomers to determine alternative signaling complexes, attachment, and assembly responses. *Genes Dev.*, **12**, 667-678.

Stein,R., Orit,S. & Anderson,D.J. (1988) The induction of a neural-specific gene, SCG10, by nerve growth factor in PC12 cells is transcriptional, protein synthesis dependent, and glucocorticoid inhibitable. *Dev.Biol.*, **127**, 316-325.

Steinmetz,M.P., Horn,K.P., Tom,V.J., Miller,J.H., Busch,S.A., Nair,D., Silver,D.J. & Silver,J. (2005) Chronic enhancement of the intrinsic growth capacity of sensory neurons combined with the degradation of inhibitory proteoglycans allows functional regeneration of sensory axons through the dorsal root entry zone in the mammalian spinal cord. *J.Neurosci.*, **25**, 8066-8076.

Sternberger,N.H., Quarles,R.H., Itoyama,Y. & Webster,H.D. (1979) Myelin-associated glycoprotein demonstrated immunocytochemically in myelin and myelin-forming cells of developing rat. *Proc.Natl.Acad.Sci.U.S.A*, **76**, 1510-1514.

Steward,O., Zheng,B., Banos,K. & Yee,K.M. (2007) Response to: Kim et al., "axon regeneration in young adult mice lacking Nogo-A/B." Neuron 38, 187-199. *Neuron*, **54**, 191-195.

Steward,O., Zheng,B., Ho,C., Anderson,K. & Tessier-Lavigne,M. (2004) The dorsolateral corticospinal tract in mice: an alternative route for corticospinal input to caudal segments following dorsal column lesions. *J.Comp Neurol.*, **472**, 463-477.

Stewart,H.J. (1995) Expression of c-Jun, Jun B, Jun D and cAMP response element binding protein by Schwann cells and their precursors in vivo and in vitro. *Eur.J.Neurosci.*, **7**, 1366-1375.

Stichel,C.C., Hermanns,S., Luhmann,H.J., Lausberg,F., Niermann,H., D'Urso,D., Servos,G., Hartwig,H.G. & Muller,H.W. (1999) Inhibition of collagen IV deposition promotes regeneration of injured CNS axons. .*Eur.J.Neurosci.*, **11**, 632-646.

Stichel,C.C., Wunderlich,G., Schwab,M.E. & Muller,H.W. (1995) Clearance of myelin constituents and axonal sprouting in the transected postcommissural fornix of the adult rat. *Eur.J.Neurosci.*, **7**, 401-411.

Stoll,G., Griffin,J.W., Li,C.Y. & Trapp,B.D. (1989) Wallerian degeneration in the peripheral nervous system: participation of both Schwann cells and macrophages in myelin degradation. *J.Neurocytol.*, **18**, 671-683.

Stoll,G., Jander,S. & Myers,R.R. (2002) Degeneration and regeneration of the peripheral nervous system: from Augustus Waller's observations to neuroinflammation. *J.Peripher.Nerv.Syst.*, **7**, 13-27.

Streit,W.J. (2002) Microglia as neuroprotective, immunocompetent cells of the CNS. *Glia*, **40**, 133-139.

Streit,W.J., Hurley,S.D., McGraw,T.S. & Semple-Rowland,S.L. (2000) Comparative evaluation of cytokine profiles and reactive gliosis supports a critical role for interleukin-6 in neuron-glia signaling during regeneration. *J.Neurosci.Res.*, **61**, 10-20.

Strittmatter,S.M., Fankhauser,C., Huang,P.L., Mashius,H. & Fishman,M.C. (1995) Neuronal pathfinding is abnormal in mice lacking the neuronal growth cone protein GAP-43. *Cell*, **80**, 445-452.

Sugiura,Y. & Mori,N. (1995) SCG10 expresses growth-associated manner in developing rat brain, but shows a different pattern to p19/stathmin or GAP-43. *Develomental Brain Research*, **90**, 73-91.

Sun,Y. & Zigmond,R.E. (1996) Leukaemia inhibitory factor induced in the sciatic nerve after axotomy is involved in the induction of galanin in sensory neurons. *Eur.J.Neurosci.*, **8**, 2213-2220.

Svensson,M. & Aldskogius,H. (1993a) Infusion of cytosine-arabinoside into the cerebrospinal fluid of the rat brain inhibits the microglial cell proliferation after hypoglossal nerve injury. *Glia*, **7**, 286-298.

Svensson,M. & Aldskogius,H. (1993b) Regeneration of hypoglossal nerve axons following blockade of the axotomy-induced microglial cell reaction in the rat. *Eur.J.Neurosci.*, **5**, 85-94.

Svensson,M. & Aldskogius,H. (1993c) Regeneration of hypoglossal nerve axons following blockade of the axotomy-induced microglial cell reaction in the rat. *Eur.J.Neurosci.*, **5**, 85-94.

Swiercz,J.M., Kuner,R., Behrens,J. & Offermanns,S. (2002) Plexin-B1 directly interacts with PDZ-RhoGEF/LARG to regulate RhoA and growth cone morphology. *Neuron*, **35**, 51-63.

Szczepanik,A.M., Fishkin,R.J., Rush,D.K. & Wilmot,C.A. (1996) Effects of chronic intrahippocampal infusion of lipopolysaccharide in the rat. *Neuroreport.*, **70**, 57-65.

Takeda,M., Kato,H., Takamiya,A., Yoshida,A. & Kiyama,H. (2000) Injury-specific expression of activating transcription factor-3 in retinal ganglion cells and its colocalized expression with phosphorylated c-Jun. *Invest Ophthalmol.Vis.Sci.*, **41**, 2412-2421.

Talts,U., Kuhn,U., Roos,G. & Rauch,U. (2000) Modulation of extracellular matrix adhesiveness by neurocan and identification of its molecular basis. *Exp.Cell Res.*, **259**, 378-388.

Tan,A.M., Colletti,M., Rorai,A.T., Skene,J.H. & Levine,J.M. (2006) Antibodies against the NG2 proteoglycan promote the regeneration of sensory axons within the dorsal columns of the spinal cord. *J.Neurosci.*, **26**, 4729-4739.

Tanaka,K. & Webster,H.D. (1991) Myelinated fiber regeneration after crush injury is retarded in sciatic nerves of aging mice. *J.Comp Neurol.*, **308**, 180-187.

Tang,S., Qiu,J., Nikulina,E. & Filbin,M.T. (2001) Soluble myelin-associated glycoprotein released from damaged white matter inhibits axonal regeneration. *Mol.Cell Neurosci.*, **18**, 259-269.

Tang,X., Davies,J.E. & Davies,S.J. (2003) Changes in distribution, cell associations, and protein expression levels of NG2, neurocan, phosphacan, brevican, versican V2, and tenascin-C during acute to chronic maturation of spinal cord scar tissue. *J.Neurosci.Res.*, **71**, 427-444.

Taniuchi,M., Clark,H.B. & Johnson,E.M., Jr. (1986) Induction of nerve growth factor receptor in Schwann cells after axotomy. *Proc.Natl.Acad.Sci.U.S.A*, **83**, 4094-4098.

Taylor,L., Jones,L., Tuszynski,M.H. & Blesch,A. (2006) Neurotrophin-3 gradients established by lentiviral gene delivery promote short-distance axonal bridging beyond cellular grafts in the injured spinal cord. *J.Neurosci.*, **26**, 9713-9721.

Tello F (1911) La influencia del neurotropismo en la regeneracion de los centros nerviosos. *Trab.Lab.Invest.Biol.*, **9**, 123-159.

Teng,F.Y. & Tang,B.L. (2005) Why do Nogo/Nogo-66 receptor gene knockouts result in inferior regeneration compared to treatment with neutralizing agents? *J.Neurochem.*, **94**, 865-874.

Tetzlaff,W., Alexander,S.W., Miller,F.D. & Bisby,M.A. (1991) Response of facial and rubrospinal neurons to axotomy: changes in cytoskeletal proteins and GAP-43. *J.Neurosci.*, **11**, 2528-2544.

Tetzlaff,W., Bisby,M.A. & Kreutzberg,G.W. (1988) Changes in cytoskeletal proteins in the rat facial nucleus following axotomy. *J.Neurosci.*, **8**, 3181-3189.

Tetzlaff,W., Kobayashi,N.R., Giehl,K.M., Tsui,B.J., Cassar,S.L. & Bedard,A.M. (1994) Response of rubrospinal and corticospinal neurons to injury and neurotrophins. *Prog.Brain Res.*, **103**, 271-286.

Thallmair,M., Metz,G.A., Z'Graggen,W.J., Raineteau,O., Kartje,G.L. & Schwab,M.E. (1998) Neurite growth inhibitors restrict plasticity and functional recovery following corticospinal tract lesions. *Nat.Neurosci.*, **1**, 124-131.

Thallmair,M., Ray,J., Stallcup,W.B. & Gage,F.H. (2006) Functional and morphological effects of NG2 proteoglycan deletion on hippocampal neurogenesis. *Exp.Neurol.*, **202**, 167-178.

Thoenen,H., Bandtlow,C., Heumann,R., Lindholm,D., Meyer,M. & Rohrer,H. (1988) Nerve growth factor: cellular localization and regulation of synthesis. *Cell Mol.Neurobiol.*, **8(1)**, 35-40.

Timmusk,T., Belluardo,N., Metsis,M. & Persson,H. (1993) Widespread and developmentally-regulated expression of neurotrophin-4 messenger-RNA in rat-brain and peripheral-tissues. *Eur.J.Neurosci.*, **5(6)**, 605-613.

Timpl,R. (1996) Macromolecular organization of basement membranes. *Curr.Opin.Cell Biol.*, **8**, 618-624.

Tobias,C.A., Shumsky,J.S., Shibata,M., Tuszynski,M.H., Fischer,I., Tessler,A. & Murray,M. (2003) Delayed grafting of BDNF and NT-3 producing fibroblasts into the injured spinal cord stimulates sprouting, partially rescues axotomized red nucleus neurons from loss and atrophy, and provides limited regeneration. *Exp.Neurol.*, **184**, 97-113.

Tona,A. & Bignami,A. (1993) Effect of hyaluronidase on brain extracellular matrix in vivo and optic nerve regeneration. *J.Neurosci.Res.*, **36**, 191-199.

Tornqvist,E. & Aldskogius,H. (1994) Motoneuron survival is not affected by the proximo-distal level of axotomy but by the possibility of regenerating axons to gain access to the distal nerve stump. *J.Neurosci.Res.*, **39**, 159-165.

Tropea,D., Caleo,M. & Maffei,L. (2003) Synergistic effects of brain-derived neurotrophic factor and chondroitinase ABC on retinal fiber sprouting after denervation of the superior colliculus in adult rats. *J.Neurosci.*, **23**, 7034-7044.

Tseng,G.F., Wang,Y.J. & Lai,Q.C. (1996) Perineuronal microglial reactivity following proximal and distal axotomy of rat rubrospinal neurons. *Brain Res.*, **715**, 32-43.

Tsujino,H., Kondo,E., Fukuoka,T., Dai,Y., Tokunaga,A., Miki,K., Yonenobu,K., Ochi,T. & Noguchi,K. (2000) Activating transcription factor 3 (ATF3) induction by axotomy in sensory and motoneurons: A novel neuronal marker of nerve injury. *Mol.Cell Neurosci.*, **15**, 170-182.

Tuszynski,M.H., Gabriel,K., Gage,F.H., Suhr,S., Meyer,S. & Rosetti,A. (1996) Nerve growth factor delivery by gene transfer induces differential outgrowth of sensory, motor, and noradrenergic neurites after adult spinal cord injury. *Exp.Neurol.*, **137**, 157-173.

Tuszynski,M.H., Grill,R., Jones,L.L., Brant,A., Blesch,A., Low,K., Lacroix,S. & Lu,P. (2003) NT-3 gene delivery elicits growth of chronically injured corticospinal axons and modestly improves functional deficits after chronic scar resection. *Exp.Neurol.*, **181**, 47-56.

Tuttle,R. & O'Leary,D.D. (1998) Neurotrophins rapidly modulate growth cone response to the axon guidance molecule, collapsin-1. *Mol.Cell Neurosci.*, **11**, 1-8.

Ughrin,Y.M., Chen,Z.J. & Levine,J.M. (2003) Multiple regions of the NG2 proteoglycan inhibit neurite growth and induce growth cone collapse. *J.Neurosci.*, **23**, 175-186.

Vallieres,N., Berard,J.L., David,S. & Lacroix,S. (2006) Systemic injections of lipopolysaccharide accelerates myelin phagocytosis during Wallerian degeneration in the injured mouse spinal cord. *Glia.*, **53**, 103-113.

van der Zee,C.E.E.M., Nielander,H.B., Vos,J.P., da Silva,S.L., Verhaagen,J., Oestreicher,A.B., Schrama,L.H., Schotman,P. & Gispen,W.H. (1989) Expression of growth-associated protein B-50 (GAP-43) in dorsal root ganglia and sciatic nerve during regenerative sprouting. *J.Neurosci.*, **9**, 3505-3512.

Vaudano,E., Campbell,G., Anderson,P.N., Davies,A.P., Woolhead,C., Schreyer,D.J. & Lieberman,A.R. (1995) The effects of a lesion or a peripheral nerve graft on GAP-43 upregulation in the adult rat brain: an in situ hybridization and immunocytochemical study. *J.Neurosci.*, **15**, 3594-3611.

Vaudano,E., Campbell,G., Hunt,S.P. & Lieberman,A.R. (1998) Axonal injury and peripheral nerve grafting in the thalamus and cerebellum of the adult rat: upregulation of c-jun and correlation with regenerative potential. *Eur.J.Neurosci.*, **10**, 2644-2656.

Vaudano, E., Woolhead, C., Anderson, P. N., Lieberman, A. R., and Hunt, S. P. Molecular changes in Purkinje cells (PC) and deep cerebellar nuclei (DCN) neurons after lesion or insertion of a peripheral nerve graft into the adult rat cerebellum. Society for Neuroscience Abstracts 19, 1510. 1993.

Vaughan,D.W. (1992) Effects of advancing age on peripheral nerve regeneration. *J.Comp Neurol.*, **323**, 219-237.

Venkatesh,K., Chivatakarn,O., Lee,H., Joshi,P.S., Kantor,D.B., Newman,B.A., Mage,R., Rader,C. & Giger,R.J. (2005) The Nogo-66 receptor homolog NgR2 is a sialic acid-dependent receptor selective for myelin-associated glycoprotein. *J.Neurosci.*, **25**, 808-822.

Verdu,E., Buti,M. & Navarro,X. (1995) The effect of aging on efferent nerve fibers regeneration in mice. *Brain Res.*, **696**, 76-82.

Verge,V.M., Tetzlaff,W., Richardson,P.M. & Bisby,M.A. (1990) Correlation between GAP43 and nerve growth factor receptors in rat sensory neurons. *J.Neurosci.*, **10**, 926-934.

Vinson,M., Strijbos,P.J., Rowles,A., Facci,L., Moore,S.E., Simmons,D.L. & Walsh,F.S. (2001) Myelin-associated glycoprotein interacts with ganglioside gt1b. a mechanism for neurite outgrowth inhibition. *J.Biol.Chem.*, **276**, 20280-20285.

von Bartheld,C.S., Byers,M.R., Williams,R. & Bothwell,M. (1996) Anterograde transport of neurotrophins and axodendritic transfer in the developing visual system. *Nature*, **379**, 830-833.

Wahl,S., Barth,H., Ciossek,T., Aktories,K. & Mueller,B.K. (2000) Ephrin-A5 induces collapse of growth cones by activating Rho and Rho kinase. *J.Cell Biol.*, **149**, 263-270.

Waller,A. (1850) Experiments on the section of the glossopharyngeal and hypoglossal nerves of the frog, and observations of the alterations produced thereby in the structure of their primitive fibres. *Philos.Trans.R.Soc.Lond B Biol.Sci.*, **140**, 423-429.

Walz,W. (2000) Controversy surrounding the existence of discrete functional classes of astrocytes in adult gray matter. *Glia.*, **31**, 95-103.

Walz,W. & Lang,M.K. (1998) Immunocytochemical evidence for a distinct GFAP-negative subpopulation of astrocytes in the adult rat hippocampus. *Neurosci.Lett.*, **257**, 127-130.

Wang,K.C., Kim,J.A., Sivasankaran,R., Segal,R. & He,Z. (2002a) p75 interacts with the Nogo receptor as a co-receptor for Nogo, MAG and OMgp. *Nature*, **420**, 74-78.

Wang,K.C., Koprivica,V., Kim,J.A., Sivasankaran,R., Guo,Y., Neve,R.L. & He,Z. (2002b) Oligodendrocyte-myelin glycoprotein is a Nogo receptor ligand that inhibits neurite outgrowth. *Nature*, **417**, 941-944.

Wang,X., Baughman,K.W., Basso,D.M. & Strittmatter,S.M. (2006) Delayed Nogo receptor therapy improves recovery from spinal cord contusion. *Ann.Neurol.*, **60**, 540-549.

Wang,Y.S. & White,T.D. (1999) The bacterial endotoxin lipopolysaccharide causes rapid inappropriate excitation in rat cortex. *J.Neurochem.*, **72**, 652-660.

Weber,J.R. & Skene,J.H. (1998) The activity of a highly promiscuous AP-1 element can be confined to neurons by a tissue-selective repressive element. *J.Neurosci.*, **18**, 5264-5274.

Weidner,N., Grill,R.J. & Tuszynski,M.H. (1999) Elimination of basal lamina and the collagen "scar" after spinal cord injury fails to augment corticospinal tract regeneration. *Exp.Neurol.*, **160**, 40-50.

Weis,C. & Humpel,C. (2002) Evidence that toxicity of lipopolysaccharide upon cholinergic basal forebrain neurons requires the presence of glial cells in vitro. *Brain Res.Bull.*, **58**, 91-98.

Weiss,J.M., Downie,S.A., Lyman,W.D. & Berman,J.W. (1998) Astrocyte-derived monocyte-chemoattractant protein-1 directs the transmigration of leukocytes across a model of the human blood-brain barrier. *J.Immunol.*, **161**, 6896-6903.

Welch,B.L. (1947) The generalization of "Student's" problem when several different population variances are involved. *Biometrika*, 28-35.

Werner,A., Willem,M., Jones,L.L., Kreutzberg,G.W., Mayer,U. & Raivich,G. (2000) Impaired axonal regeneration in alpha7 integrin-deficient mice. *J.Neurosci.*, **20**, 1822-1830.

Wetmore,C., Ernfors,P., Persson,H. & Olson,L. (1990) Localization of brain-derived neurotrophic factor mRNA to neurons in the brain by in situ hybridization. *Exp.Neurol.*, **109**, 141-152.

Widenfalk,J., Lundstromer,K., Jubran,M., Brene,S. & Olson,L. (2001) Neurotrophic factors and receptors in the immature and adult spinal cord after mechanical injury or kainic acid. *J.Neurosci.*, **21**, 3457-3475.

Wigley,R., Hamilton,N., Nishiyama,A., Kirchhoff,F. & Butt,A.M. (2007) Morphological and physiological interactions of NG2-glia with astrocytes and neurons. *J.Anat.*, **210** (6), 661-70.

Williamson,T., Gordon-Weeks,P.R., Schachner,M. & Taylor,J. (1996) Microtubule reorganization is obligatory for growth cone turning. *Proc.Natl.Acad.Sci.U.S.A*, **93**, 15221-15226.

Willson,C.A., Irizarry-Ramirez,M., Gaskins,H.E., Cruz-Orengo,L., Figueroa,J.D., Whittemore,S.R. & Miranda,J.D. (2002) Upregulation of EphA receptor expression in the injured adult rat spinal cord. *Cell Transplant.*, **11**, 229-239.

Wintergerst,E.S., Fuss,B. & Bartsch,U. (1993) Localization of janusin mRNA in the central nervous system of the developing and adult mouse. *.Eur.J.Neurosci.*, **5**, 299-310.

Wong,S.T., Henley,J.R., Kanning,K.C., Huang,K.H., Bothwell,M. & Poo,M.M. (2002) A p75(NTR) and Nogo receptor complex mediates repulsive signaling by myelin-associated glycoprotein. *Nat.Neurosci.*, **5**, 1302-1308.

Woodhall,E., West,A.K. & Chuah,M.I. (2001) Cultured olfactory ensheathing cells express nerve growth factor, brain-derived neurotrophic factor, glia cell line-derived neurotrophic factor and their receptors. *Brain Res.Mol.Brain Res.*, **88**, 203-213.

Woolf,C.J. (2003) No Nogo: now where to go? *Neuron*, **38**, 153-156.

Woolf,C.J., Reynolds,M.L., Molander,C., O'Brien,C., Lindsay,R.M. & Benowitz,L.I. (1990) GAP-43 a growth associated protein, appears in dorsal root ganglion cells and in the dorsal horn of the rat spinal cord following peripheral nerve injury. *Neuroreport.*, **34**, 465-478.

Woolhead,C.L., Zhang,Y., Lieberman,A.R., Schachner,M., Emson,P.C. & Anderson,P.N. (1998) Differential effects of autologous peripheral nerve grafts to the corpus striatum of adult rats on the regeneration of axons of striatal and nigral neurons and on the expression of GAP-43 and the cell adhesion molecules N-CAM and L1. *J.Comp.Neurol.*, **391**, 259-273.

Wu,D., Zhang,Y., Bo,X., Huang,W., Xiao,F., Zhang,X., Miao,T., Magoulas,C., Subang,M.C. & Richardson,P.M. (2007) Actions of neuropoietic cytokines and cyclic AMP in regenerative conditioning of rat primary sensory neurons. *Exp.Neurol.*, **204**, 66-76.

Xiao,D., Miller,G.M., Jassen,A., Westmoreland,S.V., Pauley,D. & Madras,B.K. (2006) Ephrin/Eph receptor expression in brain of adult nonhuman primates: implications for neuroadaptation. *Brain Res.*, **1067**, 67-77.

Xiao,Z.C., Ragsdale,D.S., Malhotra,J.D., Mattei,L.N., Braun,P.E., Schachner,M. & Isom,L.L. (1999) Tenascin-R is a functional modulator of sodium channel beta subunits. *J.Biol.Chem.*, **274**, 26511-26517.

Xu,X.M, Guenard,V., Kleitman,N., Bunge,M.B. (1994) Axonal regeneration into Schwann cell-seeded guidance channels grafted into transected adult rat spinal cord. *J.Comp.Neurol.*, **351**, 145-160

Yamada,H., Fredette,B., Shitara,K., Hagihara,K., Miura,R., Ranscht,B., Stallcup,W.B. & Yamaguchi,Y. (1997) The brain chondroitin sulfate proteoglycan brevican associates with astrocytes ensheathing cerebellar glomeruli and inhibits neurite outgrowth from granule neurons. *J.Neurosci.*, **17**, 7784-7795.

Yamashita,T., Higuchi,H. & Tohyama,M. (2002) The p75 receptor transduces the signal from myelin-associated glycoprotein to Rho. *J.Cell Biol.*, **157**, 565-570.

Yamashita,T. & Tohyama,M. (2003) The p75 receptor acts as a displacement factor that releases Rho from Rho-GDI. *Nat.Neurosci.*, **6**, 461-467.

Yang,B., Slonimsky,J.D. & Birren,S.J. (2002) A rapid switch in sympathetic neurotransmitter release properties mediated by the p75 receptor. *Nat.Neurosci.*, **5**, 539-545.

Yang,L.J., Zeller,C.B., Shaper,N.L., Kiso,M., Hasegawa,A., Shapiro,R.E. & Schnaar,R.L. (1996) Gangliosides are neuronal ligands for myelin-associated glycoprotein. *Proc.Natl.Acad.Sci.USA*, **93**, 814-818.

Yang,Z., Suzuki,R., Daniels,S.B., Brunquell,C.B., Sala,C.J. & Nishiyama,A. (2006) NG2 glial cells provide a favorable substrate for growing axons. *J.Neurosci.*, **26**, 3829-3839.

Ye,J.H. & Houle,J.D. (1997) Treatment of the chronically injured spinal cord with neurotrophic factors can promote axonal regeneration from supraspinal neurons. *Exp.Neurol.*, **143**, 70-81.

Ygge,J. (1989) Neuronal loss in lumbar dorsal root ganglia after proximal compared to distal sciatic nerve resection: a qualitative Andy in the rat. *Brain Res.*, **478**, 193-195.

Yick,L.W., So,K.F., Cheung,P.T. & Wu,W.T. (2004) Lithium chloride reinforces the regeneration-promoting effect of chondroitinase ABC on rubrospinal neurons after spinal cord injury. *J.Neurotrauma.*, **21**, 932-943.

Yick,L.W., Wu,W., So,K.F., Yip,H.K. & Shum,D.K. (2000) Chondroitinase ABC promotes axonal regeneration of Clarke's neurons after spinal cord injury. *Neuroreport.*, **11**, 1063-1067.

Yin,Y., Cui,Q., Li,Y., Irwin,N., Fischer,D., Harvey,A.R. & Benowitz,L.I. (2003) Macrophage-derived factors stimulate optic nerve regeneration. *J.Neurosci.*, **23**, 2284-2293.

Yin,Y., Henzl,M.T., Lorber,B., Nakazawa,T., Thomas,T.T., Jiang,F., Langer,R. & Benowitz,L.I. (2006) Oncomodulin is a macrophage-derived signal for axon regeneration in retinal ganglion cells. *Nat.Neurosci.*, **9**, 843-852.

Yiu G. & He Z. (2006) Glial inhibition of CNS axon regeneration. *Nat.Rev.Neurosci.*, **7**, 617-627.

Yoo,S. & Wrathall,J.R. (2007) Mixed primary culture and clonal analysis provide evidence that NG2 proteoglycan-expressing cells after spinal cord injury are glial progenitors. *Dev.Neurobiol.*, **67**, 860-874.

Yoshitomi,H., Sakaguchi,N., Kobayashi,K., Brown,G.D., Tagami,T., Sakihama,T., Hirota,K., Tanaka,S., Nomura,T., Miki,I., Gordon,S., Akira,S., Nakamura,T. & Sakaguchi,S. (2005) A role for fungal {beta}-glucans and their receptor Dectin-1 in the induction of autoimmune arthritis in genetically susceptible mice. *J.Exp.Med.*, **201**, 949-960.

You,S.W., Chen,B.Y., Liu,H.L., Lang,B., Xia,J.L., Jiao,X.Y. & Ju,G. (2003) Spontaneous recovery of locomotion induced by remaining fibers after spinal cord transection in adult rats. *Restor.Neurol.Neurosci.*, **21**, 39-45.

Z'Graggen,W.J., Metz,G.A., Kartje,G.L., Thallmair,M. & Schwab,M.E. (1998) Functional recovery and enhanced corticofugal plasticity after unilateral pyramidal tract lesion and blockade of myelin- associated neurite growth inhibitors in adult rats. *J.Neurosci.*, **18**, 4744-4757.

Zander,H., Reineke,U., Schneider-Mergener,J. & Skerra,A. (2007) Epitope mapping of the neuronal growth inhibitor Nogo-A for the Nogo receptor and the cognate monoclonal antibody IN-1 by means of the SPOT technique. *J.Mol.Recognit,*. **20 (3)**, 185-196.

Zhang,Y., Anderson,P.N., Campbell,G., Mohajeri,H., Schachner,M. & Lieberman,A.R. (1995a) Tenascin-C expression by neurons and glial cells in the rat spinal cord: changes during postnatal development and after dorsal root or sciatic nerve injury. *J.Neurocytol.*, **24**, 585-601.

Zhang,Y., Bo,X., Schoepfer,R., Holtmaat,A.J., Verhaagen,J., Emson,P.C., Lieberman,A.R. & Anderson,P.N. (2005) Growth-associated protein GAP-43 and L1 act synergistically to promote regenerative growth of Purkinje cell axons in vivo. *Proc.Natl.Acad.Sci.U.S.A*, **102**, 14883-14888.

Zhang,Y., Campbell,G., Anderson,P.N., Martini,R., Schachner,M. & Lieberman,A.R. (1995b) Molecular basis of interactions between regenerating adult rat thalamic axons and Schwann cells in peripheral nerve grafts. II. Tenascin-C. *J.Comp.Neurol.*, **361**, 210-224.

Zhang,Y., Roslan,R., Lang,D., Schachner,M., Lieberman,A.R. & Anderson,P.N. (2000) Expression of CHL1 and L1 by neurons and glia following sciatic nerve and dorsal root injury. *Mol.Cell.Neurosci.*, **16**, 71-86.

Zhang,Y., Tohyama,K., Winterbottom,J.K., Haque,N.S., Schachner,M., Lieberman,A.R. & Anderson,P.N. (2001) Correlation between putative inhibitory molecules at the dorsal root entry zone and failure of dorsal root axonal regeneration. *Mol.Cell Neurosci.*, **17**, 444-459.

Zhang,Y., Winterbottom,J.K., Schachner,M., Lieberman,A.R. & Anderson,P.N. (1997) Tenascin-C expression and axonal sprouting following injury to the spinal dorsal columns in the adult rat. *J.Neurosci.Res.*, **49**, 433-450.

Zhang,Y., Zhang,X., Yeh,J., Richardson,P. & Bo,X. (2007) Engineered expression of polysialic acid enhances Purkinje cell axonal regeneration in L1/GAP-43 double transgenic mice. *Eur.J.Neurosci.*, **25**, 351-361.

Zheng,B., Atwal,J., Ho,C., Case,L., He,X.L., Garcia,K.C., Steward,O. & Tessier-Lavigne,M. (2005) Genetic deletion of the Nogo receptor does not reduce neurite inhibition in vitro or promote corticospinal tract regeneration in vivo. *Proc.Natl.Acad.Sci.U.S.A*, **102**, 1205-1210.

Zheng,B., Ho,C., Li,S., Keirstead,H., Steward,O. & Tessier-Lavigne,M. (2003) Lack of enhanced spinal regeneration in nogo-deficient mice. *Neuron*, **38**, 213-224.

Zhou,L., Baumgartner,B.J., Hill-Felberg,S.J., McGowen,L.R. & Shine,H.D. (2003) Neurotrophin-3 expressed in situ induces axonal plasticity in the adult injured spinal cord. *J.Neurosci.*, **23**, 1424-1431.

Zhou,L. & Shine,H.D. (2003) Neurotrophic factors expressed in both cortex and spinal cord induce axonal plasticity after spinal cord injury. *J.Neurosci.Res.*, **74**, 221-226.

Zhu,J.X., Goldoni,S., Bix,G., Owens,R.T., McQuillan,D.J., Reed,C.C. & Iozzo,R.V. (2005) Decorin evokes protracted internalization and degradation of the epidermal growth factor receptor via caveolar endocytosis. J.Biol.Chem., **280**, 32468-32479.

Ziskin,J.L., Nishiyama,A., Rubio,M., Fukaya,M. & Bergles,D.E. (2007) Vesicular release of glutamate from unmyelinated axons in white matter. *Nat.Neurosci.*, **10**, 321-330.

Zorick,T.S., Syroid,D.E., Arroyo,E., Scherer,S.S. & Lemke,G. (1996) The transcription factors SCIP and Krox-20 mark distinct stages and cell fates in Schwann cell differentiation. *Mol.Cell Neurosci.*, **8**, 129-145.